Evaluation des StrAtégies de LUTte contre la pollution de l'AIR à longue distance dans le contexte du changement climatique

Assessing Long Term Air Quality Mitigation Strategies in the Face of Long Range Transport and Climate Change

Programme PRIMEQUAL 2

Rapport de fin de contrat

Augustin Colette, Simone Schucht, Bertrand Bessagnet, Sophie Szopa,
Robert Vautard, Laurent Menut, Om Tripathi, Gaelle Clain, Juliette Lathière,
Philippe Drobinski, Hiba Omrani, Didier Hauglustaine,
Frédérik Meleux, Elsa Réal, Marjorie Délias, Alessandro Anav

INERIS,
Parc Technologique Alata, BP2
60550 Verneuil-en-Halatte

Responsables du projet:
Bertrand Bessagnet, Sophie Szopa

N° de contrat: 0962C0033

Date du contrat: 29/05/2009

Date du rapport: 02/07/2013

Funding : Primequal, ADEME – MEDDE

.

List of staff involved in the study:

INERIS:

Augustin Colette, Bertrand Bessagnet, Simone Schucht, Frédérik Meleux, Elsa Réal, Marjorie Délias

LMD/IPSL/CNRS:

Laurent Menut, Om Tripathi, Alessandro Anav, Philippe Drobinski, Hiba Omrani

LSCE/IPSL/CEA:

Sophie Szopa, Robert Vautard, Gaelle Clain, Juliette Lathière

LIVE:

Didier Hauglustaine

External collaborations:

The project benefited from interactions with partners that were not included in the initial work plan. They were actively involved in the publications produced in the course of the project or currently being produced, however the responsibility of the content of the present report remains with the core team of authors.

LSCE/IPSL/CEA:

Mathieu Vrac

EMRC:

Mike Holland

IIASA:

Shilpa Rao, Zig Klimont, Wolfgang Schöpp, Peter Kolp

Univ l'Aquila:

Gabriele Curci

DISCLAIMER

This report was drawn up on the basis of the information provided to INERIS and the objective (scientific or technical) data available as well as applicable regulations.

INERIS cannot be held liable if the information received was incomplete or erroneous.

Any findings, recommendations, suggestions or equivalents that are recorded by INERIS as part of the services it is contracted to perform may assist with decision making. Given the tasks entrusted to INERIS on the basis of the decree founding the organization, INERIS cannot be involved in the decision making process itself. INERIS cannot therefore take responsibility in lieu and place of the decision maker.

The addressee shall use the results comprised in this report in whole or at least in an objective manner. Using this information in the form of excerpts or summary memos may take place only under the full and complete responsibility of the addressee. The same applies to any modification made to this report.

INERIS declines any liability for any use of this report outside of the scope of the service provided.

	Drafting	Checking	Approval
Name	Augustin Colette Bertrand Bessagnet Salut'AIR team	Jean-Marc Brignon	Laurence Rouïl
Quality	Ingénieurs et Resp. Unité DRC/DECI/MOCA	Responsable d'Unité DRC/DECI/EDEN	Responsable du Pôle DRC/DECI
Signature			

Résumé

Le changement climatique, le transport intercontinental de polluants atmosphériques, et la qualité de l'air partagent de nombreux mécanismes d'interaction. La définition de mesures de réduction de la pollution atmosphérique efficientes à long terme nécessite de prendre en compte des facteurs externes qui peuvent légitimement être négligés pour des projections à court terme. Un nouveau système de modélisation régionale de climat et de la qualité de l'air a donc été conçu, développé, et mis en œuvre afin de prendre en compte les pénalités que sont susceptibles de constituer le changement climatique ou le transport à longue distance de polluants pour la qualité de l'air Européenne. Afin de s'assurer de la pertinence de cet outil pour l'aide à la décision, ce système de modélisation est intégré à un cadre d'analyse quantitative coût-bénéfice.

Le développement de la chaîne de modélisation a fourni une occasion d'étudier plus en détails certains composants de cette chaîne. Une avancée significative a été possible dans le domaine de la modélisation régionale du climat en évaluant et améliorant les performances de la descente d'échelle dynamique, et en explorant des techniques de correction de biais. Les interactions entre la végétation, le climat et la chimie atmosphérique ont aussi été étudiées.

La chaîne de modélisation a permis de conduire une évaluation de la qualité de l'air en Europe en 2050. L'influence dominante des réductions d'émissions de polluants atmosphériques anthropiques en Europe a été mise en évidence. La pénalité climatique pesant sur la pollution à l'ozone a été confirmée, et le fort impact du transport à longue distance en 2050 a été souligné. Pour les particules, le transport à longue distance est moins important, le changement climatique joue dans ce cas un rôle significatif mais plus incertain.

Nous avons évalué les coûts de l'atténuation du changement climatique et de la réduction de la pollution atmosphérique en utilisant des projections fondées sur des facteurs d'émission représentatifs de la législation actuelle. Il apparaît que les politiques climatiques apportent indirectement une baisse des coûts de la réduction de la pollution de l'air, une société économe en carbone nécessitant moins de mesures technologiques de réduction d'émission de polluants atmosphériques en aval. Le coût total de l'atténuation (climat et pollution) demeure cependant plus élevé avec le scénario comportant une politique climatique ambitieuse qu'en l'absence de politique climatique.

Les bénéfices sanitaires de la réduction de la pollution atmosphérique ont été monétisés grâce à une étude d'impact sanitaire reposant sur les résultats de modélisation de la qualité de l'air et du climat à l'échelle Européenne. Il est essentiel de noter que les bénéfices sanitaires monétisés excèdent les coûts des politiques environnementales (atténuation du changement climatique et réduction de la pollution atmosphérique), démontrant l'intérêt pour la pollution de l'air des co-bénéfices induits par les investissements relatifs à la politique climatique.

Abstract

Climate change, long range transport of pollutants and surface air quality share multiple interaction pathways. Tailoring efficient air quality mitigation strategies over the long term requires taking into account such external factors that can be neglected for short term projections. We designed, developed and implemented a new regional air quality and climate modelling system to account for the possible penalties of climate change and long range transport of pollutants on European air quality. In order to ensure its relevance for environmental policy making, this modelling system is embedded in a quantitative cost-benefit analysis framework.

The development of the modelling system provided an opportunity to investigate individual components of the suite. A breakthrough in terms of regional climate modelling was achieved by carefully documenting and improving the performance of the dynamical downscaling and by exploring bias correction techniques. Interactions between vegetation, climate, and air were also investigated.

The regional air quality and climate modelling suite allowed proposing an assessment of European air quality in 2050. We highlighted the dominating influence of mitigation of anthropogenic emissions of pollutants in Europe. But the penalty brought about by climate change on ozone pollution was also confirmed, and the large impact of long range transport at the 2050 horizon was emphasized. For particulate matter, long range transport is less important; the impact of climate change is significant but also uncertain.

Thanks to the use of air pollutant emission projections based on emission factors reflecting the current legislation, we could assess the costs of climate mitigation and air quality legislation. We point out the economic benefit of climate policies for air quality legislation due to a low carbon economy requiring fewer (end-of-pipe) technological measures against air pollution. The total cost of mitigation (air and climate) remains however higher under the mitigation than under the business as usual pathway.

The analysis of air and climate modelling results within a monetised health impact assessment framework allowed assessing expected sanitary benefits. It is important to highlight that the expected monetised sanitary benefits exceed the costs, showing the air quality co-benefit of investing in climate mitigation.

Note de Synthèse

La qualité de l'air, le transport à longue distance de polluants et le changement climatique sont fortement liés dans leur fonctionnement et leurs impacts. Par conséquent, leur atténuation nécessite des mesures conjointes.

- Les politiques climatiques impliquent des mesures d'efficacité énergétique et d'autres mesures technologiques qui concernent un vaste panel d'activités humaines, et par conséquent, influent en retour sur les émissions de polluants et donc la chimie atmosphérique.
- Les mesures de réduction d'émission de polluants ont aussi un impact indirect sur les émissions de gaz à effet de serre.
- La chimie atmosphérique est sensible au changement climatique (qui, en modifiant les caractéristiques physiques de l'atmosphère, contraint la fréquence des phénomènes météorologiques susceptibles de conduire à la formation d'épisodes de pollution).
- Certains polluants (gazeux ou particulaires) ont un impact direct ou indirect sur l'équilibre radiatif terrestre.
- La distinction entre qualité de l'air et transport de polluants à longue distance est induite par la durée de vie des espèces traces mais, pour nombre d'entre elles, cette durée de vie est telle qu'elles peuvent jouer un rôle à travers les échelles spatiales.

Le projet SALUT'AIR a permis à un consortium de groupes de recherche de sciences de l'atmosphère et d'économie de l'environnement de redéfinir les méthodes d'évaluation intégrées relatives aux stratégies de réduction de la pollution atmosphérique. Le principal résultat de ce projet est un nouveau système de modélisation exhaustif de la qualité de l'air et du climat régional dans un cadre d'analyse coût-bénéfice. Ce nouvel outil permet de prendre en compte les facteurs externes pesant sur la qualité de l'air en Europe - tels que le transport intercontinental de polluants et le changement climatique – tout en proposant une évaluation quantitative de l'impact des mesures réglementaires relatives à la pollution de l'air sur la santé. Ce système de modélisation repose sur des modèles existants de climat et de chimie-transport, l'innovation réside dans leur intégration pour le cas spécifique des études à long terme. Un nouvel outil a été ajouté à la panoplie à la disposition du consortium : Alpha-RiskPoll-France, version adaptée de l'outil utilisé par la Commission Européenne, par exemple dans le cadre du programme CAFE[1]. Cette chaîne de modélisation peut à présent être utilisée pour des études d'évaluation intégrées mais elle a aussi prouvé son utilité pour des études scientifiques plus ciblées sur certains compartiments du système étudié.

La chaîne de modélisation régionale, explicite, et intégrée des coûts et des bénéfices du climat et de la qualité de l'air est schématisée sur la Figure 1, elle permet :

- D'analyser les scénarios prospectifs d'émission de polluants atmosphériques (ici issus du Global Energy Assessment) en proposant une quantification des coûts économiques associés ;
- De raffiner spatialement les projections des modèles climatiques globaux (ici le modèle IPSL-CM5-MR, raffiné en utilisant WRF) effectuées dans le cadre de projets internationaux coordonnés (tel que CMIP[2], conçu pour informer le travail du GIEC[3]) afin d'atteindre des échelles spatiales pertinentes pour les études d'impact ;

[1] Clean Air For Europe
[2] Climate Model Intercomparison Exercise
[3] Groupe d'experts intergouvernemental sur l'évolution du climat

- D'utiliser les projections globales de chimie atmosphérique et de climat afin de tenir compte de l'évolution de la pollution dans les régions éloignées (on utilise ici le modèle de chimie-climat global LMDz-OR-INCA) ;
- De proposer un focus sur une région donnée pour la qualité de l'air (ici l'Europe) qui tient compte de tous les facteurs mentionnés ci-dessus (avec le modèle de chimie transport CHIMERE) ;
- D'utiliser ces résultats pour des études d'impact sanitaire afin de quantifier les bénéfices des politiques de gestion et de les comparer à leurs coûts.

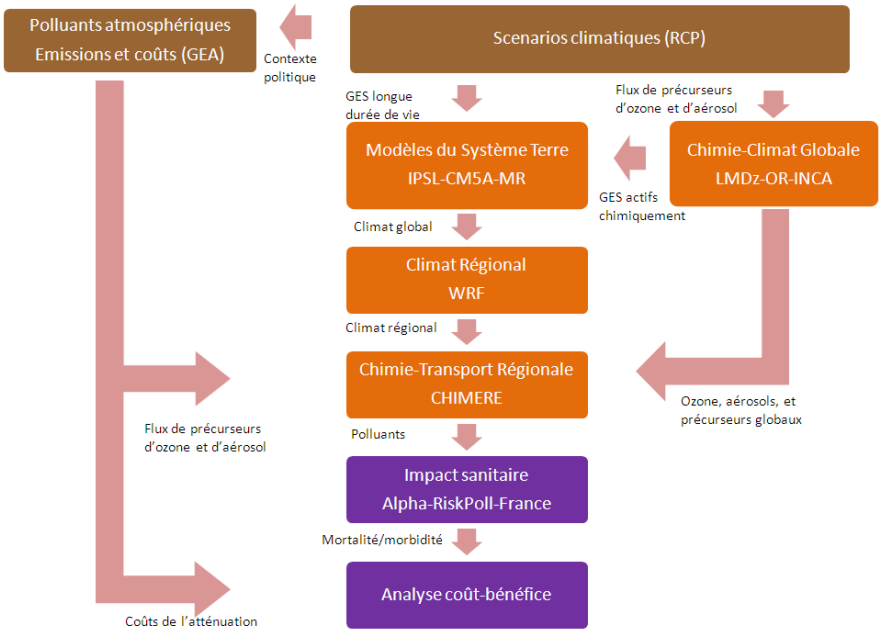

Figure 1: Schéma de fonctionnement du système de modélisation de la qualité de l'air et du climat régional (orange), les projections d'émissions en entrée sont données en marron, et les outils relatifs à l'étude d'impact sanitaire monétisée sont en violet.

Des développements techniques et méthodologiques significatifs ont été nécessaires avant de pouvoir explorer les projections de qualité de l'air à l'horizon 2050. Un effort particulier a été consacré à la descente d'échelle des projections climatiques :

- Les projections climatiques globales doivent être raffinées spatialement pour les études d'impact. Ce travail a été accompli en privilégiant une approche dynamique. La sensibilité physique et numérique du modèle de climat régional a été documentée et ses forces et faiblesses ont été soigneusement évaluées. **Une technique innovante de correction de biais a aussi été développée**.
- Les efforts consacrés à la modélisation régionale du climat ont permis au partenariat IPSL-INERIS de rejoindre le consortium international CORDEX sur les projections climatiques régionales.

Les interactions entre végétation et qualité de l'air, dans le contexte spécifique du changement climatique, ont aussi été étudiées :

- L'impact du climat sur les émissions biogéniques futures a été quantifié, en particulier en ce qui concerne l'importance des changements d'occupation des sols, de l'augmentation des concentrations de CO_2, et la sensibilité à la température et au rayonnement solaire. Cette

étude a montré que **l'effet inhibant de l'augmentation du CO_2 peut contrebalancer l'effet du changement climatique sur les émissions d'isoprène**.
- Les rétroactions directes et inverses entre qualité de l'air et climat ont été documentées à l'aide d'une nouvelle version du modèle de chimie-transport CHIMERE couplée au modèle de biosphère ORCHIDEE

Les principaux résultats de l'étude intégrée du climat et de la qualité de l'air régionale sont résumés ci-dessous.

Quelles tendances d'émission de polluant sont envisagées dans les décennies à venir, comment sont-elles liées aux politiques climatiques et quels sont les coûts associés ?

- Deux scénarios prospectifs ont été analysés. Ils sont identiques en termes de politique de gestion de la qualité de l'air mais diffèrent en termes de politiques climatiques. L'un d'entre eux ignore tout type de mesure spécifique au changement climatique, alors que le deuxième ambitionne de limiter le réchauffement global à 2°C d'ici la fin du siècle. **Les mesures de gestion de la qualité de l'air planifiées à ce jour conduisent à des réductions d'émission de polluant significatives selon les deux scénarios. Les politiques climatiques apportent un co-bénéfice additionnel important**.
- En termes économique, l'atténuation du changement climatique conduit à une augmentation des dépenses dans le système énergétique de 107 000M€, mais les coûts de la lutte contre la pollution sont indirectement réduits de 42 000M€, grâce au co-bénéfice des politiques climatiques (un nombre moins importants de technologies de dépollution en aval étant nécessaire dans une société économe en carbone tel qu'on le voit sur les deux premières paires de colonnes de la Figure 2). Le coût net de l'atténuation du changement climatique demeure toutefois 65 000M€, soit 15%, au dessus du coût du scénario qui ignore toute forme de politique climatique.

Quel est l'impact net du changement climatique, du transport à longue distance, et de l'atténuation des émissions de polluants sur la qualité de l'air future?

- En utilisant des projections d'émissions de polluants quantitatives dans la chaîne de modélisation intégrée nous avons pu proposer une **évaluation de la qualité de l'air en 2050 en Europe**, et des études de sensibilité ont permis d'isoler les contribution individuelles de chaque facteur.
- La réduction des émissions de polluants atmosphériques en Europe demeure le facteur dominant de l'évolution des concentrations futures d'ozone et de particules, son influence est supérieure à celle du changement climatique ou du transport à longue distance de ces polluants.
- La pénalité que fait poser le changement climatique sur la pollution atmosphérique (i.e. l'augmentation de la pollution attribuée à l'augmentation des températures, via une photochimie plus active ou des émissions de précurseurs biogéniques renforcées) est confirmée pour l'ozone mais apparaît moins robuste pour les particules.

Quels seront les impacts de la pollution de l'air à venir sur la santé ? Quels sont les coûts nets réels des mesures de gestions lorsque l'on prend en compte les bénéfices sanitaires ?

- En l'absence de politique d'atténuation du changement climatique, les impacts sanitaires relatifs à l'exposition à l'ozone augmenteront d'ici 2050 à cause de l'effet conjoint du changement climatique et du transport à longue distance de polluants, qui compensent les

politiques de qualité de l'air. L'augmentation de la population jouera également un rôle dans la hausse des impacts. Le scénario d'atténuation réduirait fortement ces impacts.

- **Les impacts sanitaires totaux sont largement dominés par l'exposition aux particules fines** (95 à 98% des coûts sanitaires totaux, le reste étant attribué à l'ozone). Par conséquent, l'évolution future des $PM_{2.5}$ régit les coûts associés à la mortalité et à la morbidité qui devraient décroître de 60% entre 2005 et 2050 selon le scénario ignorant toute politique climatique. Une réduction additionnelle de 50% serait atteinte grâce au scénario ambitieux en termes de politique climatique (voir la 3^{e} paire de colonnes de la Figure 2).
- Le scénario d'atténuation du changement climatique comporte d'importants co-bénéfices pour la qualité de l'air qui sont reflétés dans la réduction des coûts de la gestion de la qualité de l'air. Avec une consommation et une production d'énergie réduite, les obligations relatives à la qualité de l'air nécessitent des investissements réduits. On peut citer en exemple le transport routier, où la part de l'électricité serait de 5% dans le scénario ignorant les politiques climatiques et passe à un tiers dans le scénario d'atténuation, avec un gain important pour la qualité de l'air qui s'affranchi dès lors de mesures technologiques de dépollution des gaz d'échappement.
- L'analyse coût bénéfice conclut à un bénéfice net des politiques environnementales ambitieuses, avec des coûts additionnels de l'atténuation du changement climatique (énergie et qualité de l'air) atteignant 66 milliard d'euros (€2005) par an en 2050, alors que les bénéfices sanitaires sont estimés à 79 milliards d'euros (€2005) par an en 2050 (ce qui fait une économie nette de 13 milliards d'euros €2005 par an en 2050, voir la dernière paire de colonne de la Figure 2). Les analyses de sensibilité explorant toutes les sources d'incertitudes à l'exception des coûts énergétiques confirment que dans toutes les configurations, les bénéfices excèderont probablement les coûts. Il faut souligner que l'analyse des bénéfices se focalise sur les bénéfices sanitaires d'une amélioration de la qualité de l'air. Tous les bénéfices des politiques ne sont pas pris en compte dans cette analyse. L'analyse ne quantifie pas les dommages de la pollution atmosphérique sur les écosystèmes, les cultures et les matériaux qui sont évités grâce à la réduction de la politique atmosphérique. Il ne prend pas non plus en compte des impacts de la réduction des gaz à effet de serre autres que ceux sur la qualité de l'air. Les bénéfices totaux des réductions d'émissions (air et gaz à effet de serre) sont alors clairement sous-estimés.

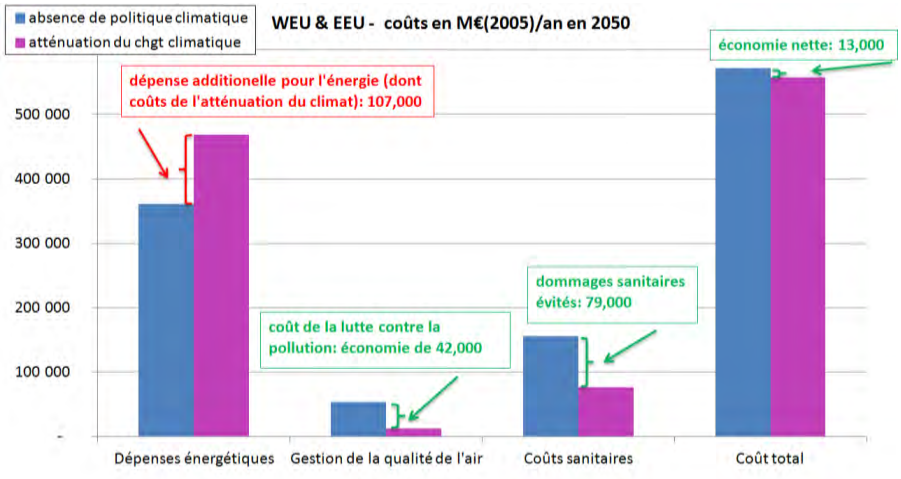

Figure 2: Coûts (dépenses énergétiques, lutte contre la pollution de l'air, impacts sanitaires et coût total net) selon les deux scénarios en M€(2005)/an en 2050.

Executive Summary

Air pollution, long-range transport of pollutants and climate change are closely inter-related in their functioning and their impacts. As a consequence, their mitigation requires considering them synergistically.

- Climate policies imply energy efficiency and other technical measures that have an impact on a wide range of human activities and, in turn, on atmospheric emissions of air pollutants, hence on atmospheric chemistry.
- Air pollution mitigation measures may also have an impact on co-emitted greenhouse gases.
- Atmospheric chemistry is sensitive to climate change (which affects physical properties of the atmosphere and therefore drives the frequency of weather events yielding favourable conditions to the build up of pollution episodes).
- Some air pollutants (both gaseous and particulate) have direct and indirect impacts on the atmospheric radiative forcing.
- The lifetimes of trace species govern their impact on local air quality and/or intercontinental long-range transport; however, for many species, their lifetime is such that they may have impacts at both local and long-range scales.

The SALUT'AIR project allowed a consortium of research groups involved in atmospheric science and environmental economics to revisit assessment methodologies devoted to air quality mitigation strategies. The main asset of the project is a new comprehensive regional air quality and climate modelling system embedded in a quantitative cost-benefit analysis framework. This new tool allows taking into account the main external factors bearing upon European air pollution, namely intercontinental transport and climate change, while remaining focused on quantitative assessment of air pollution legislation and its impact on human health. The modelling system relies on existing climate and chemistry models, the innovation being in their integration in the very specific context of long-term projections. One new model was added in the panel available to the consortium: Alpha-RiskPoll-France, adapted from the version being used in European Policy analyses such as the CAFE[4] programme. The suite of models can now be used for operational integrated assessment but it has also demonstrated its relevance for more focused scientific studies on individual components of the modelling system.

The operational explicit and integrated tool for the cost-benefit assessment of regional air quality and climate change is sketched in Figure 3, it allows:

- Analysing emission projection scenarios (here the Global Energy Assessment pathways) by including a quantitative evaluation of the associated mitigation costs;
- Downscaling global climate (IPSL-CM5-MR global climate model, downscaled with WRF) projections produced in international experiments (such as CMIP[5] designed to inform the IPCC[6] process) to reach spatial scales relevant to climate impacts issues;
- Making use of global atmospheric projections that combine projected climate change and atmospheric composition trends in distant locations (given by the global chemistry-transport model LMDz-OR-INCA);
- Producing a focus on air quality over a given region (here Europe) that takes into account the above-mentioned factors (with the regional Chemistry-Transport CHIMERE);

[4] Clean Air For Europe
[5] Climate Model Intercomparison Exercise
[6] Intergovernmental Panel on Climate Change

– Using these results in a health impact assessment framework (Alpha-RiskPoll-France) to derive monetized sanitary benefits that shall be compared with the mitigation costs allowing a quantitative comparison.

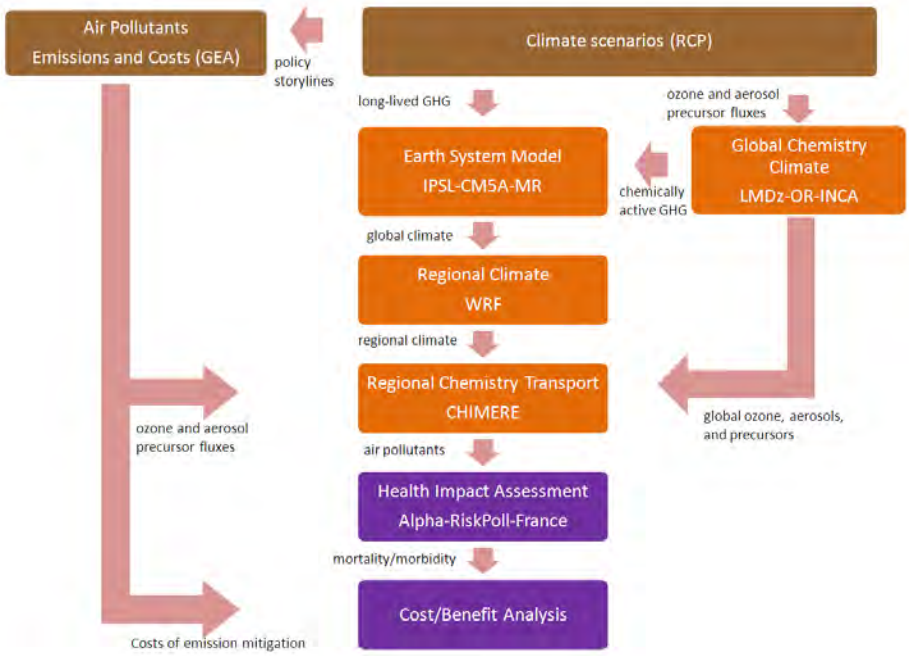

Figure 3: Conceptual flowchart of the regional air quality and climate modelling system (orange boxes), input emission sources for greenhouse gases and pollutant are given in the brown boxes, and the health impact assessment and monetisation tools are given in the violet boxes.

Important technical and methodological developments were required in order to explore air quality projections at the 2050 horizon. In particular, a large effort was devoted to regional climate downscaling:

– Global climate projections need to be spatially refined for climate impact assessments. This refinement is performed using a dynamical approach. The sensitivity of the regional climate model setup (in physical and numerical terms) was documented, and the strength and weaknesses of the result carefully assessed. **An innovative technique to bias-correct regional climate projections was also developed**.
– The efforts related to regional climate modelling allowed the IPSL-INERIS partnership to join the international CORDEX consortium on regional climate projections.

The interactions between vegetation and air quality under the context of a changing climate were also investigated:

– The impact of climate on future biogenic emissions was explored, in particular in relation with changes in land use, inter-linkages with increasing CO_2 levels, and sensitivity to temperature and incoming solar radiation. This study showed that **the inhibiting effect of increased CO_2 on isoprene emissions can counterbalance the increase expected from atmospheric warming**.
– The two-ways feedbacks between air quality and climate were documented with a new version of the CHIMERE Chemistry-Transport model coupled with the biosphere model ORCHIDEE.

The key results of the integrated regional air and climate assessment are summarized hereafter.

What are the possible European air pollutant emission trends in the coming decades, how do they relate to climate policies, and what are the associated costs?

- We explored two emission projection scenarios, identical in terms of air quality legislation but differing in terms of climate policy. One of them assumes no specific climate measures (no climate policy), while the other aims at limiting global warming below 2°C by the end of the century (mitigation). **The currently planned air quality legislation leads to substantive reduction of air pollutant emissions in Europe under both scenarios, climate policies contribute an important additional co-benefit**.
- In economical terms, climate mitigation leads to an increase of 107 000M€ of energy expenditures in Europe, but at the same time horizon **air pollution mitigation costs are reduced by 42 000 M€ thanks to the co-benefit of climate policies on air pollutant emissions** (fewer end of pipe measures are required in a low carbon economy as shown in the first and second bars of Figure 4). The net cost of climate mitigation remains however 65 000M€, or 15%, higher than the no climate policy scenario.

What is the net impact of climate change, long range transport and mitigation of air pollutant emissions in Europe on future air quality?

- Using the quantitative emission projections to inform the suite of climate and chemistry models, we could propose an **assessment of air quality in Europe in 2050**, and a number of sensitivity scenarios to isolate the individual contribution of each driver.
- **Reduction of air pollutant emissions in Europe is the main factor influencing ozone and particulate air quality at the 2050 horizon** dominating external drivers such as climate change and intercontinental transport of air pollution.
- The penalty of climate change on air pollution (increase of pollution due to temperature increase - for instance - through more active photochemistry and enhanced biogenic emission of precursors) is confirmed for ozone but appears less robust for particulate matter.
- **Intercontinental transport of air pollution is a major driver for future ozone** (the global composition projections switches from increasing ozone to decreasing ozone background depending on the selected scenario) even dominating the climate penalty, while it is less important for particulate matter.

What are the impacts of future air pollution on human health? What are the true net costs of mitigation accounting for the sanitary benefits in addition to the technological costs?

- Health impacts from acute exposure to ozone will increase by 2050 compared to 2005 under the no-climate policy scenario as a result of penalties from climate change and intercontinental transport exceeding the efficiency of mitigation, combined with European population increases. The climate mitigation pathway would strongly reduce such impacts.
- **Overall health damages are strongly dominated by exposure to $PM_{2.5}$** (95 to 98% of total sanitary costs, the remainder being attributed to ozone). As a consequence, its evolution drives the future changes of the costs associated with mortality and morbidity that are anticipated to decrease by 60% between 2005 and 2050 under the no-climate policy scenario, while an additional 50% decrease can be achieved in 2050 by implementing an ambitious climate policy (see the third couple of bars of Figure 4).

- The ambitious climate mitigation policy scenario leads to important co-benefits for air pollution policy that are mirrored in air pollution cost-savings relative to the no climate policy scenario. With overall lower energy consumption and production, air quality requirements require fewer investment in end-of-pipe measures to reduce atmospheric emissions. As an example, the share of electricity in transportation amounts to approximately one third in overall transportation fuel consumption in the mitigation scenario in 2050, it only counts for approximately 5% in the no climate policy scenario.
- In all, the cost-benefit analysis concludes to the **net benefit of ambitious environmental policies, with net additional costs of climate mitigation (energy + air pollution) reaching 66 billion €(2005)/year in 2050, while the sanitary benefits are estimated to 79 billion €(2005)/year in 2050** (resulting in a net cost saving of 13 billion €(2005)/year in 2050 between the last couple of bars of Figure 4). The sensitivity analysis exploring all uncertainties but those related to energy costs, confirms the finding that benefits are likely to exceed costs. It is also worth noting that the benefits analysis is focused on health benefits from improved air quality. Not all benefits of the policies have therefore been accounted for. The analysis does not quantify avoided damages of air pollution onto ecosystems, crops and materials, nor does it account for impacts - other than on air quality - of reduced greenhouse gases, and in this clearly underestimates benefits of emission (atmospheric and greenhouse gases) reductions.

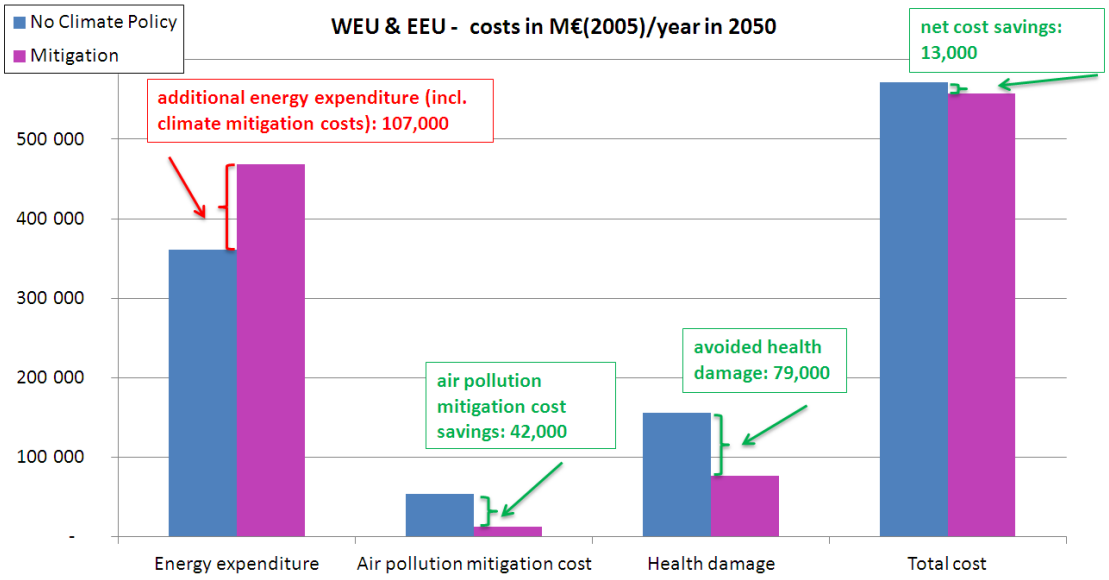

Figure 4: Costs (energy expenditure, air pollution mitigation, health damage, and net overall cost) under the two scenarios, in M€(2005)/year in 2050.

1 Introduction

1.1 Scientific context and scope

Climate change resulting from greenhouse gas emissions (IPCC, 2007), is expected to yield substantial impacts on air quality (Jacob and Winner, 2009). Meteorological conditions that drive the dispersion, accumulation and formation of pollutants might undergo significant changes in the future. In order to be exhaustive, one should take into account the changes in typology, frequency and intensity of synoptic events yielding favourable conditions for the onset of pollution episodes. It is therefore important to develop tailored long-term measures in mitigating air pollution, taking into account climate change. While policies designed to mitigate climate change aim at reducing greenhouse gases, the indirect impact of these policies on emissions of air pollutants is not systematically taken into account. One should have in mind the example of domestic wood burning strongly supported to increase the share of renewables, but that also contributes to increase particulate matter episodes. At the same time, stakeholders are lacking an appropriate tool to explore long term perspectives. In Europe, the most established model to investigate portfolios of air quality mitigation options is GAINS[7] (Amann et al., 2011a) which limits its scope to the 2030 horizon because (1) explicit technological and social changes after that date are speculative, (2) external factors such as climate change and long range transport might play a significant role at such long time scales and these factors are ignored in the source/receptor matrices used to build the model.

The major external factors that are expected to play a significant role in long term air quality assessment are (1) long range transport and (2) climate change:

1. An increase in background levels of ozone at the a global scale, due to increased human activities would lead to an increase in radiative forcing and a change of pollution levels at the regional scale (Prather et al., 2003). (Jacob et al., 1999) showed that multiplying by a factor three Asian emissions of ozone precursors between 1985 and 2010 would have increased the monthly concentrations of 2 to 6 ppb in the western United States. According to these authors, this amount is greater than would result from a reduction of NOx and VOC domestic emissions by 25% in the West of the United States. Thus, as confirmed in (Szopa et al., 2006), even modest rises of background levels may jeopardise regional strategies for air pollution control that are based on non-exceedance of target and limit values. However the way (and even the direction) of how global ozone will evolve in the future is strongly dependent on the scenario considered (Stevenson et al., 2006), showing at the same time that (1) there is still scope for mitigation if appropriate actions are taken, (2) appropriate tools taking into account a global perspective are needed.
2. Over the past few years, there has been a growing body of literature showing that climate change would contribute to increasing ozone levels in Europe, either through the effect of incoming solar radiation, water vapour increase (Stevenson et al., 2006) and temperature impact on the photochemistry or conversion of reservoir species such as peroxyacetyl nitrate (Hauglustaine et al., 2005), or through the emission of biogenic precursors of ozone.

[7] GAINS was launched in 2006 as an extension to the RAINS model which is used to assess cost-effective response strategies for combating air pollution, such as fine particles and ground-level ozone.
GAINS provides an authoritative framework for assessing strategies that reduce emissions of multiple air pollutants and greenhouse gases at least costs, and minimize their negative effects on human health, ecosystems and climate change. GAINS is used for policy analyses under the Convention on Long-range Transboundary Air Pollution (CLRTAP), e.g., for the revision of the Gothenburg Protocol, and by the European Commission for the EU Thematic Strategy on Air Pollution and the air policy review.

3. The term “ozone climate penalty” has emerged and was confirmed by (Andersson and Engardt, 2010;Hedegaard et al., 2008;Hedegaard et al., 2012;Katragkou et al., 2011;Langner et al., 2012a;Langner et al., 2012b;Manders et al., 2012;Meleux et al., 2007). But climate change might also weight upon particulate pollution (Hedegaard et al., 2012;Manders et al., 2012), through the frequency of stagnation episodes, the washout sink, but also presumably by altering the formation of secondary aerosols (in a similar fashion as for ozone). The latter was already envisaged in an exploratory internal study (Bessagnet, 2008) that showed that climate change alone led to strong regional in-homogeneities in the evolution of the concentrations of PM_{10} and $PM_{2.5}$.

These two main drivers are however rarely compared to other influential factors (such as local mitigation measures) whereas the latest evidences suggested that reductions in air pollutant emissions would largely compensate the climate penalty (Hedegaard et al., 2012;Langner et al., 2012a).

In addition, because air quality and climate modelling is often tackled by distinct research communities, synergetic approaches were often overlooked, and the uncertainties brought about by the climate modelling on the air quality assessment are not systematically assessed. Similarly, the link between climate, vegetation and atmospheric chemistry deserved more investigation. The expected changes in vegetation, and in turn in chemical deposition and biogenic emission fluxes could drastically affect the atmospheric composition (Hauglustaine et al., 2005).

The project provides a unique opportunity to investigate sensitive processes and feedback mechanisms that are not well documented in the literature. But the ultimate ambition is to produce quantitative integrated air quality and climate projections that are relevant to support environmental decision making. Besides the requirement of an operational suite of models, this objective also calls for the use of realistic prospective scenario, for which economic costs of mitigation measures can be assessed. Air pollution impacts on health and subsequent sanitary benefits of mitigation should also be computed, rather than limiting the scope to the discussion of air pollutant concentrations.

To sum up, the Salut’AIR project aims at bringing together expertise from different research communities: Global and Regional Climate, Global and Regional Chemistry, Vegetation modelling, projection of technical measures and anthropogenic emission, health impact assessment and monetary valuation.

The overarching aim of the project is to provide guidance to the public authorities to determine the best air quality and climate mitigation strategies in Europe. To achieve this goal, it is necessary to document the efficiency of European mitigation measure under the context of external penalties such as climate change and long range transport and better estimate the robustness of such projections. They will in particular contribute to the debates on the subjects that take place in forums and working groups of the United Nations Convention on Long-Range Transboundary Air Pollution (Economic Commission for Europe of the United Nations): Task Forces on Hemispheric Transport of Air Pollutant (TF-HTAP), Measurement and Modelling (TFMM), Integrated Assessment Modelling (TFIAM). They will also contribute to the assessment of the European Environment Agency, for which INERIS leads the air quality and climate interlinkages sub-projects within the European Topic Centre on air and climate mitigation. This project is also a continuation of long-term commitments of the partners: INERIS through its support programs to the Ministry in charge of Ecology, and IPSL through its long term strategy on climate change. Salut’AIR is also inscribed in the momentum created by the *Groupement d'Intérêt Scientifique Climat-Environnement-Societé*.

1.2 Workplan

In order to encompass all the processes playing a role, one should implement four types of models in a synergetic way summarized in Figure 5 from (Jacob and Winner, 2009):

1. A global atmosphere-ocean coupled climate model (GCM) that produces future projections of climate at a coarse resolution but covering the whole globe hence taking into account feedbacks with the cryosphere, the biosphere, and the ocean.
2. A regional climate model (RCM) nested at its boundaries within the GCM, offering a dynamical downscaling at a higher resolution.
3. A global chemistry transport model (GCTM) at coarse resolution but that represents distant sources of pollutants: either anthropogenic (intercontinental transport of pollution) or natural (desert dusts, volcanoes, biomass burning). Such models may be coupled with the GCM in order to capture the radiative impact of short lived trace species.
4. A regional chemistry transport model (RCTM), nested within the GCTM for the chemical boundary conditions and driven by the RCM for the meteorological forcing, refined over a given area hence offering a better understanding of local scale exposure of population and also scope for scenario analysis.

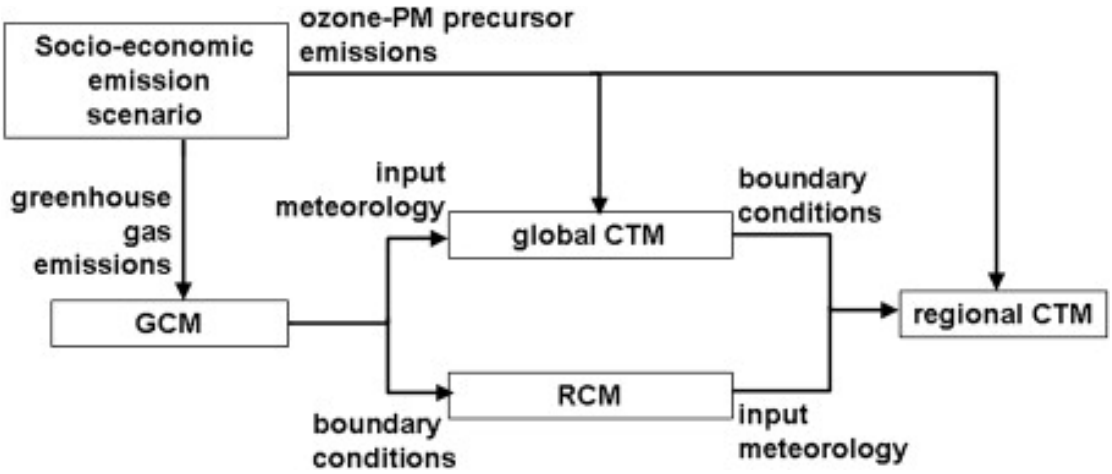

Figure 5: General flowchart of the Global / Regional coupling to simulate the Air Quality and Climate interactions (GCM: General Circulation Model, CTM: Chemical Transport Model, RCM: Regional Climate Model), source: (Jacob and Winner, 2009).

This complete suite of models and interactions is considered in Salut'AIR. And all the models, with the exception of the GCM, are specifically operated for this project. At the same time, the simulations produced in the framework of Salut'AIR will be delivered to internationally coordinated modelling experiments (ACCMIP for the GCTM, Euro-CORDEX for the RCM).

In addition to the components highlighted in Figure 5, we will also give a specific focus on vegetation emissions and landuse changes, as well as on upstream emission modelling and downstream health impact assessment and monetary valuation.

In order to keep the scope of the project within realistic boundaries, we deliberately decided to discard the whole issue of impacts of air quality on climate at the regional scale (thereby strictly following the framework of (Jacob and Winner, 2009)). Whereas many air pollutants have direct or indirect radiative properties (Forster et al., 2007) we decided to leave that topic out of our scope for the regional modelling. There are ongoing initiatives to assess such impacts on long term climate change at the global scale (Shindell et al., 2012;Young et al., 2012), but at the

regional scale, such assessments are limited to short episodes, or at best monthly or annual assessment (Jacobson et al., 2007;Péré et al., 2012;Zhang et al., 2010) while our aim in the present study is to assess multi-decadal projections.

The present report follows the chronology of Figure 5. After presenting the emission projections and investigating the associated costs in Section 2, we focus on specific sensitivity studies for individual components of the modelling chain in Section 3 (regional climate) and Section 4 (vegetation interactions). The finale regional air quality and climate model results are investigated in Section 5. The report ends with a section (6) on health impact and benefit valuation that is in turn compared to the costs of mitigation to perform a cost-benefit analysis.

1.3 Management of the project

This project running for a period of 36 months is divided into 4 parts possibly divided into sub-components (Figure 6). The first work package WP1 is dedicated to the development of "advanced" emission scenarios for Europe by 2050 in line with climate change projected for this date. A second work package WP2 (available in two sub-components) is devoted to two sources of uncertainties in the methodologies used to study the evolution of pollutant concentrations at the regional level, namely, the methodology downscaling Global to Regional (WP21) and evolution of vegetation (WP22). A third work package WP3 was dedicated to the simulations of air quality in Europe in the context of climate change and the analysis of their results, based on the scenarios used in the WP1 component. Based on the simulation results, we compute the sanitary costs due to pollution in a final work package (WP4).

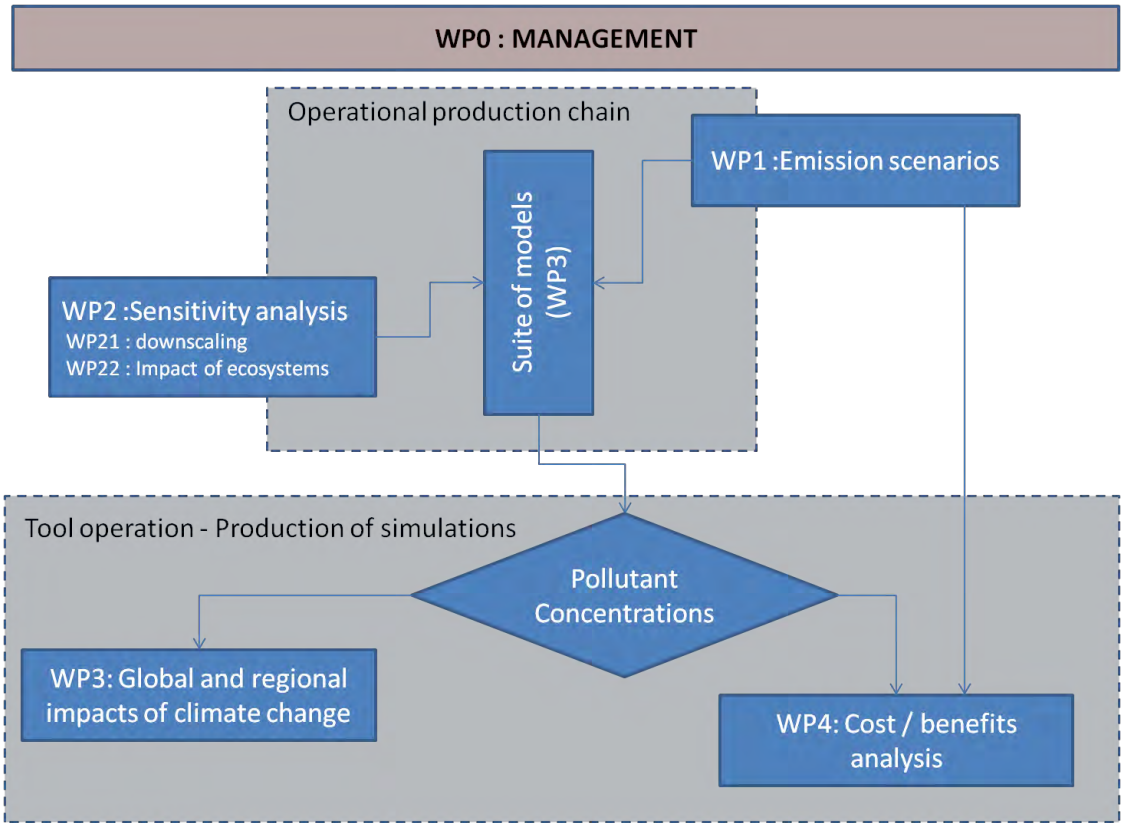

Figure 6: Project flowchart

The project was coordinated by INERIS and co-coordinated by LSCE (**WP0**). The partners are listed below with their associated tasks in the project.

Table 1: List of Partners and main tasksInstitute/Lab	Tasks
Institut National de l'Environnement Industriel et des Risques (INERIS)	-Management – WP0 -Regional modelling (air quality and meteorology) – WP3 -Regional emission inventory – WP3 -Emissions scenarios (with subcontracting : IIASA) – WP1 -Cost benefit analysis (with subcontracting : EMRC) – WP4
Laboratoire de Météorologie Dynamique (LMD) : CNRS / Ecole Polytechnique / Institut Pierre Simon Laplace (IPSL)	-Meteorological modelling (Coupling, test on nudging) – WP2 -Interactions Air quality/Ecosystems models - WP2
Laboratoire des Sciences du Climat et de l'Environnement (LSCE) : CNRS / CEA / UVSQ / IPSL	-Management – WP0 -Global modelling (atmospheric composition and climate, including provision of boundary conditions to the regional scale models) – WP3-Global emissions inventories – WP3 -Regional modelling (air quality and meteorology) – WP3 -Interactions Air quality/Ecosystems models - WP2
Laboratoire Image, Ville, Environnement (LIVE) : CNRS / Université de Strasbourg	-Expertise on global boundary conditions – WP3

Within the Salut'AIR project, INERIS also set up two collaborative projects with European experts. This is firstly, collaboration with IIASA (International Institute for Applied Systems Analysis) in Laxenburg (Austria) in order to get access to the GEA (Global Energy Assessment) emission scenarios and detailed assumptions underlying these scenarios, especially with respect to air pollution mitigation measures applied to various economic activities, and to the related emissions reductions and costs (WP1). This subcontract involved a collaboration of INERIS with two IIASA programmes, the Energy Programme (ENE) and the Mitigation of Air Pollution & Greenhouse Gases Programme (MAG). It resulted in important information for the cost assessment carried out in Salut'AIR as well as for the analysis of driving factors behind the scenario results.

Secondly, this is collaboration with the UK consultant Michael Holland (EMRC), to implement at INERIS the French version of the health impact and benefits assessment tool Alpha-RiskPoll, initially developed by Michael Holland and Joe Spadaro, and regularly used for cost-benefit analyses of European policy proposals in the air pollution domain. Implementation of this tool at INERIS was crucial for carrying out the assessment of health impacts and of health and air pollution policy co-benefits of a climate mitigation policy within Salut'air (WP4).

One of the aims of the project was to develop a full chain to simulate air quality under climate and emissions changes. Two main streams of development and analysis were undertaken: an operational production chain and a set of sensitivity and exploratory analyses.

The operational production suite of models

The main outreach of WP3 is the development and use of an operational chain (suite of fortran, shell and R routines) to simulate the air quality under climate change for different scenarios in a consistent way at both regional and global scales Figure 7. Output results were

analysed for scenarios and fed into WP4 for the cost-benefit analysis. The four institutions and laboratories worked together to reach this goal by sharing input/output files, INERIS and LMD were focussing on the regional simulations while LSCE and LIVE were more focussed on the global scale, although INERIS and LSCE also closely worked to produce the regional climate projections delivered as part of the CORDEX project. LSCE used the climate context "Coupled Model Intercomparison Project Phase 5" (CMIP5).

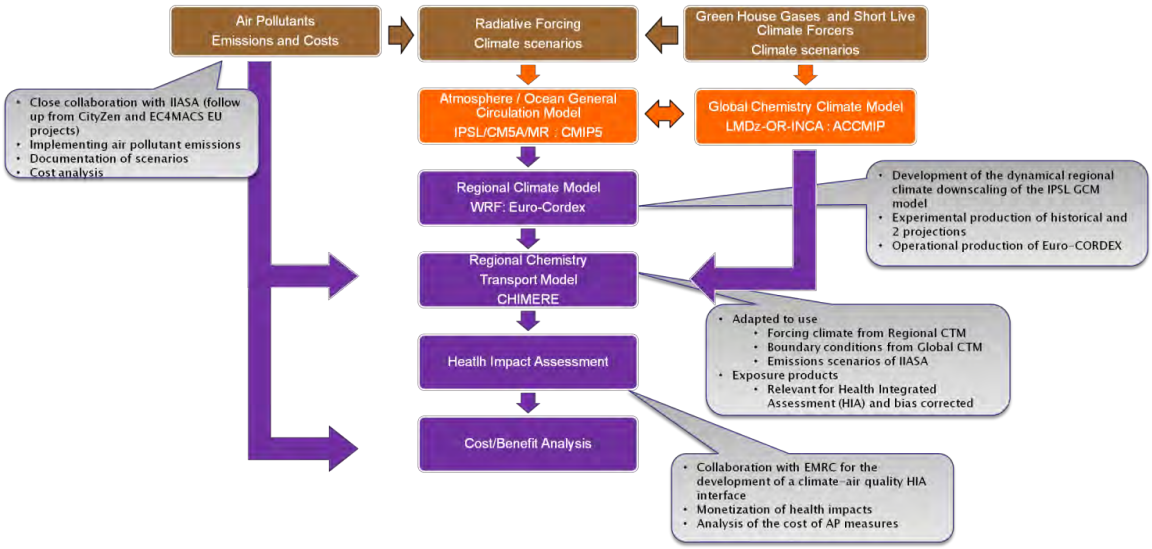

Figure 7: Architecture of the production chain in SALUT'AIR. The components that have been developed in the project are in purple.

Sensitivity and explorative analysis

The WP2 was defined to assess the climate fields and to perform sensitivity and explorative analyses. INERIS and LMD worked together in this work package to define the best nudging procedures, the most appropriate configuration parameters of the mesoscale meteorological model (in WP21). The feedback of the vegetation on air quality simulation is assessed in WP22. The main outcome of the work package WP2 was (1) to assess the influence of input data and (2) to define the configuration files of the suite of models (3) used to infer the impact air quality and ecosystems interactions in the models.

2 Prospective scenarios of air pollutant emissions

Salut'AIR uses two emission scenarios from the Global Energy Assessment (GEA[8]), an international project that was coordinated by IIASA (International Institute for Applied Systems Analysis). In the GEA, a set of four scenarios was constructed (Riahi et al., 2012), which differ with respect to levels of future air quality legislation and with respect to levels of policies towards climate change and energy efficiency, and access to energy. It is one of the stated aims of the GEA modelling exercise to identify the impact of the different scenarios in terms of air quality and human health. In this they are particularly adapted to the aims of Salut'AIR.

To some extent Salut'AIR uses information that is a direct outcome of the GEA. This includes data sets of gridded air pollutant emissions, regional (European) projections for air pollutant emissions, greenhouse gas trajectories and information on energy expenditure corresponding to the selected scenarios.

Additionally, within Salut'AIR, a collaboration project between IIASA and INERIS was set up with the aim to get access to additional and more detailed data, necessary especially for the analysis of air pollution scenarios (in this chapter) and for the cost-benefit assessment (cf. chapter 6). This concerns in particular the provision of detailed information about economic activities and the application of air pollution mitigation measures that drive and explain atmospheric emissions and air pollution mitigation costs.

For this, the link between the models MESSAGE (Model for Energy Supply Strategy Alternatives and their General Environmental Impact, (Messner and Strubegger, 1995;Riahi et al., 2007;Riahi et al., 2011)) and GAINS (Greenhouse Gas - Air Pollution Interactions and Synergies), described in section 2.1 below, had to be applied and was presented in an explicit way (cf. section 2.4). The results of this collaboration enabled the analyses and results presented in sections 2.4 to 2.6 and in Annex C.

The emission pathways produced in the Global Energy Assessment include various degrees of uncertainty sources. There is structural uncertainty of the policy options to be chosen in the future (which make them "pathways" rather than "scenarios"), but they also include modelling uncertainty (Amann et al., 2011a). Such uncertainties will be propagated to emission projections. The sources of uncertainty for this specific set of projections are discussed in (Riahi et al., 2012) and the overall Global Energy Assessment report.

2.1 General characteristics of the emission scenarios

The GEA scenarios are based on modelling by IIASA with the global energy model MESSAGE (energy system) and GAINS (air quality). Information about air pollutant inventories and air quality legislation (control options) from GAINS was linked with the MESSAGE energy scenarios until 2030 to derive sector based estimates of air pollutant emissions. The combination of the two models could however only be achieved with some assumptions with regards to the granularity of the economic activities and the energy mix. Implied emission factors that are compatible with the sector-fuel combinations in MESSAGE are derived from GAINS, and subsequently applied to the energy scenarios from MESSAGE. Computing GAINS emission factors thus requires some aggregation for application to the GEA scenarios, i.e. country-scale GAINS information (emission factors, technological and economic information, control measures, etc.) have to be aggregated to match the granularity of MESSAGE (Rafaj et al., 2010). Post 2030, MESSAGE makes additional assumptions on declines of emission factors based on income development (Riahi et al., 2011).

[8] http://www.iiasa.ac.at/web/home/research/Flagship-Projects/Global-Energy-Assessment/Home-GEA.en.html

MESSAGE distinguishes 11 world regions, amongst which Western Europe (WEU[9]) and Central & Eastern Europe (EEU[10]). The GEA emission trajectories were developed for the period from 2005 up to 2100. In the Salut'AIR project, we focus on the year 2050.

The sectoral coverage in MESSAGE includes power plants, industry (combustion and processes), domestic (residential/commercial), road transportation, international shipping and aviation, waste, agriculture (fertilizer application), agricultural waste burning, and biomass burning (deforestation, savannah burning and forest fires).

The following greenhouse gases and air pollutants are included in the scenarios, of which all but CO_2 were gridded based on methodology described in (Riahi et al., 2011): CO_2, CH_4, SO_2, NOx, CO, VOCs, BC, OC & $PM_{2.5}$.

In all scenario variants, global population is assumed to increase to 9.2 billion inhabitants in 2050. The European population is expected to amount to 623 million in 2050, following a stabilization phase after 2030 and a decline after 2040[11]. For the period from 2005 to 2050 the scenarios assume an annual average GDP growth rate of 2.8% for the world and of 1.6% for Europe (Colette et al., 2012b).

For the Salut'air project we chose two amongst the four GEA emission scenarios: the scenario called CLE1 which represents the reference situation for energy and climate policy, and the scenario named CLE2, describing the mitigation energy and climate policy. The major policy assumptions behind theses two GEA scenarios are summarized in Table 2.

Table 2 : Assumptions behind the GEA scenarios CLE1 (reference) and CLE2 (mitigation). Source: (Riahi et al., 2012).

<table>
<tr><th colspan="2" rowspan="2">Scenarios</th><th colspan="4">Policies</th><th rowspan="2">Climate context</th></tr>
<tr><th>Air pollution</th><th>Climate change</th><th>Energy efficiency</th><th>Energy access</th></tr>
<tr><td>CLE1</td><td>Reference case (climate policy) with current air pollution legislation (CLE)</td><td rowspan="2">All current and planned air quality legislations implemented by 2030; further improvement of emission factors with economic growth after 2030</td><td>No climate change policy</td><td>Annual energy intensity reduction of 1.5% until 2050</td><td>No specific energy access policy; medium improvement in quality of cooking fuels</td><td>RCP8.5</td></tr>
<tr><td>CLE2</td><td>Sustainable policy with current air pollution legislation</td><td>Limit on temperature change to 2°C in 2100</td><td>Annual energy intensity reduction of 2.6% until 2050</td><td>Policies to ensure global access to clean energy by 2060</td><td>RCP2.6</td></tr>
</table>

These two scenarios (Rao, 2013) make equal assumptions about policies and measures assumed for air pollution control: the application of current legislation by 2030 (cf.Table 3) and improvements of emission factors occurring with technology improvements, as well as a convergence of emission factors across regions as welfare increases (environmental Kuznets curve theory) in later years[12]. The scenarios differ however in their assumptions about policies towards climate change. Whereas the reference scenario assumes no climate policy at all, the mitigation scenario assumes policies leading to a stabilisation of global warming (2°C target) in 2100. In

[9] Western Europe (Andorra, Austria, Azores, Belgium, Canary Islands, Channel Islands, Cyprus, Denmark, Faeroe Islands, Finland, France, Germany, Gibraltar, Greece, Greenland, Iceland, Ireland, Isle of Man, Italy, Liechtenstein, Luxembourg, Madeira, Malta, Monaco, Netherlands, Norway, Portugal, Spain, Sweden, Switzerland, Turkey, United Kingdom).

[10] Central and Eastern Europe (Albania, Bosnia and Herzegovina, Bulgaria, Croatia, Czech Republic, Estonia, The former Yugoslav Rep. of Macedonia, Latvia, Lithuania, Hungary, Poland, Romania, Slovak Republic, Slovenia, Yugoslavia).

[11] The reference for the population data in GEA is UN, 2009, World Population Prospects: The 2008 Revision. United Nations, Department of Economic and Social Affairs, Population Division, New York.

[12] Air pollutant emission reductions in GEA after 2030 are due to changes in total energy use or changes in the energy mix and to assumed improvements in emission reduction technologies.

terms of global radiative forcing, CLE1 is coherent with the RCP8.5[13], and CLE2 with the RCP2.6 (cf. also Section 2.3).

Table 3 : Specific Policies and Measures for Air Pollution Control in the CLE Scenarios. Source: (Riahi et al., 2012).

	Transportation	Industry and power plants	International shipping	Other
SO_2	OECD: directives on the sulphur content in liquid fuels Non-OECD: national legislation on the sulphur content in liquid fuels	OECD: emission standards for new plants from the Large Combustion Plant Directive (LCPD, OJ 1988) Non-OECD: increased use of low sulphur coal, increasing penetration of flue gas desulphurisation (FGD) after 2005 in new and existing plants	MARPOL Annex VI regulations	Reduction in gas flaring, reduction in agricultural waste burning
NOx	OECD: emission controls for vehicles and off-road sources up to the Euro-VI and Euro-V standard Non-OECD: national emission standards equivalent to approximately Euro III-IV standards (vary by region)	OECD: Emission standards for new plants and emission ceilings for existing plants from the LCPD (OJ 1988); national emission standards if stricter than in the LCPD Non-OECD: primary measures for controlling of NOx	Revised MARPOL Annex VI regulations	Reduction in gas flaring, reduction in agricultural waste burning
CO	As above for NOx			Reduction in gas flaring, reduction in agricultural waste burning
VOC	End-of-pipe measures as described above for NOx	Solvent Directive of the EU (COM(96), 538, 1997); 1999 UNECE Gothenburg Protocol to Abate Acidification, Eutrophication and Ground-level Ozone		Reduction in gas flaring, reduction in agricultural waste burning
NH_3		End of pipe controls in industry (fertilizer manufacturing)		Substitution of urea fertilizers
$PM_{2.5}$*		EU and national legislation on power plants and industrial sources limiting stack concentrations of PM		Reduction in gas flaring, reduction in agricultural waste burning
*: Legislation is for PM2.5 only, but black carbon and organic carbon emissions can be expected also to decline as a result.				

2.2 Energy related characteristics of the scenarios

The two energy trajectories underlying the scenarios CLE1 and CLE2 are fundamentally different. Compared to the reference scenario, the mitigation scenario is characterised by a distinctly lower energy demand due to energy efficiency improvements and shifts in the energy mix (less coal/oil and more renewables).

Global energy demand increases until 2100 across all GEA scenarios, although in the climate mitigation scenarios demand growth is very limited and almost stable by the end of the century.

[13] RCP designates the "Representative Concentration Pathways" developed for the IPCC (Intergovernmental Panel on Climate Change) fifth assessment report (AR5).

For specific regions, however, demand declines in the mitigation scenario because of the much larger emission intensity improvements compared to the rest of the world. For Europe this is the case from 2010 onwards.

2.2.1 Evolution of energy consumption and electricity production

Figure 8 illustrates on an aggregate level (all sectors, sum over WEU and EEU) the evolution of primary[14] and final energy[15] consumption as well as of electricity generation in Europe under the two scenarios. The important decrease in energy demand in the mitigation scenario relative to the reference scenario is mirrored in distinctly lower energy consumption and electricity production in the mitigation case.

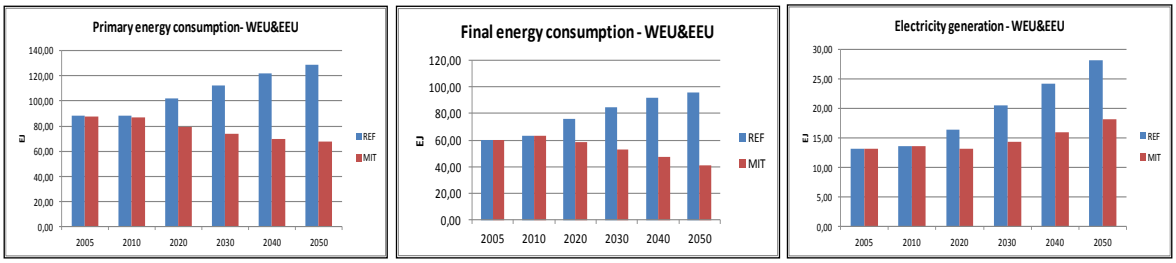

Figure 8: Evolution of primary (left) and final energy consumption (middle) and of electricity generation (right), (in EJ = Exa Joules) by scenario

Figure 9 illustrates for primary energy consumption the considerable shifts in the energy mix when moving from CLE1 to CLE2. Coal is almost phased-out by 2050 under the mitigation scenario, the amount of oil almost divided by 4 and the consumption of gas halved. Biomass, wind, solar and geothermal energy show increases. Nuclear energy consumption is phased out in 2050.

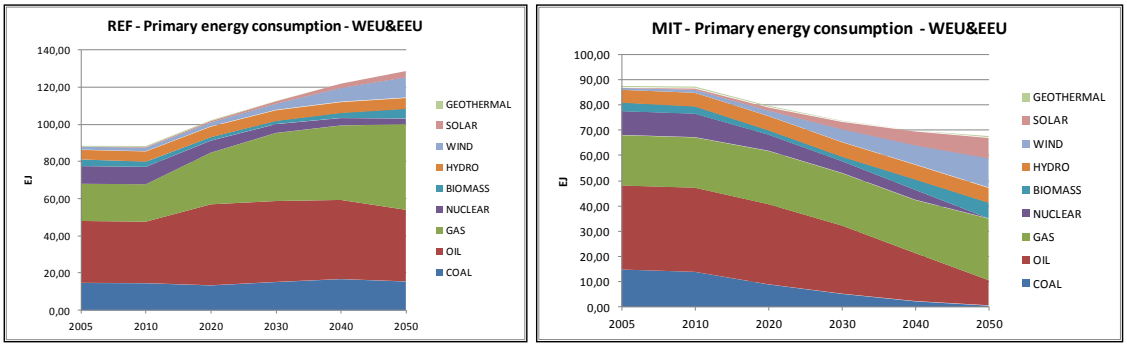

Figure 9: Primary energy consumption (in EJ) by fuel type and scenario

Figure 10 describes the share of different sectors in overall final energy consumption. Instead of increases between 2005 and 2050 in the energy consumption by all sectors under the reference scenario, energy consumption in the mitigation scenario decreases in the transportation and the residential and commercial sector, and remains largely stable in industry. When moving from CLE1 to CLE2, final energy consumption of the residential and commercial sector and of the transportation sector are divided by three in 2050, consumption of industry is halved.

[14] Primary energy consumption refers to the direct use at the source, or supply to users without transformation, of crude energy, that is, energy that has not been subjected to any conversion or transformation process (UN, 1997).

[15] The total energy consumed by end users, such as households, industry and agriculture. It is the energy which reaches the final consumer's door and excludes that which is used by the energy sector itself (http://epp.eurostat.ec.europa.eu/statistics_explained).

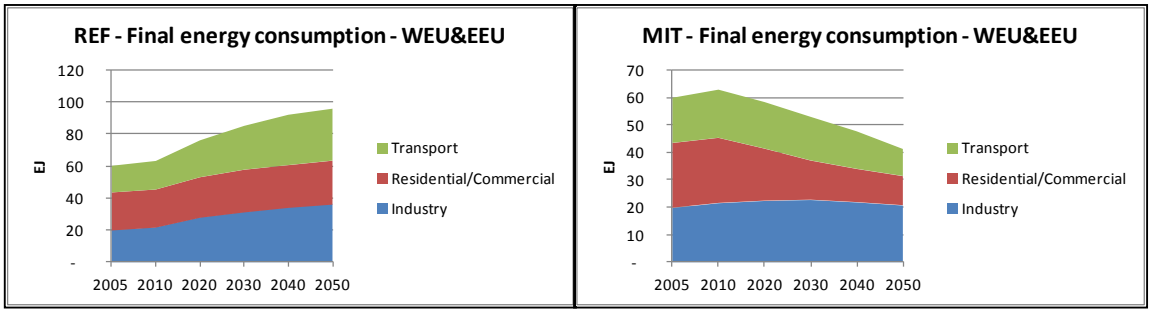

Figure 10: Final energy consumption (in EJ) by sector and scenario

Table 4 then shows the evolution in the energy mix between the two scenarios for the same final energy demand sectors. Concerning the evolution of the energy mix in 2050 when moving from the reference to the mitigation scenario, in industry, consumption of all fuels decrease, except for on-site solar. In the residential and commercial sector the high demand reduction leads to a decrease in the consumption of all fuels, with a phase-out of solid fuels which occurs around 2020. In the transportation sector, finally, consumption of liquid fuels is almost divided by 5 in 2050, while the share of electricity use (referred to as "grids" in the table) increases between the reference and the mitigation scenario.

Table 4 : Final energy consumption (in EJ) in the different sectors by fuel type and scenario

WEU & EEU		2005		2050	
Final energy consumption, in EJ		REF	MIT	REF	MIT
Industry	Solids (Biomass and Coal)	2,6	2,6	14,3	5,0
	Liquids	6,6	6,6	8,9	4,8
	Grids	10,6	10,6	12,7	9,6
	On Site Solar	0,0	0,0	0,0	1,3
Residential/commercial	Solids (Biomass and Coal)	2,3	2,3	0,1	0,0
	Liquids	4,7	4,7	1,1	0,4
	Grids	16,8	16,8	23,4	9,5
	On Site Solar	0,0	0,0	2,9	0,7
Transport	Solids (Biomass and Coal)	0,0	0,0	0,0	0,0
	Liquids	16,3	16,3	30,7	6,6
	Grids	0,3	0,3	1,6	3,3

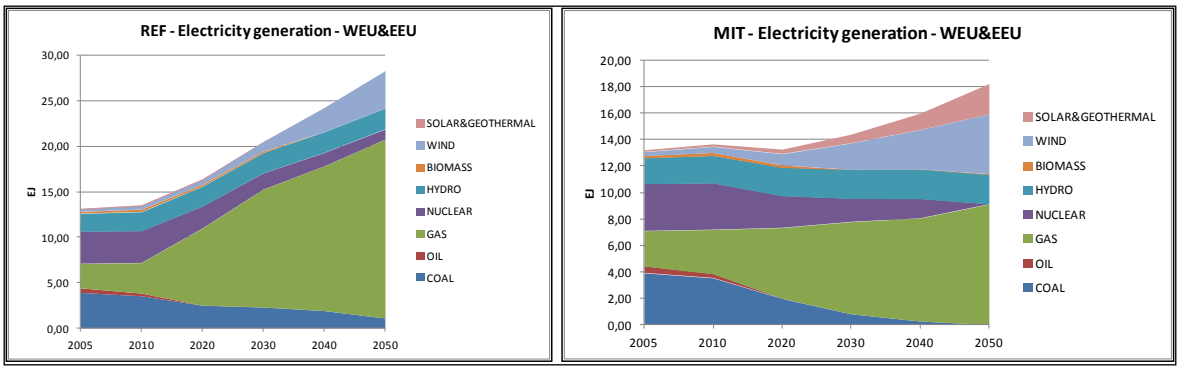

Figure 11: Electricity generation by energy source and scenario

While electricity generation from liquid fossil fuels is phased-out by 2030 under both scenarios (Figure 11), coal use and nuclear based electricity generation continue on a low level in the reference scenario while they are phased out in the mitigation scenario. When switching from CLE1 to CLE2, gas based electricity generation is halved in 2050 while the share of the renewable energy sources increases.

2.3 Greenhouse gas related characteristics of the scenarios

Projections of greenhouse gas emissions in the GEA scenarios are developed with the global energy model MESSAGE. Table 5 illustrates CO_2 emission projections for the reference and the mitigation scenarios. Contrary to the reference scenario, under which emissions are assumed to increase continuously over the period investigated, under the mitigation scenario emissions decrease after 2010. CO_2 emissions in 2050 are reduced by around 75% when moving from the reference scenario to the mitigation scenario[16].

Table 5: CO2 emissions in Mt/year per scenario, all sectors, WEU & EEU

in Mt/year	CO_2 emissions in WEU & EEU					
Scenarios	**2005**	**2010**	**2020**	**2030**	**2040**	**2050**
REF	4 930	5 119	6 194	6 849	7 224	7 234
MIT	4 930	5 072	4 494	3 686	2 695	1 764

2.4 Air pollution related characteristics of the scenarios

To some extent, emissions of airborne pollutants in the GEA scenarios were modelled based on detailed information about air quality legislation, control options and related emission factors from the GAINS model for various pollutants and a number of fuel-sector-technology combinations. This holds for the sectors, economic activities and pollutants for which MESSAGE and GAINS were linked, via the consumption of energy, in the construction of the GEA scenarios. The activities for which the link between GAINS and MESSAGE was made are in the following referred to under the aggregates “power plants” (PPL), “industry” (IND), “ground transportation” (GRT) and “residential and commercial sector” (RES), and for 3 pollutants, SO_2, NOx and $PM_{2.5}$.[17]. However, MESSAGE and GAINS were not linked for all activities falling under these four sectors. Exceptions are, for example, extraction and mining activities, gas flaring and industrial processes in industry.

MESSAGE is not linked to GAINS for non-energy sectors. GEA thus used other sources than GAINS to determine emission factors for these sectors and activities, and their emissions were modelled in GEA independently of the GAINS model.

In order to obtain information as detailed as possible about the drivers of air pollution emissions (and related abatement costs) for Salut’AIR, INERIS sub-contracted with IIASA to understand in more detail the more aggregated detail in MESSAGE by looking closer at the underlying control technologies from GAINS. In the development of the GEA emission projections, detailed emission factors from GAINS, applicable to specific economic activities, fuels and abatement measures were aggregated to match the granularity of MESSAGE sector and fuel categories and then applied to the respective energy projections from MESSAGE (cf. Section 2.1). For the purposes of Salut’AIR, more disaggregated information from GAINS was provided, showing more detail for the energy and emission projections and identifying at the same time the abatement technology mix assumed to be applied in each scenario.

This work resulted in an estimate for emissions and costs for the pollutants SO_2, NOX and $PM_{2.5}$ and the 4 sectors listed above. It was performed for two years: for 2030 for which GAINS emission factors were used in MESSAGE, and for 2050, for which MESSAGE assumes a further improvement in emission factors based on assumption of continuing legislation with income growth, while in

[16] A direct comparison between the CO_2 trajectory of the GEA mitigation scenario for Europe and that of the RCP 2.6 (Colette et al., 2012) showed that their regional profiles differ. However, the two are similar in terms of their global climate response.

[17] GAINS and MESSAGE are also linked for CO and VOCs but the detailed hypotheses were not made available to the Salut’AIR assessment.

GAINS emission factors are kept fixed after 2030. For 2050, the matching of MESSAGE energy scenarios with GAINS for Salut'AIR purposes hence consists in the application of GAINS controls as available in 2030 applied to the MESSAGE energy structure in 2050. This is a first reason for why the inverse match is not perfect. A second reason is that MESSAGE also includes technological shifts that cannot directly be captured by this link. Examples are technology shifts to integrated gasification combined cycles (IGCC) in the power sector or biomass gasifiers in industry, which are modelled in MESSAGE and which often become active post 2030, especially in the climate mitigation runs. These technologies have relatively low emissions associated with them, but assumptions on emissions are based on available estimates other than from GAINS, and such technological shifts are not captured by the link (personal communication with IIASA). Nevertheless, the scenarios are very detailed with respect to pollution control and represent the first long-term scenarios available from integrated assessment modelling that have such a high level of detail. They provide useful information on activity levels, abatement measures applied and atmospheric emissions emitted at a detailed sectoral level.

To sum up this discussion, the different modelling levels (MESSAGE only versus MESSAGE-GAINS link) imply that:

- For sectors and pollutants for which the link between GAINS and MESSAGE was made, detailed information on various air pollution mitigation measures and their impacts on emission reductions (and on costs, cf. section 2.4) are available.
- For sectors or specific activities for which MESSAGE is not linked to GAINS, no detailed information is available on emission reduction measures (and on their costs). The emissions of these activities, however, are estimated in MESSAGE and used in the air quality assessment presented in this report.
- We have detailed information on the drivers of air pollution emissions (in terms of changes in energy use and mitigation measures applied) only for the share of overall GEA emissions that is explained via the link between GAINS and MESSAGE. In 2050, this link explains a bit more than 70% (about 65%) of overall atmospheric emissions of NOx in CLE1 (CLE2), about 90% (65%) of SO_2 in CLE1 (CLE2), and about 60% (50%) of $PM_{2.5}$ in CLE1 (CLE2).

2.4.1 Development of total GEA air pollutant emissions

Figure 12 illustrates the overall airborne emissions in the two GEA scenarios (those based on assumptions about emission factors coming from GAINS and those estimated based on further hypotheses). It highlights that while the implementation of current legislation (and further improvements of emission factors with economic growth after 2030) leads to important emission reductions especially for NOx, SO_2 and VOCs by 2050 in the reference scenario (continuous lines), emission levels are even lower under the mitigation scenario (dashed lines). These further emission reductions represent co-benefits of the ambitious climate policy (as regulations concerning air pollutants are the same in both scenarios). Co-benefits are highest for SO2 and NOx, and lowest for $PM_{2.5}$.

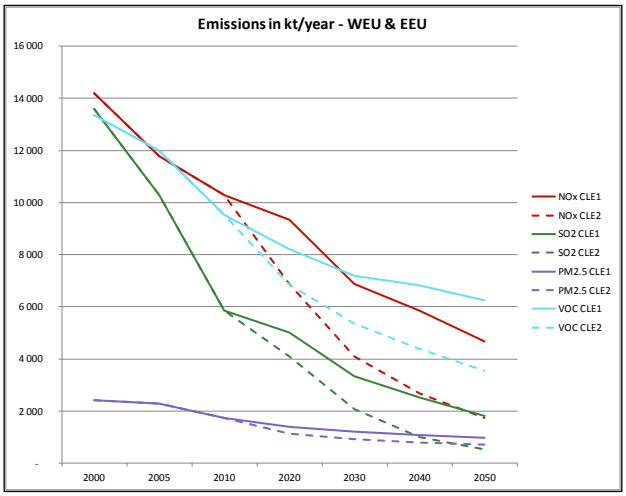

Figure 12: Emissions of atmospheric pollutants in kt/year per scenario, all sectors

2.4.2 Air pollutant emissions determined via a link between GAINS and MESSAGE

The following two tables show detailed assumptions on the emissions of NOx and $PM_{2.5}$ in the sectors power plants (PPL), industry (IND), ground transportation (GRT) and residential and commercial sector (RES) for which GAINS provided emission factors for the GEA assessment and for which the detailed assumptions were made available to the Salut'AIR assessment. This information was provided thanks to the collaboration with IIASA. Annex C presents a complementary table for SO_2 emissions as well as tables that indicate the changes between the two scenarios CLE1 and CLE2.

Table 6 shows for the part of the NOx emissions (in kt/year in 2050) that is determined via GAINS its distribution between different sectors and European sub-regions for the two scenarios. The total of the four sectors and Europe overall is also given. The data are provided for each scenario, CLE1 (reference climate scenario) and CLE2 (climate mitigation scenario). In line with Figure 12 above, emissions in CLE2 are significantly lower than in CLE1. These changes are brought about by the more ambitious climate and energy policy underlying the scenario CLE2. Table 7 presents the same information for $PM_{2.5}$ emissions.

Table 6: NOx emissions in kt/year in 2050 for the scenarios CLE1 and CLE2

in kt/year in 2050	Scenarios	Nox emissions		
		WEU	EEU	WEU & EEU
PPL	CLE-1	535	170	706
	CLE-2	228	32	260
IND	CLE-1	604	121	725
	CLE-2	329	49	378
GRT	CLE-1	1 376	347	1 724
	CLE-2	289	77	366
RES	CLE-1	204	58	262
	CLE-2	68	23	91
Sum 4 sectors	CLE-1	2 720	697	3 416
	CLE-2	914	181	1 094

The major reductions of NOx emissions when moving from CLE1 to CLE2 occur in the sectors ground transportation followed by power plants and then by industry. Changes in these sectors explain over 90% of the overall reduction in NOx emissions. WEU alone accounts for over 72% of these.

Table 7: $PM_{2.5}$ emissions in kt/year in 2050 for the scenarios CLE1 and CLE2

in kt/year in 2050	Scenarios	$PM_{2.5}$ emissions		
		WEU	EEU	WEU & EEU
PPL	CLE-1	5	26	31
	CLE-2	2	1	2
IND	CLE-1	288	105	393
	CLE-2	221	96	318
GRT	CLE-1	106	16	122
	CLE-2	22	3	26
RES	CLE-1	12	1	13
	CLE-2	4	0	4
Sum 4 sectors	CLE-1	411	148	559
	CLE-2	249	101	350

The emission reductions in $PM_{2.5}$ between CLE1 and CLE2 are mainly driven by changes in the industrial and ground transportation sectors in WEU and by the power plant sector in EEU. Together these sectors explain over 80% of the reduction. Emission reductions of SO_2 between CLE1 and CLE2 are most important in the power plant and industrial sectors and this in both regions (cf. Annex C). These explain over 90% of the overall reductions in SO_2.

For the sectors and regions contributing the most to the observed emission reductions, the drivers are summarized in Section 2.6 and presented in more detail in Annex C.

2.5 Cost related characteristics of the scenarios

Energy expenditure for the GEA scenarios was determined by the energy model MESSAGE. Energy expenditure comprises both application of emission mitigation technologies and investment in the energy system itself (such as modification of processes to increase efficiency or the construction of new power plants). Air pollution mitigation costs are the costs assumed for individual technical emission reduction measures as assumed in GAINS. They were determined via the link that was established for some sectors and activities between the models GAINS and MESSAGE (cf. section 2.3). For the sectors and activities for which the two models were not linked, no air pollution mitigation costs are available, i.e. air pollution mitigation costs in GEA are limited to those provided via the link of the two models MESSAGE and GAINS[18]. For the air pollution mitigation costs available in the GEA scenarios, IIASA provided us with detailed information on the drivers (in terms of changes in energy use and mitigation measures applied) of changes when switching from the scenario CLE1 to the scenario CLE2.

2.5.1 Energy expenditure derived via MESSAGE

Energy expenditure is available at an aggregated level (Table 8). illustrates the difference in annual energy expenditure in 2050 between the reference and the mitigation scenario for Europe and its two sub-regions.

Table 8: Energy expenditure by sub-region and scenario in 2050

Energy expenditures in M€2005/year in 2050			
	WEU	EEU	WEU & EEU
CLE 1 (REF)	303 212	57 981	361 193
CLE 2 (MIT)	386 245	82 324	468 569

Energy expenditure in Europe in 2050, expressed in million €/year (price base 2005), is almost 30% higher in the mitigation scenario than it is under the reference scenario. This is due to

[18] It is worth noting that VOC costs in the energy sector are small, and that CO costs are indirectly related to NOx and therefore indirectly accounted for.

additional demand side investments[19] in the mitigation scenario (which explain the lower energy demand), while supply side[20] costs are lower. The additional costs in 2050 in CLE2 relative to CLE1 can be considered as climate mitigation costs.

2.5.2 Air pollution mitigation costs determined via a link between GAINS and MESSAGE

The following table presents the air pollution mitigation costs assumed in the GEA scenarios in 2050 that were determined through the link between the models GAINS and MESSAGE for NOx, SO_2 and $PM_{2.5}$. As noted before, they represent the costs for mitigation measures that respect current legislation from 2030 onwards and an estimate of the costs for further improvements in emission factors that occur between 2030 and 2050 and are induced by economic growth.

Table 9 indicates the annual costs, in million €/year (price base 2005) in 2050, for the sum over the three air pollutants by sector and sub-region and for the respective aggregates. The data are provided for CLE1 and CLE2. Tables providing corresponding cost data for each pollutant individually, as well as tables indicating the changes between the two scenarios, are given in Annex C.

Table 9 shows that overall air pollution mitigation costs are significantly lower in CLE2 than in CLE1. These cost savings are brought about by the more ambitious climate and energy policy underlying the scenario CLE2. Measures taken to mitigate climate change in fact imply that due to changes in the energy system, shifts in the fuel mix and the general energy demand reduction, less air pollution mitigation measures are necessary to comply with emission limits defined under current legislation. The relative savings in air pollution mitigation expenditure when going from CLE1 to CLE2 thus represent tangible economic co-benefits of the ambitious climate policy. The same results hold for the costs that can be attributed to the reduction of each of the pollutants individually (cf. Annex C).

Changes in three sectors, power plants, industry and ground transportation, and in both regions, WEU and EEU, contribute in an important way to the overall reduction in air pollution mitigation costs when moving from CLE1 to CLE2 (Table 9). These sectors account for approximately 97% of the overall cost reduction.

Table 9: Overall air pollution mitigation costs in million €/year in 2050 for the scenarios CLE1 and CLE2

in million EUR 2005/year	Emission reduction costs (SO2, PM2.5 & NOx)			
	Scenarios	WEU	EEU	WEU & EEU
PPL	CLE-1	6 998	3 731	10 729
	CLE-2	3 053	674	3 726
IND	CLE-1	12 150	3 121	15 271
	CLE-2	2 054	219	2 273
GRT	CLE-1	21 995	4 437	26 432
	CLE-2	4 614	1 021	5 635
RES	CLE-1	1 512	112	1 624
	CLE-2	500	46	546
Sum 4 sectors	CLE-1	42 656	11 401	54 057
	CLE-2	10 222	1 959	12 181

[19] Demand side investment refers to investment in equipment, vehicles etc. which make up for the final consumption of energy. This is often investment to increase the efficiency of energy use.
[20] Supply side refers to the production of energy and electricity.

The corresponding findings for mitigation costs of individual pollutants, for which tables are presented in Annex C, are:

- SO_2: the same sectors - with the exception of the power plant sector in WEU - drive cost reductions and explain about 98 % of these when moving from CLE1 to CLE2.
- NOx: cost reductions are also largely explained by changes in the sectors power plants, industry and ground transportation. It should be noted however, that WEU on its own accounts for almost 80% of the cost reduction when moving from CLE1 to CLE2.
- $PM_{2.5}$: the sectors power plants, industry and ground transportation are also characterised by the major reductions in air pollution mitigation costs for this pollutant when moving from CLE1 to CLE2. Both regions contribute significantly to these reductions, with the exception of the power plant sector in WEU which has a relatively low impact on overall cost reductions.

Drivers behind the observed cost reductions are summarized in Section 2.6 and presented in more detail in Annex C.

2.5.3 Aggregate climate and air pollution mitigation costs

Figure 13 presents energy expenditure next to air pollution mitigation costs. It illustrates the overall cost development when moving from CLE1 to CLE2. These costs are used in the cost-benefit analysis in chapter 6.

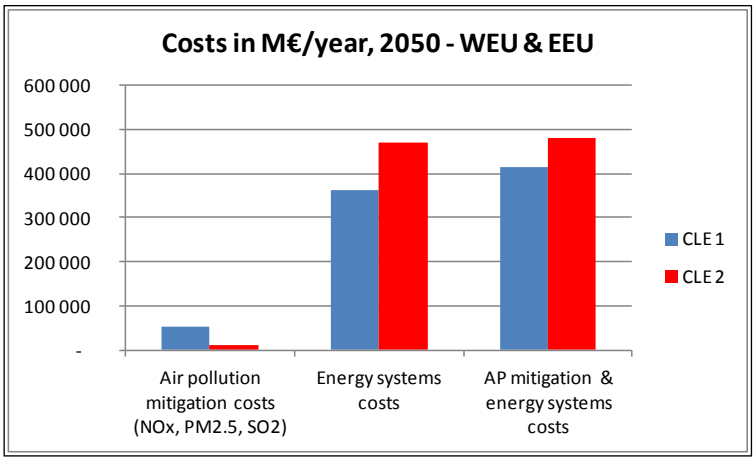

Figure 13: Energy/climate and air pollution mitigation expenditure (in M (2005)€/year) by scenario in 2050

The bars in the middle recall the energy expenditure presented in Table 8 above. Air pollution costs from Table 9 are represented in the left hand side bars and show the co-benefits in terms of cost savings that arise when moving from the reference to the mitigation climate scenario. Air pollution mitigation costs are approximately 78% lower under CLE2 than under CLE1. The bars on the right hand side of the graph indicate that the net cost increase (sum over the reduction in air pollution mitigation costs and the increase in energy expenditure) between the two scenarios is approximately 15%.

2.6 Drivers of air pollutant emission and cost reductions when moving from CLE1 to CLE2

The sectors most important in the observed emission and cost reductions are power plants, industry and ground transportation. For these, examples of the developments explaining the observed trends in emissions and costs are presented here. These drivers are presented in more detail in Annex C.

The important reduction in energy use when moving from the reference to the mitigation climate scenario is clearly the major driver behind the emission and cost reductions.

- This holds for example for emission and/or cost reductions in the power plant sector, explained by the phase-out of coal in the EEU or the reduction in the activity of biomass heating plants and oil refineries, especially in WEU.

Partly emissions and costs are also strongly affected by shifts between different plant types.

- An example in the power plant sector is an important decrease in the activity of gas combined cycle plants and a shift of parts of this activity to combined cycle gas plants equipped with CCS (carbon capture and storage). The reductions in emissions and costs from the former over-compensate additional emissions and costs that come from increased activity of the latter.

Reductions in activity combined with shifts between different fuel types sometimes permit to use more advanced technology while reducing costs overall, or to apply less effective abatement technologies, while still meeting the requirements of current legislation.

- In the industry sector, for example, reductions in NOx emission and related abatement costs are mainly explained by the net effect of a strong decrease in the use of coal and an increase in the use of biomass and gas. The cost increase for additional application of combustion modification and selective catalytic reduction (SCR) on solid fuel fired industrial boilers and furnaces using biomass to reduce NOx emissions is low compared to the decrease in costs brought about by the declining share of coal capacity for which comparable measures are applied. Coal and biomass combustion also determine changes in $PM_{2.5}$ emissions from industry and related costs (in WEU). The emission reductions from reduced coal use are higher than the emission increases due to increased use of biomass. Increases in costs to control emissions from the higher biomass use are low compared to the cost savings attained through reduced coal use. And concerning SO_2 emissions (in EEU) the phase-out of coal and the increase in biofuel use are combined with a limited use of flue gases desulphurisation (FGD) in the mitigation scenario and with more capacities remaining uncontrolled. As a result, the increased biofuel use does not increase costs in this region.
- The transportation sector also shows examples for more advanced technology being applied at lower cost overall when moving from CLE1 to CLE2. In EEU, for example, activity reductions from light duty vehicles (LDV) and heavy duty vehicles (HDV) imply cost reductions that are higher than the relative increase in costs that comes from a trend to more recent Euro standards for diesel vehicles.

A final note on the residential and commercial sector appears useful. As mentioned in previous sections, the contribution of changes that take place in this sector when moving from CLE1 to CLE2 are less important in overall emission and cost reductions than those of the sectors discussed above. This does not imply that no important changes take place in this sector over time. However, in the comparison in 2050 between the two scenarios they are not that important. This is partly due to the fact that no biomass use is assumed in the scenarios in 2050. In fact, as established in direct communication with IIASA, direct use of biomass in the residential sector in WEU and EEU is still significant in 2010 and 2020 but zero by 2030. The scenario moves the biomass to biofuels production and increases the district heating capacity in WEU and EEU. So biofuels use increases in the transportation but also in the residential sector in the longer term while district heating and grid based systems become important in the medium term[21].

As a further reason, major energy use by the residential and commercial sector is actually electricity (cf. Table 4 in section 2.2), which does not lead to emissions of air pollutants in this sector and therefore does not require abatement measures. The related emissions will occur in

[21] For developing countries however biomass continues to be used as a direct fuel in the residential sector up to 2060 and even beyond.

the electricity production sector and the necessary investment is energy related, and thus included in the energy costs.

3 Sensitivity analyses: regional climate downscaling

3.1 Introduction

Global Climate Models (GCM) are designed to capture the sensitivity of the global climate to changes in natural and anthropogenic forcing. Their fairly low resolution does not allow for the detailed simulation of local atmospheric processes. And their main focus being the global energy balance, coupled models may exhibit significant regional biases in important variables such as temperature or precipitation. Climate risk assessment tools require horizontal resolution of the order of half a degree or below. In addition impact models (e.g., with regards to food safety, energy, water, or here air pollution) are tuned and validated for the current climate, their validity on the basis of coarse, and sometimes biased, global climate models, should be demonstrated.

Alternatives technique to refine and correct GCM outputs can be divided into two broad types of approaches: statistical or dynamical downscaling.

- Statistical downscaling builds upon a prior knowledge of statistical relationships between the GCM and observational data. Statistical models representing those relationships are then applied over future time periods, without involving any additional physical modelling in addition to the GCM(Maraun et al., 2010;Semenov et al., 1998;Vrac et al., 2007;Wilks and Wilby, 1999).
- To downscale a global model in a dynamical way, one implements a Regional Climate Model (RCM) forced by the global fields at the boundaries (Giorgi et al., 2009;Laprise, 2008). Similarly to the GCM, the RCM provides a comprehensive physically-consistent representation of the climate system.

In short, the strength of statistical downscaling is that it is better tuned to observations. Its weakness is that its outcome lacks physical consistency. Dynamical downscaling offers this physical consistency but it is weakly constrained and can exhibit biases. Given the ultimate goal of Salut'AIR to produce regional air quality projections, physically consistent 3D atmospheric fields are required to drive the regional atmospheric chemistry model. Therefore, the choice of a dynamical downscaling approach is straightforward. However, potential biases must be carefully documented and reduced if possible.

In this section we introduce the downscaling model used (Section 3.2), how it was setup (Section 3.3 and 3.4) and evaluated (3.5), and we explore potential techniques to reduce its bias when used in a climate mode (3.6).

3.2 The Weather Research and Forecast Model

The regional model used in this study is the Weather Research and Forecasting (WRF) model (Skamarock et al., 2008) in its non-hydrostatic configuration. WRF is one of the more established mesoscale meteorological models worldwide. Although it was primarily designed for short to medium term application, the recent evolution of computing resources now allows for its implementation as a regional climate model, a field that was limited only 5 years ago to hydrostatic models.

One of the main assets of the WRF model, thanks to its large community of users and developers is the very wide range of possible setups, based on a variety of physical, dynamical, microphysical and numerical configurations. The related drawback is that it requires a careful setup for each application. In the following paragraph we summarise the choices made within the projects.

3.3 Towards an optimal physical configuration of WRF

The Salut'AIR project provided for a unique opportunity to invest in the definition of an optimal setting of WRF. While regional air quality forecasting relied on mesoscale models to obtain meteorological forcing fields (the MM5 model has been widely used over the years 2000's in conjunction with CHIMERE), the gradual increase of resolution of global forecast is such that the forecasting community switched directly from MM5 to global models (such as the IFS model of ECMWF) that now deliver assimilated worldwide fields at almost 10km of resolution.

Today, mesoscale models such as WRF are being used either for very high resolution (which is not the purpose here), or regional climate modelling for which we – still – need to downscale global climate models whose resolution (of the order of 2-3degrees) is not suitable for regional studies. That is why we revisited the definition of an optimal setup of WRF for this specific context.

The various possible physical configurations of WRF were explored using case studies of the order of a couple of weeks, for which the scores of the model against observations were computed to derive empirically an optimal configuration. Winter and summer time pollution episodes were targeted, and besides sole performances of WRF in reproducing observed meteorological variables, the subsequent performances of CHIMERE, driven by each of these WRF configuration was also tested. Such an analysis was already introduced in the Salut'AIR Progress report of 2011.

The details of this activity are provided in Annex D. The optimal configuration is summarized below, the references for specific parameterizations can be found in the general description of WRF (Skamarock et al., 2008).

- For the microphysics, the WRF Single Moment-5 class scheme is used allowing for mixed phase processes and super cooled water.
- The radiation scheme is RRTMG scheme with the MCICA method of random cloud overlap.
- The cumulus parameterization uses the ensemble scheme of Grell.
- The surface layer scheme is based on Monin-Obukhov with Carslon-Boland viscous sub-layer.
- The surface physics is calculated using the Noah Land Surface Model scheme with four soil temperature and moisture layers.
- The planetary boundary layer physics is processed using the Yonsei University scheme.

3.4 Relaxation of the regional model (nudging)

Because of the very nature of atmospheric dynamics, the regional mesoscale model shall diverge from the large scale forcing fields, even when it is forced at the boundaries. That is why a relaxation in the inner part of the simulation is sometimes used.

The empirical approach of testing various configurations and evaluating the performances of the model against observations was also explored to investigate the importance of nudging (see annex D). This method reaches however a limit when it comes to the sensitivity of nudging. The large scale meteorological fields used for the case studies are reanalyses that make use of assimilation techniques. A small divergence of the mesoscale model is thus likely to degrade the performances, so that a very strong relaxation is often optimal, even if in such a configuration the added value of the mesoscale model can be questioned.

We decided to work on this issue in collaboration with H. Omrani and P. Drobinski who were planning a series of numerical experiment at the time the project started to face this challenge. By using the big-brother / little-brother framework, they could investigate the added value of

mesoscale modelling when using various type and intensity of nudging. This work is summarized in Annex E.

Following the findings of this initiative we decided to use a slight relaxation towards large scale forcing fields using a spectral nudging for all wavelength greater than 2000km (wavenumbers less than 3 in latitude and longitude), for wind, temperature and humidity and only above 850 hPa. However, the specific simulations performed in the framework of the project to be ultimately delivered to the Euro-Cordex we did not use any nudging to comply with the practices of the European Regional Climate Modelling Community. The main aversion of this community relies in the fact that nudging mixes physical and dynamical processes with a mathematical relaxation that makes very difficult any interpretation of the added value, with no consideration on the 'performances' of the regional model in terms of scores or production of small scale features. These non-nudged results are only mentioned in the present report in Section 5.2.

3.5 Evaluation of the regional climate simulations

Foreword: this section is a synthesis of (Menut et al., 2013b), in the following the reader is referred implicitly to that paper for further details.

In order to evaluate the future potential benefits of emission regulation on regional air quality, while taking into account the effects of climate change, off-line air quality projection simulations are driven using weather forcing taken from regional climate models. These regional models are themselves driven by simulations carried out using global climate models (GCM) and economical scenarios. Uncertainties and biases in climate models introduce an additional "climate modelling" source of uncertainty that is to be added to all other types of uncertainties in air quality modelling for policy evaluation.

The aim of this study is to evaluate the skill of a GCM-forced regional climate model to simulate meteorological variables to which air pollution is most sensitive, in order to help understand the simulated impact of future emission scenarios accounting for climate change in subsequent CTM simulations (Section 5.3). In particular, we investigate the changes in the statistics of such variables when moving from reanalyses-forced to GCM-forced regional climate simulations.

The variables considered for investigation are those that are critical for air quality modelling. Temperature (hereafter denoted T2 for "2m temperature") is essential to gas-phase chemical reactions and thermodynamics of aerosols. Its variability is highly correlated with that of ozone concentrations, although most of the links are due to common radiative forcing. Therefore we also investigate short-wave radiation (SWR), which is the driver of photochemistry. Wind speed (WS for 10m wind speed) is essential to dispersion, as well as the planetary boundary layer height (PBLH). Finally precipitation (RAIN) is also investigated for being an important control of aerosols through scavenging and for emissions, plume transport (like fires and volcano ashes).

The fate of chemical concentrations depends on numerous sources and sinks. First of all, the two drivers are the meteorological fields (transport, mixing, deposition) and the emissions (anthropogenic, biogenic, natural...). These drivers are integrated into chemistry-transport models in order to predict pollutants concentrations. These concentrations are evaluated for specific species (ozone, nitrogen oxides, particulate matter etc.) in order to evaluate the air quality.

The general strategy is summarized in Figure 14. The models and data are used in this study:

- The E-OBS European database (EOBS)
- The ERA-interim global ECMWF reanalysis (ERAi)
- The IPSL global coupled climate model (IPSLcm)

- The WRF regional model forced by ERA-interim (WRF-ERAi) and by IPSLcm (WRF-IPSLcm).

The observations used in this study are daily average 2m temperature and precipitation amount taken from the European Climate Gridded dataset (E-OBS).

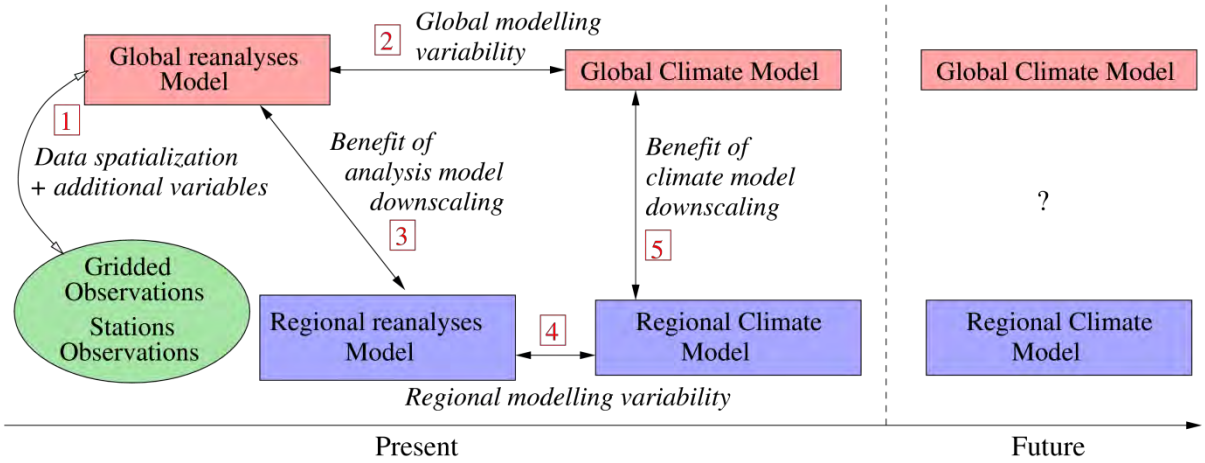

Figure 14: General flowchart of the strategy to compare global and regional scale models for present (typically 1990-2010) and future (typically 2040-2060) simulations. In this study, the global models are ERA-interim and IPSL coupled model. The regional model is WRF, forced by the global models. The observations are extracted from the E-OBS database.

We have compared several simulations in order to quantify their differences and identify the possible origins of biases. The study was conducted over an evaluation period of 17 years (1989-2005) and over an area covering Europe, as defined for the EURO-CORDEX exercise. We have compared the GCM-forced simulation with the ERA-interim (ERAi) reanalyses, observations, a WRF simulation driven by the reanalyses, and the driving GCM simulation itself (IPSLcm). ERAi provides a reference information, the difference between ERAi and ERAi-WRF allows the identification of differences induced by the RCM itself, and the comparison between ERAi and IPSLcm provides indications on the differences induced by the GCM. The same set of parameterization is used in the two RCM simulations.

We use a domain covering the larger Europe at about 50 km resolution on a lambert projection with 119x116 grid points (Figure 15). The vertical grid covers 32 levels from the surface to 50hPa and the integration time step is 4mn.

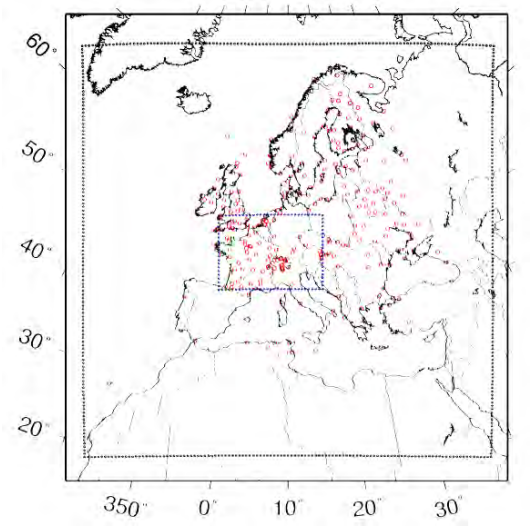

Figure 15: Geographical domains of the WRF simulation in lambert projection.

The results are presented according to the meteorological variables that will have a direct impact on the quality modelling: air temperature and surface wind speed, the short-wave downward radiative flux, precipitation and boundary layer height. The main conclusions are summarized in Figure 16. The results are expressed using several statistics (mean values, standard deviation and extremes) and the four models configurations are compared with the E-OBS available observations. The results are obviously dependent on the model configuration (resolution, parameterizations) and the selected ones correspond to those that will be used for chemistry-transport simulations in future studies.

Parameter	WRF-IPSLcm / WRF-ERAi	Expected impact on air quality
Mean values		
T2m	< (-4K winter, -1K summer)	Less biogenic emissions, less photochemistry
WS	> 0.5m/s (winter) and < 1m/s (summer)	Low impact, less natural particles emissions in summer
BLH	> (+20%)	More dilution, less surface concentrations
SWR	> (+10%)	More photochemistry, more ozone
RAIN	> (+1mm/day)	More scavenging, less pollutants in the atmospheric column (gas and particles)
Variability and extremes		
T2m	≈	Negligible impact
WS	<	More stagnation episodes
SWR	>	More fluxes leading to more photochemistry

Figure 16: Synthesis of all differences between the model configurations and expected impact on air quality.

For the mean biases of 2m temperature, the ERAi global meteorological fields are more or less unbiased when compared to EOBS. For precipitation, a positive bias of +0.5 mm/day is observed. The IPSLcm global model has a strong cold bias of -2K in temperature and -1m/s for wind speed. WRF tends to increase the temperature cold bias (by -2K) and the precipitation positive bias by +1 mm/day (Figure 17).

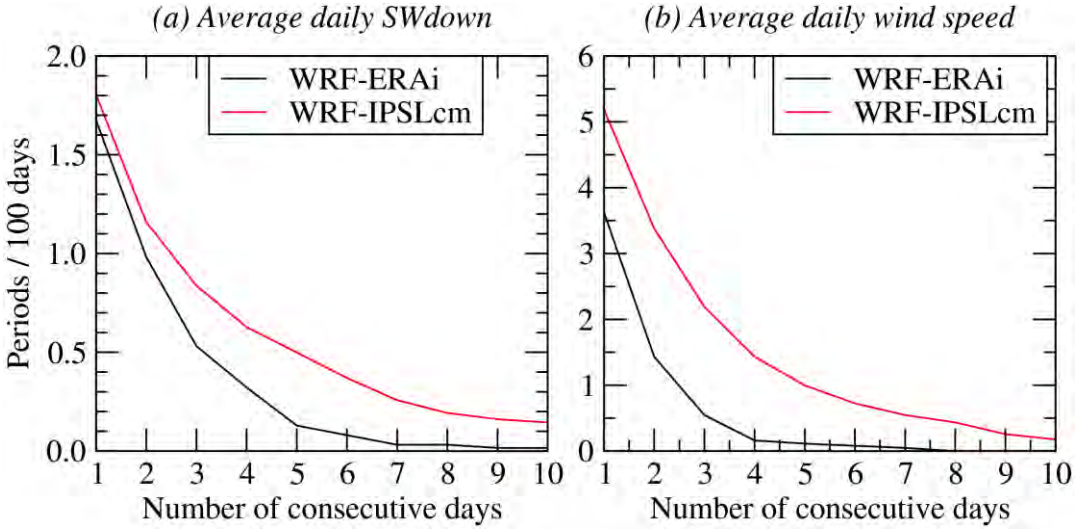

Figure 17: Number of periods with more than n consecutive days when (a) the average radiation (over the day and the Western-Central Europe area) exceeds 300 W/m2 which is about the 95th percentile for the WRF-ERA interim distribution, and (b) the average daily wind speed remains below 3.5 m.s-1 which is about its 5th percentile.

Over land, WRF tends to increases the wind speed by ~1 to 2m/s, independently of the global model used. The short-wave radiation is higher with WRF-IPSLcm than with WRF-ERAi, leading to more photochemistry (more ozone and less nitrogen oxides). At the same time, the boundary layer height is also higher with WRF-IPSLcm than with WRF-ERAi, leading to more dilution of primary pollutants (such as anthropogenic emissions in large urbanized areas) and thus, to less surface concentrations (both for gases and particles).

Pollutants are sensitive to mean meteorological values but also to variability and extremes: for example, photochemistry increases exponentially with temperature. If a significant cold temperature bias was found, the temperature variability was relatively close between all models. The WRF-IPSLcm showed much more periods with low wind speed and high short-wave-radiation fluxes: during summer, we can expect more stagnation periods and more frequent continuous sunshine periods, leading to more episodes of high pollution during drought periods. For some periods, this could be offset by more raining days. Finally, the differences observed on precipitations suggest a more general discrepancy affecting the water cycle, this will have strong implications on the aerosol chemistry.

3.6 Upstream CDF-t

Foreword: this section is a synthesis of (Colette et al., 2012c), in the following the reader is referred implicitly to that paper for further details.

3.6.1 Introduction

We propose here an innovative climate downscaling methodology that combines both dynamical and statistical approaches. In a nutshell, our hybrid approach consists in applying a statistical correction of the GCM fields with respect to atmospheric reanalyses prior to performing a dynamical downscaling of these corrected fields. As such, this approach constitutes a hybrid climate downscaling technique building upon upstream statistical correction and downstream physical modelling.

Like any probabilistic downscaling technique, the upstream statistical correction may alter the integrity of the forcing fields by matching it to reanalyses. The main strength of our hybrid approach lies in the implementation of a mesoscale model after the probabilistic downscaling that guarantees the physical consistency of the resulting fields and hence constitutes an essential advantage for climate impact studies (Parry et al., 2007).

3.6.2 Methodology

Large scale climate model : The large scale climate model that we use to demonstrate the efficiency of our hybrid statistical and dynamical technique is the coupled climate model IPSLcm (Institut Pierre Simon Laplace Coupled Model) GCM (Marti et al., 2010) in its “low resolution” version (3.75 x 1.875 degrees) prepared for the CMIP5 (Climate Model Intercomparison Project) stream of the Intergovernmental Panel on Climate Change (IPCC).

Statistical downscaling : The probabilistic downscaling methodology is the CDF-t (Cumulative Distribution Function transform) of (Michelangeli et al., 2009), based on a variant of the “quantile-matching” technique (Déqué, 2007). Quantile-matching consists in associating to a modelled value, the value in a control distribution (e.g. observations) that has the same probability. In other words, from a quantile in the CDF of the simulations, the corresponding quantile in the CDF of the control data (e.g. observations) is determined. By scaling the quantile-quantile relationship, the correction changes the shape of the distribution so that the events whose frequency (or probability) is systematically biased in the model are better captured. While classical applications of quantile-matching consider that the CDF of the simulations is stationary in time (Maraun et al., 2010;Wilks and Wilby, 1999), the scope of CDF-t consists in expanding this technique for the case where the CDF of the simulations for the future has changed. This is done, first, by estimating the CDF of the corrected variable for the future time period of interest (Michelangeli et al., 2009). Then, projections are obtained through a quantile-quantile technique between future uncorrected and corrected CDFs (Vrac et al., 2012). The methodology implemented here thus applies for future projections even though we decided to limit the scope of the present paper to historical periods in order to discuss its validation.

Dynamical downscaling : We use the Weather Research and Forecasting (Skamarock et al., 2008) mesoscale model to downscale the IPSLcm fields in a dynamical way. The spatial resolution is 50km and the domain covers the whole of Europe with 119x116 grid points. The setup is the same as that of (Menut et al., 2012b) who present a detailed evaluation of the performance of the IPSLcm/WRF regional climate modelling suite. However no nudging was applied in the present case in order to evaluate the full effect of prior correction on dynamical downscaling.

Experimental design : We perform a CDF-t based correction of the large-scale input fields produced with the IPSLcm model so that corrected fields will be used for the dynamical downscaling. Distributions of 3D zonal and meridional wind, 3D relative humidity, and 3D and surface (skin) temperature are matched with those of reanalysed fields of the ERA-interim reanalysis at every gridpoint. To account for seasonality, training distributions are taken on a monthly basis. For 3D and surface temperature, the correction is performed independently for the 4 daily time steps to account for the diurnal cycle. Surface pressure and geopotential height are not matched in order to maintain flow consistency and quasi-geostrophy at the boundaries, but they are indirectly modified by the matching of the 3D temperature field. The hydrostatic balance of the corrected input field is recomputed before launching the mesoscale model in order to ensure physical consistency along the columns.

Evaluation: Two 10-year simulations are carried out for the assessment of the technique. The first one is done without applying the GCM correction prior to dynamical downscaling, while the second is done with application of the prior CDF-t approach. The two simulations are then compared to E-OBS data (Haylock et al., 2008) over the same time period.

3.6.3 Results

Surface temperature

The bias of temperature averaged over the 10-year time period is given in Figure 18 for the reanalysis (ERA-i), the large-scale climate model (IPSLcm) and its statistically corrected version, the dynamically downscaled climate model (IPSLcm/WRF) and our hybrid statistical/dynamical downscaling (IPSLcm/CDF-t/WRF). For all the models the temperature is interpolated at 950hPa while the observations are provided at 2-m altitude. The discrepancies between E-OBS and ERA-i are confined to the outskirts of the domain where the gap filling procedure used in E-OBS has uncertainties as a result of the scarcity of the monitoring network. In addition, important differences are found over mountainous areas due to lack of resolution and methodological differences. On average, the difference between ERA-i and the observations is -1.41K (standard deviation σ=2.03) over the Western part of the domain (5W, 15E, 40N, 55N). Raw GCM temperatures exhibit a strong negative bias (—4.78K, σ=0.6), except over mountainous areas where the positive biases result from an artefact of the smooth orography. This strong negative bias of the low resolution version of the IPSLcm model was discussed before (Hourdin et al., 2012) and was improved in a more recent version of the model including a higher resolution (Cattiaux et al., 2012). This feature constitutes a somewhat good test case for the hybrid downscaling methodology presented here. The statistical correction is efficient at reducing the temperature bias of IPSLcm, the average bias of the corrected GCM is -1.36 (σ=2.07) and its pattern resembles that of ERA-i.

The negative bias of IPSLcm is amplified in the raw regional climate model simulations (—5.06K, σ=1.49), as was observed by (Menut et al., 2012b). The dynamical downscaling does not constrain the distribution in any ways, and it appears that a negative feedback occurs here as the RCM increases the negative biases of forcing fields. On the contrary, the situation is better for the hybrid downscaling, the average bias is limited to -2.33K (σ=1.35). The mesoscale still tends to cool down the GCM, and the average bias is larger than for the corrected version of IPSLcm since the compensation that occurred over high elevation terrain vanishes. Despite the reduction of the

mean bias, it still exhibits a regional pattern with negative values in Western and Northern areas and positive values in Mediterranean areas.

Precipitation

Beyond its relevance for climate impact studies, precipitation is an interesting variable to evaluate our methodology since, unlike temperature, this variable was not directly corrected by the prior statistical CDF-t method. The absolute differences between modelled and observed precipitations are provided on Figure 19.

The GCM exhibits an overestimation of precipitations throughout the domain. Only West-facing coastal areas have a deficit, presumably because of the too coarse resolution that is not able to capture the precipitation local maxima over the coastlines. The overestimation is less pronounced over mountainous areas because of a compensation of errors.

The dynamical downscaling of the raw GCM outputs yields an even stronger overestimation of the precipitation because of a negative feedback related to the low temperature bias. The deficit over coastlines and mountains is compensated by the higher resolution of the model.

It is only with the hybrid downscaling that the results are significantly improved. The model still exhibits an overestimation of precipitation but, over low-lying area of Western Europe, the bias is decreased by a factor of two. An excess is found over the Alps. Precipitation deficits are found around the Mediterranean, the spatial patterns of these deficits do not appear highly correlated to coastlines. It may thus be attributable to other uncorrected deficiencies such as weather regime frequencies rather than resolution issues.

The distribution of daily precipitation shows that the hybrid downscaling constitutes an improvement over the whole range of the distribution. Nevertheless, all the simulations still exhibit an overestimation of low precipitations and an underestimation of higher quantiles.

3.6.4 Conclusion

We introduced an innovative climate downscaling methodology that combines state-of-the-art statistical and dynamical approaches. We apply a statistical correction to large-scale fields of a Global Climate Model (GCM) prior to a regional simulation. The statistical correction makes use of the Cumulative Distribution Function transformation (CDF-t) designed by (Michelangeli et al., 2009). The GCM field distributions are matched to those of reanalysed fields in order to apply a correction over the whole 3D domain for several variables. The corrected fields are then provided to a dynamical Regional Climate Model (RCM), so that we can produce bias-corrected, yet physically consistent, 3D fields at higher spatial resolution.

An application to present-day climate shows that the statistical upstream correction leads to a reduction of the surface temperature bias of a factor four in the regional climate simulation. This improvement yields, in turn, a lower overestimation of precipitations.

The CDF-t upstream correction does not address yet spatial and temporal variability (climate modes, persistence and weather regimes), the technique remains sensitive to the choice of variables included in the correction and the location of the domain since the forcing is applied at the boundaries. The methodology carries some error compensation mechanisms whose effect is minimised thanks to the implementation of a dynamical downscaling in the lee of the statistical correction.

Nevertheless, considering the magnitude of the improvement in terms of mean bias we conclude that this innovative hybrid statistical/dynamical climate downscaling offers promising perspectives for climate impact studies requiring unbiased, balanced, high-resolution 3D fields.

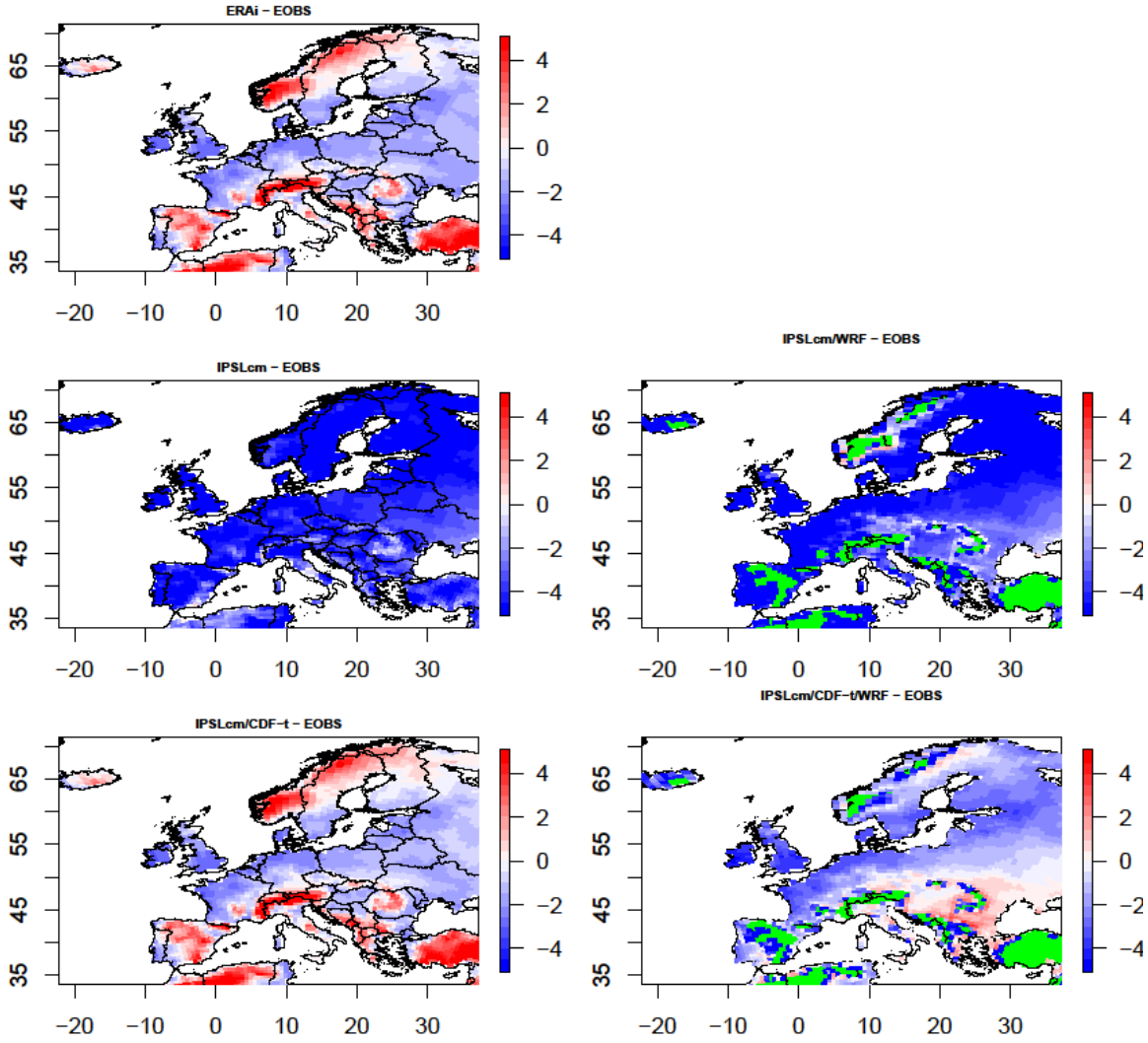

Figure 18 : Difference between the mean modelled 950hPa temperature and observed (E-OBS) 2-m temperature (K) over the 1990-1999 decade for ERA-interim, the GCM IPSLcm as well as its corrected version and the RCM WRF driven by raw IPSLcm fields and by downscaled IPSL fields corrected with the CDF-t technique. The green-shaded areas in the WRF field are unavailable because located below the 950hPa level in the hybrid coordinates.

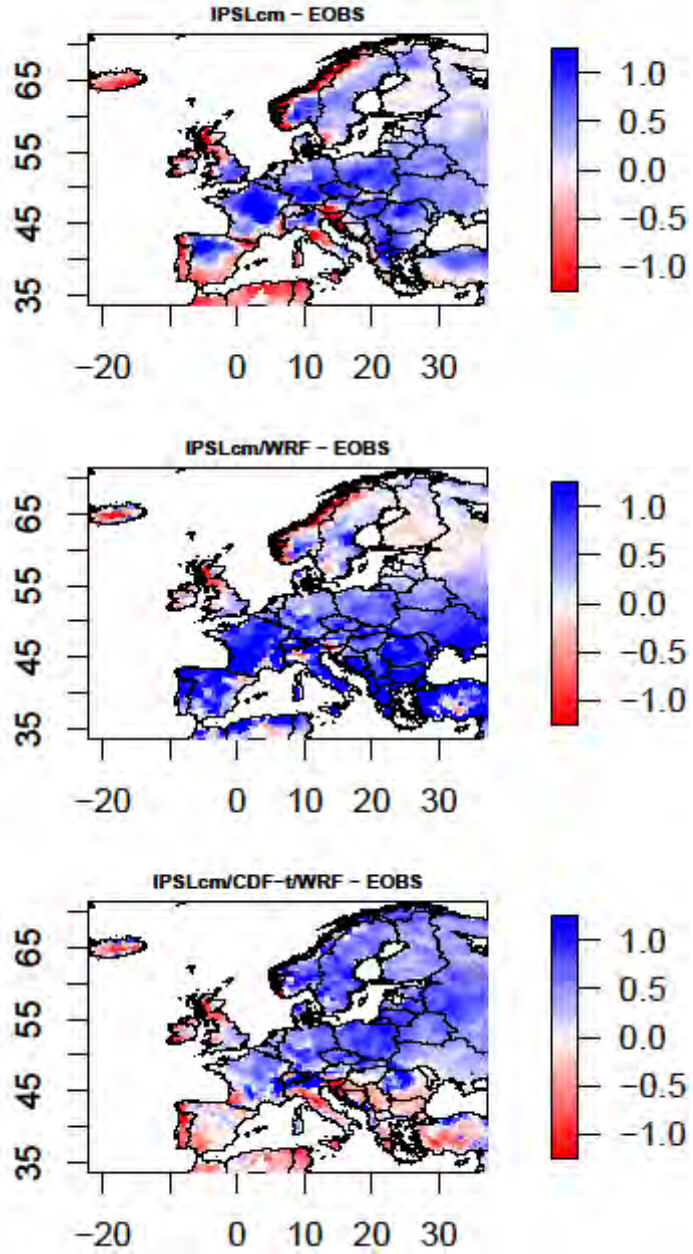

Figure 19 : Same as Figure 18 for the precipitations (mm/day) except that only the results of the climate models are given and the colour scale is reversed.

4 Sensitivity analyses: vegetation and air quality

4.1 Introduction

In addition to anthropogenic emissions of pollutants introduced in Section 2, natural sources bear upon current and future air quality. Natural sources of particulate matter such as desert dust, volcanic emissions, or sea-salt, were not in the scope of Salut'AIR, but we included in the workplan a focus on gaseous biogenic emissions of ozone precursors.

The impact of meteorological variability on biogenic emissions has been acknowledged for about a decade and all state of the art chemistry transport models now take into account this factor rather than prescribing constant biogenic emissions fluxes. But the specific goal of using CTM to investigate the impact of climate change requires taking another look on these processes that are expected to be substantially modified under future climate.

This section summarizes the work that was performed with global CTM on the impact of CO_2 concentrations (Section 4.2) and landuse changes (Section 4.3) on biogenic emissions. While we found that landuse change had little impacts in Europe, the inhibiting role of CO_2 is crucial. At the regional scale, we focused on the quantification of the feedbacks between vegetation and pollution (Section 4.4) and point out significant impacts. This chapter ends in Section 4.5 with an assessment of the sensitivity of biogenic emission of isoprene (a major precursor of ozone) under various climate scenarios and confirm the high uncertainty reported by e.g. by (Langner et al., 2012b) who found a factor 5 differences using an ensemble of regional CTM.

The roadmap of the project did not allow for an attempt to reduce these uncertainties in the operational projections introduced in Section 5.3. Rather given the ultimate goal of Salut'AIR to lead to a cost-benefit analysis, we preferred to focus our efforts on anthropogenic emissions for the operational projections.

4.2 Global biogenic emissions under increasing CO_2 concentrations

Biogenic emissions represent the major source of hydrocarbons at the global scale. Isoprene is the first volatile organic compound (VOC) emitted by the terrestrial biosphere. However the intensity of this source remains highly uncertain with total amount of present-day isoprene emissions varying from 400 and 600 TgC/yr depending on the inventories. Furthermore, since these emissions are linked to several natural processes (vegetation physiology as well as climate), they show large interannual variability. Recently, several experiments carried out in experimental chamber showed, however, that an elevation of CO_2 concentration can partly inhibit the faculty of plants to emit isoprene (Possell et al., 2005;Wilkinson et al., 2009). This could significantly change estimates previously published, especially when studying isoprene emissions at past or future periods. In the future, changes in climate, land-use or atmospheric CO_2 concentrations could therefore affect significantly biogenic isoprene emissions and, consequently, impact atmospheric concentrations of key compounds such as ozone or nitrogen oxides.

The ORCHIDEE model used in this study includes an emission module based on Guenther et al. (1995) to calculate fluxes of isoprene, monoterpenes and other VOCs (Lathière et al., 2006). Two sets of parameterisations were implemented in ORCHIDEE in order to take into account the inhibition effect of atmospheric CO_2 on isoprene emissions, based on both approaches developed by (Possell et al., 2005;Wilkinson et al., 2009). The objective is not only to consider this impact when estimating isoprene emissions in the future, but also to give a range of uncertainty in these estimates, based on the current knowledge. The function derived by (Possell et al., 2005) stands for the impact of changes in atmospheric CO_2 concentration on isoprene emissions during leaf growth as a long-term effect, while the algorithm from (Wilkinson et al., 2009) also integrates the response of emissions to short-term variation of intercellular CO_2 concentration during a single

day. Both functions are included in the ORCHIDEE model as an additional correction of isoprene emissions to atmospheric CO_2 concentration and normalized for a present-day atmospheric CO_2 of 350 ppm.

Simulations were performed for the present-day and the 2050s considering the AR4 scenarios for climate and land-use change (Figure 20). For the present-day, a global annual isoprene emission of 598 TgC/yr is calculated by our model. Taking into account future changes in atmospheric CO_2 concentrations and climate leads to an increase in global emissions ranging from 16% for the B1 scenario to 23% for the A1B scenario. When a 2050s vegetation distribution is considered, accounting for possible evolution of agricultural surfaces in the future, global annual isoprene emissions increase only by 3-9% for the different scenarios compared to the present-day. Together with land-use change, accounting for the CO_2 inhibition effect significantly counteracts the impact of future climate and CO_2 on isoprene emissions, for both approaches, either derived from(Wilkinson et al., 2009) or (Possell et al., 2005). Isoprene emissions calculated for the 2050s CCLuIn simulation decrease by 26-31% when the parameterization from (Possell et al., 2005) is considered, and by 14-16% when the parameterization from (Wilkinson et al., 2009) is considered.

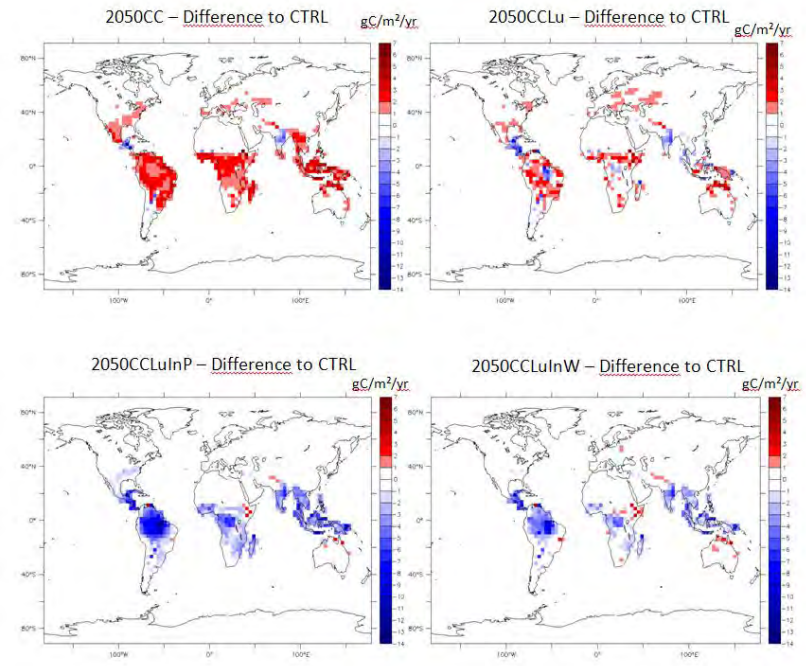

Figure 20: Future difference in isoprene emissions (gC/m²/yr) for the future compared to the presend-day control run when including changes in climate and atmospheric CO2 concentration (2050CC) together with the evolution of vegetation distribution in relation with land-use change (2050CCLu) and the CO2 inhibition effect based on the work by (Possell et al., 2005)(2050CCLuInP) or (Wilkinson et al., 2009)(2050CCLuInW).

4.3 Sensitivity of future biogenic emissions to landuse changes

The potential inhibiting effect of atmospheric CO2 on isoprene emissions from plants has been implemented in the ORCHIDEE model, based on recent studies by (Possell et al., 2005) and (Wilkinson et al., 2009) to estimate emissions for the present-day and the future.

We quantified the impact of this emission change on tropospheric chemistry in 2050 and compared it to the impact of landuse, climate or anthropogenic emission changes. When all global changes of climate, land-use and atmospheric CO_2 are taken into account together, our results

show a decrease in biogenic VOC emissions while an increase is calculated when the global increase in temperature, or the fertilizing effect of CO_2 on vegetation in considered (Figure 21). As can be seen the biogenic emissions are very weakly affected by the landuse change over Europe (<2%) and this modification becomes close to zero when considering all the 3 effects which could act simultaneously in the future.

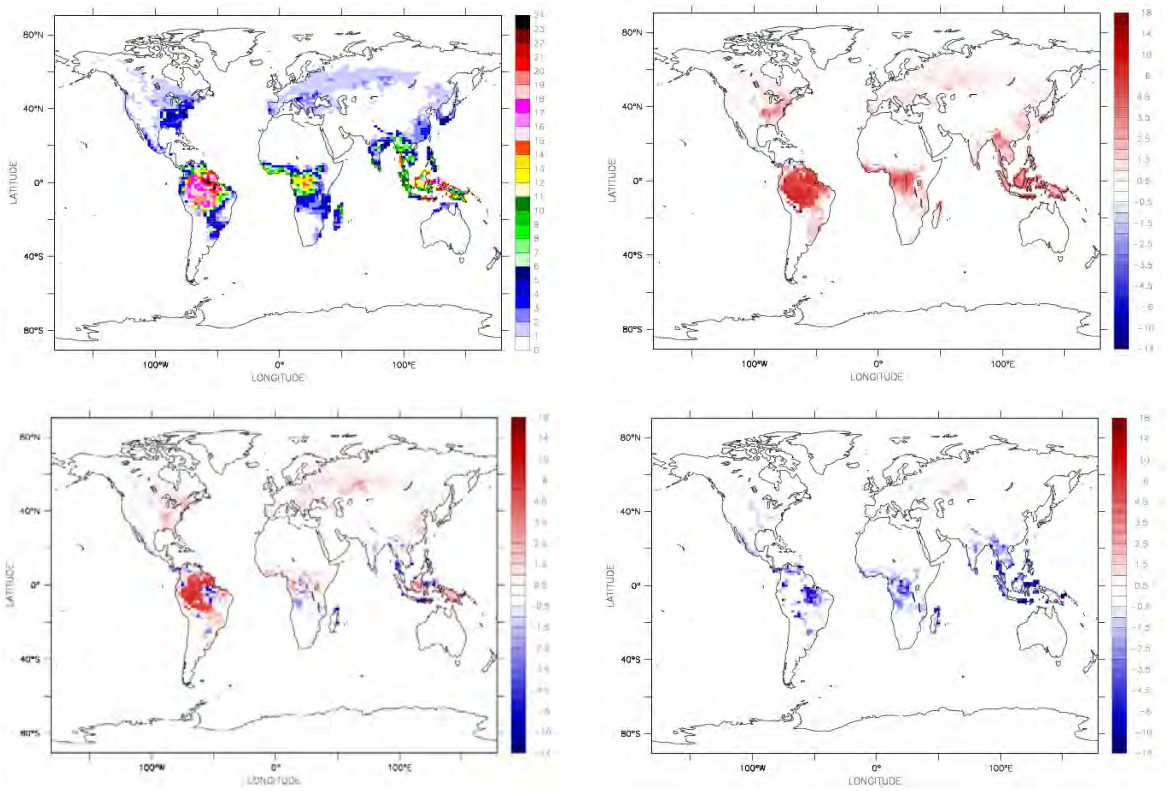

Figure 21: Biogenic isoprene emissions for present-day conditions (mgC/m²/h, upper left panel) and impact of future changes (2050) on biogenic isoprene emissions considering climate and [CO2] modifications (upper right), added to landuse change (lower left, +16%) and added to the inhibition effect linked to CO2 (lower right, -10%) as proposed by (Wilkinson et al., 2009).

4.4 Feedback between vegetation and air quality

If anthropogenic emissions are considered to be an essential part of the future evolution of atmospheric composition, other types of emissions can vary depending on the climate change and therefore interfere with the atmospheric chemistry. Biogenic emissions are thus highly dependent on ecosystems environmental factors such as tree species, soil moisture and air temperature. To estimate the impact of land cover changes on pollutants concentrations, as well as the impact of high concentrations on vegetation, we coupled two different models: the chemistry-transport model CHIMERE and the vegetation/hydrology model ORCHIDEE. The high ozone concentrations partially inhibit the ability of plants to remove it by dry deposition. But this process is not well known and it is unclear if it can be the cause of errors in the simulations, particularly in the case of extreme weather events such as heat waves.

The coupling between CHIMERE and ORCHIDEE was conducted in two stages in order to individually assess the feedback impacts.

The first step was to update the Leaf Area Index (LAI). In the current release of the CHIMERE model, biogenic emissions are calculated using the MEGAN model. This model needs several input parameters such as meteorological fields and parameters describing the status of the vegetation. One of these required parameters is the Leaf Area Index. Originally, CHIMERE is using

climatological LAI maps derived from MODIS satellite data. These values are constant in time and thus not able to reproduce the daily and seasonal variabilities observed in Europe. In this study, we replaced this climatological LAI by the one daily calculated with ORCHIDEE.

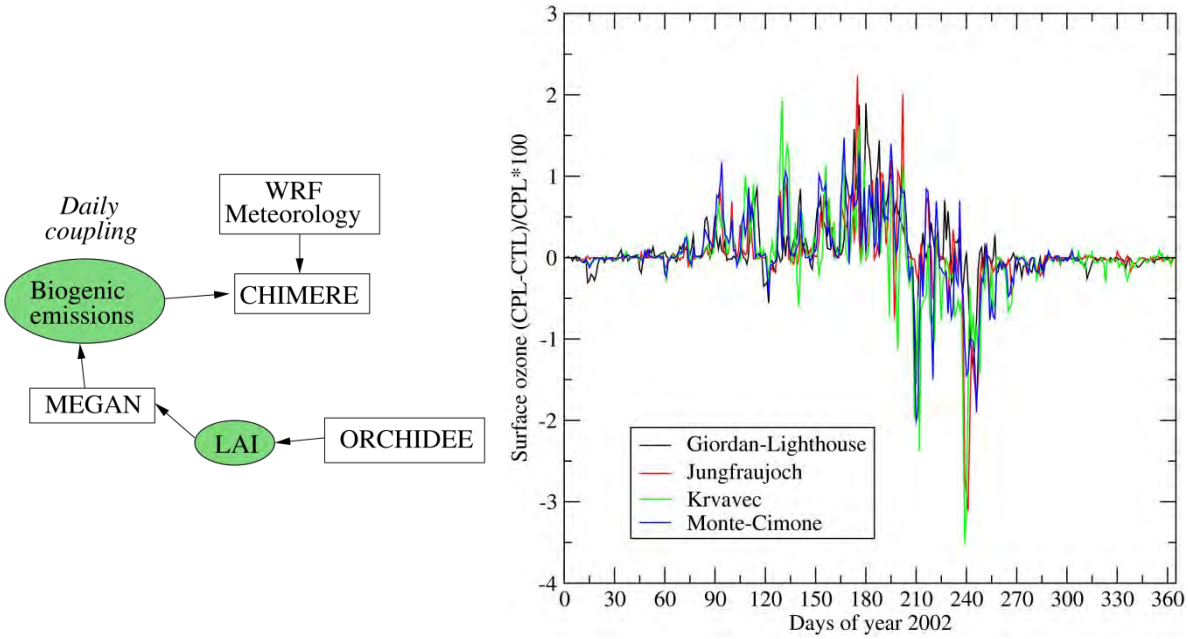

Figure 22: Offline coupling between ORCHIDEE biogenic emissions and atmospheric chemistry, and impact on modelled surface ozone.

Figure 22 shows the principle of the new LAI forcing (left side) and time series of results (right part). For the whole year of 2002, the curves present the relative difference between the simulation with the LAI climatology (CTL) and the new ORCHIDEE LAI (CPL).Results are presented for several AIRBASE stations. During the winter, the vegetation being rare in Europe, the impact is cloise to zero. During the spring and the beginning of the summer, the impact is positive and may reach +2%. At the end of the summer, the impact becomes negative and can reach -3%. This shows that the use of a daily variable LAI may change the surface concentrations results by a few percents, a moderate impact.

The second step was to make a more important loop between processes to really taken into account feedbacks between meteorology, vegetation and dry deposition of surface ozone concentrations. Compared to the step 1, a feedback is added between ozone modelled by CHIMERE and needed by ORCHIDEE. The conductance term depending on vegetation evolution, is updated by ORCHIDEE and sent to CHIMERE to update the dry deposition process. The results are presented in Figure 23. In this case, the impact is significant and can change the ozone concentrations of 20% (winter) to 40% (in summer). These large changes in ozone concentrations will have a significant impact in the case of simulations in Europe and a framework for monitoring air quality, particularly for studies related to extreme weather, particularly in the case of anticyclonic conditions in summer and Europe.

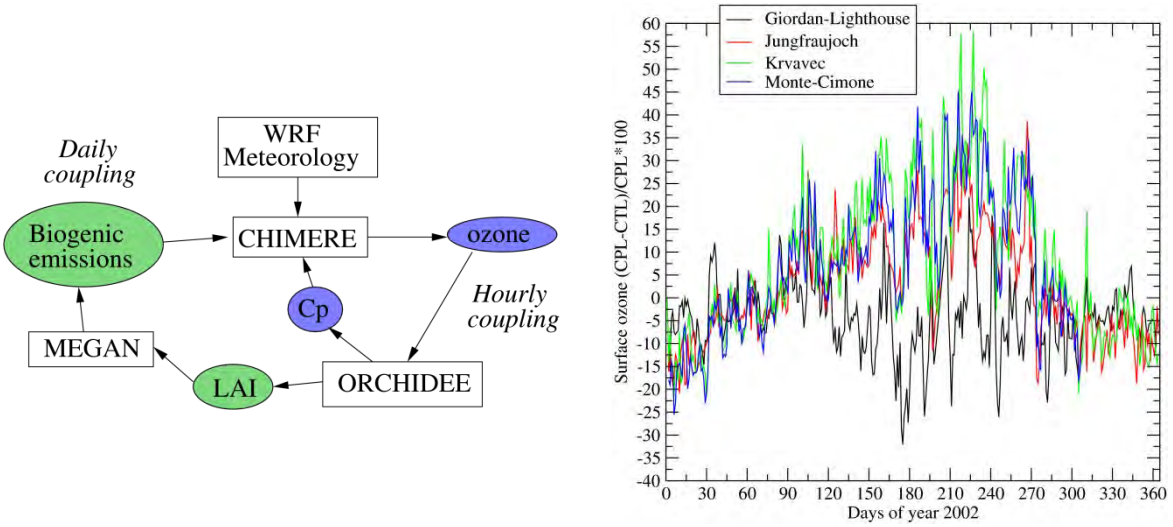

Figure 23: Online coupling (including feedbacks) between ORCHIDEE biogenic emissions and atmospheric chemistry, and impact on modelled surface ozone

4.5 Regional biogenic emissions in a changing climate

4.5.1 Projections of biogenic emissions

The projected changes in biogenic emissions of air pollutant precursors were computed using the MEGAN model (Guenther et al., 2006) for the present-day climate and at the horizon 2050. The MEGAN model will be introduced in more details in Section 4.5.2 devoted to the investigation of the most sensitive factors influencing biogenic emissions.

Using the downscaled climate model we computed that total isoprene emission over Europe reached about 5300Gg/yr for the present-climate, while it would increase in 2050 to 6086Gg/yr and 7091Gg/yr under the RCP2.6 (mitigation) and RCP8.5 (reference) scenarios, respectively. Note that we ignore the inhibiting impact of increased CO_2 concentrations on biogenic emissions whereas global-scale studies showed that this factor could significantly counterbalance this increase (Section 4.2).

A comparison of present-day isoprene emission using reanalyses (downscaled ERA-interim) instead of a realisation of the present climate as seen with a GCM showed the magnitude of the uncertainty related to isoprene emissions with a total of 8797Gg/yr, i.e. a 66% higher than the same estimate obtained with the GCM.

Significant uncertainties related to isoprene projections were reported in the past in multi-model ozone projections experiments. Over Europe, (Langner et al., 2012b) found a factor 5 differences across the model ensemble, while at the global scale (Stevenson et al., 2006) reported a factor 3. When compared to the ensemble of (Langner et al., 2012b), it appears that Chimere is in the mid to upper part of the envelope that ranges from 1592 Gg yr^{-1} to 8018 Gg yr^{-1} for the present climate.

4.5.2 The MEGAN biogenic emission model

Biogenic emissions for the six species relevant to CHIMERE (isoprene, α-pinene, β-pinene, limonene, ocimene, and NO) are based on the MEGAN model version 2.04 (Guenther et al., 2006). As described in (Bessagnet et al., 2008b;Menut et al., 2013a). For each grid cell a species-specific reference emission rate E_0 is modulated according to environmental conditions to produce the instantaneous emission:

$$E = E_0 \times \gamma_{LAI} \times \gamma_{AGE} \times \gamma_T \times \gamma_{PPFD}$$

Annual reference emissions for each species (E_0) factors are static and refer to the years 2000-2001.

The variation of monthly emission activity is due to changes in the leaf area index (LAI), which also drives leaf age changes in order to represent the fact that biogenic emissions peak several weeks after the onset of photosynthesis and decrease with the aging of the leaves. For the full expression of γ_{LAI} and γ_{AGE} the reader is referred to equations 15-19 in (Guenther et al., 2006). The LAI database is given as a monthly mean product derived from satellite (MODIS) observations for the year 2000.

The meteorological modulation is included in the hourly emission activity that is the product of two correction factors: γ_T (function of temperature) and γ_{PPFD} function of photosynthetic photon flux density (PPFD, directly related to the incoming short wave radiation). The expression of γ_T for isoprene is given in equation 14 of (Guenther et al., 2006) and reported here for convenience:

$$\gamma_T = E_{opt} \frac{C_{T_2} \exp(C_{T_1} x)}{C_{T_2} - C_{T_1}(1 - \exp(C_{T_2} x))}$$

where:

$$x = \left(\frac{1}{T_{opt}} - \frac{1}{T} \right) \Big/ 0.00831$$

$$T_{opt} = 313 + 0.6(T_{day} - 297)$$

$$E_{opt} = 1.75 \exp(0.08(T_{day} - 297)$$

$$C_{T_2} = 200$$

$$C_{T_1} = 80$$

and T_{day} is the daily temperature. The expression of γ_{PAR} is given in equations 11-13 of (Guenther et al., 2006) and also reported here for convenience:

$$\gamma_{PPFD} = \cos(SZA)\left[2.46\left(1 + 0.0005\varphi(PPFD_{day} - 400)\right) - 0.9\varphi^2\right]$$

where SZA is the Solar Zenith Angle, ϕ is the above canopy PPFD transmission, and $PPFD_{day}$ is the daily photosynthetic photon flux density.

4.5.3 Sensibility of the biogenic modulation factors to the meteorological forcing

Using the equations provided in Section 4.5.1, it is possible to quantify the impact a given difference in surface temperature or incoming short wave radiation on the modulation of biogenic emissions. We used the daily average meteorological variables computed with the downscaled GCM-historical and ERA-hindcast to assess the impact of the meteorological driver on biogenic emissions.

The maps of γ_T and γ_{PAR} are given in Figure 24 for the climate and reanalysed forcing as well as the difference, in the last row. Over land surfaces of Western Europe, the difference between the γ_{PAR} obtained with the GCM and ERA driver is -0.074, while this value is only -0.035 for γ_T, hence

the statement on a sensitivity to incoming radiation 216% or about twice as large as the sensitivity to temperature.

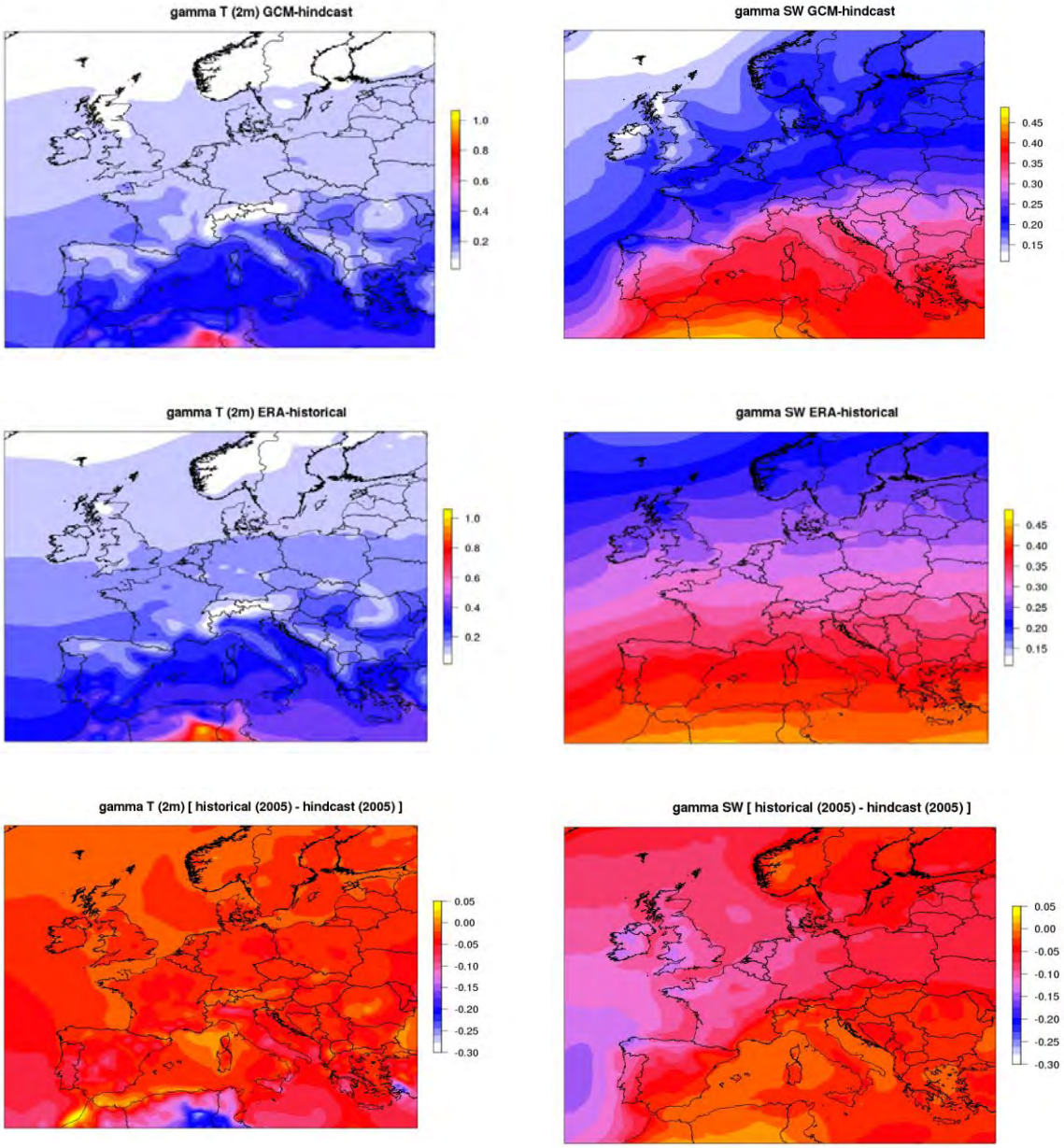

Figure 24 : Map of the modulation factors attributed to surface temperature (T2m, left) and to incoming short wave radiation (SW, right), when using the climate model (GCM-historical) or meteorological reanalyses (ERA-hindcast) as a driver. The last line provides the difference between the first two.

5 Global climate change and regional air quality

5.1 Global chemistry and climate

Foreword: this section is a synthesis of (Szopa et al., 2012b) , in the following the reader is referred implicitly to that paper for further details.

In order to take into account the global atmospheric composition changes in the future, simulations were performed using a general circulation model coupled with a chemistry module (LMDz-OR-INCA). Simulations of the global aerosol (dust, sea-salt, black carbon, particulate organic matter and sulphates) and tropospheric ozone distributions between 2000 and 2100 have been performed following the Representative Concentration Pathways (RCP) emission dataset for the future. In these simulations, only biomass burning and anthropogenic sources are varying from year-to-year. The RCP projections, defined in the IPCC-AR5 framework, allow investigating four emission trajectories for the 2000-2100 period. Each emission trajectory is compatible with a distinct climate pathway and includes gridded emissions for aerosol and ozone precursors in decadal increment. These simulations were also subsequently used by the two French Earth System Models (ESMs) to account for the spatial and temporal evolution of both radiatively and chemically active compounds, when simulating the climate evolution in the CMIP5 frame work. The methodology used to prepare such climatologies for ESMs and the main characteristics and trends shown by the climatologies are discussed for both ozone and aerosols in (Szopa et al., 2012a).

The model-calculated present-day distribution of tropospheric ozone is qualitatively compared with two space-borne thermal infrared spectrometers (Figure 25). Overall, the zonal distribution appears to be correctly reproduced in the model-calculated climatology including the summer increase of ozone in the lower levels of Northern mid-latitudes. The discrepancies between the model results and satellite datasets are rather small compared with the differences between the two remote sensor-based datasets.

The present-day global mean optical depth for each type of aerosol is compared with a large multi-model database (Figure 26). The model results are found to be consistent with the multi-model dataset for total aerosol, even if the sulphate content is slightly higher than the multi-model median.

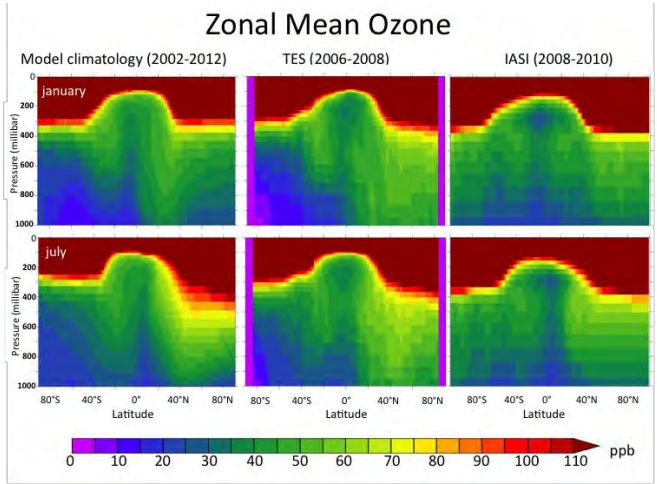

Figure 25: Monthly averaged zonal-mean ozone distribution in ppbv. The model results (left column) are averaged over a 11 year period centered around 2007. The remote sensing based ozone is obtained using the TES dataset averaged over the 2006-2008 period (middle column) and using the IASI dataset over the 2008-2010 period (right column).

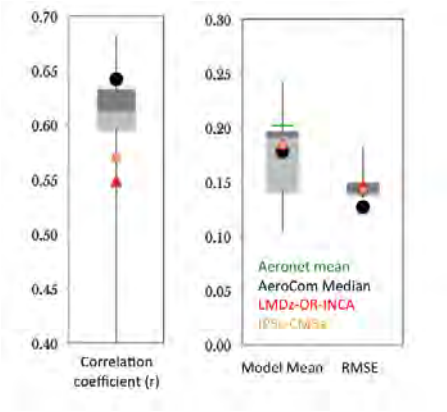

Figure 26: Statistics of evaluation of aerosol optical depth of the INCA model and the IPSL-CM5a evaluation against monthly worldwide Aeronet data climatological mean 2000-2009. Correlation coefficient, model mean at Aeronet sites (Observations show mean of 0.202) and RMS error are shown. For comparison AeroCom phase II model median is also shown (black dots). The spread of corresponding recent AeroCom phase II results is shown as box and whiskers plot with minimum, 25% percentile, median, 75% percentile and maximum.

5.1.1 Tropospheric Ozone changes between 2000 and 2100

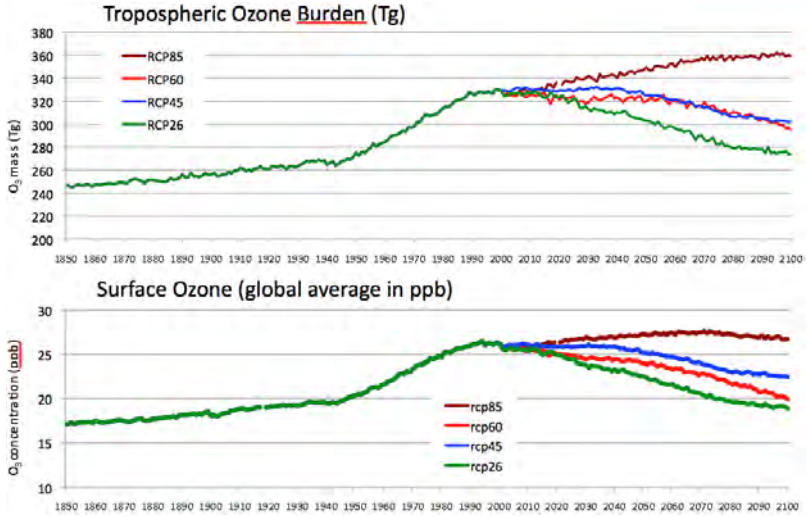

Figure 27: Evolution of ozone between 1850 and 2100 shown as tropospheric ozone burden in the INCA simulation (in Tg, upper panel) and surface ozone in the INCA simulation (in ppbv, lower panel).

Figure 27 depicts the evolution of the global tropospheric ozone content at the surface as well as for tropospheric burden. Starting with the year 2000, the four trajectories correspond to the four RCP emission scenarios. They start to differ significantly (considering global mean) from 2010 onwards. Then the RCP8.5 emission projection leads to a significant increase of the ozone burden (+30 Tg from 2010 to 2100), mainly due to the increase from 2010 to 2070. Moreover, the global surface ozone increases until 2070 in this scenario (reaching up to 27.6 ppbv) and then shows a slight decrease. At the global scale, however, all the precursor emissions from this scenario decrease strongly after 2030, with the exception of methane. The global tropospheric ozone increase is mainly due to CH_4 and regional precursor emission increases over India and some parts of Africa (Central and South Africa as well as Gulf of Guinea).

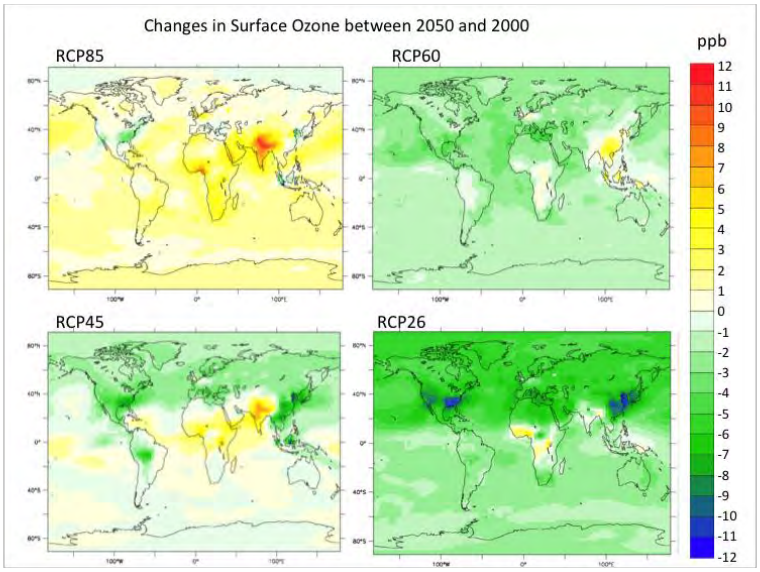

Figure 28: Distribution of surface ozone changes in 2050 compared with 2000 for the 4 RCP scenarios (using ten year means)

Figure 28 shows the map of surface ozone differences for each RCP scenario in the 2050s compared to the present-day. For RCP8.5 (upper left), a significant decrease of surface ozone in North America is simulated together with a strong increase over India (> 8 ppbv locally). African surface ozone also exhibits a large increase (4-8 ppbv) over a large part of the continent and particularly over the tropics. The responses of Europe and South America are spatially contrasted and range in 2050 between [0 ; 4.5] ppbv and [-1.5 ; 3.5] ppbv respectively. The three other scenarios (RCP6.0, 4.5 and 2.6) lead to an ozone decrease either following a stabilization period (e.g. between 2010-2040 for RCP4.5) or as early as 2010. Looking at the global scale Figure 27, the RCP4.5 and RCP6.0 trajectories are relatively close. However the ozone evolution corresponds to relatively different regional patterns. As shown in Figure 28, not only the amplitude of regional changes is different (e.g. a stronger decrease over USA in RCP4.5 compared with RCP6.0) but also the socio-economical hypotheses underlying the emission projection as is the case for Asia. The RCP6.0 leads to an increase of surface ozone over China and Indonesia whereas RCP4.5 results in a significant decrease over China/Indonesia but in a strong increase over India. In 2100, while RCP6.0 global surface ozone decrease is greater than the one of RCP4.5, the global ozone burden remains close to each other.

The RCP2.6 shows a strong and almost constant ozone decrease of about 0.07 ppbv/yr. The surface ozone decreases in the northern hemisphere but increases in some tropical regions. However in this scenario it is surprising to see that global surface ozone is lower than the 1950s level from 2070 until the end of the century.

In 2030, the surface ozone trajectories of the four RCPs lie in the range of previous projections performed with LMDz-INCA during the PHOTOCOMP project (Szopa S. et al., 2006). The RCP projections are comprised between the scenarios corresponding to the storyboards 'Maximum Feasible Reduction' (matching the RCP2.6) and 'Current Legislation' (matching the RCP8.5) (Dentener et al., 2005).

5.1.2 Aerosol changes between 2000 and 2100

Figure 29 shows the evolution of the global aerosol optical depth at 550 nm between 1850 and 2100 as simulated by LMDz-OR-INCA and averaged using a 11-year running mean. In the 21st century simulations, an increase with a growth rate equivalent to that of the 1950-1990 period is

simulated for the first decade of the 21st century. It is explained by a strong increase of particulate organic matter over central Africa and sulphates over Asia for the four RCPs. After 2010, the projections show different evolutions both in term of types of aerosols and regional features. The common characteristic is the general decline in the global aerosol content (and for all anthropogenic components) between 2010 and 2100. However, two exceptions to this general decline occur. First, a burst of sulphates over Asia between 2030 and 2080 in the RCP6.0 scenario leads to a subsequent slowdown of the global total aerosol decrease. The second notable feature is a delay (compared to other RCP) of the inversion of the growth rate in the RCP2.6 scenario due to a large increase of black carbon content over Asia which precedes a faster decline of aerosol content finally reaching in 2100 a level close to the one simulated before 1950 (also for the RCP4.5). The final content in 2100 for RCP6.0 and 8.5 is equivalent to the 1960s level. Whereas wind fields used to generate dust and sea-salt uplifts remain the same throughout the entire simulations, as described above, the dust and sea-salt contents evolve with time. The large increase of dust AOD (> 10%) is correlated in these simulations with a longer lifetime, due to a changed pattern of wet deposition in future climate. Indeed, even if the global value of precipitation increases in a warmer climate, the precipitation changes vary in amplitude and sign depending on the location (Dufresne et al., 2013). Regarding dust, the wet deposition is strongly weakened around 40°N due, in particular, to the precipitation decrease over a large area around the Black Sea.

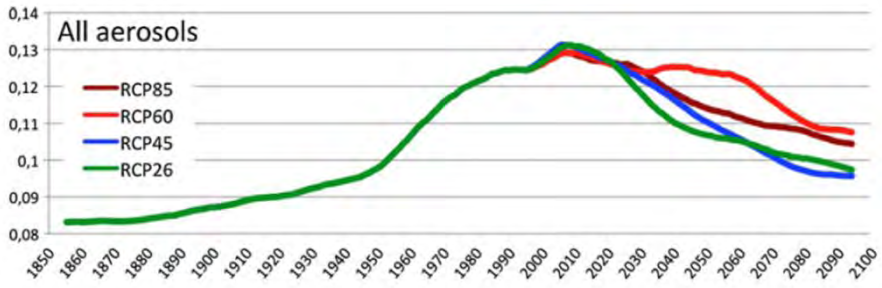

Figure 29: Evolution of the global aerosol optical depth at 550nm between 1850 and 2100 shown by types of aerosols simulated by the LMDz-OR-INCA model and then averaged using a 11-year running mean. The evolution after 2000 is simulated according to the 4 RCP scenarios.

In the previous CMIP exercise, the IPSL-CM4 considered only sulphate evolutions computed by (Boucher and Pham, 2002) for historical period and (Pham et al., 2005) for future projections based on the SRES scenarios. For the historical period, the values and distribution of emissions provided by (Lamarque et al., 2010) are similar to those of (Boucher and Pham, 2002). The slight decline of global emissions between 1980 and 1990 is similar. The (Lamarque et al., 2010) dataset extends longer (up to the year 2000), with a strong emission decline (> 16%) over the last decade. Some very large differences can be pointed out between the RCP trajectories and the SRES scenarios for future projections. In the SRES trajectories, four of the six scenarios lead to a peak in sulphate content followed by a rapid decrease, which slowed down around 2080. The two other scenarios exhibited an almost constant value of sulphate load throughout the whole 21st century or a constant decrease leading, at the end of the century, to a value equivalent to 37% of the 2000 global content. This last SRES scenario (A1T) is intermediate between the RCP2.6 and RCP4.5 projections regarding sulphate evolution. However, this scenario was skewed towards non-fossil energy source. Besides this drastic scenario, the cleanest realistic scenarios are the B1 family relying on the introduction of clean and resource efficient technologies together with reductions in material intensity. Such clean scenarios exhibit higher sulphate content than the RCP simulations, either temporarily or over the whole century.

Hence, according to the RCP scenarios, after peaking around 2010, the aerosol content is projected to decline strongly during the 21st century either monotonically for RCP8.5, 4.5 and 2.6

or after peaking around 2050 for the RCP6.0 scenario. This common feature in the emission scenario is strongly different from the SRES trajectories used for the previous IPCC report.

5.2 Regional climate modelling

5.2.1 Coordinated climate downscaling: Prudence, Ensembles, Euro-CORDEX

In Europe, regional climate modelling initiatives have been coordinated over the last decade through the PRUDENCE, ENSEMBLES and CORDEX experiments (the focus of the later including also other regions of the world beyond Europe). In the framework of each of these projects, a number of mesoscale climate models were implemented in a coordinated manner to document the spread of the models as well as forcing constrains (global models, emission projections, etc.). Given the sensitivity of regional air quality projections to the underlying regional climate model, we summarize in this section the main findings of previous initiative related to climate change projection in Europe in order to have a better insight on the uncertainties brought about by the RCM in the overall projection modelling system.

PRUDENCE (Christensen et al., 2007) was the first initiative in the early 2000's to produce 30 years time-slices simulations corresponding to the recent past and the end of the 21st century with regional climate models at about 50km resolution. The validation of the ensemble over the recent past showed that the models tend to produce a warm bias in summer and winter with a more limited cold bias in the transition seasons, and that these biases were larger for extreme warm and low temperatures (Jacob et al., 2007). The regional models were found to be less sensitive to the boundary conditions derived from global models in summer, highlighting the role of internal processes (such as the land surface models) for that season, whereas synoptic scale processes dominate in winter (Christensen and Christensen, 2007). For the same reason, the year to year variability was overestimated in summer (Jacob et al., 2007) and all the models projected an increase in the variability in the future (Vidale et al., 2007) even though the model spread was reduced in the prospective scenario compared to the control historical simulations (Christensen and Christensen, 2007).

ENSEMBLES was an opportunity to expand the work initiated in PRUDENCE by increasing the time period, producing transient simulations, investigating a larger array of large scale boundary conditions, etc. Some regional models were forced by several different global climate models which led to the conclusion that the spread between the scenarios was somewhat dominated by the spread between the boundary conditions obtained from global climate models. It was only by the end of the 21st century that the differences between the scenarios exceeded the variability of the regional and global models (Kjellström et al., 2011).

The current exercise, CORDEX (Giorgi et al., 2009) builds upon previous expertise and offers a framework for downscaling the latest CMIP5 global climate model results in a coordinated way for different regions of the world. This initiative is supported by the World Climate Research Programme. The European simulations are conducted in the EURO-CORDEX consortium (Gobiet and Jacob, 2012) and include the added value compared to the rest of the world to aim at a resolution of about 12km over Europe (covering Europe, North Africa, and European Russia), see Figure 30. The objectives of reaching such a resolution are:

- to improve, as compared to previous experiments (PRUDENCE, ENSEMBLES) the representation of extreme events, especially concerning the water cycle
- to have projections for impact studies of climate change with a more resolved nature, particularly for the development of climate services.

However one must keep in mind that fine scale representation does not remove much of the uncertainty, arising mainly from the simulation of synoptic structures and large-scale flow, when the limited area model is forced to the limits by a GCM.

EURO-CORDEX also used a lower resolution, 50 km, so that a maximum number of groups in the world, with limited computer power, can achieve the simulations. The use of two resolutions has also the advantage of allowing the study of the added value of a higher resolution.

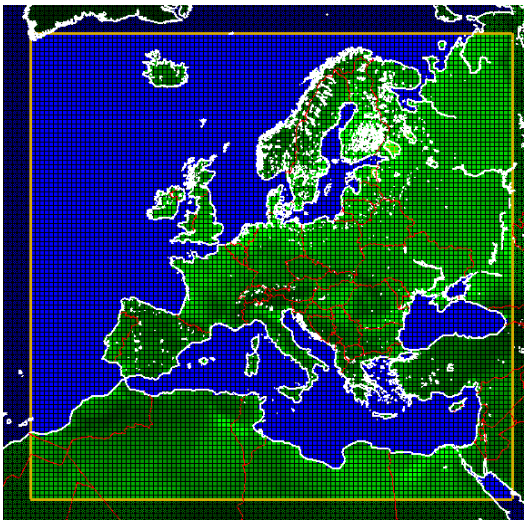

Figure 30: The Euro-Cordex domain for Regional Climate Projections at 0.11 or 0.44 degrees of resolution

Climate impact studies at the regional scale benefit today from a decade of research on the capacity of regional models to capture the European climate. There is now a well coordinated community of regional climate researchers that produces simulations that can be made available for the purpose of impact investigations in a similar way as being done at the global scale in the IPCC framework.

Thanks, in part, to the Salut'AIR project, IPSL and INERIS were able to develop an operational climate downscaling tool based on the IPSLcm5A coupled global climate model and the WRF mesoscale model in order to deliver 0.11 and 0.44 degree resolution projections and hindcast and join the European community of regional climate modelling. Beyond the simulations described in the present report, the IPSL-INERIS partnership also produced:

- an evaluation high-resolution simulation (12 km), forced by ERA-Interim reanalysis at the boundaries, over a period of 20 years (1989 - 2008), no nudging in order to properly assess the quality of the model and not that of a mixture and re-analysis and model;
- an evaluation simulation but at low resolution (50 km)
- an historical simulation starting in 1968 and ending in 2005 using the IPSL-GCM CM5MRA limits, and always without nudging, high resolution
- a simulation of scenario RCP4.5 from 2006 to 2100 at high resolution
- a simulation of scenario RCP4.5 from 2006 to 2100 at low resolution
- a simulation of scenario RCP8.5 from 2006 to 2100 at low resolution
- a simulation of scenario RCP2.6 from 2006 to 2100 at low resolution (still in progress)

The production of regional climate projections within the Euro-Cordex also offers a unique opportunity to participate in several international studies using the ensemble of simulations:

- a study on the evaluation of the simulation of heat waves (Vautard et al., 2013), also discussed in Section 5.2.2;
- a study on climate projections from the entire Euro-CORDEX (Jacob and al., 2013);
- an ongoing study about general evaluation of the ensemble (Kolarski et al, in prep);
- a study on the representation of the hydrology of the ensemble (Georgievski et al., in prep);
- a study on the representation of snow cover.

5.2.2 Evaluation of the IPSL-INERIS member of Euro-Cordex

Foreword: this section is a synthesis of (Vautard et al., 2013), in the following the reader is referred implicitly to that paper for further details.

The first published Euro-Cordex paper was performed in the framework of Salut'AIR and devoted to the capability of regional climate models to capture heat waves and extreme temperatures, which is of particular importance with regard to air quality, as these extremes generate acute pollution episodes. The Figure 31 shows for 21 simulations (including 7 high resolution), the bias of the 90th percentile of summer temperatures, often used as an indicator of high temperatures.

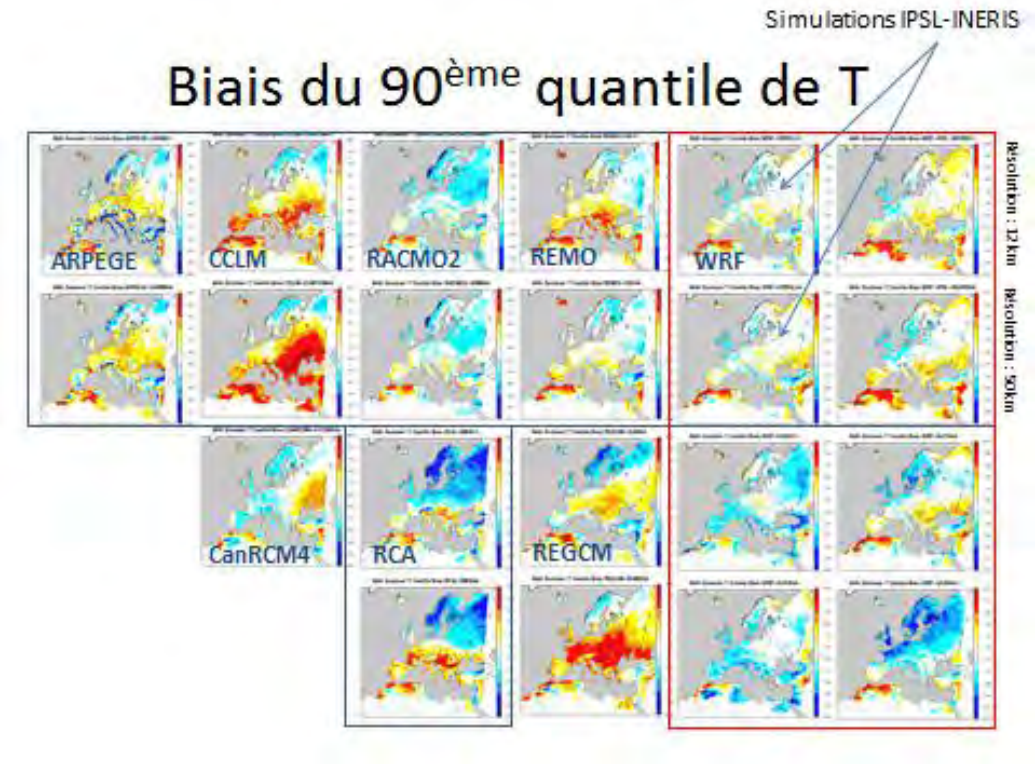

Figure 31: bias of the 90th percentile of summer temperatures for each of the 21 simulations used in the ensemble. The first line, and the upper box to the RCA model shows high-resolution simulations. The second line represents the simulation using the same model but with low resolution. The block of eight simulations on the right represents those using the WRF model.

Thanks to this study, we found that:

- the dispersion of simulations is large for the whole ensemble, as well as for the subset of various configurations of WRF;

- the high-resolution simulations (0.11 degrees versus 0.44) did not yield and improvement in the representation of heat waves;
- regional climate models tend to overestimate high temperatures in the South of Europe and underestimate in the North of Europe, which is consistent with previous studies (Boberg and Christensen, 2012)

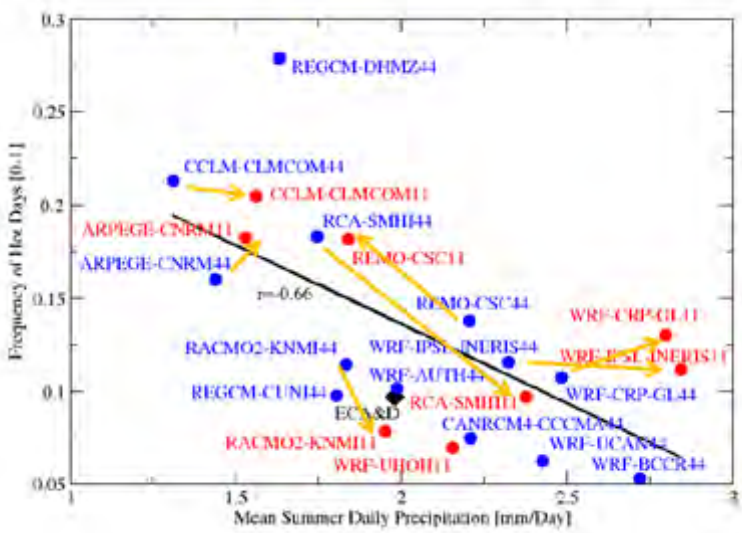

Figure 32: average frequency of days exceeding the 90th temperature centile vs. mean summer precipitation. High-resolution simulations are in red and the low-resolution simulations in blue.

In addition, with relation to air quality, we have shown that the models, in general, produced episodes of high temperature too persistent and of too high amplitude compared to observations. This could lead to overestimated average concentrations of ozone and aerosols.

The analysis of the models behaviour under climate scenarios is currently underway. Preliminary analyses confirm the previous results (ENSEMBLES, PRUDENCE) on the structure of warming expected in the summer, including a sharper rise in temperatures in southern Europe than in the north.

5.3 Regional air quality projections

Foreword: this section is a synthesis of (Colette et al., 2013), in the following the reader is referred implicitly to that paper for further details.

In order to investigate the impact of climate change on future air quality in Europe, the CHIMERE Chemistry-Transport model was used using future conditions provided by the other activities of the project. Anthropogenic emissions of pollutants and precursors in Europe are obtained from the Global Energy Assessment (Section 2). Global Climate projected with the IPSLcm5 coupled climate model downscaled with WRF is obtained from the first iteration of the IPSL-INERIS stream contributing to Euro-Cordex (Section 5.2). Chemical boundary conditions prescribing future intercontinental transport of pollution are obtained from the LMDz-OR-INCA contribution to the ACCMIP experiment (Section 5.1, see also Annex F for a focus on how is performed the coupling between LMDz-OR-INCA and Chimere in terms of particulate matter).

5.3.1 Anthropogenic emissions of pollutants

We focused on the two scenarios from the GEA set that include an identical representation of all current air quality legislation in Europe but differ in terms of policies on climate change and energy access. The Reference scenario (also called CLE1) assumes no specific climate policy and has a climate response almost identical to the RCP8.5 while the mitigation scenario (CLE2) includes climate policies leading to a stabilisation of global warming (hence resembling the RCP2.6). These scenarios are based on modelling with MESSAGE (Model for Energy Supply Strategy Alternatives and their General Environmental Impact) for the energy system (Messner and Strubegger, 1995;Riahi et al., 2007). The emissions (CH_4, SO_2, NOx (nitrogen oxides), CO, NMVOC (non-methane volatile organic compounds), Black and Organic Carbon, PPM (fine primary particulate matter)) are subsequently spatialised on a 0.5 degree geographical grid using ACCMIP emission data for the year 2000 (Lamarque et al., 2010). Further details of the GEA air pollution modelling framework are available in (Rao et al., 2012).

The total emissions of the main anthropogenic pollutants or precursors thereof are given in **Erreur ! Source du renvoi introuvable.**. The Reference or CLE1 scenario in absence of climate policy already shows a decline by 2050 of about 35-45% (depending on the constituent) of the current level of emissions emphasizing the efficiency of current legislation with regards to air pollutant emissions in Europe. The decrease is even larger when climate policy is implemented as in the CLE2 scenario. NOx and VOC decrease to 14-22% of current level, indicating a 50% co-benefit of climate policy for air quality. For particulate matter, given here as black and organic carbon, the decrease reaches almost a factor 10 in the case of BC in the mitigation scenario.

Table 10: Total annual anthropogenic emissions (Ggyr-1) of NOx (in NO2 equivalent), non-methane VOCs, sulphur dioxide (SO2), ammonia (NH3), carbon monoxide (CO) and black and organic carbon aggregated over Europe (15W, 40E, 30N, 65N) in the gridded GEA emission projections for 2005 (historical year), and 2050 under the Reference (CLE1) and Mitigation (CLE2) scenarios. Note that the geographical domain differs from the list of countries in Section 2 and we include here all activities sector instead of the 4 sector used before.

	GEA 2005	GEA CLE1/2050	GEA CLE2/2050
NOx	21 180	9 849	4 195
NMVOC	18 882	13 003	6 115
SO_2	19 872	4 929	1 689
NH_3	7 446	9 978	9 918
CO	63 865	20 019	10 520
$PPM_{2.5}$	4 284	2 101	1 540
BC	780	254	89
OC	1 696	397	319

5.3.2 Future Scenarios

We investigate two possible future scenarios (CLE1: reference – business as usual- and CLE2: mitigation) that we compare to the present-day situation. In order to assess the impact of using a climate model instead of meteorological reanalyses, the present-day situation is duplicated with the two types of possible forcing. In the following, we will thus refer to four experiments:

- ERA-hindcast: Meteorology computed using the ERA-interim reanalysis for the 1998-2007 decade, downscaled with WRF at 50km resolution. The boundary conditions are provided by the LMDz-OR-INCA for the present day (average centred on 2005) using historical ACCMIP emissions. Anthropogenic emissions of air pollutants over Europe are given by the GEA dataset for the year 2005.

- GCM-historical: Same boundary conditions and anthropogenic emissions as ERA-hindcast, but the meteorological driver is a downscaled version (with WRF at 50km) of the IPSLcm5 coupled climate models for the years 1995-2004.
- 2050-Reference: The 2045-2054 decade of the downscaled IPSLcm5 model along the RCP8.5 pathway provides the meteorological forcing. The RCP8.5 pathway is also used for the LMDz-OR-INCA boundary conditions of trace species. The reference (CLE1) projection of GEA provides European emissions of pollutants.
- 2050-Mitigation: Same meteorological forcing and boundary conditions as for 2050-Reference but along the RCP2.6 pathway. The GEA mitigation (CLE2) projection of GEA provides emissions of pollutants.

5.3.3 Regional Climate Projections

SALUTAIR was a pioneer project, but its timing, combined with the overall delay of the completion of the CORDEX exercise (all groups), did not allow the use of the high-resolution simulations introduced in Section 5.2. Their use, with a chemistry-transport model of the same resolution, still remains to be tested because the required resources are very important for simulations over time periods of several decades. The project however used the first low-resolution simulations (50km), carried out under EURO-CORDEX and presented in Section 3.5.

5.3.4 Projected changes in air quality concentration

Figure 33 and Figure 34 display the GCM-historical, ERA-hindcast and projections for ozone and total $PM_{2.5}$ (including secondary aerosols) concentration fields. Absolute values are given for the GCM-historical simulation while differences relative to the GCM-historical simulation are provided for the remaining configurations. Such differences are only plotted where found to be statistically significant with a student t-test at the 95% confidence level (the difference being set to zero where insignificant).

Ozone

Projected ozone changes are discussed on the basis of two different metrics in Figure 33. The average summertime daily maxima (based on 8-hr running means) of ozone (O_3^{max}) is provided since it can be readily compared with the literature. However, in order to perform an assessment relevant for health impacts we also focus on SOMO35, an indicator designed to capture detrimental impacts of ozone on human health and defined as the annual sum of daily maximum over 35ppbv based on 8-hr running means (expressed in $\mu g.m^{-3}$.day according to (EEA, 2009)).

The average situation for the GCM-historical (2005) simulation resembles the usual picture (e.g. (Colette et al., 2011)): a sharp latitudinal gradient with the exception of pollution hotspots over Europe. The difference between the GCM-historical and ERA-hindcast simulation provided on the second row confirms that the climate model is less favourable to ozone build-up than the actual meteorology over the recent past.

A closer look into the frequency of stagnation episodes suggests a limited responsibility of unfavourable weather regimes in the climate model. Even if (Manders et al., 2012) pointed out this factor, in our case the GCM-historical simulation is actually more conducive to stagnant summertime episodes that the ERA-hindcast with a frequency of calm days (average wind speed below 3.5m s^{-1}) of 31% and 23%, respectively, and a mean duration of calm spells of 2.45 and 2.16 days (see the similar findings of (Menut et al., 2012a;Vautard et al., 2012)).

As mentioned in Section 4.5, future biogenic emissions also play a major role in the formation of ozone.

Last, we can mention that temperature, incoming radiation, or even specific humidity can also play a direct role onto atmospheric chemistry, although these factors are much more difficult to isolate (Menut, 2003).

Both projections for 2050 indicate a decrease of daily maximum ozone compared to the GCM-historical climate simulation, but the magnitude of this decrease is moderate for the reference scenario. The situation is however more complex under the reference scenario for the ozone human health exposure index, since SOMO35 actually increases over a significant part of Europe. The mitigation scenario achieves a much higher degree of emission reduction. As a result, SOMO35 decreases sharply, especially in the Mediterranean area where the levels were highest. On a more quantitative basis, in order to emphasize the projected changes in high-exposure areas, we apply a weighting function to the SOMO35 fields depending on the population density. We find that the population-weighted SOMO35 increases by 7.4% (standard deviation ±5.4) in the reference scenario whereas it decreases by 80.4% (±2.1) in the mitigation case.

Particulate matter

In addition to primary particulate matter prescribed in anthropogenic emissions (black carbon – BC – and organic carbon – OC) and derived in the natural emissions (dust and sea salt), CHIMERE accounts for the formation of secondary aerosols that undergo a range of microphysical transformations including nucleation, coagulation, and absorption. For inorganic species such as nitrate (NO3p), sulphate (SO4p) and ammonium (NH4p) the thermodynamic equilibrium is diagnosed using the ISORROPIA model (Nenes et al., 1998). For semi-volatile organic species, the Pankow (Pankow, 1994) partition coefficient is used for hydrophobic particles and aerosols derived from isoprene, while the Henry law is used for hydrophilic compounds. Chemical formation of secondary organic aerosols (SOA) is represented with a single step oxidation of the relevant precursors and gas-particle partitioning of the condensable oxidation products (Bessagnet et al., 2008a).

The average fields of fine particles ($PM_{2.5}$) in Figure 34 for the GCM-historical (2005) simulation display local maxima over the main air pollution hotspots besides the large influx at the southern boundary of the domain (desert dust). The bias towards too high precipitations (Section 5.2) in the GCM-historical climate simulation has a limited impact on the average load of $PM_{2.5}$ over Western Europe that is 12.14µg m^{-3} and 12.11µg m^{-3} in the GCM-historical and reanalysis simulations, respectively GCM-historical ERA-hindcast. The decrease by 2050 is very large, with $PM_{2.5}$ concentrations dropping down to 4.1 and 2.3µg m^{-3} over Western Europe areas in the reference and mitigation scenarios, respectively.

A closer look in the average individual aerosol components over Western Europe is provided in Figure 35. Note that individual PM components sum up to PM_{10}, instead of the $PM_{2.5}$ that are used elsewhere in the paper because of their higher relevance for air quality purposes.

All the secondary aerosols decrease in the future as a result of decreasing anthropogenic emission of precursors. Secondary organic aerosols are the only species that maintain their relative importance due to the contribution of biogenic precursors in their formation process. As far as secondary inorganic aerosols are concerned it is worth mentioning that the small increase of NH_3 emissions in the GEA projections - Section 5.3.1 and (Colette et al., 2012b) - is not reflected in the projected formation of particulate NH_4^+. Whereas NH_3 emissions increase by 22% and 21% for the reference and mitigation scenario, respectively, between 2005 and 2050, we find that NH_4^+ decreases from 4.05µg m^{-3} in the GCM-historical 2005 simulation to 1.43µg m^{-3} and 0.49 µg m^{-3} in the reference and mitigation projection, respectively. This feature emphasises the probable limiting role of NOx emissions through the availability of HNO_3 in rural areas (Hamaoui-Laguel et al., 2012) that do exhibit a strong decrease in the future. The reason why such behaviour is not reported in coarse global chemistry transport model projections deserves further investigation

(Fiore et al., 2012;Shindell et al., 2012). The most prominent feature in the projection of aerosol composition is the increase of the relative importance of natural aerosols such as dust and sea salts in the future (right panel of Figure 35).

We find that population-weighted $PM_{2.5}$ decreases by 61.8% (±3.1)and 78.0% (±1.8) in the reference and mitigation scenarios, respectively. It appears that air quality legislation (that is identical in both scenarios) somewhat dominates the relative change in population-weighted $PM_{2.5}$ concentrations, the impact of the climate policy (that differs in both scenarios) is not as large as observed for the ozone population-weighted concentrations.

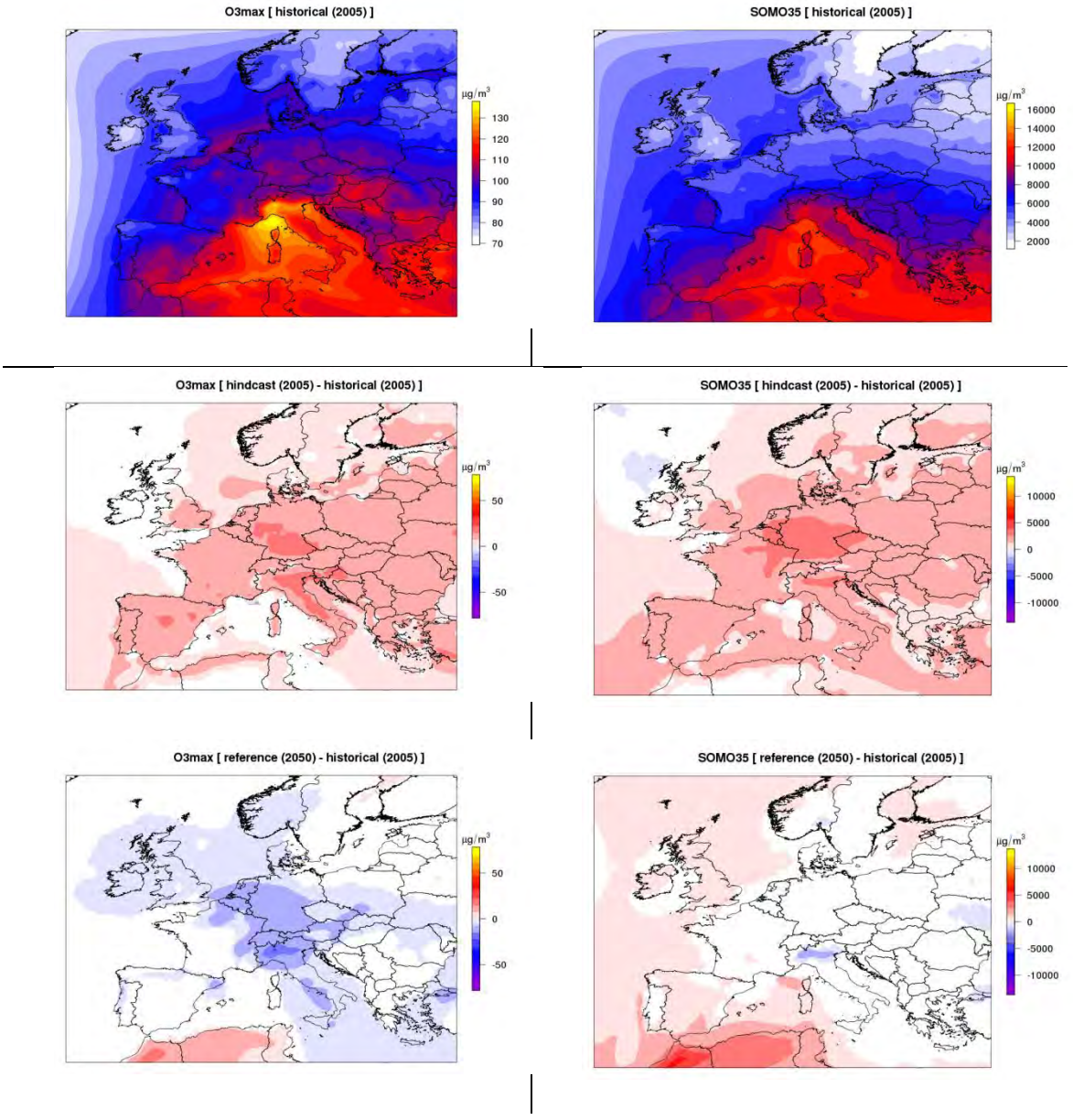

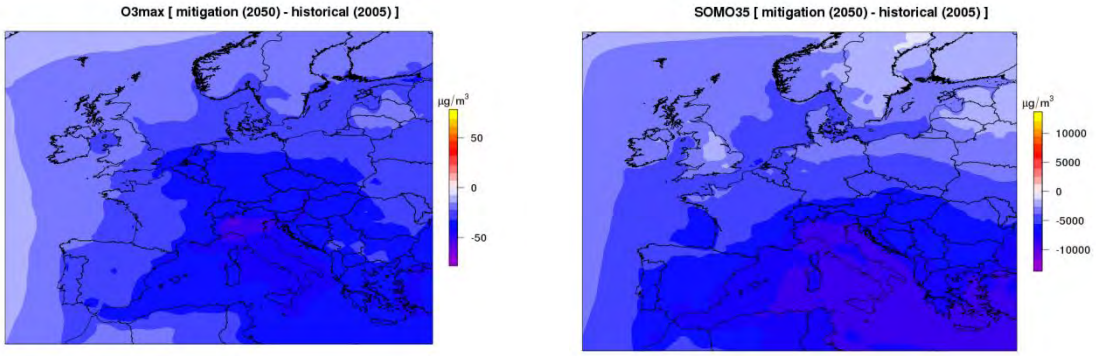

Figure 33: Top row (from left to right): average fields of O_3 as summertime average of the daily maxima (O_3^{max}, µg m^{-3}), and SOMO35 (µg m^{-3} day) in the control (2005) simulation (averaged over 10 years corresponding to the current climate). Following rows: difference between the simulations for the reanalysedERA-hindcast and then for the reference (CLE1) and mitigation (CLE2) 2050 projections taken with respect to the GCM-historical climate simulation (2005). The differences are only displayed where significant given the interannual variability of ten years.

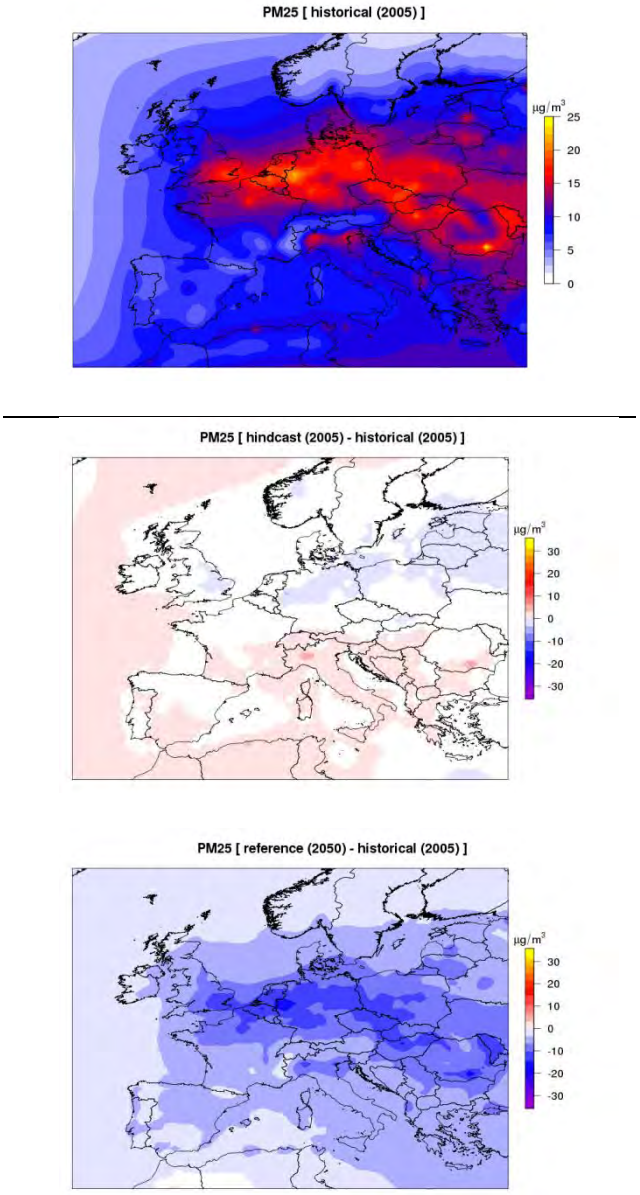

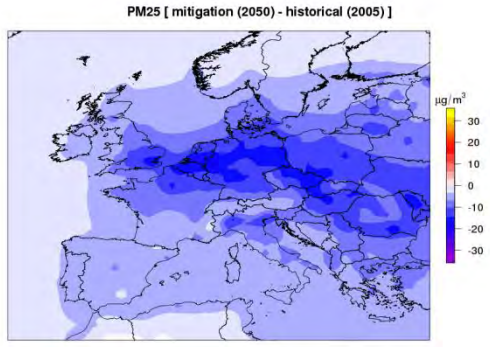

Figure 34 : Same as Figure 33, for $PM_{2.5}$ (annual mean, µg m^{-3})

5.3.5 Disentangling the driving factors

A comprehensive sensitivity analysis replicating the above mentioned experiment but changing the drivers one by one allow concluding on the quantitative contribution of (1) anthropogenic emissions, (2) long range transport and (3) climate change to the net response (Figure 36). This experiment is described in details in (Colette et al., 2013). The main findings are:

The climate penalty bearing upon ozone is compensated by the projected changes in precursor emissions and to a lesser extent by intercontinental transport of pollution. Whereas the first studies on the sole impact of climate on ozone pointed toward a strong penalty brought about by climate change (Meleux et al., 2007), more recent assessments including air pollutant emission projections already emphasized the larger role of the latter (Hedegaard et al., 2012;Langner et al., 2012a). As far as intercontinental transport of pollution is concerned, a significant contribution was already envisaged by (Langner et al., 2012a;Szopa et al., 2006).

We conclude that the overall climate penalty bearing upon ozone is confirmed, and its geographical patterns present some degree of robustness. At the same time, its importance should not be overstated. On a quantitative basis, we find that the air quality legislation being envisaged today should be able to counterbalance the climate penalty. On the contrary, the sensitivity to background changes (resulting from both intercontinental transport of pollution and the impact of global climate change on the ozone burden) was overlooked in the literature, whereas its impact competes even more than the climate penalty with the beneficial air quality legislation.

For particulate matter, the small benefit brought about by climate change is largely dominated by the response attributed to changes in air pollutant emissions. As noted in Section 2.4.2, mitigation in the industrial and ground transportation sectors dominates in WEU while the power plant sector offers larger scope for reduction in EEU. The contribution of boundary conditions is moderate. We note however that there is no consensus whether climate change constitutes a penalty or a benefit for particulate matter (Jacob and Winner, 2009). At the same time a considerable attention is devoted to the investigation of direct and indirect impacts of aerosols on climate. Increasing the robustness of the anticipated impact of climate change on particulate matter should become a key research priority in the coming years.

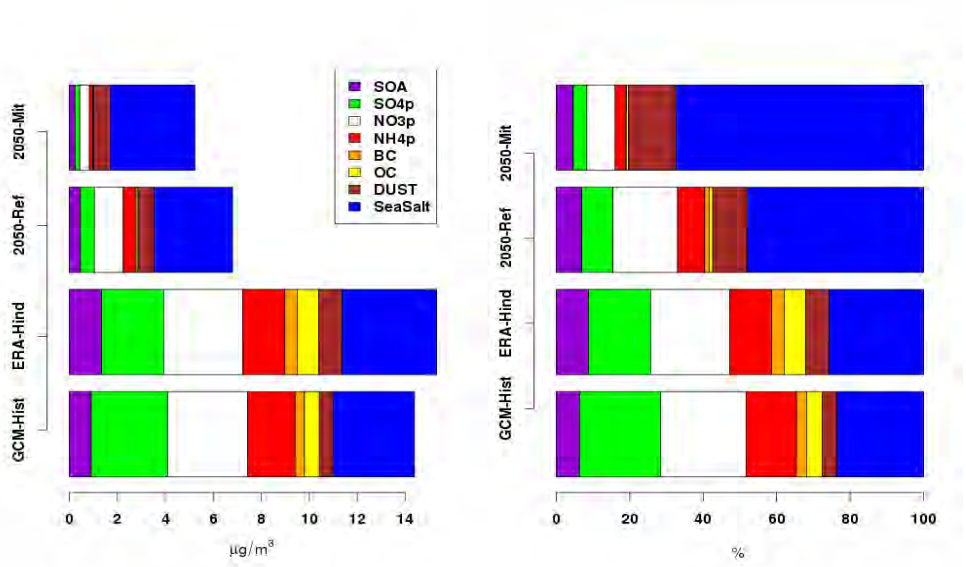

Figure 35 : Average aerosol composition over Western Europe for the two simulations corresponding to the present-day conditions (GCM-historical and ERA-hindcast) as well as the two scenarios for 2050 (CLE1: Reference and CLE2: Mitigation). Absolute concentrations are given on the left panel and relative contributions to total PM_{10} (expressed in percentages) are given on the right panel.

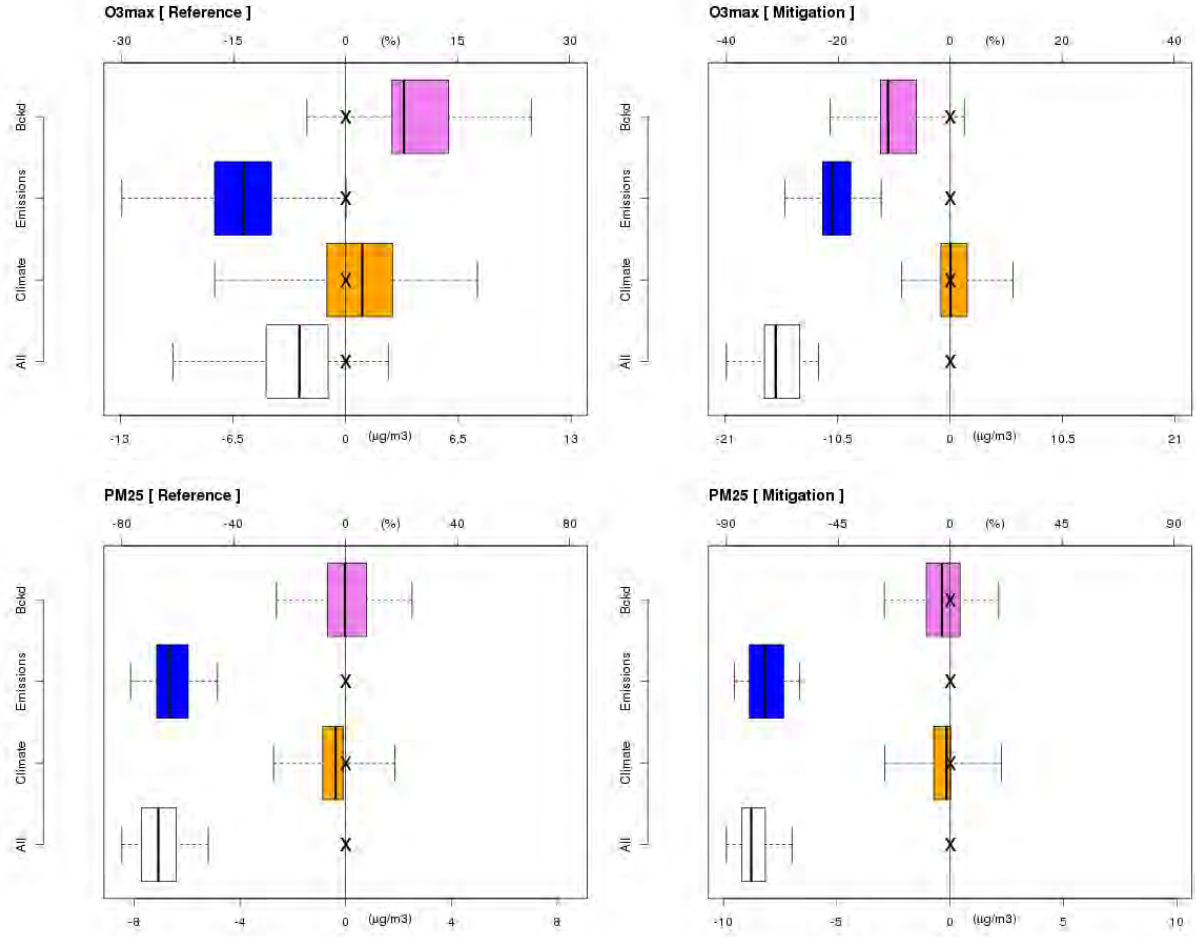

Figure 36: Quantitative decomposition of the relative contribution of climate, European anthropogenic emissions, and intercontinental transport (Bckd) to the net (all) change of ozone daily maxima and PM2.5 annual mean for the Reference and Mitigation scenarios.

5.3.6 Bias correction and population-weighting modelling

In order to be able to produce integrated air quality and climate projection we had to alter two key characteristic of the operational air quality modelling chain: (1) the meteorological driver was changed from a reanalysis to a climate model and (2) the spatial resolution was reduced from about 10-25km to 50km. These changes bear upon the confidence we have the results, it is therefore legitimate to do our utmost to document the associated uncertainty and attempt to correct any potential bias.

Biases of the climate model

As mentioned in Section 3.5, the global climate model and its downscaled version suffer from a cold and wet bias when compared to reanalysis over the present period. That being said, we should add upfront that it is not because the climate model exhibits a bias that its projections are not reliable. An over-fitted climate would perform ideally for the past, yet being very poor for future projections. That is why, in the vast majority of climate literature, model variability is investigated rather than absolute differences. When it comes to climate impact modelling the perspective changes however; and the absolute differences do matter, hence raising new challenges. Ideally, one should make use of model ensembles to cope for biases of individual models, but ensemble raise a significantly larger computational challenge for regional air quality and climate projections.

An alternative to ensemble modelling consist in using statistical methods to correct the biases of the climate model. Such an endeavour was introduced in Section 3.6 where we performed an upstream quantile matching of the climate model. Here we implement the same statistical correction, but in a downstream manner.

We compare the end results of the Regional air quality and climate modelling system (output from Chimere) for the current period driven with reanalyses or with the downscaled climate model (Section 5.3.4). The differences observed over the current period are combined with the differences between the simulation for the present and 2050 in order to propose a correction of the projection. The statistical technique used to perform this correction is the Cumulative Distribution Function transform (CDF-t) (Michelangeli et al., 2009)that builds upon the quantile-matching strategy, i.e. associating to a modelled value, the value in a control distribution that has the same probability (Déqué, 2007). It has been extensively used in the past to downscale and correct climate model output (Flaounas et al., 2011;Vrac et al., 2012), and (Colette et al., 2012a) introduced the potential of the method for air quality modelling. We show here the results for ozone only but the same correction was applied to $PM_{2.5}$.

The cumulative distribution functions of Figure 37 illustrate the efficiency of the technique. At a given grid point, the Y-axis provides frequency of occurrence of the O_3^{max} levels given in the x-axis. The underestimation brought about by the change of meteorological driver can be seen through the comparison of the CDF in the ERA-hindcast and GCM-historical simulations. After applying the quantile matching, the CDF become virtually identical. And a similar correction can be applied to the future projections, provided a bias-corrected view of future air quality.

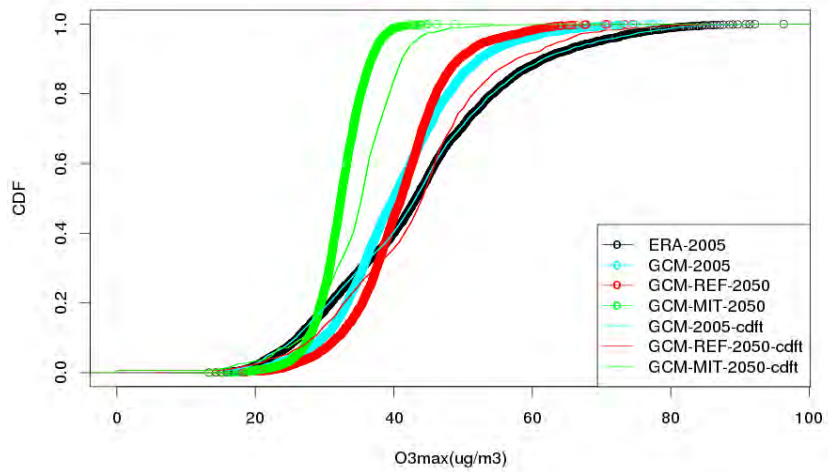

Figure 37: Cumulative Distribution Function of daily O_3 maxima in Paris over ten years in the four regional air quality and climate model decades (ERA-2005: ERA-hindcast, GCM-2005: GCM-historical, GCM-REF-2050: Reference projection, GCM-MIT-2050: Mitigation projection) and after applying the CDF-t correction.

The maps of Figure XX show the average SOMO35 fields in the projections before and after applying the CDF-t correction thanks to which the average of the GCM-historical scenario becomes identical to ERA-hindcast. These fields will be use for the Health Impact Assessment presented in Section 6. Although this type of approach solves a major source of uncertainty in climate modelling (the discrepancies of climate models that we can document over the historical periods), it does not guarantee an increased robustness of the results which, when it comes to climate modelling, can only be achieved through ensemble approaches.

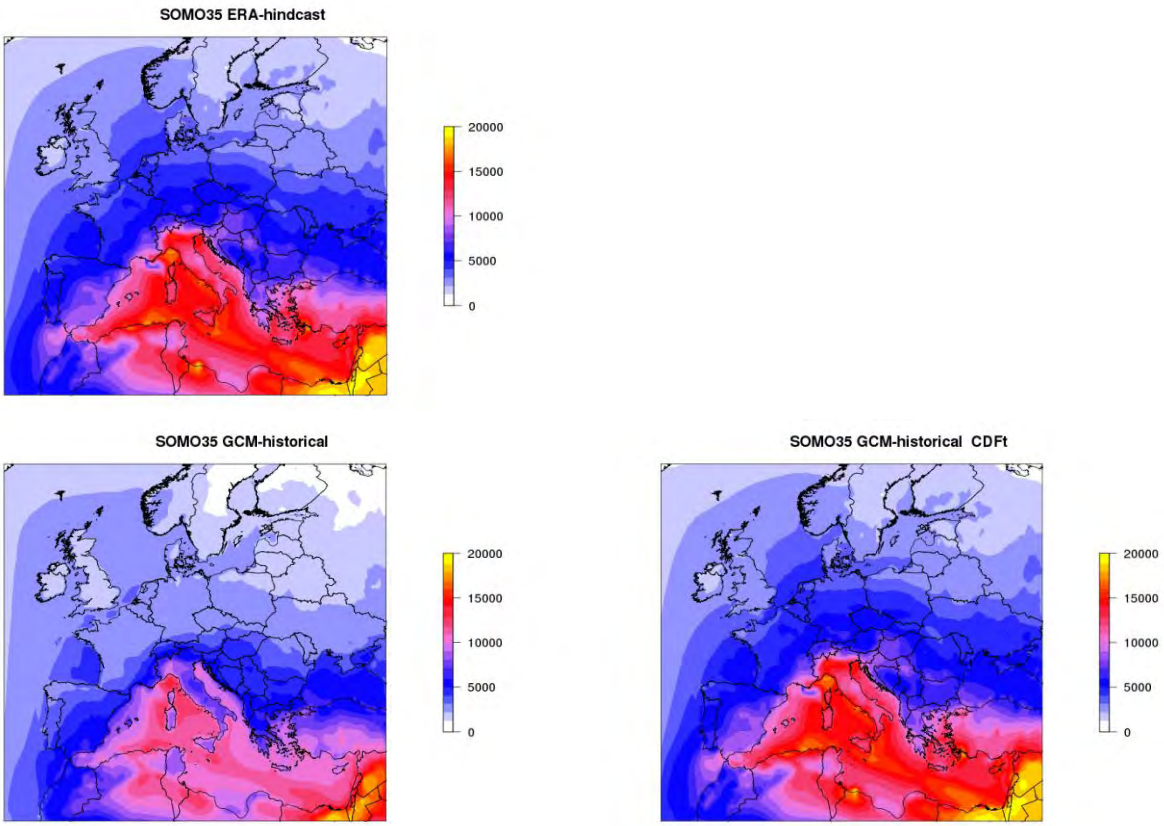

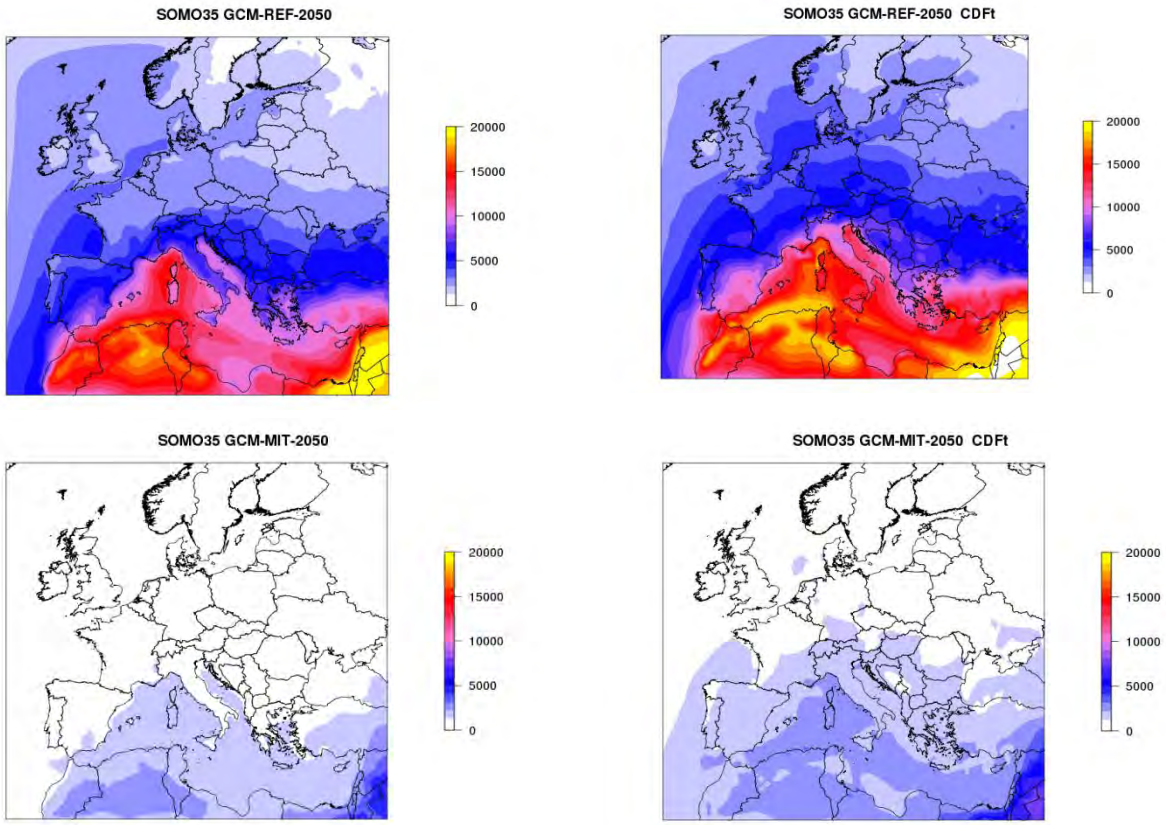

Figure 38: Average SOMO35 fields for the four regional air quality and climate model decades (left) and after applying the CDF-t correction (right)

Population weighting modelling

The approximations related to the use of a coarse (50km) resolution should also be corrected for, to the extent possible. Using a coarse setup for the Chemistry-Transport model alters non-linear processes (in particular in relation with chemistry) but also ignores sub-gridscale covariance between population and pollutant concentration. We developed an innovative technique designed to capture the impact of sub-gridscale covariance but also included implicitly a correction for non-linear high-resolution chemistry. By targeting primarily population weighted concentrations, our approach is closer to that of (Denby et al., 2011) rather than the urban increments used in GAINS (Amann et al., 2011a).

We used two annual Chimere simulations at 50km and 7km resolution and compared the daily population weighted concentrations at each grid point (Figure 39). The fact that some emission sources and population density are strongly correlated leads to much higher population weighted concentrations estimates in high-resolution air quality model outputs. For illustration purposes, Figure 39 also gives the ratio of $PM_{2.5}$ population weighted concentrations in the high and low model outputs (after they have been interpolated on the coarser grid. In parts of Europe, the population-PM2.5 covariance yields on average a ratio higher than unity, although in large parts of Europe the ratio is smaller than one, presumably as a result of spatial differences in the role of secondary aerosols. Would $PM_{2.5}$ population weighted concentrations be exclusively driven by primary species emitted in densely populated areas, this ratio would exceed unity in urban areas and be close to 1 elsewhere. The more complex geographical variability obtained here illustrates the important of secondary aerosol transport and transformation and the un-even balance of regional versus local pollution across Europe. In order to capture at the same time increments of

primary PM and decrements for secondary PM, we develop a downscaling strategy for total PM2.5, therefore aggregating all factors together.

Rather than using a multiplicative factor (the ratio of the lower right panel of Figure 39) we compute a simple first order linear regression at each grid point, on the basis of daily values. This regression is then applied to the population weighted concentrations in the coarse model. By dividing this coarse population weighted concentrations - that has been corrected for the subgrid-scale covariance of population and pollution - by the average population, we obtain an "effective pollution" load (Figure 40). This new "effective pollution", shall not be compared to observed concentration, yet it captures the amount of pollutant that "effectively" bear upon human health, in a way it can be presented as an analogous of the wind-chill of meteorologists.

This methodology is presented here for PM2.5 but we also developed an analogous technique for O_3^{max}, although in that case the correlation with population is mostly negative.

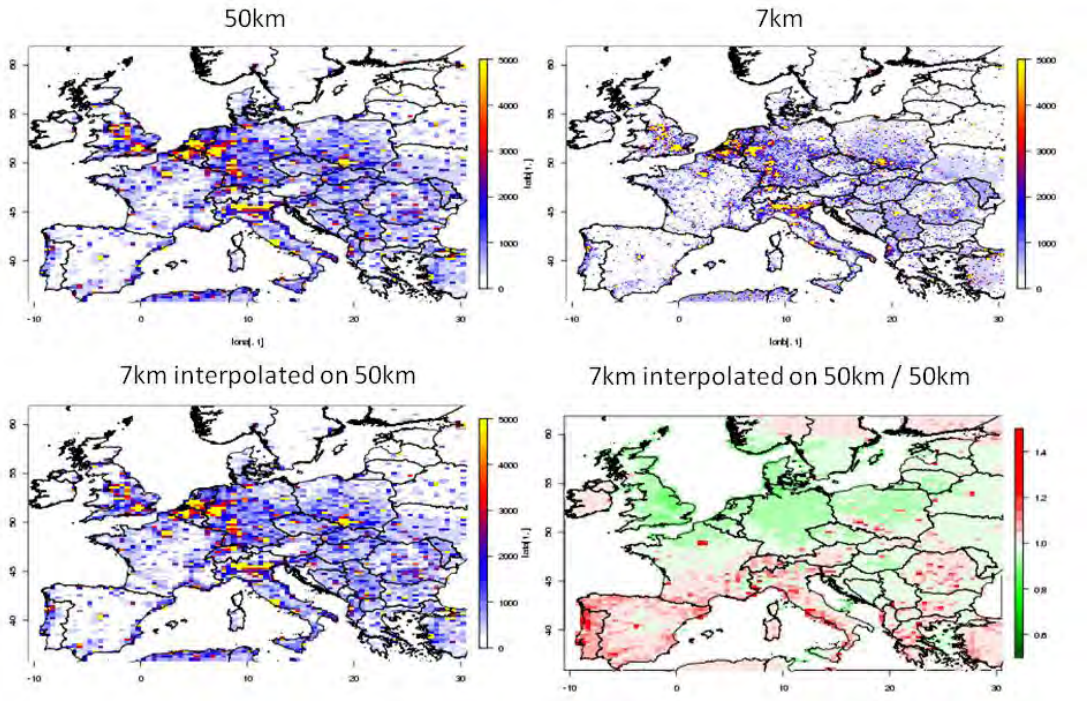

Figure 39: Population weighted concentrations of PM2.5 (as µg/m3 x khab) in two 1-yr Chimere simulation at 50 and 7km (top). The bottom row gives the population weighted concentrations modelled at 7km aggregated on the 50km grid (left) and the right panel gives the ratio of population weighted concentrations in both resolution once they have been aggregated on a common grid.

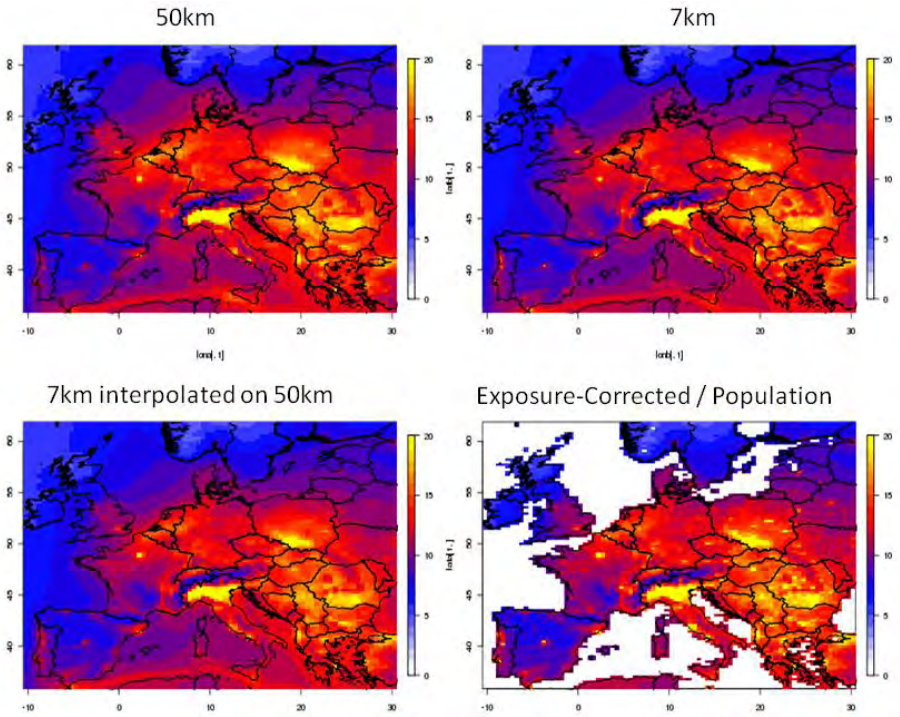

Figure 40: Top: row: average annual $PM_{2.5}$ level in the 50km and 7km model versions. Lower row: left: average $PM_{2.5}$ in the 7km simulation, aggregated on the 50km grid, right: corrected population weighted concentrations divided by the average population yielding an "effective $PM_{2.5}$ concentration".

Summary

Two new techniques designed to minimize the potential biases of regional climate and air quality projections were developed in the framework of the Salut'AIR project. A third approach (upstream CDF-t, Section 3.6) was also explored although it was not implemented in the operational production stream of simulation. In the following (Section 6) on Health Impact Assessment, we will focus primarily on the CHIMERE outputs, corrected of both climate and population weighted concentrations bias (Figure 41). A subsection on uncertainty will be devoted to the quantification of the relative impact of each of these corrections.

This work will be the focus of a paper to be submitted by fall 2013, and until this study has been accepted for publication the results should be seen as preliminary.

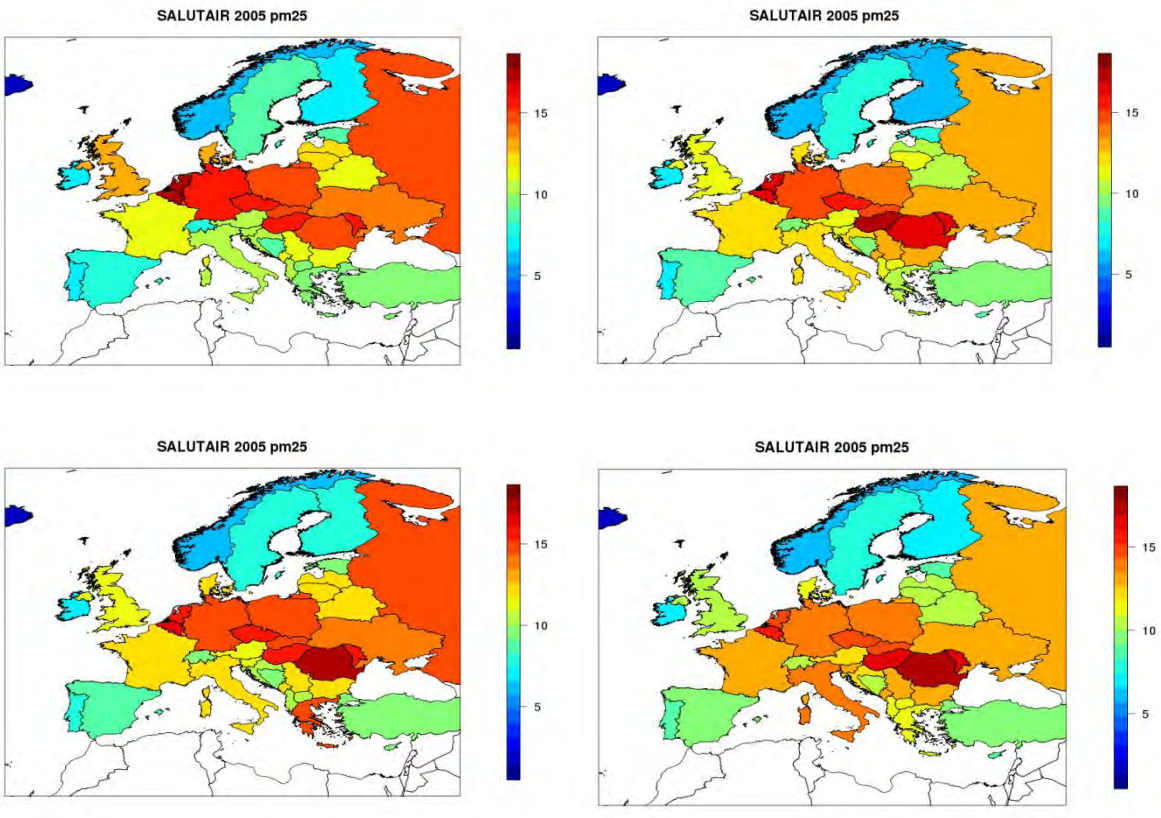

Figure 41: Average PM2.5 in the GCM-historical experiment, before any statistical correction (top left), after applying only the CDF-t correction for climate (top right), after applying only the sub-gridscale population weighted concentrations correction (bottom left), and after applying both corrections (bottom right).

6 Health impact assessment and cost-benefit analysis

Within the Salut'AIR project, a collaboration was developed between INERIS and the UK consultant Michael Holland (EMRC), involved since the 1990s in the development and application of cost-benefit analyses for the evaluation of European policy proposals. This collaboration led to the implementation, at INERIS, of the French version of the health impact and benefits assessment tool Alpha-RiskPoll[22]. The French version of the tool, Alpha-RiskPoll-France (ARP-FR), was set up to use pollution data coming from the chemistry-transport model CHIMERE.

The quantitative analysis of benefits in this report is focused on (monetised) health impacts. The effects of air quality on crops and materials, for which simple approaches to monetisation are available, remain out of the scope of this study. Health impacts are shown to represent the largest part of the quantifiable portion of overall monetised effects ((Holland et al., 2005a;Holland et al., 2005b;Holland et al., 2011;Amann et al., 2011b). Equally outside the scope of this study are the effects of air quality on ecosystems, for which monetization methodologies are still under development. The uncertainty induced by this limitation is considered in a qualitative way further below (Section 6.2.2).

6.1 Assessing health impacts with ARP-FR

The health impact and benefits assessment in Salut'AIR uses the ARP-FR tool. ARP uses the methods for benefits assessment that were first developed under the EC funded ExternE Project (External cost of Energy[23]) during the 1990s. These methods have been applied since the end of the 1990s to cost-benefit assessments of EC and UNECE policies and were thoroughly reviewed for use for the EU's CAFE programme (Krupnick et al., 2005). They are currently again under review for the revision of the EU Thematic Strategy for Air Pollution (WHO, 2013a, b)[24]. The methodology is extensively documented in (Holland et al., 2005a;Holland et al., 2005b;Holland et al., 2005c;Hurley et al., 2005;Holland et al., 2011;Amann et al., 2011b) and the above cited reviews.

6.1.1 Impact pathway approach

The health impact analysis carried out with ARP-FR uses the approach for quantification of effects which is known as the impact pathway approach, developed amongst others under the ExternE project. It represents a logical progression from emission and pollutant dispersion to quantification of impacts and monetary damage (Holland et al., 2011;Hurley et al., 2005).

Figure 42 illustrates the different steps in the calculation of health impacts and the models providing the related data in Salut'AIR. Air pollutant emissions come from IIASA's GEA scenarios (discussed in Section 2), dispersion of pollutants is modelled in the climate and air quality modelling suite presented in the preceding chapters. This suite also delivers exposure data (expressed as population weighted concentrations). Health impacts and their monetary equivalents (= damages) are calculated in ARP-FR, which thus delivers the necessary information on benefits, in terms of avoided health damages due to ambitious policies, for the cost-benefit analysis.

[22] The ARP version used for health impact assessment in the framework of EC and UNECE policies was developed by Michael Holland and Joe Spadaro.

[23] http://www.externe.info/externe_d7/

[24] Under the jointly funded WHO-EC projects REVIHAAP ('Review of evidence on health aspects of air pollution') and HRAPIE ('Health Risks of Air Pollution in Europe').

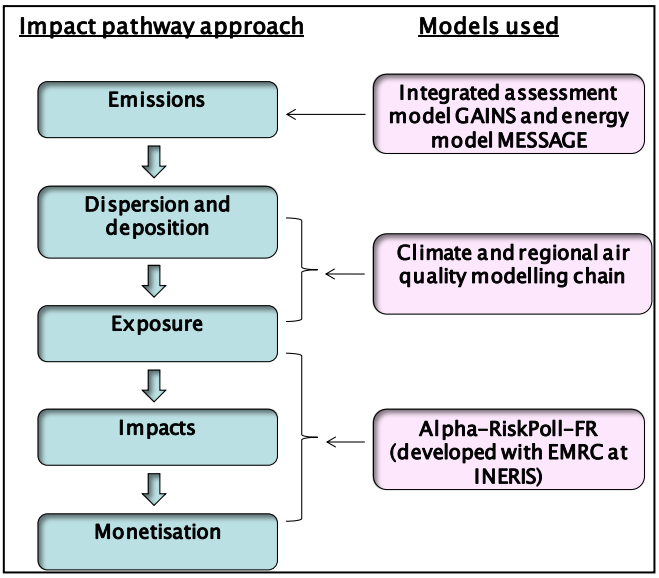

Figure 42: The impact pathway approach and models providing the calculation of emissions, dispersion, exposure (in terms of population weighted concentrations) and (monetized) impacts in Salut'air

ARP quantifies annual health impacts in terms of morbidity and mortality due to exposure to (inhalation of) $PM_{2.5}$[25] and ground level ozone. Effects of other pollutants such as PM_{10}, NO_2 and SO_2 on health are not separately included. While it is considered reasonable to add together the estimated health impacts of PM and of ozone, the addition of further impacts from NO_2 and SO_2, would create a risk of double counting, in particular with the estimated effects of fine particulate matter (Hurley et al., 2005). This approach was confirmed by (Miller et al., 2011).

The generic form of the equations for the calculation of impacts and then damage is (Holland et al., 2011):

- Impact = pollution x population at risk x dose-response function
- Economic damage = impact x unit value of impact

"Pollution" here refers to annual mean concentrations of $PM_{2.5}$ and to SOMO35[26]. The "population at risk" refers to the amount of sensitive people, where the distribution of population and of effects on demographics within the population (children, elderly, and people at working age) are accounted for[27]. For each type of impact quantified (cf. Table 11 below) incidence rates that are considered representative of the rate of occurrence of different health conditions across Europe are used to modify the population at risk (Holland et al., 2011).

6.1.2 Health end-points and monetary values used to quantify health impacts

The health impacts quantified in this analysis, together with the respective population at risk, the exposure metric used and the monetary unit value of impact are listed in Table 11. The table distinguishes 'core' health impacts (shaded in light blue in the table), for which concentration-response functions are considered most robust for use in a European policy context, and 'sensitivity' health impacts (shaded in pink) for which quantification is considered less robust. Mortality effects from chronic exposure to $PM_{2.5}$ are expressed in two metrics, in terms of loss of

[25] In line with WHO advice, all particles are treated as equally harmful, irrespective of source and chemical composition. This is because a precise quantification of the health effects of PM emissions from different sources or of individual PM components, is not possible according to current knowledge (WHO, 2007;Miller et al., 2011).

[26] The use of SOMO35 does not imply that a threshold for the effects of ozone on human health was found. Using SOMO35 results of the wish to limit quantification to ozone levels where there is positive evidence of an effect (Hurley et al., 2005;Miller et al., 2011).

[27] ARP-FR in its current version employs population data from the UN's World Population Prospects 2010 Revision (http://esa.un.org/unpd/wpp/index.htm).

life expectancy (total number of life years lost per year across the population) and in terms of premature deaths brought forward (number of deaths per year). These two estimates are not additive. Neither are the alternative monetary values (median, mean) for a given health end point. Following the methodology developed in the CAFE programme (which was itself under the guidance of the WHO-CLRTAP Task Force on Health[28]) we did not explicitly account for the adverse impacts of acute exposure to PM2.5. There is a growing body of evidence of impacts of short term exposure to PM2.5 although the effects of long-term are much larger (WHO, 2013a). Accounting for such effects in a health impact assessment raises important methodological challenges to avoid double counting (acute and long-term effects are partly interrelated, but the long-term effects are not the sum of all short-term effects).

Table 11: Health end-points for which impacts are assessed and corresponding monetary values, end-points contributing to the 'core impact indicator' are highlighted in blue.

End point	Population	Core or sensitivity	Aggregate monetised core indicator ("best estimate") in Salut'AIR	Impact	Pollutant	Exposure metric (population weighted)	Valuation (€, 2005)
Acute Mortality low VOLY	all ages	Core		Premature deaths	O3	SOMO35	40 000
Acute Mortality median VOLY	all ages	Core	X	Premature deaths	O3	SOMO35	57 700
Acute Mortality mean VOLY	all ages	Core		Premature deaths	O3	SOMO35	138 700
Respiratory Hospital Admissions	over 65 years	Core	X	Cases	O3	SOMO35	2 220
Minor Restricted Activity Days (MRADs)	15 - 64 years	Core	X	Days	O3	SOMO35	42
Respiratory medication use	over 20 years	Core	X	Days	O3	SOMO35	1
Minor Restricted activity days	over 65 years	Sensitivity		Days	O3	SOMO35	42
Respiratory symptoms	over 15 years	Sensitivity		Days	O3	SOMO35	42
Chronic Mortality LYL median VOLY	all ages	Core		Life years lost	PM	PM2.5 annual average	40 000
Chronic Mortality LYL median VOLY	all ages	Core	X	Life years lost	PM	PM2.5 annual average	57 700
Chronic Mortality LYL mean VOLY	all ages	Core		Life years lost	PM	PM2.5 annual average	138 700
Chronic Mortality deaths median VSL	over 30 years	Core		Premature deaths	PM	PM2.5 annual average	1 090 000
Chronic Mortality deaths mean VSL	over 30 years	Core		Premature deaths	PM	PM2.5 annual average	2 220 000
Chronic Mortality deaths mean VSL	over 30 years	Core		Premature deaths	PM	PM2.5 annual average	2 800 000
Infant Mortality median VSL	0-1 years	Core	X	Premature deaths	PM	PM2.5 annual average	1 635 000
Infant Mortality mean VSL	0-1 years	Core		Premature deaths	PM	PM2.5 annual average	3 330 000
Infant Mortality mean VSL	0-1 years	Core		Premature deaths	PM	PM2.5 annual average	4 200 000
Chronic Bronchitis	over 27 years	Core	X	Cases	PM	PM2.5 annual average	208 000
Respiratory Hospital Admissions	all ages	Core	X	Cases	PM	PM2.5 annual average	2 220
Cardiac Hospital Admissions	all ages	Core	X	Cases	PM	PM2.5 annual average	2 220
Restricted Activity Days (RADs)	15 - 64 years	Core	X	Days	PM	PM2.5 annual average	92
Respiratory medication use	5-14 years	Core	X	Days	PM	PM2.5 annual average	1
Respiratory medication use	over 20 years	Core	X	Days	PM	PM2.5 annual average	1
LRS symptom days	5-14 years	Core	X	Days	PM	PM2.5 annual average	42
LRS among adults with chronic symptoms	over 15 years	Core	X	Days	PM	PM2.5 annual average	42
Restricted Activity Days (RADs) - ext. days	over 65 years	Sensitivity		Days	PM	PM2.5 annual average	75
Asthma Consultations	0-14 years	Sensitivity		Consultations	PM	PM2.5 annual average	59
Asthma Consultations	15 - 64 years	Sensitivity		Consultations	PM	PM2.5 annual average	59
Asthma Consultations	over 65 years	Sensitivity		Consultations	PM	PM2.5 annual average	59
Consultations for URDs	0-14 years	Sensitivity		Consultations	PM	PM2.5 annual average	59
Consultations for URDs	15 - 64 years	Sensitivity		Consultations	PM	PM2.5 annual average	59
Consultations for URDs	over 65 years	Sensitivity		Consultations	PM	PM2.5 annual average	59

The health impacts and associated unit values of impact marked with an "x" in the fourth column designate those aggregated to the core impact indicator (highlighted in blue in Table 11) in the following used as "best estimate" in Salut'AIR. This choice follows a precautionary approach, by using, as equally done in current EC and UNECE policy analyses

- the median values for mortality valuation:

  Although (Krupnick et al., 2005) argue that conceptually, the mean would be the appropriate measure because mean values fully summarize the heterogeneity of values in the sample, the median is here preferred. The reason is that it is a conservative measure, being lower than the mean. Also, it may be considered as more robust, being not influenced by outliers, which can be prevalent in stated preference studies[29] as used for establishing the monetary values for mortality used in ARP.

[28] http://www.euro.who.int/document/e79097.pdf

[29] These studies estimate the willingness to pay for a modification in the risk of death.

- the loss of life expectancy as metric for $PM_{2.5}$ adult mortality:

  Loss of life expectancy – and not number of deaths - is the preferred approach in the CAFE analysis which followed WHO recommendations (Hurley et al., 2005). This is because there is a question on how fundamental air pollution has been to the death - the actual loss of life is likely to be small, the death might in any case have occurred within the same year (Krupnick et al., 2005;Hurley et al., 2005). Furthermore, the simplified approach used in CAFE estimating premature deaths without using life-tables tends to over-estimate effects. It actually fails to take into account that extra deaths under a higher air pollution scenario are in fact deaths postponed, but not avoided (Hurley et al., 2005). Further reasons for the preference of the life expectancy indicator are that results in terms of life years lost (or gained) are a direct outcome of cohort studies – considered in (Hurley et al., 2005) as the principal and most accurate representation of the effects of particles on mortality - and are based on the use of life tables.

  However, the estimate of the monetary value for a VSL (Value of Statistical Life, used for valuing premature deaths) is more easily defended methodologically than that for a VOLY[30] (Value Of Life Year, used for valuing loss of life expectancy), which led the CAFE peer review team to recommend the use of both metrics. Attributable deaths, valued by VSL, are therefore used in sensitivity analyses in current European policy analyses. The monetary values used for life expectancy changes are lower than those for estimates of deaths brought forward, in so far this is in line with a conservative estimate of damages (and benefits).

  Note that infant mortality due to PM exposure is assessed in terms of attributable cases, rather than life-years, thus using a different approach than for adults. Also mortality impacts (all ages) due to acute exposure to ozone are initially expressed in terms of premature deaths. In line with the CAFE methodology which assumes that people whose deaths are brought forward by higher air pollution are likely to have had serious pre-existing cardio-respiratory disease and that the actual loss of life expectancy may be small, the number of deaths is then converted to life years lost. This conversion assumes that on average each death brought forward involves a loss of life of 12 months.

- only core health impacts for mortality and morbidity:

  The CAFE approach distinguishes two sets of response functions. The core set groups those for which evidence was considered being more robust, the sensitivity set those for which quantification was considered less robust (Holland, 2013). The sensitivity functions are seldom used and their contribution to total damage is relatively small (cf. also Section 6.2.2.1).

However, the alternative metrics (VSL for all age chronic mortality from fine particulate matter) and aggregates also comprising the sensitivity health impact categories are used to calculate sensitivity ranges in the cost-benefit analysis below (Section 6.2.2.1). Sensitivity ranges also use alternative monetary values given in **Erreur ! Source du renvoi introuvable.**Table 11 for mortality, including next to CAFE mean estimates the recent updates for VOLY and VSL estimates (Desaigues et al., 2011;OECD, 2012).

Except for chronic bronchitis, the valuation of morbidity endpoints is less important for the overall health damage results than those of mortality. Still it seems worth mentioning that methods applied to develop monetary unit values for these end points partly differ from the methods applied to mortality. While valuation for the indicators chronic bronchitis and restricted activity days is based on willingness to pay studies (as also used for mortality), valuation for

[30] The value of life year is computed from the value of statistical life. For a more detailed discussion of methodological differences between estimates in terms of life expectancy and in terms of deaths brought forward (CGDD, 2012;Hurley et al., 2005;Krupnick et al., 2005).

medication use is based on tangible costs for the medical treatment, and valuations for medical consultations and hospital admissions are based on both, willingness to pay and medical treatment costs. Morbidity costs thus cover both, tangible treatment costs, opportunity costs and intangible costs, such as costs of anxiety or pain (CGDD, 2012).

All valuation data are expressed in 2005 prices to be consistent with the cost data for the GEA scenarios used in this analysis.

It is worth mentioning that we have opted for not applying any discounting in the cost-benefit analysis presented in Section 6.2. The practical reason is that cost numbers provided by the model GAINS are annual abatement costs; and that ARP was set up accordingly to provide annual benefits numbers. The analysis therefore takes a snapshot of a year. In principle, a policy analysis aimed at determining how much a policy is going to cost for a country or region should calculate the present value of costs and hence discount future costs and benefits. Doing this however opens an important discussion about which interest rate to use to discount future benefits. There might be a point in using the same interest rate as the one used to discount cost data. If this was done, the benefit cost ratio, i.e. the relative importance of benefits and costs would stay the same. For this reason we have opted for working with undiscounted data. This implies however, that the absolute numbers given have less meaning than the relative comparison of benefits and costs and hence the benefits/costs ratios.

6.1.3 Exposure to air pollution and associated health impacts and damage

The CHIMERE results[31] introduced in Section 5.3 are fed into ARP-FR in order to assess the health impact of the reduction in the exposure of the population to fine particles and to ozone. Figure 43 illustrates the reduction in the exposure of the population to fine particles between 2005 and 2050 (CLE 1 versus 2005) which is due to atmospheric policy (and occurs despite climate change). Additional reductions in the exposure are brought about by the ambitious climate policy (CLE 2 versus CLE 1).

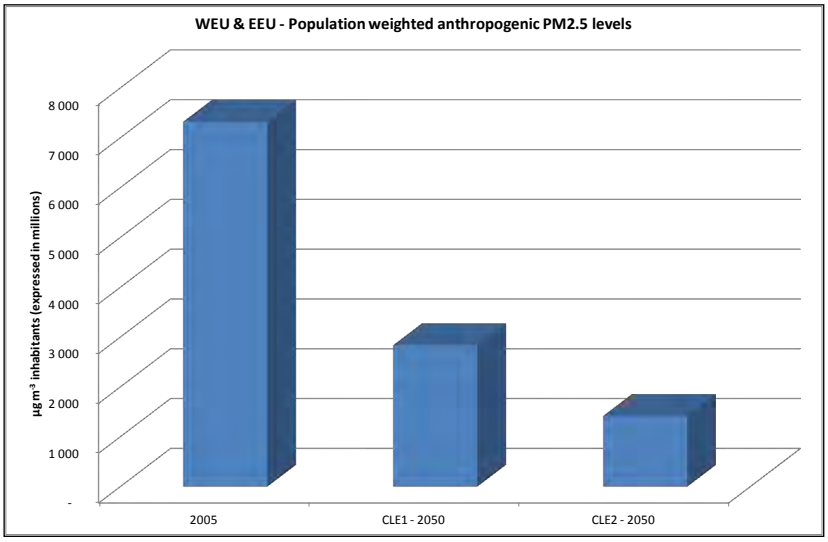

Figure 43: Population weighted concentrations of fine particles in 2005 and in 2050 according to the two scenarios

The quantification with ARP-FR of the corresponding effects on health in terms of life years lost from chronic exposure to $PM_{2.5}$ show a similar pattern (Figure 44).

[31] All results presented for the health impact assessment and cost-benefit analysis correspond to the model run with climate correction and urban increment/decrement.

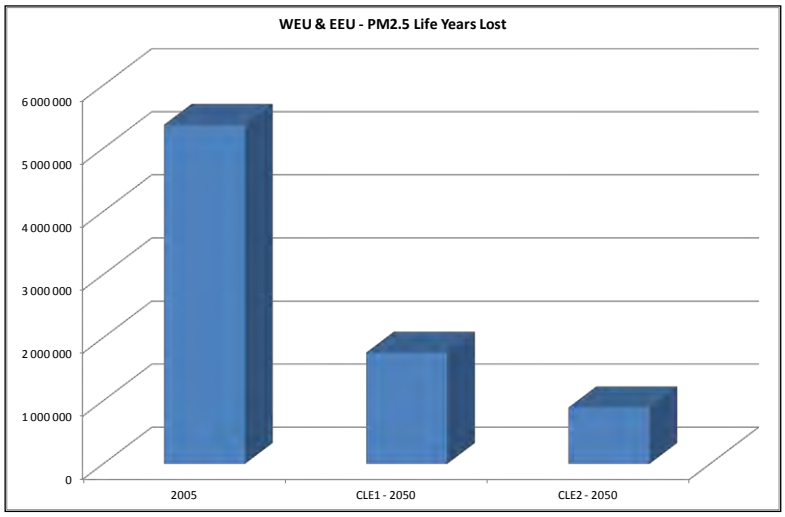

Figure 44: Life years lost from chronic exposure to $PM_{2.5}$ in 2005 and in 2050 according to the two scenarios

Exposure to ozone (SOMO35) shows a different pattern (Figure 45). There is only a small reduction between 2005 and 2050 in the reference scenario (CLE1 versus 2005) which is explained by a joint effect of global climate change and hemispheric transport which counterbalances the effects of the European atmospheric policy. A large part of long range transport is due to the fact that air quality policies are less developed, or actually absent, in some other world regions. Indeed, the climate conditions corresponding to CLE1 are those of the RCP8.5 which does show an increase in global ozone. When moving from CLE1 to CLE2 (both in 2050), the ambitious climate policy of the mitigation scenario does bring about a significant reduction in exposure to ozone. The climatic conditions of CLE2 correspond to those of the RCP2.6.

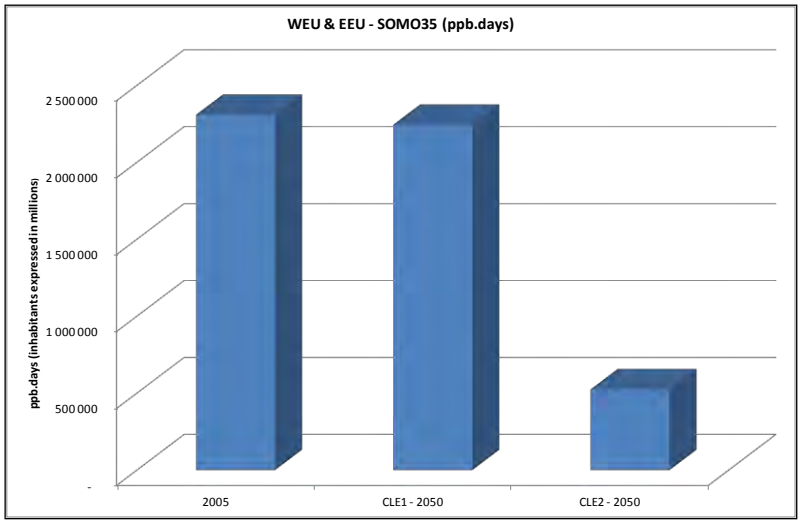

Figure 45: Population weighted concentrations to ozone in 2005 and in 2050 according to the two scenarios

Despite the low reduction in population weighted concentrations between 2005 and 2050 (CLE1 versus 2005) in Figure 45, health effects in terms of premature deaths from acute exposure to ozone (Figure 46) increase between 2005 and 2050 in the reference scenario (CLE1 versus 2005). This is the effect of an increase in Europe's population between 2005 (below 620 million inhabitants) and 2050 (almost 700 million inhabitants). The ambitious climate mitigation scenario however strongly reduces these health impacts (CLE2 versus CLE1).

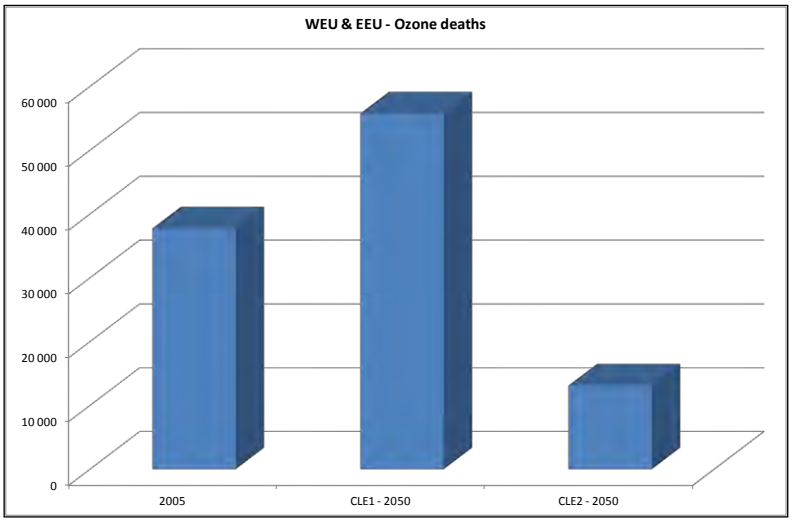

Figure 46: Premature deaths from acute exposure to ozone in 2005 and in 2050 according to the two scenarios

All annual health impacts comprised in the core aggregate indicator for Salut'air are quantified in Table 12.

Table 12: Estimated annual health impacts due to air pollution in 2005 and in 2050 according to the two scenarios (core indicator)

Impacts	WEU & EEU	Pollutant	2005	CLE1 - 2050	CLE2 - 2050
Acute Mortality (All ages) median VOLY	Premature deaths	O3	37 736	55 767	13 102
Respiratory Hospital Admissions (65yr +)	Cases	O3	29 669	61 361	14 399
Minor Restricted Activity Days (MRADs 15-64yr)	Days	O3	100 171 110	90 021 573	21 294 845
Respiratory medication use (adults 20yr +)	Days	O3	33 516 583	39 475 865	9 309 955
Chronic Mortality (All ages) LYL median VOLY	Life years lost	PM	5 370 638	1 761 520	891 230
Infant Mortality (0-1yr) median VSL	Premature deaths	PM	2 161	319	169
Chronic Bronchitis (27yr +)	Cases	PM	210 441	100 359	51 092
Respiratory Hospital Admissions (All ages)	Cases	PM	83 150	35 941	18 254
Cardiac Hospital Admissions (All ages)	Cases	PM	51 282	22 166	11 258
Restricted Activity Days (RADs 15-64yr)	Days	PM	453 169 956	157 534 882	79 757 470
Respiratory medication use (children 5-14yr)	Days	PM	5 081 740	1 871 472	952 977
Respiratory medication use (adults 20yr +)	Days	PM	37 161 881	16 944 013	8 616 990
LRS symptom days (children 5-14yr)	Days	PM	249 824 045	89 015 374	45 007 712
LRS among adults (15yr +) with chronic symptoms	Days	PM	383 215 915	171 076 139	86 974 976

The monetized equivalents of these health impacts are given in Table 13.

Table 13: Estimated annual health damage due to air pollution in 2005 and in 2050 according to the two scenarios (core indicator)

Damage, €M/year	WEU & EEU	Pollutant	2005	CLE1 - 2050	CLE2 - 2050
Acute Mortality (All ages) median VOLY	Premature deaths	O3	2 177	3 218	756
Respiratory Hospital Admissions (65yr +)	Cases	O3	66	136	32
Minor Restricted Activity Days (MRADs 15-64yr)	Days	O3	4 207	3 781	894
Respiratory medication use (adults 20yr +)	Days	O3	34	39	9
Chronic Mortality (All ages) LYL median VOLY	Life years lost	PM	309 886	101 640	51 424
Infant Mortality (0-1yr) median VSL	Premature deaths	PM	3 533	521	276
Chronic Bronchitis (27yr +)	Cases	PM	43 772	20 875	10 627
Respiratory Hospital Admissions (All ages)	Cases	PM	185	80	41
Cardiac Hospital Admissions (All ages)	Cases	PM	114	49	25
Restricted Activity Days (RADs 15-64yr)	Days	PM	41 692	14 493	7 338
Respiratory medication use (children 5-14yr)	Days	PM	5	2	1
Respiratory medication use (adults 20yr +)	Days	PM	37	17	9
LRS symptom days (children 5-14yr)	Days	PM	10 493	3 739	1 890
LRS among adults (15yr +) with chronic symptoms	Days	PM	16 095	7 185	3 653
Total, with VOLY, median			432 295	155 775	76 975

Figure 47 and Figure 48 illustrate the contribution of different health impacts to overall (monetized) health damage in 2050. What is important to note is, firstly, the fact that health costs

are dominated by $PM_{2.5}$ effects, and especially by chronic mortality (accounting for ≈ 66% of the overall health damage in the core aggregate indicator), chronic bronchitis (≈ 13%) and restricted activity days (≈ 10%). Secondly, the two graphs underline the difference in health costs when moving between the two scenarios. Health costs from ozone amount to approximately 4.6 % in overall health costs in CLE 1 in 2050, and to approximately 2.1 % in CLE 2.[32]

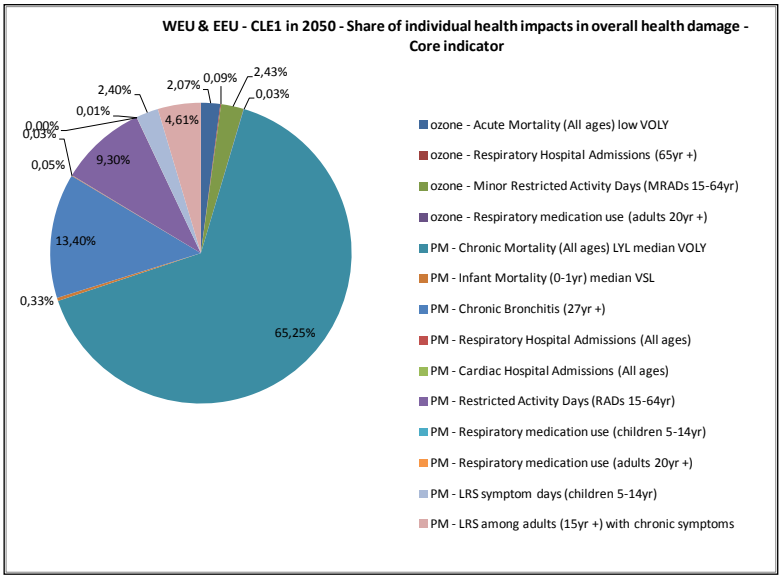

Figure 47: Contribution of individual health impacts to the overall health damage, CLE 1 in 2050 (core indicator)

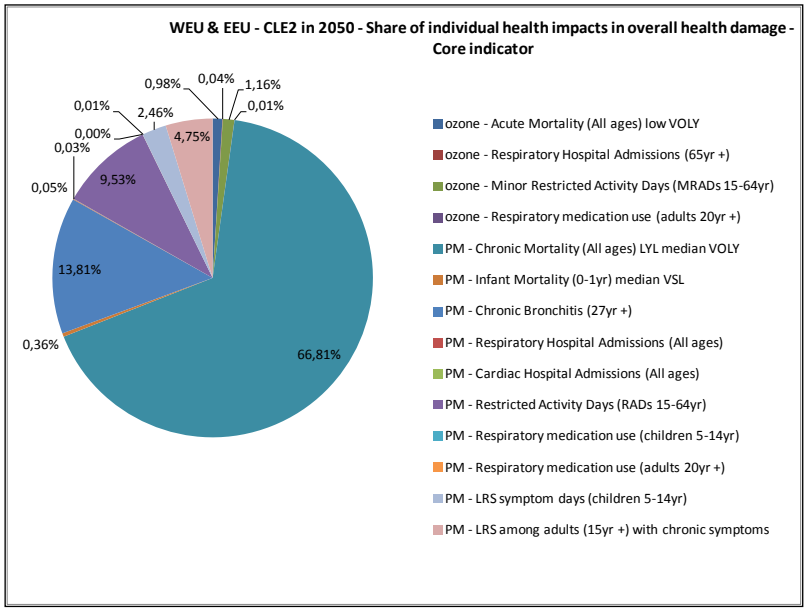

Figure 48: Contribution of individual health impacts to the overall health damage, CLE 2 in 2050 (core indicator)

Given that the total health damage is largely dominated by $PM_{2.5}$ health effects, the aggregate health damage (monetized core indicator, Figure 49) resembles the pattern shown in Figure 44 above for the $PM_{2.5}$ health effects. The implementation of current air pollution policy in 2030 and additional improvements in emission factors with economic growth in later years reduce total health damage by approximately 60% between 2005 and 2050 under the reference scenario (CLE

[32] In 2005, health costs from ozone account for approximately 1.5% in overall health costs (figure not shown here).

1 versus 2005). When moving from CLE1 in 2050 to CLE2 in 2050 (implementation of climate policy) health damage is reduced by approximately 50%.

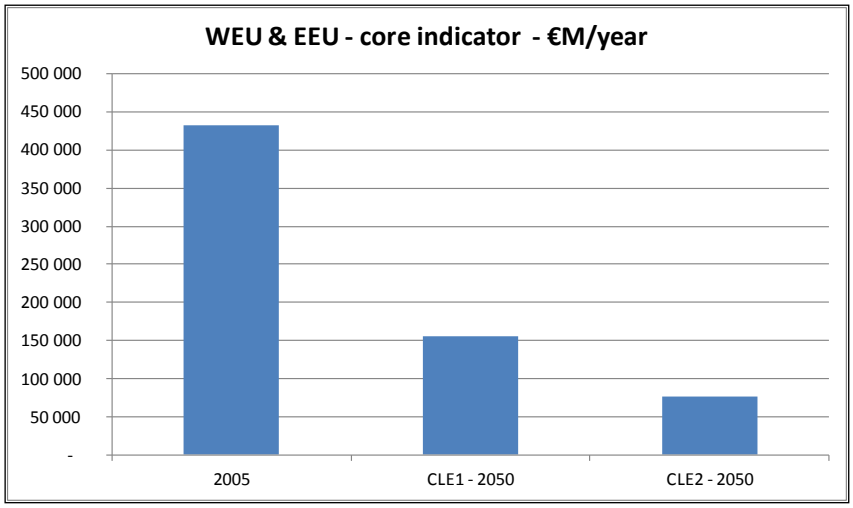

Figure 49: Estimated total health damage from air pollution in 2005 and in 2050 according to the two scenarios (core indicator)

6.1.4 Benefits – avoided health impacts and damage under different scenarios

The following two tables quantify the benefits, by calculating the health impacts (Table 13) and health damage (Table 14) avoided:

- in 2050 relative to 2005 through the application of air pollution policies (2005 – CLE1),
- in 2050 relative to 2005 through the application of air pollution policies and ambitious climate policy (2005 – CLE2),
- in 2050 when moving from the reference to the mitigation climate scenario (CLE1 – CLE2).

Positive values in these tables indicate a reduction representing a health benefit (avoided health impacts and damage); negative values indicate an increase (and thus additional health impacts and damage). The results in the last column of the tables quantify the co-benefits for health impacts from air pollution brought about by the ambitious climate policy.

Table 14: Change in estimated annual health impacts between years and scenarios (core indicator). A negative sign indicates an increase, a positive sign a reduction in impacts.

Benefits (units as shown)	WEU & EEU	Pollutant	2005 - CLE1	2005 - CLE2	CLE1 - CLE2
Acute Mortality (All ages) median VOLY	Premature deaths	O3	- 18 031	24 635	42 665
Respiratory Hospital Admissions (65yr +)	Cases	O3	- 31 691	15 270	46 961
Minor Restricted Activity Days (MRADs 15-64yr)	Days	O3	10 149 538	78 876 265	68 726 728
Respiratory medication use (adults 20yr +)	Days	O3	- 5 959 281	24 206 628	30 165 909
Chronic Mortality (All ages) LYL median VOLY	Life years lost	PM	3 609 118	4 479 408	870 290
Infant Mortality (0-1yr) median VSL	Premature deaths	PM	1 842	1 992	150
Chronic Bronchitis (27yr +)	Cases	PM	110 082	159 349	49 267
Respiratory Hospital Admissions (All ages)	Cases	PM	47 208	64 896	17 688
Cardiac Hospital Admissions (All ages)	Cases	PM	29 115	40 024	10 909
Restricted Activity Days (RADs 15-64yr)	Days	PM	295 635 074	373 412 486	77 777 412
Respiratory medication use (children 5-14yr)	Days	PM	3 210 268	4 128 764	918 496
Respiratory medication use (adults 20yr +)	Days	PM	20 217 869	28 544 892	8 327 023
LRS symptom days (children 5-14yr)	Days	PM	160 808 671	204 816 333	44 007 661
LRS among adults (15yr +) with chronic symptoms	Days	PM	212 139 776	296 240 939	84 101 164

The finding of Minor Restricted Activity Days due to ozone exposure decreasing when moving from 2005 to CLE1 in 2050, while the other ozone related health end-points show increasing

impacts (column 4 in Table 14 and Table 15), is explained by the demographic development between 2005 and 2050. Whereas the overall population and the age classes of people over 20 years and over 65 years increase between these two years in WEU & EEU, the population at working age (15 to 64 years) decreases.

Table 15: Change in estimated annual health damage between years and scenarios (core indicator). A negative sign indicates an increase, a positive sign a reduction in damage.

Benefits, €M/year	WEU & EEU	Pollutant	2005 - CLE1	2005 - CLE2	CLE1 - CLE2
Acute Mortality (All ages) median VOLY	Premature deaths	O3	- 1 040	1 421	2 462
Respiratory Hospital Admissions (65yr +)	Cases	O3	- 70	34	104
Minor Restricted Activity Days (MRADs 15-64yr)	Days	O3	426	3 313	2 887
Respiratory medication use (adults 20yr +)	Days	O3	- 6	24	30
Chronic Mortality (All ages) LYL median VOLY	Life years lost	PM	208 246	258 462	50 216
Infant Mortality (0-1yr) median VSL	Premature deaths	PM	3 012	3 257	245
Chronic Bronchitis (27yr +)	Cases	PM	22 897	33 145	10 248
Respiratory Hospital Admissions (All ages)	Cases	PM	105	144	39
Cardiac Hospital Admissions (All ages)	Cases	PM	65	89	24
Restricted Activity Days (RADs 15-64yr)	Days	PM	27 198	34 354	7 156
Respiratory medication use (children 5-14yr)	Days	PM	3	4	1
Respiratory medication use (adults 20yr +)	Days	PM	20	29	8
LRS symptom days (children 5-14yr)	Days	PM	6 754	8 602	1 848
LRS among adults (15yr +) with chronic symptoms	Days	PM	8 910	12 442	3 532
Total, with VOLY, median			276 520	355 320	78 800

6.2 Comparing costs with benefits

In this sub-section, results of the benefit/cost analysis are presented, first for the core aggregate health damage indicator, and then taking into account sensitivity ranges for the health damage estimation (Section 6.2.2.1). The potential impact omitted variables might have on the overall results are analysed in a qualitative way in Section 6.2.2.2. Further sensitivity analysis focuses on a quantification of the impact on the results of several corrections used in the regional air quality and climate modelling (Section 6.3): correction for the bias of the climate model and correction of population weighted concentrations through calculation of increments/decrements.

6.2.1 Comparison of costs and co-benefits of climate policy

In policy evaluations for which the ARP tool has traditionally been applied (e.g. UNECE Gothenburg Protocol, EC National Emission Ceilings Directive), benefits achieved when moving from less to more ambitious air pollution mitigation strategies were assessed. In Salut'AIR we assess the health effects of only one air pollution mitigation strategy under two energy/climate policy contexts. This implies that unlike the 'traditional' benefit/cost analyses we cannot assess benefits in monetary terms relative to costs of air pollution policy[33]. We hence do not calculate the classical benefit/cost ratio here[34].

Instead we calculate a co-benefit/cost ratio. This ratio compares the increase in energy/climate policy costs when moving from the scenario without climate policy to the ambitious climate policy scenario (incremental analysis) with the co-benefits it brings about in the form of air pollution policy cost savings (above referred to as tangible economic co-benefits) and of avoided health damages (which partly consist in intangible cost savings).

[33] We have no information on air pollution mitigation costs in 2005 and none on air pollution mitigation costs in 2050 for a less ambitious GEA air pollution policy scenario.

[34] In the 'traditional' benefit/cost analysis an air pollution mitigation strategy would be considered as socially acceptable when its benefit/cost ratio exceeded 1.

The result of this analysis is illustrated in Figure 50. The two graphs contain the same numbers, but present them differently. The left hand side of the figure indicates the additional monetised health impacts next to the additional air pollution costs and additional energy policy costs. The right hand side directly sets the monetised health benefit in relation to net additional policy costs (sum over air pollution mitigation cost savings and additional energy policy costs). Cost data used here are those presented in Figure 13 above. The numbers for the monetized health damage come from **Erreur ! Source du renvoi introuvable.**.

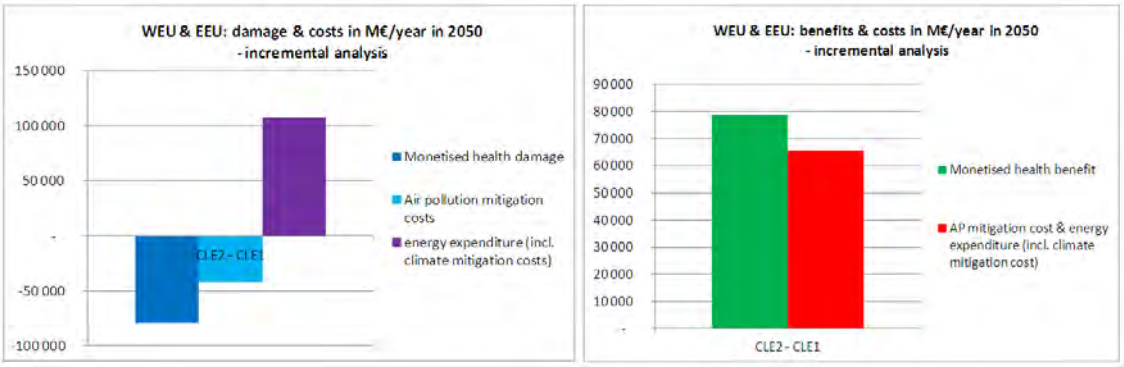

Figure 50: Additional costs and co-benefits of an ambitious climate policy – incremental analysis between CLE1 and CLE2 in 2050

The results can be summarized as follows:

- The additional costs for climate/energy measures when moving from CLE1 to CLE2 amount to approximately 107 billion €(2005)/year in 2050.
- The co-benefits of the ambitious energy policy are composed of savings in air pollution mitigation costs that amount to approximately 42 billion €(2005)/year in 2050 (tangible economic co-benefits) and of avoided health damages from reduced air pollution that amount to approximately 79 billion €(2005)/year in 2050 (partly intangible co-benefits of climate policy).
- The monetised health benefits (core indicator) of 79 billion € (2005)/year in 2050 thus exceed the additional net aggregate air pollution mitigation and climate policy costs of 107 - 42 = 65 billion €(2005)/year in 2050.

6.2.2 Some considerations on uncertainties

Two types of uncertainty analyses are explored here. This is firstly the calculation of sensitivity ranges for estimating health benefits. Secondly, the potential direction of the impact on results of omitted variables and of factors for which we cannot quantify uncertainty is analysed in a qualitative approach. The sensitivities of the results to corrections used in atmospheric modelling are discussed in Section 6.3.

6.2.2.1 Sensitivity ranges for health damage calculation

Calculating a sensitivity range for the changes in the health damage when moving from CLE1 to CLE2 by applying alternative monetary values (mean values) for the core indicators for mortality and the alternative metric for chronic $PM_{2.5}$ mortality (VSL) listed in Table 11 (above) leads to the spread for the monetized health benefit as indicated in Figure 51. The bars give the mid values (the Salut'AIR "best estimate" is indicated by a red circle), and the end points of the uncertainty ranges indicate the minimum and maximum monetary values for the core indicators for VOLY and VSL respectively.

If the additional sensitivity indicators were taken into account, they would add approximately 20 M€/year in 2050 to each of these values. Additional information about the respective

aggregations of indicators to the total health damage indicators (and benefit in the incremental analysis) employed in this Figure is given in Annex 0.

Co-benefits for health of the ambitious climate policy range from 63 billion €/year to 384 billion €/year for core indicators, with our conservative "best" estimate amounting to 79 billion €/year in 2050, which have to be compared to the additional policy costs of 65 billion €/year.

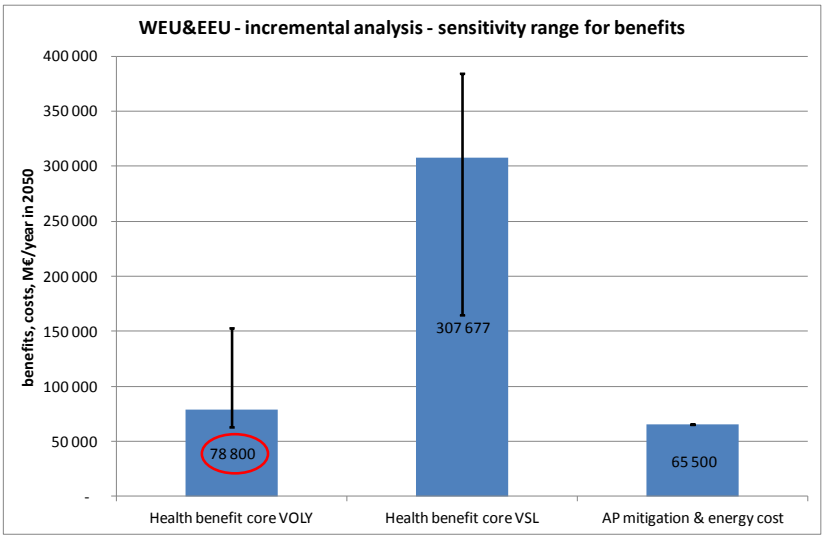

Figure 51: Sensitivity range for the monetised health benefit estimate (indicating the low, mid and high VOLY and VSL values) and comparison to overall additional policy cost

As mentioned in Section 5.1.2 above, within the scientific community there is no agreement on whether to use VOLY or VSL for valuing mortality related to air pollution. While some authors suggest using both (cf. Krupnick et al., 2005), others dismiss the use of VSL estimates for methodological reasons[35] (CGDD, 2012). Yet others follow the approach suggested by the(OECD, 2006)[36] and use VSL for acute and VOLY for chronic mortality (Brandt et al., 2013). We followed for our core value the approach adopted under CAFE and use VSL for infant mortality from PM, and VOLY for chronic mortality from PM and for acute mortality from ozone. There is also no consensus within the scientific community on whether to use mean or median values as first choice.

While it is hence difficult to come to clear conclusions in terms of robustness of the different core estimates in Figure 51, following a precautionary and conservative approach would suggest placing more confidence in the lower values, i.e. using median values for mortality in general and VOLY estimates for valuing chronic mortality from PM. This is the case for the minimum and mid levels in the bar on the left hand side of the figure. Nevertheless, the core high VOLY (using the mean CAFE VOLY) cannot be dismissed on theoretical grounds either.

With less evidence available for the sensitivity indicators than for the core indicators (cf. Section 6.1.2), the aggregates based on core indicators can be considered as more robust than the aggregates comprising also sensitivity indicators (not shown in the figure).

The preliminary conclusion that can be drawn from this is that it is more likely than not that the health co-benefits from the ambitious climate policy, according to the Salut'AIR analysis of

[35] Notably the issue of transferring VSL estimates often based on reductions in life expectancy around 35 or 40 years as associated with traffic accidents to the domain of air pollution, where the related reduction in life time is likely to be some weeks to months.

[36] In OECD (2006) an issue related to that discussed in CGDD (2012) is discussed, namely that VSLs are often established in non-environmental contexts, which tend to be associated with immediate risks such as accidents. These authors suggest that valuations of immediate risk might be transferred to environmental immediate risk contexts and that future risks need to be valued separately.

GEA scenarios, will be close to or even exceed the additional policy costs, indicated in the right hand bar in the figure.

6.2.2.2 Qualitative assessment of uncertainties

Caveats to the co-benefit/cost assessment presented here consist for example in air pollution mitigation costs for the GEA scenarios being quantified mainly for the mitigation measures applied to reduce three pollutants (NOx, SO_2, $PM_{2.5}$). While this covers the majority of air pollution costs for energy sectors, some underestimation is likely for air pollution mitigation costs that might occur in non-energy sectors. On the other hand, various further benefit categories are also not included in the analysis, such as the impacts of reduced air pollution on material and crop damage and ecosystems; and any benefits other than on air quality related to the reduction of greenhouse gases. Lack of account of these impacts drives the analysis towards an underestimation of benefits.

To assess at least qualitatively what impact omitted variables or factors for which we cannot quantify uncertainty may have on the ratio of benefits and costs is the objective of this section. It aims at giving an indication of the likely direction in which such factors may bias results and of whether or not their influence is important, as suggested in the methodology developed in Holland et al. (2005b and 2005c).

Hereafter, factors are listed that are not accounted for in the modelling and which may bias the balance of costs and benefits. The analysis focuses on four modelling areas: emissions modelling, dispersion modelling, health impact assessment and modelling of air pollution mitigation costs.

Sources of potential biases in the former three modelling areas may affect the overall damage under each scenario and thus the ***benefit*** calculated when passing from CLE1 to CLE2. Examples are discussed hereafter and presented in table form in Annex 0. In the following, a negative bias implies an underestimation of damage, a positive bias an overestimation of damage.

Modelling of atmospheric emissions:

- Uncertainty in emission inventories, used for establishing emissions of historic years in the scenarios, may introduce a significant negative or positive bias. In other words it may under- or over-estimate emissions and hence damage.
- The same holds for emission factors estimated in relation to economic growth (Kuznets curve hypothesis), an approach applied to estimating improvements in air pollutant related emission factors after 2030, while we assume that GAINS emission factors (applied up to 2030) are well researched and that there is no evidence of any significant bias.

Dispersion modelling:

- Overall, ozone and $PM_{2.5}$ concentrations are exempt from any systematic bias[37], largely thanks to the statistical increment/decrement calculated to counterbalance the impact of the degraded spatial resolution of the air quality model (50 km) (cf. Section 5.3.6).
- Hot spot ozone and hot spot $PM_{2.5}$ are not accounted for in the modelling. In line with Holland et al. (2005b and c) this is not considered to entail very important biases as the models are calibrated against background concentrations.
- Variability in meteorology can be an important source of bias. On the one hand, we can assume that such bias is limited by the fact that meteorological data for 10 years is used in the analysis. On the other hand we use here a climate model rather than reanalyses, which may introduce a bias. In Salut'air this bias is also handled in the atmospheric post-

[37] It is worth noting that the inclusion of some dust from natural sources in CHIMERE is likely to lead to higher PM damage than would be calculated based on data from models excluding natural dust.

processing (see Section 5.3.6). In order to get a clearer idea of the likely direction and importance of this bias, various climate models would need to be used.

Benefits analysis:

- The monetised health impact assessment in this report does not cover all health impacts. Excluded are, for example, chronic health effects of exposure to ozone and effects of coarse particles on health. However, the potential overall underestimation of health damage is not considered important, especially as it is suggested that valuation for chronic bronchitis is possibly too high (cf. Holland, 2013). We hence assume that the assessment of health impacts is not subject to important biases.
- It is also likely that the lack of assessment of impacts from air pollution on materials in cultural heritage and in agriculture other than crops is of limited importance for the overall results.
- The lack of assessment of impacts from air pollution on utilitarian buildings/constructions, on crops and on ecosystems, however, may introduce an important negative bias in the results, and thus underestimate total damage.
- The fact that we only estimate health impacts in Europe underestimates the benefits of a reduction of emissions from Europe (Holland et al., 2005b).
- A further issue which may introduce important biases is the lack of accounting for different particle composition. Depending on which particle species prevail, the bias may be positive or negative (ibid.).
- The estimation of premature deaths based on simple techniques that are not based on life tables (as is the case in our analysis) introduces a risk of double counting and hence overestimation of damage (Holland et al., 2005b). While this factor may have a significant impact on overall results, in the Salut'air analysis it is of limited importance as premature deaths are only used for sensitivity ranges.
- SOMO35 being the indicator for ozone health impacts, the analysis uses a cut-point, which might introduce a tendency of underestimating health damage from ozone. However, given the low share of the ozone impacts in the overall health damage, this bias is not likely to be significant (Holland et al., 2005c).
- Finally, Salut'air does not account for impacts - other than on air quality - of reduced greenhouse gases, and in this clearly underestimates benefits of emission reductions. Examples of such impacts are those related to sea level rise, river floods, heat related mortality and morbidity, risks to critical infrastructure (such as water and power supplies) from extreme weather events (Kovats, N/A).

Except for the issue of estimation of premature deaths (which is not relevant for our core damage and benefits estimate), all biases for which the direction is unambiguous and which are likely to be important point to an underestimation of damages from air pollution. The more important the damage category is that is underestimated or omitted, the more important is the underestimation of benefits in an incremental analysis between CLE1 and CLE2. An underestimation of benefits also implies an underestimation of the co-benefit/cost ratio.

Concerning the modelling of ***air pollution mitigation costs***, several factors are identified that might constitute a source for biases towards an under- or overestimation of costs and thus of the overall costs when passing from CLE1 to CLE2. As was the case for the benefits side, not all of these factors are considered to be important (cf. also Annex 0):

- The lack of account in GAINS of the development of the costs for abatement measures over time, and of a future technical development of existing measures may imply that costs are estimated to be higher than they might be. However this may be counterbalanced by the application, in the overall GEA modelling, of the Kuznets curve assumptions post 2030, assuming improvement of emission factors with economic growth. This also incorporates an assumption of learning effects. The overall effect is unclear.
- For the GEA scenarios, air pollution mitigation costs were calculated for energy sectors and mainly for NOx, SO_2 and $PM_{2.5}$. CO costs are indirectly related to NOx, so in a sense they are accounted for. VOC costs in the energy sector are small. It can therefore be assumed that the majority of costs are accounted for and that any remaining bias is small.
- For non-energy sectors (e.g. agricultural or savannah burning) MESSAGE and GAINS were not linked. While emissions are estimated for such activities and sectors, no information was taken into account for assessing related mitigation costs. This is likely to imply some underestimation of air pollution mitigation costs. It is worth mentioning however that costs in these sectors are very uncertain. While air pollution mitigation costs have not been assessed for these sectors, assessments for methane mitigation suggest direct costs are low (Rao and Riahi, 2006).
- The modelling framework used here does not necessarily account for the full range of behavioural and structural changes. We nevertheless assume that the lack of modelling of structural measures in GAINS is to some extent compensated by the use of MESSAGE energy scenarios which incorporate such changes, especially in the mitigation scenario. This scenario also implies an important reduction in demand relative to the reference scenario.

The screening of potential biases for the air pollution mitigation cost assessment did not allow identifying any for which the effect was known to be important. While the net effect is not completely sure, the overall impression is that the potential biases identified for the assessment of air pollution mitigation costs are likely to influence the co-benefit/cost ratio in the same direction as the potential biases identified for the benefits assessment.

Overall, therefore, the bias analysis for the benefits and air pollution cost assessment tends to increase the robustness of the result of co-benefits exceeding additional policy costs in the Salut'AIR analysis.

A thorough analysis of potential biases in the MESSAGE energy scenario modelling and of likely effects on ***energy*** (and climate mitigation***) costs*** are outside the scope of the Salut'air project. However, (Riahi et al., 2012) and (Grubler et al., 2012) report uncertainty about costs, especially for demand-side investment, due to a lack of reliable statistics and difficulties in clearly defining what constitutes a purely energy-related investment. Uncertainty about investment in specific technologies, such as nuclear power or carbon capture and storage (CCS), is also prevalent on the energy supply-side and can lead to large increases in other investments (for e.g. renewables) in scenarios where these are not deployed. The overall costs of such technology constrained scenarios are found to be much larger that a scenario with a complete technology portfolio. Finally, the authors report that while innovation and technological learning tend to lower investment costs over time, there is uncertainty in the degree to which investment costs, efficiencies, emissions, and other performance characteristics improve and that costs could either be higher or lower depending on such developments. However to the extent that stringent climate policy leads to major transformations in the energy system, the co-benefits in terms of both reduced air pollution costs and associated health benefits are likely to be significant.

Altogether, this analysis suggests that the co-benefits (for air pollution policies and for health impacts from air pollution) from the stringent climate policy modelled in the CLE2 scenario do at least account for an important share in additional climate mitigation costs.

6.3 Sensitivity of the health benefit analysis to the modelling uncertainties

The model results used in this Section are derived from the comprehensive regional modelling system introduced in Section 4, and statistically corrected to account for the bias of the climate model and the importance of subgridscale population weighted concentrations variability (Section 5.3.6). Only ensemble approaches would allow assessing the uncertainty of selecting one or another model in the climate/chemistry global/regional suite of models. But the sensitivity to the statistical corrections can be further quantified. Table 16 provides the total Core Low Voly aggregated over EU27 for the four scenarios, and the four stages of statistical correction. First, we can verify that the CDF-t correction does not affect ERA-hindcast which is the reference for the climate matching. The GCM-historical tends to underestimate air pollution compared to the reanalysis-driven CHIMERE results (Section 5.3.4). Therefore, the CDFt correction increases the damage for the GCM-historical scenario. In turn, the population weighted concentrations correction further increases the damage. These corrections, however, remain limited to below 1% of the total health impacts. For the future projections, we also find that the climate correction is relatively small. But the population weighted concentrations is now more sensitive and accounts for 10 to 20% of the damage. This higher sensitivity is induced by $PM_{2.5}$ damage rather than O_3. While there are several reasons why we could obtain such a non-linear behaviour of subgrid scale population weighted concentrations, it remains difficult to explain. This feature will undergo further investigation, possibly in connection with the Air and Climate Health Impact Assessment Project, coordinated by Patrick Kinney from Univ. Columbia (NY) and involving INERIS, LSCE, and IPSL together with INVS where the ambition is to understand the importance of scale issues in air and climate projections.

Table 16: Total sanitary costs (as Core Low VOLYs, in M€/yr) according to the four scenarios in the Air and Climate modelling, and the four stages of statistical correction.

M€/year	ERA-hindcast	GCM-historical	GCM-REF-2050	GCM-MIT-2050
raw	279 468	277 818	82 213	40 180
CDFt	279 468	280 092	83 632	42 920
CDFt+Pop-weighted correction	281 224	281 785	100 470	47 792

7 Conclusion

7.1 Summary

The Salut'AIR project allowed to design, develop and implement a new comprehensive regional air quality and climate modelling system embedded in a quantitative cost-benefit analysis framework. This new tool allows taking into account the main external factors bearing upon European air pollution, namely intercontinental transport and climate change, while remaining focused on quantitative assessment of air pollution legislation and its impact on human health. The system is now operational and can be used for long term scenario analyses or to investigate the sensitivity of individual components of the modelling suite.

A comprehensive analysis of the co-benefit of climate policies for air quality was performed and we conclude that climate mitigation, by targeting energy efficiency and a low-carbon economy, has multiple beneficial collateral consequences for air quality. First, we find that emissions of pollutants are reduced under a low-carbon scenario. But even the cost of air pollution mitigation is reduced under this more energy-efficient future, thanks to reductions in the need for end-of-pipe measures.

The project gave also the opportunity to consolidate a climate dynamical downscaling modelling suite based on the WRF model by investigating various sources of uncertainty and exploring bias correction techniques. Interactions between air and vegetation were also studied, in particular the inhibiting effect of CO_2 increase on biogenic emissions.

The future regional climate and global chemistry fields could then be provided to the CHIMERE air quality model together with emission projection data. The air quality model was thus used to better assess the dominating factors through a sensitivity analysis and to provide future air pollution projections to a health impacts assessment tool. The uncertainty associated with the air quality model were evaluated by quantifying the impact of implementing bias and exposure correction techniques. Alternative techniques to further document the robustness of such projections are mentioned in the last section of the report on research perspectives.

A decomposition analysis demonstrated that for both ozone and $PM_{2.5}$, mitigation of anthropogenic emissions is the dominating factor that drives future air quality. The analysis of prospective scenarios shows that the bulk of primary PM2.5 emission reduction is carried by the industrial and ground transportation sectors in WEU while the power plant sector offers larger scope for reduction in EEU. We confirmed that future climate change will contribute to increase ozone pollution (the so-called climate penalty), whereas this factor is less robust for $PM_{2.5}$. We also found that intercontinental transport of pollution plays a major role in the future evolution of ozone, arguing in favour of coordinated international air pollution mitigation approaches.

Last, a health impact assessment, associated to a monetary valuation approach allowed quantifying the expected sanitary benefit of mitigation. We found that the net additional mitigation cost (climate and air pollution) in 2050 (65 billion €(2005)/year in 2050) could be compensated in 2050 by the collateral sanitary benefits (79 billion €(2005)/year in 2050).

7.2 Outcomes

Besides the above mentioned scientific findings, the project also led to the following outcomes:

- Capacity building: funding of two post-docs (Gaëlle Clain, and Om Tripathi);
- Publication of 7 peer-reviewed articles and more conference communications;

- Participation of the project teams to international (self-funded) coordinated modelling exercises such as ACCMIP (Atmospheric Composition Change Model Intercomparison Project: the production of the LMDz-OR-INCA member by LSCE), and CORDEX (Coordinated Regional Climate Downscaling Experiment, the production of the IPSL-INERIS member to Euro-Cordex).
- Lessons learnt being transferred to a French daughter project focusing on bridging spatial scales in health and climate assessments (ACHIA, funded by the GIS Climat Environnement Société) and also to on-going FP7 European projects (ATOPICA, IMPACT2C);
- The project also allowed the increase in the international visibility of French teams with INERIS taking the lead of the climate and air quality interaction work of the European Topic Centre on Air and Climate Mitigation of EEA.

7.3 Perspectives

The project also conducted to the identification of key priorities for the future.

Biogenic emissions of air pollutant precursors. Large uncertainties in estimates over Europe were reported in the project and in the literature. At the same time, it appears that global models are more advanced given that they take into account additional processes such as the inhibition attributed to increased CO_2 concentrations. Reducing these uncertainties by increasing the comprehensiveness of biogenic emission models but also by attempting to validate these models against measurements should be a key priority in the future. It should be mentioned that the present report focused mostly on the impact of such emissions on ozone pollution while they also bear upon secondary particulate matter formation.

Regional climate downscaling. Potential biases brought about by the use of a single climate model in the present study are pointed out repeatedly over the report. At the same time moving to – preferred – ensemble approaches remains excessively costly for the time being. We opened the way for promising hybrid statistical and dynamical downscaling techniques, which should be further investigated in the future.

Regional air quality projections. The CHIMERE air quality model has undergone thorough operational evaluations by means of comparison with existing state-of-the-art regional chemistry transport models (e.g. (van Loon et al., 2007;Solazzo et al., 2012a;Solazzo et al., 2012b). In the present context (future projections under changing external factors), dynamical evaluations are required to better assess the confidence we can have in the sensitivity of the model to emissions and meteorological changes. Thanks to a long-term involvement in model intercomparison exercises, the performances of the CHIMERE model in responding to meteorological and emission changes have been documented in the CITYZEN ((Colette et al., 2011)) and EURODELTA exercises ((Thunis et al., 2008)), respectively, but further dynamical evaluation initiatives remain relevant. In order to address this issue, the Task Force on Measurement and Modelling of the CLRTAP Convention launched the third phase of the EURODELTA initiative and entrusted its coordination to INERIS.

Impact assessment. The concentration response functions and valuation references used in the health impact assessment model should be gradually completed in order to incorporate the results of ongoing projects such as the global burden of diseases, or European initiatives such as ESCAPE or APHEKOM, or WHO-EC projects such as REVIHAAP and HRAPIE. In the future, the analysis could also take account of impacts of air pollution on materials and crops, for which

approaches to monetisation do exist. More importantly, the analysis should be completed by the results of ongoing research aimed at developing approaches to quantify, and monetize, the impacts of pollution on ecosystems and biodiversity (e.g. the European ECLAIRE project, or the global initiative TEEB - Economics of Ecosystems and Biodiversity).

Short-lived climate forcers. Despite its comprehensiveness, the regional part of the present suite of models lacks feedback processes, in particular feedbacks of air pollutants on climate. An online version of the CHIMERE model that includes direct and indirect impacts of aerosols on climate is being developed and will be included in the present framework in the future.

8 Acknowledgements

The staff involved in the Salut'AIR project also benefited from the support of sister projects: The CityZen and ATOPICA projects, under grant agreement 212095 and 282687 of the European Union's Seventh Framework Programme (FP7/2007-2013), the ACHIA project of GIS Environnement-Climat-Société. The European Environment Agency is also acknowledged through its support to the Topic Centre on Air Quality and Climate Mitigation. The CCRT/TGCC computing facility hosted at CEA is also acknowledged.

APPENDICES

A. OUTREACH

Peer-Reviewed publications of the project (acknowledging support):

1. Colette, A., L. Rouïl, B. Bessagnet, S. Schucht, S. Szopa, R. Vautard, L. Menut, 2013, Pollution atmosphérique et climat, accepté pour publication dans Pollution atmosphérique, Numéro Spécial Climat.
2. Colette, A., Bessagnet, B., Vautard, R., Szopa, S., Rao, S., Schucht, S., Klimont, Z., Menut, L., Clain, G., Meleux, F., Rouïl, L., 2013. European atmosphere in 2050, a regional air quality and climate perspective under CMIP5 scenarios. Atmos. Chem. Phys. Discuss. 13, 6455-6499.
3. Colette, A., Granier, C., Hodnebrog, O., Jakobs, H., Maurizi, A., Nyiri, A., Rao, S., Amann, M., Bessagnet, B., D'Angiola, A., Gauss, M., Heyes, C., Klimont, Z., Meleux, F., Memmesheimer, M., Mieville, A., Rouïl, L., Russo, F., Schucht, S., Simpson, D., Stordal, F., Tampieri, F., Vrac, M., 2012a. Future air quality in Europe: a multi-model assessment of projected exposure to ozone. Atmos. Chem. Phys. 12, 10613-10630.
4. Colette, A., Vautard, R., Vrac, M., 2012c. Regional climate downscaling with prior statistical correction of the global climate forcing. Geophys. Res. Lett. 39, L13707.
5. Menut, L., Tripathi, O., Colette, A., Vautard, R., Flaounas, E., Bessagnet, B., 2013b. Evaluation of regional climate simulations for air quality modelling purposes. Climate Dynamics 40, 2515-2533.
6. Vautard, R., Brankovic, C., Colette, A., Deque, M., Fernandez, J., Gobiet, A., Goergen, K., Nikulin, G., Guettler, I., Keuler, K., Warrach-Sagi, K., Teichmann, C., Halenka, T., 2012. The simulation of European heat waves from an ensemble of regional climate models within the EURO-CORDEX project. Climate Dynamics, in press.
7. Szopa S., Y. Balkanski, M. Schulz, S. Bekki, D. Cugnet, A. Fortems-Cheiney, S. Turquety, A. Cozic, C. Déandreis, D. Hauglustaine, A. Idelkadi, J. Lathière, F. Lefevre, M. Marchand, R. Vuolo, N. Yan and J.-L. Dufresne. Aerosol and Ozone changes as forcing for Climate Evolution between 1850 and 2100. Climate Dynamics, DOI: 10.1007/s00382-012-1408-y, 2012.

Publications related to the project (involving partners and addressing overlapping scientific questions):

1. Anav A., L.Menut, D.Khvorostiyanov and N.Viovy, Impact of tropospheric ozone on the Euro-Mediterranean vegetation, Global Change Biology, vol. 17, issue 6, DOI: 10.1111/j.1365-2486.2010.02387.x
2. Anav A., L. Menut, D. Khvorostyanov, N. Viovy, Comparison of two canopy conductance parameterizations to quantify the interactions between surface ozone and vegetation over Europe, Journal of Geophysical Research - Biogeosciences, 117, G03027, 20 PP., doi:10.1029/2012JG001976
3. Omrani H., Drobinski P., Dubos T.: Nudging in regional climate modelling: what should we nudge? Clim. Dyn., submitted.
4. Omrani H., Drobinski P., Dubos T., 2013: Optimal nudging strategies in regional climate modelling: investigation in a Big-Brother Experiment over the European and Mediterranean regions. Clim. Dyn., doi:10.1007/s00382-012-1615-6
5. Omrani H., Drobinski P., Dubos T., 2012b: Spectral nudging in regional climate modelling: how strongly should we nudge? Quart. J. Roy. Meteorol. Soc., 138, 1808-1813
6. Omrani H., Drobinski P., Dubos T., 2012a: Investigation of indiscriminate nudging and predictability in a nested quasi-geostrophic model. Quart. J. Roy. Meteorol. Soc., 138, 158-169

Reports:

1. Colette, A., Koelemeijer, R., Mellios, G., Schucht, S., Péré, J.-C., Kouridis, C., Bessagnet, B., Eerens, H., Van Velze, K., Rouïl, L., 2011. Cobenefits of climate and air pollution regulations, The context of the European Commission Roadmap for moving to a low carbon economy in 2050, Technical Report of the European Topic Centre on Air Quality and Climate Mitigation, European Environment Agency, Copenhagen, p. 78.

2. Colette, A., Bessagnet, B., Rouïl, L., 2012, On the role of low carbon scenarios on 2050 European air quality and radiative forcing, Technical Report of the European Topic Centre on Air Quality and Climate Mitigation, European Environment Agency, Copenhagen, p. 39

Talks:

1. Colette, A., sollicited press conference at European Geoscience Union, 13 Avril 2013, Vienne.
2. Colette, A., F. Meleux , B. Bessagnet C. Granier O. Hodnebrog, M. Gauss, Interlinkages : Global and Regional CTM, Relevance for medium and long term air quality studies, HTAP Workshop, Pasadena, CA, 2012 (solicited)
3. Bessagnet, B., A. Colette, G. Clain, Z. Klimont, L. Menut, S. Rao, S. Schucht, S. Szopa, R. Vautard, European air quality in 2050: global and re-gional simulations accounting for climate and socio-economic changes, 32st NATO/SPS International Technical Meeting on Air Pollution Modelling and its Application, 7-11 May, 2012, Utrecht, The Netherlands.
4. Colette, A., Bessagnet, B., Vautard, R., Szopa, S., Menut, L., Schucht, S., and Rao, R., Europe in 2050, a regional air quality and climate perspective, EGU 2013
5. Schucht, S., The Salut'AIR project: Assessment of European Air Quality in 2050 in the Context of Climate Change, 42nd meeting of the Task Force on Integrated Assessment Modelling (TFIAM), 22-23 April 2013, Copenhagen, Denmark.
6. Schucht, S., Coûts et bénéfices des politiques de réduction de la pollution atmosphérique, séminaire « Monétarisation des biens et services environnementaux : quelles utilisations pour les politiques publiques et les décisions privées ? », 13 décembre 2012, Ministère de l'Ecologie du Développement Durable et de l'Energie, Paris, France.

Posters:

1. Colette, A., Bessagnet, B., Frédérik Meleux, Guido Pirovano, Dmitry Khvorostyanov, Laurent Menut, 2010, Switching from MM5 to WRF: consequences on the skills of the Chemistry Transport Model Chimere. Second International Workshop on Air Quality Forecasting Research, Quebec City, November 16-18, 2010.
2. Colette, A., Claire Granier, Agnes Nyiri, Øivind Hodnebrog, Hermann Jakobs, Alberto Maurizi, Zbigniew Klimont, 2012, Clean air for future generations: a multi-model investigation of air quality projections, International Global Biosphere Programme, Planet under Pressure, London 2012.
3. Colette, A. Meleux, F., Bessagnet, B., Claire Granier, Øivind Hodnebrog, Guido Pirovano, and Sophie Szopa, On the impact of chemical boundary conditions on air quality modelling, EGU 2011.
4. Szopa, S., Y. Balkanski, A. Cozic. D. Cugnet, C. Deandreis, J.-L. Dufresne, D. Hauglustaine, M.-A. Foujols, J. Lathière, N. de Noblet-Ducoudre, M. Schulz, N. Yan. Changes in tropospheric aerosol and reactive gases burdens and concentrations under IPCC-AR5 emission scenarios for 1850-2100. AGU Assembly, San Francisco, december 2010
5. Szopa, S., Juliette Lathière, Flavie Benardais, Patricia Cadule, Nathalie de Noblet-Ducoudré. Impatc of Biogenic Isoprene Emissions on Atmospheric Chemistry: What could the future look like? 3rd iLEAPS Science Conference, 18-23 September 2011 in Garmisch-Partenkirchen, Germany.
6. Szopa, S. G. Clain, R. Vautard, B. Bessagnet, A. Colette, O. Tripathi, L. Menut, A. Cozic, Global chemical composition modifications and European air quality changes induced by the RCP scenarios at the 2050 horizon. International Global Biosphere Programme, Planet under Pressure, London 2012.
7. Clain, G., Szopa, S., Tripati, O., Vautard, R., Colette, A., and Bessagnet, B.: Modelling the impact of global changes on summer European surface O3 levels at the 2050 horizon, Poster session, Accent Symposium on Air Quality and Climate change, Urbino, 2011

B. GLOSSARY

AR5	Fifth IPCC Assessment Report
ARP	Alpha-RiskPoll, tool for health impact and benefits assessment
ARP-FR	French version of the ARP tool
BC	Black carbon
CAFE	Clean Air for Europe programme
CCS	Carbon capture and storage technology
CH_4	Methane
CHIMERE	Regional (European) chemistry-transport model
CLE1	Reference energy scenario from GEA, also referred to as REF (reference scenario)
CLE2	Climate mitigation scenario from GEA, also referred to as MIT (mitigation scenario)
CO	Carbon monoxide
CO_2	Carbon dioxide
EC	European Commission
EJ	Exa Joules (unit for energy production and consumption), equal to 10^{18} joules
EEU	MESSAGE region Central and Eastern Europe
EMRC	UK consultant for health impact and benefits analysis
FGD	Flue gases desulphurisation
GAINS	Greenhouse Gas - Air Pollution Interactions and Synergies model (run at IIASA)
GEA	Global Energy Assessment
GRT	Ground transportation sector
HDV	Heavy duty vehicles
IIASA	International Institute for Applied Systems Analysis
IGCC	integrated gasification combined cycle
IPCC	Intergovernmental Panel on Climate Change
IND	Industry sector
Kt	Kilo tonnes (1000 metric tonnes)
LDV	Light duty vehicles
MESSAGE	Model for Energy Supply Strategy Alternatives and their General Environmental Impact (run at IIASA)
M€2005/year	Costs expressed in million Euros per year, the Euro price base being 2005
MIT	Climate mitigation scenario from GEA, also referred to as CLE2
Mt	Million metric tonnes
OC	Organic carbon
NOx	Nitrogen oxide
OECD	Organisation for Economic Co-operation and Development
$PM_{2.5}$	Fine particulate matter
PPL	Power plant sector
RCP	Representative Concentration Pathway, developed under the IPCC/AR5

REF	Reference energy scenario from GEA, also referred to as CLE1
RES	Residential and commercial sector
SCR	Selective catalytic reduction
SO_2	Sulphur dioxide
SOMO35	For ozone, the sum of means over 35 ppb (daily maximum 8-hour)
UNECE	United Nations Economic Commission for Europe
VOC	Volatile organic compounds
VOLY	Value Of Life Year
VSL	Value of Statistical Life
WEU	MESSAGE region Western Europe
WHO	World Health Organisation

C. COMPLEMENTARY INFORMATION ON EMISSIONS AND COSTS

1. Emissions

As a complement to Section 2.4.2, Table 17 shows for the part of the SO_2 emissions that is determined via the GAINS-MESSAGE link, its distribution between different sectors and European sub-regions for the two scenarios. The total of the four sectors and Europe overall is also given. The data are provided for each scenario, CLE1 (reference climate scenario) and CLE2 scenario (climate mitigation scenario).

Table 17: SO_2 emissions in kt/year in 2050 for the scenarios CLE1 and CLE2, per sector and region

in kt/year in 2050	Scenarios	SO_2 emissions		
		WEU	EEU	WEU & EEU
PPL	CLE-1	120	282	402
	CLE-2	28	26	54
IND	CLE-1	765	333	1 097
	CLE-2	152	99	251
GRT	CLE-1	54	23	77
	CLE-2	11	6	17
RES	CLE-1	54	17	72
	CLE-2	17	7	24
Sum 4 sectors	CLE-1	992	656	1 648
	CLE-2	209	138	347

As further complements to section 2.4.2 the following three tables indicate, for each of the three pollutants respectively, the emission reductions brought about by a switch from the reference climate and energy scenario (REF, CLE1) to the ambitious climate and energy scenario (MIT, CLE2). The left hand side part of each table indicates the absolute reduction in emissions in kt/year in 2050, the right hand side part the contribution (in %) of each sector and region to the overall emission reduction in Europe. For the sectors and regions contributing the most to the observed emission reduction, the drivers are presented below.

Table 18: SO_2 emission reductions when switching from CLE1 to CLE2 (left) and contribution of each sector region combination to the overall emission reduction (right)

Emission reduction in kt/year in 2050	SO2			Percentage in overall emission reduction	SO2		
	WEU	EEU	WEU & EEU		WEU	EEU	WEU & EEU
PPL	92	256	348	PPL	7	20	27
IND	612	234	846	IND	47	18	65
GRT	43	17	60	GRT	3	1	5
RES	37	10	47	RES	3	1	4
Sum 4 sectors	784	518	1 301	Sum 4 sectors	60	40	100

Emission reductions of SO_2 (Table 18) are most important in the power plant and industrial sectors and this in both regions. These explain over 90% of the overall reductions in SO_2 between CLE1 and CLE2.

Table 19: NOx emission reductions when switching from CLE1 to CLE2 (left) and contribution of each sector region combination to the overall emission reduction (right)

Emission reduction in kt/year in 2050	NOx			Percentage in overall emission reduction	NOx		
	WEU	EEU	WEU & EEU		WEU	EEU	WEU & EEU
PPL	307	138	445	PPL	13	6	19
IND	275	72	347	IND	12	3	15
GRT	1 088	270	1 358	GRT	47	12	58
RES	136	36	172	RES	6	2	7
Sum 4 sectors	1 806	516	2 322	Sum 4 sectors	78	22	100

The major reductions of NOx emissions (Table 19) occur in the sectors ground transportation followed by power plants and then by industry. Changes in these sectors explain over 90% of the overall reduction in NOx emissions, WEU alone accounts for over 72% of these.

Table 20: $PM_{2.5}$ emission reductions when switching from CLE1 to CLE2 (left) and contribution of each sector region combination to the overall emission reduction (right)

Emission reduction in kt/year in 2050	PM2.5			Percentage in overall emission reduction	PM2.5		
	WEU	EEU	WEU & EEU		WEU	EEU	WEU & EEU
PPL	3	26	29	PPL	1	12	14
IND	67	8	75	IND	32	4	36
GRT	84	12	96	GRT	40	6	46
RES	8	1	9	RES	4	0	4
Sum 4 sectors	162	47	209	Sum 4 sectors	77	23	100

The emission reductions in $PM_{2.5}$ are mainly driven by changes in the industrial and ground transport sectors in WEU and by the power plant sector in EEU. Together these sectors explain over 80% of the reduction shown in Table 20.

2. Costs

As a complement to section 2.5.2, the following four tables present the air pollution mitigation costs assumed in the GEA scenarios in 2050 that were determined through the link between the models GAINS and MESSAGE for NOx, SO_2 and $PM_{2.5}$. They indicate the annual costs, in million €/year (price base 2005) in 2050, for each pollutant individually by sector and sub-region and for the respective aggregates. The data are provided for CLE1 and CLE2.

Table 21: SO_2 emission mitigation costs in million €/year in 2050 for the scenarios CLE1 and CLE2

in million EUR 2005/year	Emission reduction costs (SO2)			
	Scenarios	WEU	EEU	WEU & EEU
PPL	CLE-1	142	1 401	1 543
	CLE-2	21	10	31
IND	CLE-1	7 122	1 813	8 935
	CLE-2	859	52	911
GRT	CLE-1	10 958	2 428	13 386
	CLE-2	2 299	557	2 856
RES	CLE-1	375	99	475
	CLE-2	119	40	159
Sum 4 sectors	CLE-1	18 597	5 742	24 339
	CLE-2	3 298	660	3 958

Table 22: NOx emission mitigation costs in million €/year in 2050 for the scenarios CLE1 and CLE2

in million EUR 2005/year	Emission reduction costs (NOx)			
	Scenarios	WEU	EEU	WEU & EEU
PPL	CLE-1	6 636	1 319	7 955
	CLE-2	2 972	652	3 623
IND	CLE-1	2 823	724	3 547
	CLE-2	585	87	672
GRT	CLE-1	5 603	1 016	6 619
	CLE-2	1 175	236	1 411
RES	CLE-1	979	7	986
	CLE-2	331	3	334
Sum 4 sectors	CLE-1	16 041	3 066	19 107
	CLE-2	5 064	977	6 041

Table 23: $PM_{2.5}$ emission mitigation costs in million €/year in 2050 for the scenarios CLE1 and CLE2

in million EUR 2005/year	Emission reduction costs (PM2.5)			
	Scenarios	WEU	EEU	WEU & EEU
PPL	CLE-1	221	1 011	1 231
	CLE-2	60	12	71
IND	CLE-1	2 205	584	2 789
	CLE-2	610	80	690
GRT	CLE-1	5 434	993	6 427
	CLE-2	1 140	228	1 368
RES	CLE-1	158	6	164
	CLE-2	50	3	53
Sum 4 sectors	CLE-1	8 017	2 594	10 611
	CLE-2	1 860	323	2 182

The following four tables indicate, for the sum over the three pollutants and for each of the three pollutants individually, the cost reductions brought about by a switch from CLE1 to CLE2. The left hand side part of each table indicates the absolute reduction in million €/year in 2050, the right hand side part the contribution (in %) of each sector and region to the overall air pollution mitigation cost reduction in Europe. The drivers behind the most important developments of costs between CLE1 and CLE2 are presented further below.

Table 24: Air pollution mitigation cost reductions when switching from CLE1 to CLE2 (left) and contribution of each sector region combination to the overall cost reduction (right)

Cost reduction in million EUR 2005/year in 2050	SO2, NOx, PM2.5			Percentage in overall cost reduction	SO2, NOx, PM2.5		
	WEU	EEU	WEU & EEU		WEU	EEU	WEU & EEU
PPL	3 946	3 057	7 003	PPL	9	7	17
IND	10 096	2 902	12 998	IND	24	7	31
GRT	17 380	3 416	20 797	GRT	42	8	50
RES	1 012	66	1 078	RES	2	0	3
Sum 4 sectors	32 434	9 442	41 876	Sum 4 sectors	77	23	100

Changes in three sectors, power plants, industry and ground transportation, and in both regions, WEU and EEU, contribute in an important way to the overall reduction in air pollution

mitigation costs (Table 24). These sectors account for approximately 97% of the overall cost reduction.

When looking at SO_2 mitigation costs individually (Table 25), the same sectors - with the exception of the power plant sector in WEU - drive cost reductions and explain about 98 % of these.

Table 25: Decrease in SO_2 emission reduction costs when switching from CLE1 to CLE2 (left) and contribution of each sector region combination to the overall cost reduction (right)

Cost reduction in million EUR 2005/year in 2050	SO2			Percentage in overall cost reduction	SO2		
	WEU	EEU	WEU & EEU		WEU	EEU	WEU & EEU
PPL	120	1 391	1 512	PPL	1	7	7
IND	6 263	1 761	8 024	IND	31	9	39
GRT	8 659	1 871	10 530	GRT	42	9	52
RES	256	59	315	RES	1	0	2
Sum 4 sectors	15 299	5 082	20 381	Sum 4 sectors	75	25	100

Cost reductions for NOx mitigation measures are also largely explained by changes in the sectors power plants, industry and ground transportation (Table 26). It should be noted however, that WEU on its own accounts for almost 80% of the cost reduction.

Table 26: Decrease in NOx emission reduction costs when switching from CLE1 to CLE2 (left) and contribution of each sector region combination to the overall cost reduction (right)

Cost reduction in million EUR 2005/year in 2050	NOx			Percentage in overall cost reduction	NOx		
	WEU	EEU	WEU & EEU		WEU	EEU	WEU & EEU
PPL	3 664	667	4 331	PPL	28	5	33
IND	2 238	637	2 875	IND	17	5	22
GRT	4 427	780	5 208	GRT	34	6	40
RES	648	4	652	RES	5	0	5
Sum 4 sectors	10 978	2 088	13 066	Sum 4 sectors	84	16	100

The sectors power plants, industry and ground transportation are also characterised by the major reductions in air pollution mitigation costs for $PM_{2.5}$ emissions (Table 27). Both regions contribute significantly to these reductions, with the exception of the power plant sector in WEU which has a relatively low impact on overall cost reductions.

Table 27: Decrease in $PM_{2.5}$ emission reduction costs when switching from CLE1 to CLE2 (left) and contribution of each sector region combination to the overall cost reduction (right)

Cost reduction in million EUR 2005/year in 2050	PM2.5			Percentage in overall cost reduction	PM2.5		
	WEU	EEU	WEU & EEU		WEU	EEU	WEU & EEU
PPL	161	999	1 160	PPL	2	12	14
IND	1 595	504	2 099	IND	19	6	25
GRT	4 294	765	5 059	GRT	51	9	60
RES	108	3	111	RES	1	0	1
Sum 4 sectors	6 158	2 271	8 429	Sum 4 sectors	73	27	100

3. Drivers

1. Power plants

Passing from CLE1 to CLE2 permits reducing emissions of ***NOx*** from power plants in WEU by 307 kt/year and costs by 3,665 million euros/year in 2050. In EEU emission reductions amount to 138 kt/year, cost reductions amount to 667 million euros/year in 2050.

- In ***Western Europe*** the highest contribution to the emission and cost reductions comes from an important reduction in the activity of gas combined cycle plants. A small part of this activity passes to combined cycle gas plants equipped with CCS (carbon capture and storage) where it leads to additional emissions and costs. These changes taken together explain approximately 70% in the emission reduction and 95% in the cost reduction. The second highest contribution to the overall emission reduction comes from a reduction in the activity of biomass heating plants (27%) but has only a negligible effect on costs (no control options are applied on the major part of this activity). Reduction in the activity of refineries also contributes to the emission and cost decrease (approximately 3%), while the increase in activity from gas heating plants increases emissions from this sector (3%). The complete phase-out of coal power plants only contributes marginally to the overall emission reduction.
- In ***Central and Eastern Europe*** the decrease in emissions is dominated by the effects of the phase-out of coal power plants. This contributes with approximately 65% to the emission reduction and with over 60% to the cost reduction. An important share of the emission reduction is furthermore due to the reduction in activity from gas combined cycle plants and the phase out of production from plants not equipped with SCR (selective catalytic reduction). The introduction in CLE2 of combined cycle gas plants equipped with CCS leads to additional emissions from these plants. Altogether these shifts between gas plants explain 25% of the emission reductions and approximately 28% of the cost reductions. The reduction of activity in high emitting oil refineries and the equipment of the remaining capacity with effective NOx control measures also contribute to emission reductions (4%), while the contribution to the cost reduction is negligible (1%).

Passing from CLE1 to CLE2 permits reducing emissions of ***SO_2*** from power plants in WEU by 92 kt/year and costs by 120 million euros/year in 2050. In EEU the corresponding reductions are 256 kt/year and 1,390 million euros/year in 2050.

- In ***Western Europe*** the major part of the emission reduction (55 %) comes from an important reduction in the activity of biomass heating plants. These plants not being equipped with control technology, this reduction has no impact on costs. The second highest contribution to emission reductions (37%) comes from a decrease in the activity in oil refineries. Treating the majority of this remaining activity with stage 2 control (instead of stage 3 control) is sufficient to still reach a significant overall emission reduction. These trends obviously reduce costs considerably (contribution: 64%). A complete phase-out of coal power plants under CLE2 decreases emissions and costs. There is also a slight decrease of coal use in heat plants. Together these contribute with 7% to the overall emission reduction and with 36% to the overall cost reduction. For the coal heating plants, a relatively higher use of more effective emission reduction technology (relative restructuring from wet flue-gases desulphurisation to higher efficiency flue gases desulphurisation) is possible at lower cost overall thanks to the lower activity. Finally the use of gas in gas combined cycle plants decreases while an important activity is introduced in gas combined cycle with carbon capture and storage, and the activity of gas heating plants increases as well. Still, there is an overall net reduction in gas use, which

leads to a slight decrease in emissions from gas power plants overall but has no effect on costs as no mitigation measures are applied to the gas plants.

- In ***Central and Eastern Europe*** the phase-out of coal in power plants explains almost completely the emission reduction achieved when passing from CLE1 to CLE2 (contribution of 99% to emission reduction and of 98% to cost reduction). Slight emission reductions come also from the decrease in activity in biomass heating plants. The reduction of activity in gas combined cycle plants and increase in gas combined cycle plants with carbon capture and storage do not effect emissions. The lower overall activity in refineries implies that less strict emission controls are sufficient to meet ELVs, which contributes with 1.5% to the decrease in costs.

Passing from CLE1 to CLE2 permits reducing emissions of ***$PM_{2.5}$*** from power plants in WEU by (only) 3 kt/year and costs by 161 million euros/year in 2050. In EEU emissions decrease by 26 kt/year in 2050, and costs by 1,000 million euros/year.

- The major part of the overall limited emission reduction in ***Western Europe*** is due to the reduction in activity from gas combined cycle plants. Part of the remaining activity is transferred to gas combined cycle plants equipped with CCS where it leads to additional emissions. Not being specifically equipped with technology to reduce PM, this has no impact on costs. Altogether these changes contribute with 55% to the emission reduction. The second most important factor behind emission reductions (contribution approximately 23%) is the decrease in activity from oil refineries. The remaining activity is treated by the most effective technology (high efficiency dedusters) and these modifications contribute approximately 7% to the cost reduction. The third most important factor contributing to emission reductions is the phase-out of coal power plants and contributes with 15% to the emission reduction and with 10% to the cost reduction. While the important reduction of activity from biomass heating plants does not contribute much to the emission reduction (5%), it is the most important factor for cost reduction (over 80%), as all activity assumes strict emission control (high efficiency dedusters).
- In ***Central and Eastern Europe***, the reduction in emissions and costs is almost entirely driven by the phase-out of coal power plants which explains 99% of the reduction. Although activity decreases also significantly in oil refineries and gas combined cycle plants, this does not add much to the overall emissions and costs, nor does the switch of almost 50% of the activity reduction from gas combined cycle plants to gas combined cycle plants equipped with CCS.

2. Industry

Passing from CLE1 to CLE2 permits reducing emissions of ***NOx*** from industry in WEU by 275 kt/year and costs by 2,238 million euros/year in 2050. In EEU this leads to emission reductions of 72 kt/year and cost reductions of 637 million euros/year in 2050.

- In ***Western Europe*** the overall net emission and cost reductions are mainly explained by the net effect of a strong decrease in the use of coal and an increase in the use of biomass and gas. The latter two lead to an increase in emissions which is largely overcompensated by the decrease in emissions from the lower coal use. The cost increase for additional application of combustion modification and selective catalytic reduction (SCR) on solid fuel fired industrial boilers and furnaces using biomass is low compared to the decrease in costs brought about by the declining share of coal capacity for which comparable measures are still applied under the climate mitigation scenario.

- In ***Central and Eastern Europe*** the opposing trends between coal and biomass use when passing from the reference to the mitigation scenario explain almost all net emission and cost reductions. The emission and cost reductions due to the complete phase-out of coal largely over-compensate increasing emissions and costs from increased use of biomass. Fuel oil use in industry also decreases but the related emission and cost reductions do account for a small share only in the overall result.

Passing from CLE1 to CLE2 permits reducing emissions of SO_2 from industry in WEU by 612 kt/year and costs by 6,263 million euros/year in 2050. In EEU the corresponding reductions are 234 kt/year and 1,761 million euros/year in 2050.

- The overall net emission reductions from industrial combustion in ***Western Europe*** are explained by two opposing developments. Firstly, a strong reduction of coal use in industry which explains almost all emission reductions. This also explains the largest part of the cost reductions as the capacity to be treated by wet flue gas desulphurisation is significantly lower under CLE2. Secondly, an increase in the use of biomass in industry which leads to increased emissions and costs from this activity. The reduction in coal use strongly dominates the net effect for costs and emissions. Diesel oil consumption also decreases but this only represents a small part of emission and cost reductions.
- In ***Central and Eastern Europe*** the phase-out of coal use by industry explains the major share of the emission and over 90% of the cost reduction. Here biomass use and related emissions increase as was also assumed for WEU, but because less flue gases desulphurisation (FGD) is used in the mitigation scenario and more capacities remain uncontrolled, this contributes to a slight decrease in cost. Fuel oil use decreases, entailing slight emission reductions; and a trend towards less use of flue gases desulphurisation contributes with approximately 7% to the overall cost reduction. For diesel oil activity and emissions increase, whereas costs decrease slightly due to a relative increase in the use of fuels with higher sulphur content.

Passing from CLE1 to CLE2 permits reducing emissions of $PM_{2.5}$ from industry in WEU by 67 kt/year and costs by 1595 million euros/year in 2050. In EEU emissions decrease by 8 kt/year in 2050, and costs by 504 million euros/year.

- In ***Western Europe*** PM emissions from industry and related mitigation cost changes between CLE1 and CLE 2 are also determined primarily by coal and biomass combustion. The strong decrease in coal use in industrial combustion explains all emission reductions in this sector and reduces costs owing to less abatement equipment for dust control (electrostatic precipitators and high efficiency dedusters mainly). Increased use of biomass in industry combustion however leads to additional emissions compensating 70% of the emission reductions from reduced coal combustion. Nevertheless, the additional PM deduster investment (same types mainly as for coal) needed to control PM emissions from biomass use leads to additional costs that represent only 8% of the savings attained through the reduced coal use.
- In ***Central and Eastern Europe*** the emission reductions due to the phase out of coal combustion in industry are compensated to over 90% by additional emissions from increasing biomass use. Cost reductions from the coal phase-out are only compensated to approximately 10% by additional costs from increased biomass combustion requiring abatement measures.

3. Ground transportation

Passing from CLE1 to CLE2 permits reducing emissions of ***NOx*** from ground transportation in WEU by 1,088 kt/year and costs by 4,428 million euros/year in 2050, in EEU emission reductions are 270 kt/year and cost reductions 780 million euros/year in 2050.

- In ***Western Europe***, all emission and cost reductions in this sector are explained by the decrease in the use of fossil fuels in transportation. Almost 40% of emission reductions and around 45% of cost reductions come from light duty road vehicles ((LDV) applying Euro standards), a bit more than 20 % of emission reductions and more than 50% of cost reductions from heavy duty road vehicles (HDV), almost 20% of emission but less than 1% of cost reductions from ships (large and medium vessels), around 11% of emission reductions but less than 1% of cost reductions from mobile sources on railways and inland waterways, and around 10% in emission reductions and around 1% in cost reductions from motorcycles and mopeds. Any increases in electric driven vehicles (cf. Table 4) are not accounted for in the GAINS-MESSAGE link for the transportation sector. Corresponding emissions would be accounted for in the power sector.
- In ***Central and Eastern Europe*** emission and cost reductions are dominated by a strong decrease in the activity from HDVs and LDVs. The activity reduction explains the cost decrease and over-compensates a relative increase in costs that comes from a slight trend to more recent Euro standards for diesel vehicles. Changes in the HDV activity contribute to 37% (58%) of the emission (cost) reduction. Changes in the LDV activity contribute to 47% (40%) of the emission (cost) reduction.

Passing from CLE1 to CLE2 permits reducing emissions of $\boldsymbol{SO_2}$ from ground transportation in WEU by 43 kt/year and costs by 8660 million euros/year in 2050. In EEU the corresponding reductions are 17 kt/year and 1870 million euros/year in 2050.

- In **Western Europe** the strong reduction in fossil fuel use explains the emission and cost reductions. Reductions in fuel oil and light oil explain the emission reductions (52% and 48% respectively). Amongst these, light oil reductions account for the major share of costs reductions (99%) as most of the fossil fuel used in CLE1 is of this type. Costs here refer to additional costs of use of low sulphur fuel.
- As in WEU, reductions in fuel oil and light oil explain the emission and cost reductions in ***Central and Eastern Europe***. The major part of the emission and cost reductions (78% and 99%respectively) comes from the reduction in the much more used light oil fraction.

Passing from CLE1 to CLE2 permits reducing emissions of $\boldsymbol{PM_{2.5}}$ from ground transportation in WEU by 84 kt/year and costs by 4,294 million euros/year in 2050. In EEU this leads to emission reductions of 12 kt/year and cost reductions of 765 million euros/year in 2050.

- In ***Western Europe*** activity reductions from light duty vehicles contribute with 42% to emission reductions, followed by large and medium vessels (22%), mobile sources in the railway and inland waterways sectors (16%), heavy duty vehicles (13%) and motorcycles and mopeds (8%). The corresponding contributions to the overall cost reduction are dominated by HDV (53%) and LDV (46%).
- In ***Central and Eastern Europe*** HDVs account for 43% of the emission reductions and 56% for the costs reductions, LDVs account for 22% of the emission reductions and for 43% of the cost reductions.

D. SENSITIVITY OF WRF CONFIGURATIONS

1. Introduction:

Les modèles de chimie-transport présentent une forte sensibilité aux données d'entrée, en particulier au modèle météorologique utilisé. L'objectif de cette étude est d'évaluer l'impact de la paramétrisation du modèle météorologique WRF sur la température de surface et la vitesse du vent au sol mais aussi sur les concentrations d'ozone et de particules PM10 calculées par CHIMERE.

2. Méthodologie :

1. Description de CHIMERE et de WRF

Le modèle WRF utilisé ici est « Advanced Research WRF » version 3.2.1 (Août 2010) développé et maintenu par le NCAR. Ce modèle peut être utilisé pour des applications réelles ou idéalisées, et avec des domaines imbriqués. La relaxation vers un modèle global peut se faire avec une méthode de « nudging » (spectral ou indiscriminé) ou d'assimilation 3DVAR.

Sur le plan de la physique du modèle, un large éventail de paramétrisations est disponible pour le mélange turbulent, le schéma de surface, la microphysique, la convection, le bilan radiatif …

Les champs WRF obtenus sont ensuite utilisés dans le modèle Chimère afin de discuter leur impact sur les performances en termes de qualité de l'air. La version Chimère utilisée ici est celle de 2009.

2. Données analysées :

Les données de qualité de l'air pour les stations de surveillance de la qualité de l'air sont issues de la base de données Airbase de l'EEA. Seules les données PM10 et O3 ont été étudiées ici. Seules les données des stations suburbaines et rurales ont été conservées pour l'étude.

En ce qui concerne les données météorologiques aux stations de mesures, elles ont été obtenues via l'archive ECMWF. Seuls les scores de température à 2m et de vitesse du vent à 10m ont été étudiés ici. Les données de précipitations de cette archive (principalement construite pour l'assimilation de donnée des modèles ECMWF) ne sont malheureusement pas validées car cette variable n'est pas assimilée.

3. Etudes de cas :

Le domaine géographique étudié recouvre l'ensemble de l'Europe (15W, 35E, 30N, 65N) à une résolution de 50km. Deux périodes hivernales en mars 2003 et janvier 2006 ont été sélectionnées pour évaluer le modèle. Elles correspondent à des épisodes de pic de pollution particulaire sur l'Europe occidentale. Dans cette étude, le lien sera fait avec des travaux déjà réalisés précédemment sur deux périodes estivales (août 2003 et juillet 2005) correspondant à de fortes concentrations d'ozone sur une zone étendue en Europe (voir Rapport Intermédiaire Primequal, 2011).

Pour chaque période, des simulations de 20 jours ont été menées et seuls les dix deniers jours ont été utilisés pour le calcul des scores de performance, les dix premiers servant d'initialisation.

4. Grille de test des configurations :

Dans cette étude, différents paramètres WRF : physiques (modèle de surface, paramètres dans la couche limite, paramètres de convection, de radiation, paramètres microphysiques), paramètres de forçage à grand échelle et de nudging, ont été testés.

3. Présentation des paramétrisations du modèle WRF :

1. *Modèles de surface et schémas de couche limite :*

Les **modèles de surface** (land-surface models ou LSM) fournissent des données de flux de chaleur et d'humidité dans la couche de surface et gère la représentation des bilans d'énergie entre le sol et l'atmosphère. Ces flux fournissent ainsi une condition limite inférieure pour le transport vertical dans la couche limite atmosphérique.

- Le modèle de surface **5Diff** (pour *5-layer thermal diffusion*) est un modèle à 5 niveaux de sol où la couverture neigeuse est indépendante du temps, où l'humidité du sol est seulement dépendante de la saison et du sol et où les effets de la végétation ne sont pas pris en compte.
- Le modèle de surface **Noah** est un modèle à 4 niveaux de température et d'humidité du sol. Il prend également en compte l'impact d'un sol gelé ou enneigé, l'impact de la texture du sol ainsi que celui de la végétation par catégories.
- Le modèle de surface **RUC** (pour *Rapid Update Cycle*) est un modèle à 6 niveaux de sol (plus fins que pour Noah) qui affine les échanges hydrauliques au niveau du sol par rapport au modèle précédent.
- Le modèle de surface **PX** (pour *Pleim-Xiu*) est un modèle à seulement deux niveaux de sol, qui met l'accent sur les échanges de vapeur d'eau entre le sol et l'atmosphère. Deux schémas de *nudging* permettent de corriger la température de l'air à 2m et l'humidité relative.

Les **schémas de couche limite** paramètrent le mélange vertical turbulent à l'intérieur de la couche limite atmosphérique (*Planetary Boundary Layer* ou PBL) :

- Le schéma **YSU** (pour Yonsei University) affine le schéma MRF en introduisant un traitement explicite de la couche d'entraînement en haut de la couche limite.
- Le schéma **MYJ** (pour *Mellor-Yamada-Janjic*) se base sur le modèle Mellor-Yamada Level 2.5 et utilise l'énergie cinétique turbulente comme base de calcul de la température et de la hauteur de couche limite.
- Le schéma **PX** (Asymmetrical Convective Model version 2) combine un modèle convectif Blackadar et un modèle diffusif turbulent.

2. *Convection profonde :*

Les schémas de convection permettent de prendre en compte les phénomènes convectifs qui ne sont pas représentés par le modèle à une telle résolution.

- La configuration de **Kain-Fritsch** est un schéma de flux de masse avec des courants ascendants et descendants humides et faisant intervenir les effets de détraînement et d'entraînement ainsi que de la microphysique relativement simple.
- La configuration **Grell-Devenyi**, quant à elle, moyenne l'influence de plusieurs schémas de flux de masse avec différents paramètres d'entraînement/détraînement.

3. *Bilan radiatif :*

Les schémas radiatifs calculent l'échauffement atmosphérique dû au rayonnement de courtes et de grandes longueurs d'ondes. Celui-ci peut être représenté de différentes manières.

- Le schéma **RRTM/Dudhia** (pour *Rapide Radiative Transfer Model*) est un modèle radiatif pour grandes longueurs d'ondes qui prend en compte les processus dus à la vapeur d'eau, à l'ozone et au CO_2 et se base sur un schéma Dudhia pour les courtes longueurs d'ondes.
- Le schéma **RRTMG/RRTMG**, quant à lui, est basé sur le modèle RRTM en ajoutant une approche de Monte-Carlo pour tenir compte de la superposition aléatoire de la couverture nuageuse.

4. Microphysique :

La microphysique prend en compte les processus de vapeur d'eau, de nuage et de précipitation.

- Le schéma de Lin Purdue (**MP2**) prend en compte la vapeur d'eau, l'eau et la glace des nuages, la pluie, la neige et la grêle.
- Le schéma **MP3** (*WRF Single-Moment 3-class*) prévoit trois catégories de variables : la vapeur, l'eau/glace des nuages et la pluie/neige et convient parfaitement aux simulations à méso-échelle.
- Le schéma **MP4** (*WRF Single-Moment 5-class*) est similaire au schéma précédent mais distingue l'eau de la glace contenue dans les nuages ainsi que la pluie et la neige.
- Le schéma **MP6** (*WRF Single-Moment 6-class*) est similaire au schéma précédent mais inclut la grêle dans ses variables et est adapté aux simulations à très haute résolution.

5. Forçage à grande échelle :

Le forçage de grande échelle représente les conditions météorologiques (température, vent, humidité etc …) qui sont imposées aux limites du domaine étudié. Ces conditions sont le plus souvent issues d'un modèle météorologique de grande échelle. Ici, les données ré-analysées de 2 modèles météorologiques globaux sont utilisées : Era-Interim (EI) pour le modèle européen ECMWF et GFS-AVN pour le modèle américain GFS. Le terme ré-analyse est utilisé pour des simulations avec assimilation de données météorologiques (4D-var pour EI et 3D-var pour GFS). Les ré-analyses ECMWF ont une résolution d'environ 0.75° contre 1° environ pour GFS.

6. Guidage :

Le guidage (encore appelé « nudging ») consiste à relaxer de manière optimale les variables du modèle méso-échelle avec celles des champs analysés de grande-échelle. Ainsi, en complément du forçage aux limites, le rappel vers les variables de grande échelle se fait également à l'intérieur du domaine selon un temps caractéristique de rappel qui va définir l'intensité du guidage. Convenablement appliqué, le guidage permet de laisser se propager la variabilité interne de méso-échelle. Plus l'intensité du rappel est grande (temps de rappel petit), plus les champs méso-echelle sont proches des champs du modèle global interpolés sur sa grille et plus grande est l'inhibition de la physique de ce dernier.

Ici la technique utilisée est la technique du rappel en point de grille (grid-point nudging) : en chaque point de grille, les variables suivantes sont relaxées aux valeurs du modèle global : température, humidité, hauteur du Géopotentiel et composantes horizontales du vent. La relaxation peut se faire ou non dans la couche limite, suivant que l'on veuille la laisser se développer suivant la physique propre au modèle méso-échelle. La méthode de relaxation spectrale sera présentée et étudiée en détail dans l'annexe E.

Ici les analyses de grande échelle ERA-Interim sont utilisées pour le guidage. Différentes intensité ont été testées.

4. Résultats : Paramétrisations physiques

1. *Validation des quantités météorologiques*

Modèles de surface (Land Surface Model) et schémas de couche limite

Les séries temporelles des valeurs horaires observées et calculées pour la température à 2m et la vitesse du vent à 10m pour la période de mars 2003 sont présentées respectivement Figure 52 et Figure 53. Les données de scores pour les deux périodes hivernales sont présentées dans les Table 28 et Table 29 en parallèle des scores des périodes estivales lorsqu'elles sont disponibles.

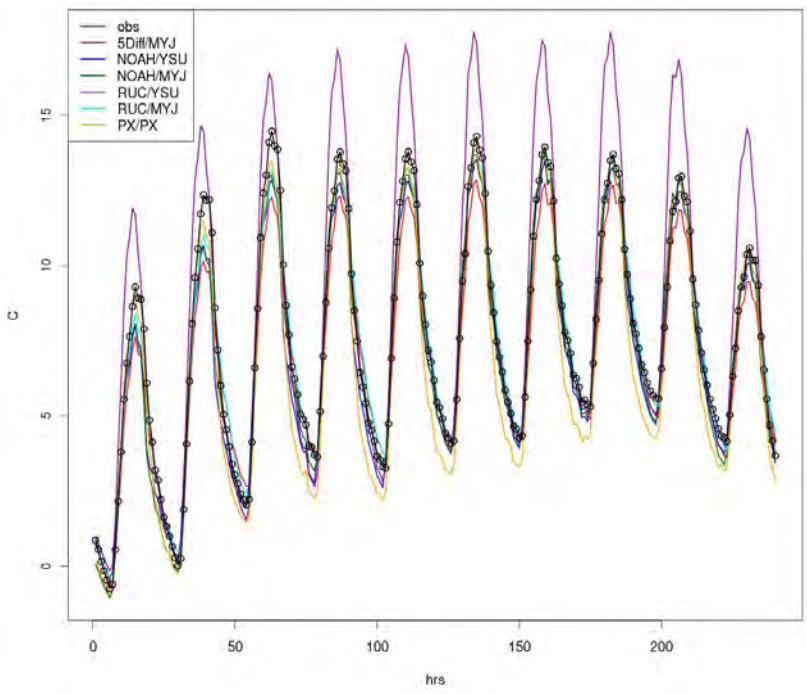

Figure 52 : Série temporelle (heures à partir du 21 mars 2003 00UT) de température à 2m observée (noir) et modélisée par les différentes combinaisons de modèles de surface et de schémas de couche limite.

La combinaison RUC/YSU a tendance à surestimer la température à 2m alors que les autres combinaisons en captent bien les variations et semblent équivalentes. Pour la vitesse de vent à 10m, toutes les configurations détectent les grandes valeurs caractéristiques. Les combinaisons 5Diff/MYJ et RUC/MYJ se détachent en surestimant la vitesse, en particulier lors des pics.

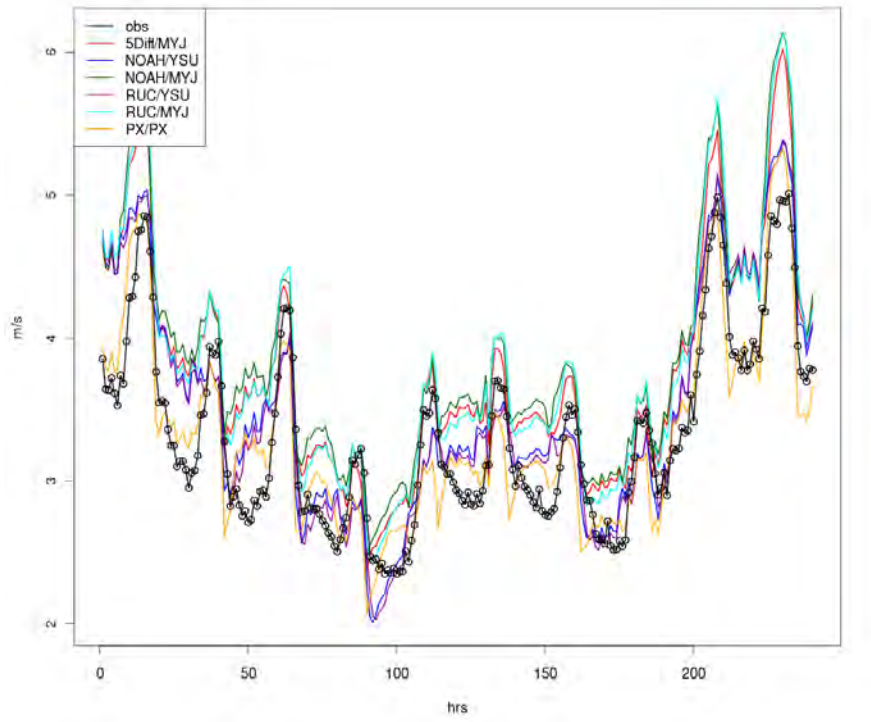

Figure 53 : Séries temporelle (heures à partir du 21 mars 2003 00UT) de vitesse du vent à 10m observée (noir) et modélisées par les différentes combinaisons de modèles de surface et de schémas de couche limite.

Table 28: Médianes des observations et des RMSE pour la température à 2m en hiver et en été pour différentes combinaisons de modèles de surface et de schémas de couche limite.

	T2 - Hiver				T2 - Eté			
	Mars 2003		Janvier 2006		Août 2003		Juillet 2005	
	Median Obs	Median RMSE	Median Obs	Median RMSE	Median Obs	Median RMSE	Median Obs	Median RMSE
	°C							
5Diff/MYJ	7,65	2,13	-0,65	---	23,35	2,18	19,45	1,76
Noah/YSU		2,03		2,05		2,00		1,70
Noah/MYJ		2,11		2,15		1,96		1,71
RUC/YSU		3,00		2,32		4,12		3,83
RUC/MYJ		1,99		2,16		1,97		1,70
PX/PX		2,12		2,17		1,83		1,60

Table 29: Médianes des observations et des RMSE pour la vitesse du vent à 10 m en hiver pour différentes combinaisons de modèles de surface et de schémas de couche limite.

	W10 - Hiver			
	Mars 2003		Janvier 2006	
	Median Obs	Median RMSE	Median Obs	Median RMSE
	m/s			
5Diff/MYJ	3	1,55	3	---
Noah/YSU		1,50		1,64
Noah/MYJ		1,62		1,70
RUC/YSU		1,50		1,63
RUC/MYJ		1,58		1,68
PX/PX		1,40		1,45

L'analyse des valeurs de RMSE confirme que RUC/YSU devrait être écarté et identifie PX/PX comme étant la meilleure configuration pour la modélisation de la vitesse du vent à 10m.

Convection profonde :

Les scores pour les données météorologiques (Table 30 et Table 31) sont équivalents avec un léger avantage pour la configuration de Grell-Devenyi.

Table 30: Médianes des observations et des RMSE pour la température à 2m en hiver et en été pour différents schémas de convection.

	T2 - Hiver				T2 - Eté			
	Mars 2003		Janvier 2006		Août 2003		Juillet 2005	
	Median Obs	Median RMSE	Median Obs	Median RMSE	Median Obs	Median RMSE	Median Obs	Median RMSE
	°C							
Kain-Fristch	7,65	3,00	-0,65	2,05	23,35	2,00	19,45	1,70
Grell-Devenyi		2,96		2,00		1,98		1,68

Table 31: Médianes des observations et des RMSE pour la vitesse du vent à 10m en hiver pour différents schémas de convection.

	W10 - Hiver			
	Mars 2003		Janvier 2006	
	Median Obs	Median RMSE	Median Obs	Median RMSE
	m/s			
Kain-Fristch	3	1,50	3	1,64
Grell-Devenyi		1,50		1,66

Bilan radiatif :

Les scores donnent un léger avantage au schéma radiatif RRTM-Dudhia (Table 32 et Table 33). Cependant la recommandation pour le schéma RRTMG-RRTMG (théoriquement pus réaliste) est maintenue.

Table 32: Médianes des observations et des RMSE pour la température à 2m en hiver et en été pour différents schémas radiatifs.

	T2 - Hiver				T2 - Eté			
	Mars 2003		Janvier 2006		Août 2003		Juillet 2005	
	Median Obs	Median RMSE	Median Obs	Median RMSE	Median Obs	Median RMSE	Median Obs	Median RMSE
	°C							
RRTM/Dudhia	7,65	2,61	-0,65	2,16	23,35	2,06	19,45	1,69
RRTMG/RRTMG		3,00		2,05		2,00		1,70

Table 33: Médianes des observations et des RMSE pour la vitesse du vent à 10m en hiver pour différents schémas radiatifs.

	W10 - Hiver			
	Mars 2003		Janvier 2006	
	Median Obs	Median RMSE	Median Obs	Median RMSE
	m/s			
RRTM/Dudhia	3	1,49	3	1,62
RRTMG/RRTMG		1,50		1,64

Microphysique :

Les 4 configurations de microphysique donnent des scores équivalents pour les données météorologiques (Table 34 et Table 35). La recommandation du WSM 5-class scheme (MP4) est maintenue.

Table 34: Médianes des observations et des RMSE pour la température à 2m en hiver pour différents modèles microphysiques.

	T2 - Hiver			
	Mars 2003		Janvier 2006	
	Median Obs	Median RMSE	Median Obs	Median RMSE
	°C			
MP2	7,65	3,00	-0,65	2,32
MP3		3,05		2,63
MP4		3,00		2,32
MP6		3,00		2,29

Table 35: Médianes des observations et des RMSE pour la vitesse du vent à 10m en hiver pour différents modèles microphysiques.

	W10 - Hiver			
	Mars 2003		Janvier 2006	
	Median Obs	Median RMSE	Median Obs	Median RMSE
	m/s			
MP2	3	1,49	3	1,64
MP3		1,50		1,63
MP4		1,50		1,63
MP6		1,50		1,63

2. Validation des quantités de la qualité de l'air

Modèles de surface (Land Surface Model) et schémas de couche limite

Plusieurs combinaisons de modèles de surface et de schémas de couche limite ont été testées et les séries temporelles des concentrations journalières observées et calculées pour les particules PM10 pour la période de mars 2003 sont présentées Figure 54. Pour chaque jour, les données de stations suburbaines et rurales ont été moyennées.

La Figure 55 présente également, de gauche à droite, de haut en bas, la distribution des concentrations de PM10 ainsi que les histogrammes des scores de performance entre modèle et observations : biais de concentrations, coefficient de corrélation et RMSE (Root Mean Square Error ou racine carrée de l'erreur quadratique moyenne).

On remarque que toutes les configurations ont tendance à sous-estimer les concentrations en particules mais détectent toutes le pic de concentration. Le modèle de surface 5Diff associé au schéma de couche limite MYJ donne le plus faible biais mais aussi le plus faible coefficient de corrélation. Par contre, si les combinaisons NOAH/MYJ et PX/PX ne donnent pas un biais minimal, elles fournissent en revanche un bon coefficient de corrélation et de bonnes valeurs de RMSE.

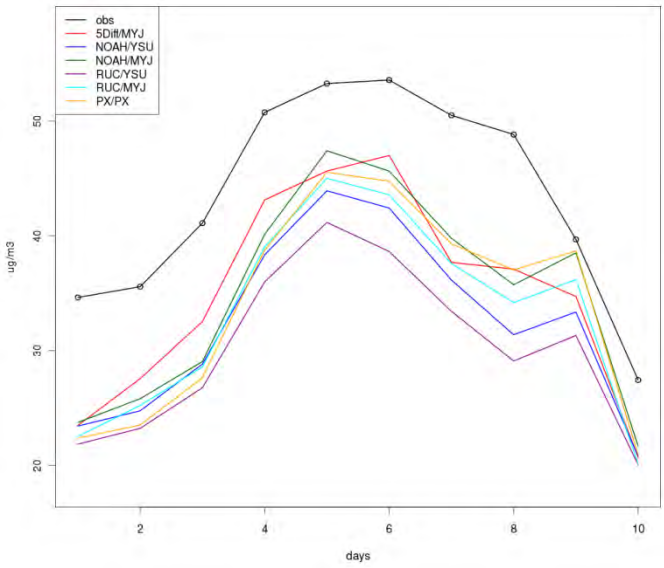

Figure 54 : Séries temporelles des moyennes de concentrations de PM10 observées aux stations suburbaines et rurales, et calculées avec différentes combinaisons de modèles de surface et de schémas de couche limite pour la période de mars 2003.

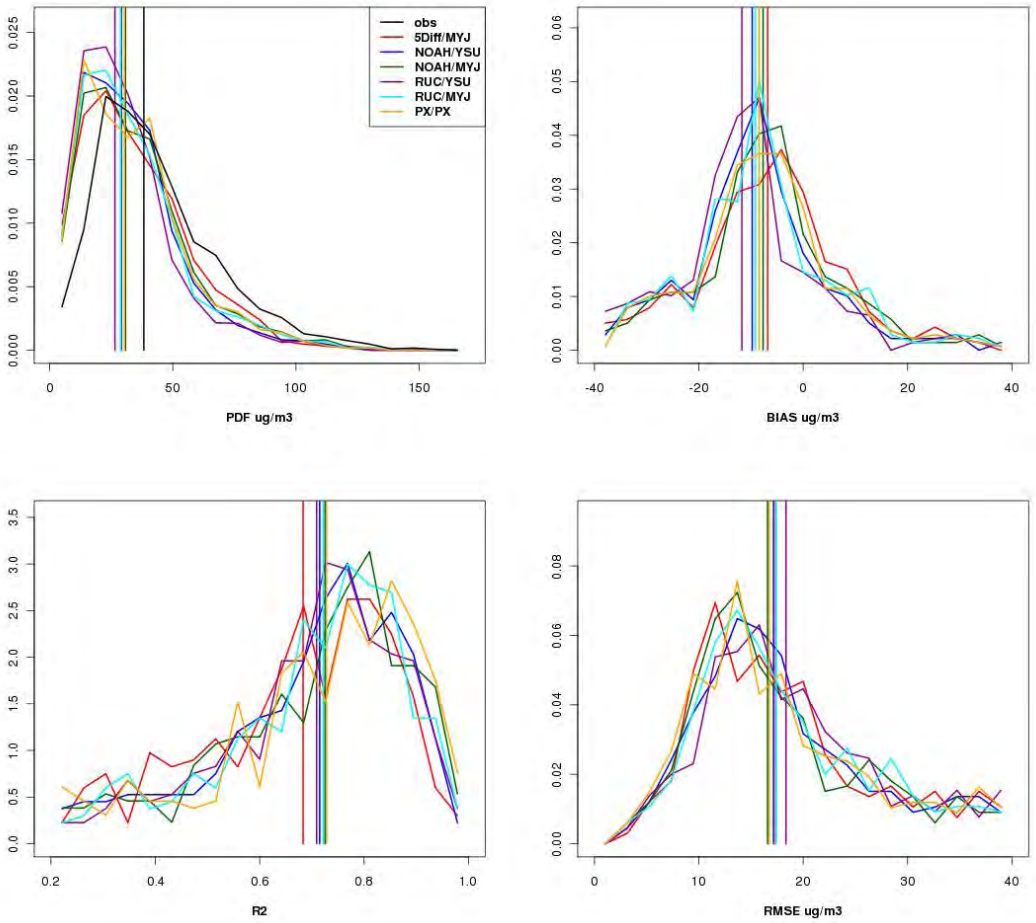

Figure 55 : (a) Densités de probabilité des concentrations de PM10 observées aux stations rurales et suburbaines sur 10 jours en mars 2003 et calculées selon différentes combinaisons de modèles de surfaces et de schémas de couche limite, (b) histogrammes des biais des concentrations moyennes temporelles, (c) histogrammes des coefficients de

corrélation, (d) histogrammes des RMSE. Sur chaque graphique, les droites verticales représentent les valeurs médianes.

La Table 36 donne les valeurs médianes des concentrations observées ainsi que les valeurs médianes de RMSE obtenues pour les PM10 sur les deux périodes hivernales et rappelle également ces valeurs pour l'ozone sur deux périodes estivales. A ce stade il apparait que la configuration RUC/YSU devrait être écartée, aucune combinaison ne se détachant réellement par ailleurs.

Table 36: Médianes des observations et des RMSE pour les PM10 en hiver et l'ozone en été pour différentes combinaisons de modèles de surface et de schémas de couche limite.

	PM10 - Hiver				O3 - Eté			
	Mars 2003		Janvier 2006		Août 2003		Juillet 2005	
	Median Obs	Median RMSE	Median Obs	Median RMSE	Median Obs	Median RMSE	Median Obs	Median RMSE
	ug/m3							
5Diff/MYJ	38,25	17,37	43,51	---	106,5	31,62	78,6	28,96
Noah/YSU		17,16		34,24		29,87		27,044
Noah/MYJ		16,58		32,68		31,46		28,577
RUC/YSU		18,35		36,62		33,45		30,866
RUC/MYJ		17,42		32,14		31,05		28,849
PX/PX		16,76		33,94		31,74		27,543

Convection profonde :

Les scores des deux configurations de WRF testées (*Kain-Fritsch* et *Grell-Devenyi*) sont équivalents (Table 37).

Table 37: Médianes des observations et des RMSE pour les PM10 en hiver et l'ozone en été pour différents schémas de convection.

	PM10 - Hiver				O3 - Eté			
	Mars 2003		Janvier 2006		Août 2003		Juillet 2005	
	Median Obs	Median RMSE	Median Obs	Median RMSE	Median Obs	Median RMSE	Median Obs	Median RMSE
	ug/m3							
Kain-Fristch	38,25	18,35	43,5	34,24	106,5	29,87	78,6	27,04
Grell-Devenyi		18,59		34,60		30,16		25,99

Bilan radiatif :

Les scores de données sur la qualité de l'air (Table 38) sont peu sensibles à la paramétrisation de bilan radiatif de WRF. Cependant le schéma RRTMG est recommandé car il offre théoriquement une représentation plus réaliste (prise en compte d'un recouvrement aléatoire de la couverture nuageuse).

Table 38: Médianes des observations et des RMSE pour les PM10 en hiver et l'ozone en été pour différents schémas radiatifs.

	PM10 - Hiver				O3 - Eté			
	Mars 2003		Janvier 2006		Août 2003		Juillet 2005	
	Median Obs	Median RMSE	Median Obs	Median RMSE	Median Obs	Median RMSE	Median Obs	Median RMSE
	ug/m3							
RRTM/Dudhia	38,25	17,64	43,5	35,25	106,5	30,23	78,6	25,83
RRTMG/RRTMG		18,35		34,24		29,87		27,04

Microphysique :

Bien que l'on ne dispose pas d'une étude de l'impact de la microphysique sur les scores de l'ozone en été, on remarque que les scores avec les configurations MP2 et MP3 sont légèrement moins bons qu'avec les autres configurations pour les PM10 en hiver (Table 39). Comme la configuration MP6 est plutôt adaptée aux simulations à haute résolution, la configuration MP4 est recommandée pour ce type de simulations à méso-échelle.

Table 39: Médianes des observations et des RMSE pour les PM10 en hiver et l'ozone en été pour différents modèles de microphysique.

	PM10 - Hiver			
	Mars 2003		Janvier 2006	
	Median Obs	Median RMSE	Median Obs	Median RMSE
	ug/m3			
MP2	38,25	18,44	43,5	37,07
MP3		19,39		37,05
MP4		18,35		36,62
MP6		18,31		36,87

5. Résultats : Forçage de grande échelle

1. *Validation des quantités météorologiques*

L'impact du forçage grande échelle sur la température de surface et le vent de surface est faible, qu'elle que soit le type de modèle de surface choisit (RUC ou NOAH).

Que ce soit pour le vent ou la température, les scores sont légèrement meilleurs avec des conditions aux limites issues de ERA-Interim (EI). Les mêmes conclusions peuvent être tirées des scores obtenus en été, excepté pour ceux de juillet 2005, où le vent est mieux reproduit avec GFS.

Table 40: Scores (RMSE, Biais normalisé et coefficient de corrélation) pour la température et le vent au sol, pour différents forçage à grande échelle.

	T2 - Hiver				T2 - Eté			
	Mars 2003		Janvier 2006		Août 2003		Juillet 2005	
	Median Obs	Median RMSE	Median Obs	Median RMSE	Median Obs	Median RMSE	Median Obs	Median RMSE
	°C							
EI/Noah	7,65	2,03	-0,65	2,05	23,35	2,00	19,45	1,70
GFS/Noah		2,12		2,23		2,19		1,81
EI/RUC		3,00		2,32		NR		NR
GFS/RUC		3,05		2,50		NR		NR

	W10 - Hiver				W10 - Eté			
	Mars 2003		Janvier 2006		Aout 2003		Juillet 2005	
	Median Obs	Median RMSE	Median Obs	Median RMSE	Median Obs	Median RMSE	Median Obs	Median RMSE
	m/s				m/s			
EI/Noah	3,00	1,50	3,00	1,64		NR		NR
GFS/Noah		1,51		1,58		NR		NR
EI/RUC		1,50		1,63		NR		NR
GFS/RUC		1,49		1,60		NR		NR

2. *Validation de la qualité de l'air*

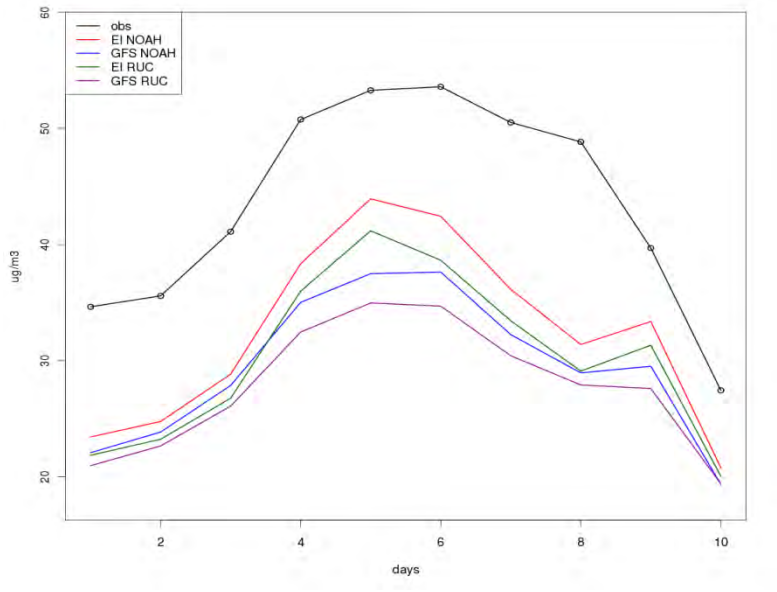

Figure 56: évolution temporelle de la concentration journalière de PM10 mesurée (ligne noire) et simulée.

L'impact du forçage grande échelle sur les concentrations de PM10 est important avec des valeurs absolues de biais qui augmente de plus de 5% lorsque les champs GFS sont utilisés, et ceux quel que soit le modèle de sol utilisé (Noah ou RUC). En revanche, les concentrations en O3 l'été ne sont que peu influencées par le choix des conditions aux limites météorologiques.

Dans tous les cas, les conditions aux limites issues des analyses ERA-Interim donnent de meilleurs scores que celles issues des analyses GFS.

	PM10 - Hiver				O3 - Eté			
	Mars 2003		Janvier 2006		Août 2003		Juillet 2005	
	Median Obs	Median RMSE	Median Obs	Median RMSE	Median Obs	Median RMSE	Median Obs	Median RMSE
	ug/m3							
EI/Noah	38,25	17,16	43,51	34,24	106,50	29,87	78,60	27,04
GFS/Noah		18,19		33,06		30,43		27,17
EI/RUC		18,35		36,62		NR		NR
GFS/RUC		19,74		34,28		NR		NR

Compte tenu des meilleurs scores obtenus à la fois sur les concentrations de PM10 en hiver, d'O3 en été et sur les données météorologiques, il est conseillé d'utiliser un forçage grande échelle à partir des champs analysés ERA-Interim.

6. Résultats : Guidage (nudging)

L'option de guidage spectral n'a été testée que pour mars 2003. Pour janvier 2006, aucune option, ni aucune intensité de guidage n'ont été testées.

1. *Validation des quantités météorologiques*

Les options de guidage (point de grille : FDDA1, spectral : FDDA2, avec ou sans guidage dans la couche limite), ainsi que le choix de l'intensité du guidage, ont une plus grande influence sur le vent de basse couche que sur la température de basse couche.

Options de guidage

Généralement, les scores sont meilleurs pour l'option « guidage en point de grille » et lorsque les variables sont guidées dans la couche limite (FDDA1/PBL).

Table 41: Scores (RMSE, Biais normalisé et coefficient de corrélation) pour la température et le vent au sol, pour différentes options de guidage.

	T2 - Hiver						T2 - Eté					
	Mars 2003			Janvier 2006			Août 2003			Juillet 2005		
	RMSE	**Norm Bias**	R	**RMSE**	**Norm Bias**	**R**	RMSE	**Norm Bias**	R	**RMSE**	**Norm Bias**	**R**
FDDA1/PBL	**2,03**	-2,79	**0,94**	NR	NR	NR	**2,00**	-2,07	0,94	**1,70**	**-1,37**	**0,94**
FDDA1/noPBL	**2,18**	-1,39	**0,91**	NR	NR	NR	**2,17**	-2,40	0,93	**1,88**	**-1,86**	**0,92**
FDDA2/PBL	**2,34**	-1,00	**0,90**	NR	NR	NR	NR	NR	NR	NR	NR	NR
FDDA2/noPBL	**2,42**	-0,27	**0,88**	NR	NR	NR	NR	NR	NR	NR	NR	NR

	W10 - Hiver					
	Mars 2003			Janvier 2006		
	RMSE	**Norm Bias**	R	**RMSE**	**Norm Bias**	**R**
FDDA1/PBL	**1,50**	11,22	**0,87**	NR	NR	NR
FDDA1/noPBL	**1,70**	23,82	**0,86**	NR	NR	NR
FDDA2/PBL	**1,74**	22,42	**0,76**	NR	NR	NR
FDDA2/noPBL	**1,84**	28,44	**0,76**	NR	NR	NR

Intensité du guidage

L'amélioration ou la dégradation des scores lorsque le guidage se fait plus intense n'est pas uniforme pour la température et le vent, ni pour toutes les périodes considérées.

En ce qui concerne la température, le biais est généralement meilleur avec une plus faible intensité de guidage (0.00002 ou 0.00005). Par contre, la RMSE et le coefficient de corrélation sont généralement meilleurs avec une intensité de guidage maximale (0.00060). Concernant la vitesse du vent, les meilleurs scores sont obtenus avec de forte intensité de guidage (0.00020 ou 0.00060).

Table 42: Scores (RMSE, Biais normalisé et coefficient de corrélation) pour la température et le vent au sol, pour différentes intensités de guidage.

	T2 - Hiver						T2 - Eté					
	Mars 2003			Janvier 2006			Août 2003			Juillet 2005		
	RMSE	Norm Bias	R	**NRMSE**	**Norm Bias**		RMSE	Norm Bias	R	**RMSE**	**Norm Bias**	**R**
2	2,12	0,51	0,92	NR	NR	NR	2,15	-2,14	0,93	**1,83**	**-1,21**	**0,92**
5	2,04	-1,65	0,93	NR	NR	NR	2,08	-2,06	0,94	**1,75**	**-1,25**	**0,93**
10	2,03	-2,81	0,94	NR	NR	NR	2,00	-2,07	0,94	**1,70**	**-1,37**	**0,94**
20	2,05	-4,31	0,94	NR	NR	NR	1,98	-2,23	0,94	**1,66**	**-1,57**	**0,94**
60	2,12	-6,36	0,93	NR	NR	NR	1,95	-2,29	0,95	**1,63**	**-1,79**	**0,94**

	W10 - Hiver					
	Mars 2003			Janvier 2006		
	RMSE	**Norm Bias**	R	**RMSE**	**Norm Bias**	**R**
2	**1,66**	**20,70**	**0,66**	NR	NR	NR
5	**1,57**	**15,99**	**0,68**	NR	NR	NR
10	**1,50**	**10,30**	**0,69**	NR	NR	NR
20	**1,42**	**3,44**	**0,69**	NR	NR	NR
60	**1,39**	**-7,85**	**0,69**	NR	NR	NR

2. *Validation de la qualité de l'air*

Le choix des options de guidage (en point de grille ou spectral, avec ou sans guidage dans la couche limite) ont un impact fort sur les concentrations de PM10 en hiver. Par exemple, le biais est doublé entre la simulation guidée en point de grille et celle guidée spectralement. Guider ou non dans la couche limite, a un impact bien moindre sur les concentrations d'O3 en été (pas de test sur le guidage spectral en été). Le choix de l'intensité de guidage influence également fortement les scores de PM10 et dans une moindre mesure, ceux d'O3.

Options de guidage

Concernant le type de guidage, les scores de PM10 sont nettement moins bons lorsque le guidage spectral est utilisé. Les scores de PM10 sont également meilleurs lorsque le guidage est maintenu dans la couche limite, alors qu'ils sont très légèrement moins bons pour l'O3 en été.

Table 43: Scores (RMSE, Biais normalisé et coefficient de corrélation) pour les concentrations dePM10 en hiver et d'O3 en été, pour différentes options de guidage.

	PM10 - Hiver						O3 - Eté					
	Mars 2003			Janvier 2006			Août 2003			Juillet 2005		
	RMSE	Norm Bias	R	**RMSE**	**Norm Bias**	**R**	RMSE	**Norm Bias**	R	**RMSE**	**Norm Bias**	**R**
FDDA1/PBL	**17,16**	-25,57	**0,71**	NR	NR	NR	**29,87**	2,67	0,82	**27,04**	**13,49**	**0,76**
FDDA1/noPBL	**20,13**	-38,48	**0,69**	NR	NR	NR	**29,55**	2,71	0,83	**27,00**	**13,28**	**0,76**
FDDA2/PBL	**23,84**	-50,51	**0,52**	NR	NR	NR	NR	NR	NR	NR	NR	NR
FDDA2/noPBL	**24,50**	-52,41	**0,54**	NR	NR	NR	NR	NR	NR	NR	NR	NR

Intensité du guidage

De manière générale, plus les simulations météorologiques sont guidées, meilleur est le biais en PM10 ainsi qu'en O3. En revanche, pour l'O3, les corrélations sont meilleures lorsque l'intensité du guidage est faible. En termes de RMSE, cela résulte en une meilleur RMSE avec des simulations fortement guidées pour les PM10 et un guidage optimal avec une intensité de 0.00010 pour l'O3.

Table 44: Scores (RMSE, Biais normalisé et coefficient de corrélation) pour les concentrations dePM10 en hiver et d'O3 en été, pour différentes intensités de guidage. L'intensité du guidage sur la 1ere colonne a été multipliée par $10^{e}5$.

	PM10 - Hiver						O3 - Eté					
	Mars 2003			Janvier 2006			Août 2003			Juillet 2005		
	RMSE	Norm Bias	R	**NRMSE**	**Norm Bias**	**R**	RMSE	Norm Bias	R	**RMSE**	**Norm Bias**	**R**
2	19,36	-33,62	0,70	NR	NR	NR	30,21	3,38	0,83	**27,25**	**14,29**	**0,76**
5	18,13	-29,06	0,72	NR	NR	NR	30,05	3,21	0,83	**27,12**	**13,79**	**0,76**
10	17,16	-25,57	0,71	NR	NR	NR	29,87	2,67	0,82	**27,04**	**13,49**	**0,76**
20	16,78	-22,57	0,72	NR	NR	NR	30,15	0,77	0,82	**27,01**	**13,13**	**0,75**
60	16,25	-14,85	0,74	NR	NR	NR	30,36	0,76	0,81	**27,10**	**13,15**	**0,75**

Le choix d'un guidage par point de grille et d'un guidage dans la couche limite se détache clairement, aussi bien pour les variables météorologiques que pour les concentrations en PM10 et O3. Concernant, l'intensité du guidage, un guidage fort des champs météorologiques résulte généralement en de meilleurs scores de vent dans les basses couches et de PM10. En revanche, un guidage faible donne de meilleurs résultats en ce qui concerne la température. Les meilleurs scores d'O3 sont obtenus avec une intensité de guidage de 0.00010 s-1. Pour éviter un guidage trop important qui aurait pour effet néfaste d'inhiber la formation de petites structures dans le modèle méso-échelle, la valeur de 0.00010 s-1 (c'est-à-dire une relaxation des champs météorologiques toutes les 2.7 heures) est recommandée.

E. THE INFLUENCE OF NUDGING ON REGIONAL CLIMATE SIMULATIONS

1. Introduction

Le système climatique couvre une large gamme d'échelles spatiales et temporelles qui interagissent entre elles d'une manière complètement chaotique et non linéaire. Les modèles du climat global appelés aussi les modèles de circulation générale (GCMs) représentent donc des outils fondamentaux pour la compréhension du climat. Cependant, de fait de leur résolution horizontale très grossières de l'ordre de 250 à 500 km, ces modèles ne sont pas adaptés aux études d'impact et aux stratégies d'adaptation associées aux changements climatiques. Ces études se font à des échelles régionales et demandent des résolutions beaucoup plus fines entre 10 et 100 km. Cette information est fournie par les modèles du climat régional (RCM), le plus souvent à aire limitée, centrés sur une région donnée et piloté aux bords par les sorties des GCM ou des (ré)analyses météorologiques. Des études antérieures ont montré la nécessité de relaxer les champs tridimensionnels des RCMs vers les champs de forçage afin d'éviter des écarts trop importants de la circulation atmosphérique à grande échelle. Cette technique de relaxation est aussi appelé "guidage". Ils existent deux types de guidage nécessitant l'ajustement adhoc d'un coefficient de relaxation : le guidage spectral qui consiste à relaxer le RCM à certaines échelles spatiales et le guidage indiscriminé qui consiste à relaxer le RCM indifféremment à toutes les échelles. L'objectif de ces études est d'étudier l'impact du guidage sur la représentation des processus de fine échelle dans la modélisation du climat régional par rapport aux différents paramètres tels que la taille du domaine, la résolution horizontale, la fréquence d'actualisation des champs de forçage et l'ensemble des variables à guider. Une approche idéalisée, appelé « the Big Brother Experiment» est utilisée. C'est une méthode où l'état de l'atmosphère est connu. Deux modèles ont été utilisés : un modèle quasi-géostrophique à deux couches et le modèle américain WRF (Weather Research and Forecast).

2. Analyse par approche "Big-Brother" dans un modèle quasi-géostrophique

Les équations régissant un modèle quasi-géostrophique (QG) à deux couches sont :

$$\text{(1a)}\ \partial_t Q_1 + J(\Psi_1, \mathrm{Q}_1) = -\upsilon\nabla^6\Psi_1$$

$$\text{(1b)}\ \partial_t Q_2 + J(\Psi_2, \mathrm{Q}_2) = -\upsilon\nabla^6\Psi_2 - \kappa\nabla^2\Psi_2$$

où les indices 1 and 2 correspondent respectivement aux couches supérieure (troposphère libre) et inférieure (couche limite) du modèle. Les quantités Ψ_i et Q_i sont les fonctions de courant et la vorticité potentielle (potential vorticity PV) pour la couche i, J est le Jacobien horizontal $J(\Psi_i, \mathrm{Q}_i) = \partial_x\Psi_i\partial_y Q_i - \partial_y\Psi_i\partial_x Q_i$ et ∇^2 est le Laplacien horizontal $\nabla^2\Psi_i = \Delta\Psi_i = \partial^2_{x^2}\Psi_i + \partial^2_{y^2}\Psi_i$. Les deux couches ont la même épaisseur H au repos. La quantité υ est la diffusion numérique et κ est la friction de surface.

Le guidage indiscriminé est un guidage encore appelé en point de grille et initialement développé pour l'assimilation (Davies and Turner, 1977). Il suppose l'ajout d'un terme de relaxation aux équations qui fournit le système suivant :

$$\text{(2a)}\ \partial_t Q_1 + J(\Psi_1, \mathrm{Q}_1) = -\upsilon\nabla^6\Psi_1 - \frac{1}{\tau}\left(Q_1 - Q_1^{GCM}\right)$$

$$\text{(2b)}\ \partial_t Q_2 + J(\Psi_2, \mathrm{Q}_2) = -\upsilon\nabla^6\Psi_2 - \kappa\nabla^2\Psi_2 - \frac{1}{\tau}\left(Q_2 - Q_2^{GCM}\right)$$

De la même façon qu'un modèle régional à aire limitée, le modèle QG a été développé avec imbrication de sous-domaines. L'approche utilisée pour évaluer la "qualité" de la simulation est celle du "Big-Brother". Le modèle QG à haute résolution est mis en œuvre sur un large domaine (c'est le Big-Brother BB). Puis le champ simulé est dégradé spatialement pour produire des champs de forçage de grande échelle (type analyses, réanalyses et modèles de circulation

générale GCM). Le rapport entre les résolutions horizontales du forçage de grande échelle et du champ simulé est dénoté α et permet pour la suite les notions de "grandes" et "petites" échelles (la grande échelle étant celle du forçage). Ces champs sont ensuite utilisés pour forcer le modèle QG sur un sous-domaine (Little-Brother LB). Les simulations réalisées avec le Little-Brother sont comparées à la "réalité" produite par le Big-Brother (Figure 57).

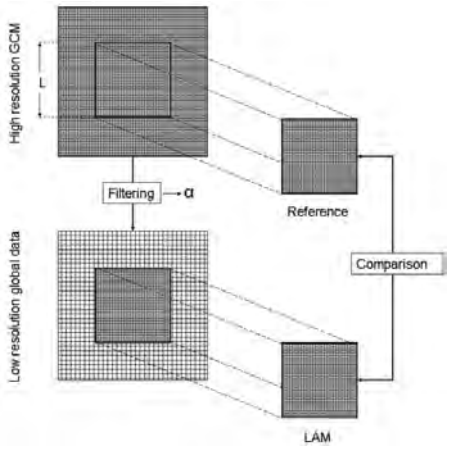

Figure 57: Schéma de l'approche "Big-Brother". Le coefficient α est un coefficient de filtrage. Source: (Omrani H. et al., 2012a).

Dans le cas d'un guidage indiscriminé, toutes les échelles spatiales simulés par le RCM sont rappelées vers le forçage de grande échelle. L'enjeu est d'établir les paramètres physiques contrôlant le temps de guidage et en particulier un temps de guidage optimal minimisant l'erreur commise à la fois sur la simulation des processus d'échelles fines (de taille inférieure à celle la plus petite l'échelle du GCM) et celle des processus de grande échelle (de taille supérieure à celle la plus petite l'échelle du GCM).

Les champs de PV obtenus pour un domaine de même taille que le Big-Brother, sont représentés sur la Figure 58.

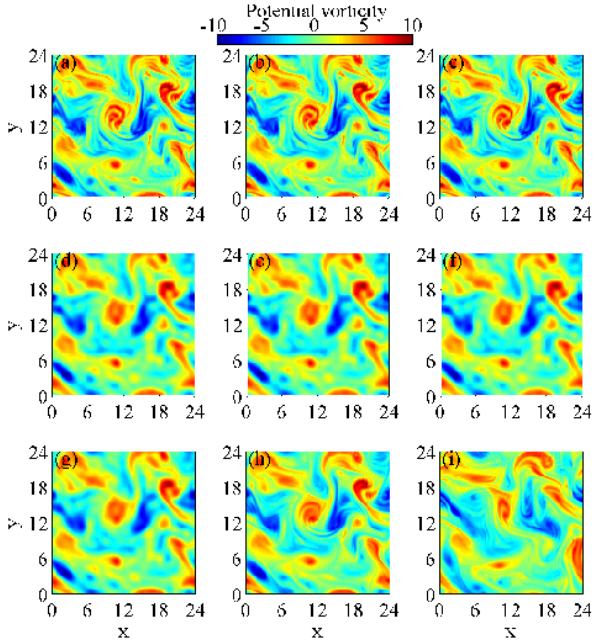

Figure 58: Champs de vorticité potentielle. Les encarts a, b et c (identiques) représentent les champs issus du "Big-Brother" (champ de référence à haute résolution). Les encarts d, e et f (identiques) représentent le champ de forçage de grande échelle avec $\alpha = 1/3$ (champ "GCM"). Les encarts g, h et i représentent les champs issus du "Little-Brother"(champs "RCM") pour $\tau=0.01\tau_p$, $0.4\tau_p$ etτ_p, respectivement. Source:(Omrani H. et al., 2012a).

Une valeur faible du temps de guidage $\tau = 0.01\tau_p$ (où τ_p est le temps de prévisibilité du système atmosphérique[38]) force le modèle à reproduire le champ de forçage à grande échelle : en effet, en comparant les figures 2g et d et les figures 2d et a, nous pouvons observer que le modèle reproduit parfaitement les tourbillons atmosphériques de grande échelle, mais pas les structures de fine échelle. D'autre part, pour $\tau = \tau_p$ (Figure 58c, f, i), le modèle est incapable de reproduire la "réalité" fournie par le Big-Brother (Figure 58c), que ce soit pour les structures de grande échelle (Figure 58f) où les structures de petite échelle (Figure 58i). Le temps de guidage correspondant à $\tau=0.4\tau_p$ est visuellement le temps de guidage optimal permettant de minimiser l'erreur sur la grande et la petite échelle. De nombreuses simulations ont été réalisées, en faisant varier le temps de guidage τ, le rapport de résolution α et la taille du modèle imbriqué (non montrés). L'étude de ces simulations permet de confirmer qu'il existe dans le modèle QG un temps optimal de guidage τ_p~$0.4\tau_p$. Dans le cas d'un modèle imbriqué, la taille du domaine du Little-Brother, plus petite que le Big-Brother, entre en jeu. Pour une taille de domaine imbriqué inférieure à 18 fois la taille des grands tourbillons atmosphériques (cyclones et anticyclones)[39], le forçage par les bords du domaine domine et l'effet du guidage est moins perceptible. On peut expliquer ceci par la raison suivante : si le domaine est "suffisamment petit", l'erreur infinitésimale induite par des conditions initiales imparfaites est évacuée en dehors du domaine par advection par la circulation atmosphérique plus vite qu'il n'est nécessaire au champ atmosphérique de grande échelle simulé de dévier du forçage atmosphérique de grande échelle.

Quant au guidage spectral (Von Storch H. et al., 2000), il suppose l'ajout d'un terme de relaxation aux équations qui fournit le système suivant :

$$\text{(3a)}\ \partial_t Q_1 + J(\Psi_1, \mathrm{Q}_1) = -\upsilon\nabla^6\Psi_1 - \frac{1}{\tau}\left(Q_1^{LS} - Q_1^{GCM}\right)$$

$$\text{(3b)}\ \partial_t Q_2 + J(\Psi_2, \mathrm{Q}_2) = -\upsilon\nabla^6\Psi_2 - \kappa\nabla^2\Psi_2 - \frac{1}{\tau}\left(Q_2^{LS} - Q_2^{GCM}\right)$$

L'exposant "LS" signifie "grande échelle" ("large scale"). Dans le cas du guidage spectral, seules les champs de grande échelle simulés par le RCM sont relaxés vers ceux du GCM. En ce cas, on peut s'interroger sur l'existence d'un temps de guidage optimal puisque en supposant le caractère "parfait" des champs du GCM, le temps de guidage devrait être égal à 0 pour assurer que $Q_1^{LS} = Q_1^{GCM}$. Or les champs du GCM, hormis le fait qu'ils ne sont pas parfaits, sont surtout fournis à intervalle de temps réguliers τ_a (généralement toutes les 6 h), bien plus grands que le pas de temps de calcul. Pour fournir les conditions aux limites du domaine à chaque pas de temps, le RCM à aire limitée interpole les champs entre 2 échéances. Cette interpolation ne permet pas de restituer la dynamique du champ de grande échelle à haute résolution temporelle. Le temps de guidage optimal est généralement compris entre $0.1\tau_p$ et $0.4\tau_p$ mais il dépend du rapport entre la résolution du RCM et celle du GCM et du rapport τ_a/τ_p. En effet, les processus d'échelle fine présentent une variabilité temporelle à haute fréquence. Même si c'est processus sont présents dans le GCM, il est inutile de guider fortement ces échelles si l'intervalle de temps entre deux forçage est trop grand. En effet, la variabilité haute fréquence de ces processus de fine échelle ne sera pas correctement représentée et induira donc du bruit dans la simulation par erreur d'échantillonnage. La Figure 59 ci-dessous indique le rapport maximal entre la résolution du RCM et celle du GCM en fonction du rapport τ_a/τ_p.

[38] Le temps de prévisibilité du système est obtenu en calculant l'exposant de Lyapounov associé à l'évolution temporelle d'une perturbation infinitésimale des conditions initiales.

[39] La taille des grands tourbillons est communément appelée le rayon de déformation de Rossby.

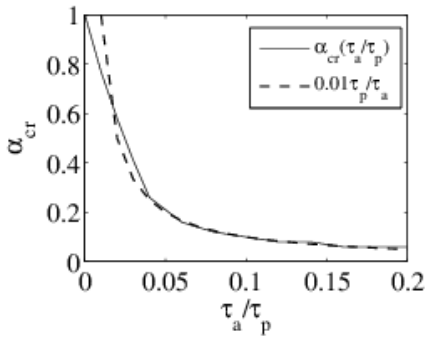

Figure 59: Rapport maximal entre la résolution du RCM et celle du GCM en fonction du rapport τ_a/τ_p. Source:(Omrani H. et al., 2012b).

Les résultats obtenus avec le modèle QG dans ses versions "guidage indiscriminé" et "guidage spectral" ont permis de mieux cerner les paramètres physiques contrôlant le comportement des simulations par RCM à aire limitée en présence de guidage. Il était alors nécessaire de déterminer le comportement aux guidages indiscriminé et spectral d'un RCM intégrant toute la complexité de l'environnement atmosphérique. Dans le cadre de SALUT'AIR et plus largement du programme international CORDEX de downscaling, le choix s'est porté sur le modèle WRF.

3. Analyse par approche "Big-Brother" dans le modèle WRF

Une approche similaire en "Big Brother" a été réalisée avec le modèle WRF sur 2 domaines correspondant aux domaines EURO-CORDEX sur l'Europe et MED-CORDEX sur la Méditerranée. Les deux domaines sont représentés sur la Figure 60.

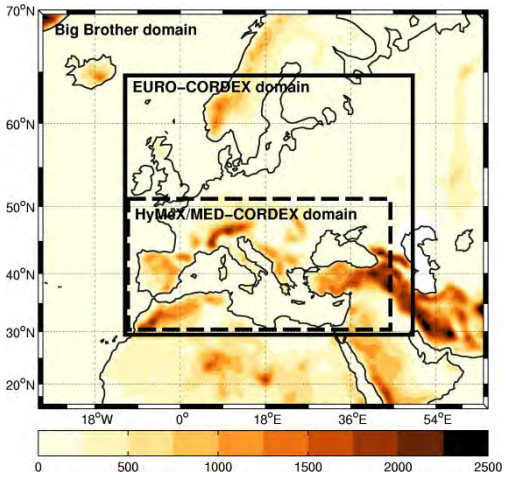

Figure 60: Domaines de simulations EURO-CORDEX et MED-CORDEX. Source: (Omrani H. et al., 2013a).

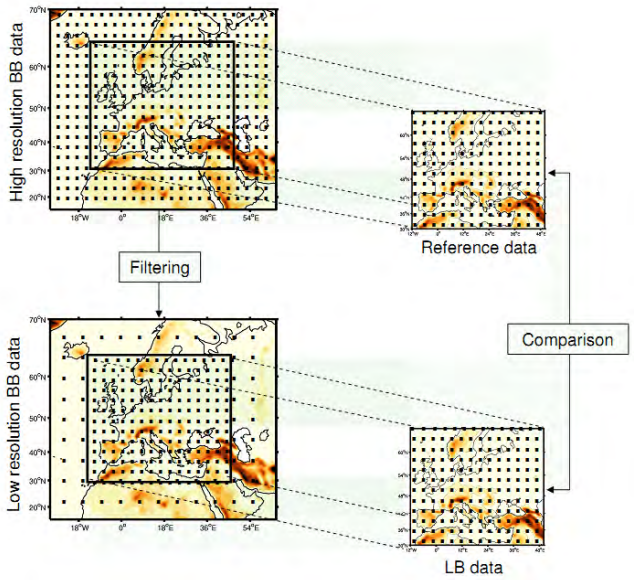

Figure 61: Schéma de l'approche "Big-Brother"avec WRF. Source: (Omrani H. et al., 2013b).

La méthode "Big-Brother" avec WRF est schématisée sur la Figure 61. Les simulations "Big-Brother" ont été réalisées à 50 km de résolution sur 4 mois d'hiver et 4 mois d'été de 1990. Les simulations ont été filtrées pour fournir des champs de grande échelle à 300 km de résolution. Les intervalles de temps des champs de forçage et les temps de guidage testés ont été respectivement τ_a = 3, 6 et 12 h et τ_p = 1, 3, 6 et 12 h.

Les résultats montrent clairement que le guidage améliore la capacité du modèle à reproduire l'état de référence de l'atmosphère indépendamment de la taille du domaine et de la variable diagnostiquée. Une illustration est reproduite en Figure 62 pour la température à 2 m. La figure mon le bais moyen par rapport à la "réalité synthétique" (simulation Big-Brother) des températures pour l'été et l'hiver pour les simulations non guidée et guidées par guidages indiscriminé et spectral pour τ_a = 3 h et τ_p = 1 h. Toutefois, les performances du modèle dépendent de la variable, la saison, la fréquence des données de forçage et du choix des variables à guider. En résumé, le temps de guidage optimal pour le guidage indiscriminé est obtenu aux alentours de 6h, ce qui confirme les résultats obtenus par (Salameh T. et al., 2010) sur la base de la théorie linéaire. En ce qui concerne le guidage spectral, τ_p = 1 h fournit les meilleurs résultats pour τ_a = 3 et 6 h et τ_p = 3 h fournit les meilleurs résultats pour τ_a = 12 h. Ceci est attribuable à l'erreur d'échantillonnage discutée dans l'analyse du modèle QG.

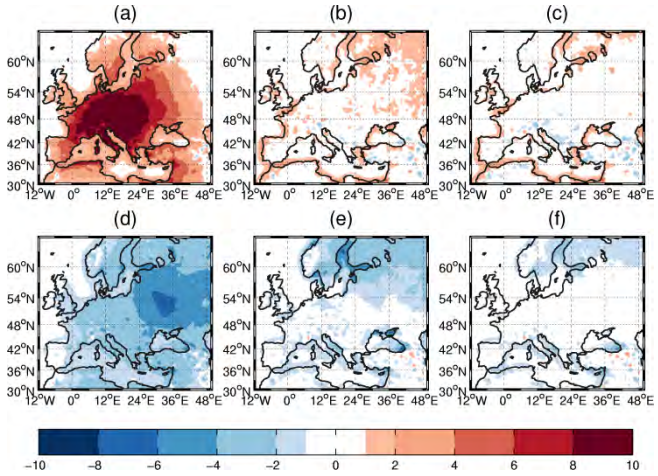

Figure 62: Bais moyen par rapport à la "réalité synthétique" (simulation Big-Brother) des températures pour l'été (encarts a,b et c) et l'hiver (encarts d, e et f). Les encarts a et d montrent la simulation non guidée, les encarts b et e montrent la simulation par guidage indiscriminé et les encarts c et f montrent la simulation par guidage spectral pour τ_a = 3 h et τ_p = 1 h. Source: (Omrani H. et al., 2013b).

Le fort biais de température centré sur l'Europe Centrale dans la simulation non guidée est purement numérique. Des tests ont été réalisés en déplaçant le domaine de simulation vers l'Ouest et vers l'Est. Cette anomalie de température par rapport à la "réalité" est toujours localisée au centre du domaine. Ceci peut s'expliquer par la rétroaction des petites échelles sur la grande (cascade inverse) en absence de guidage. Cette rétroaction va créer au centre du domaine une modification de la circulation de grande échelle incompatible avec les champs de grande échelle fournit aux limites du domaine. Cette incohérence va se traduire par une mise la simulation d'une circulation de grande échelle solution des équations et compatibles avec les conditions aux limites mais différente de la circulation de grande échelle véritable. C'est ce qu'illustre la Figure 63 présentant l'anomalie de géopotentiel à 500 hPa.

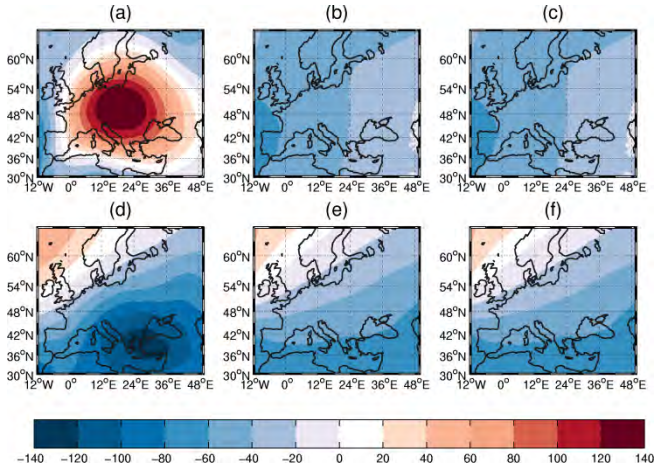

Figure 63: Bais moyen par rapport à la "réalité synthétique" (simulation Big-Brother) du géopotentiel à 500 hPa pour l'été (encarts a,b et c) et l'hiver (encarts d, e et f). Les encarts a et d montrent la simulation non guidée, les encarts b et e montrent la simulation par guidage indiscriminé et les encarts c et f montrent la simulation par guidage spectral pour τ_a = 3 h et τ_p = 1 h. Source: (Omrani H. et al., 2013b).

Cette anomalie anticyclonique d'été pourrait expliquer en partie les biais chauds simulés par (Radu R. et al., 2008;Rowell D.P. and Jones R.G., 2006;Caldwell et al., 2009).

Dans cette étude, l'ensemble des variables "guidables" dans WRF ont été guidées (température et vent, et humidité pour la version indiscriminée). Une dernière expérience a été réalisée en réalisant un ensemble de simulations intégrant toutes les combinaisons possibles de

guidage. Les résultats obtenus avec guidage indiscriminé et guidage spectral sont semblables. La Figure 64 montre les résultats obtenus pour la température avec le guidage indiscriminé.

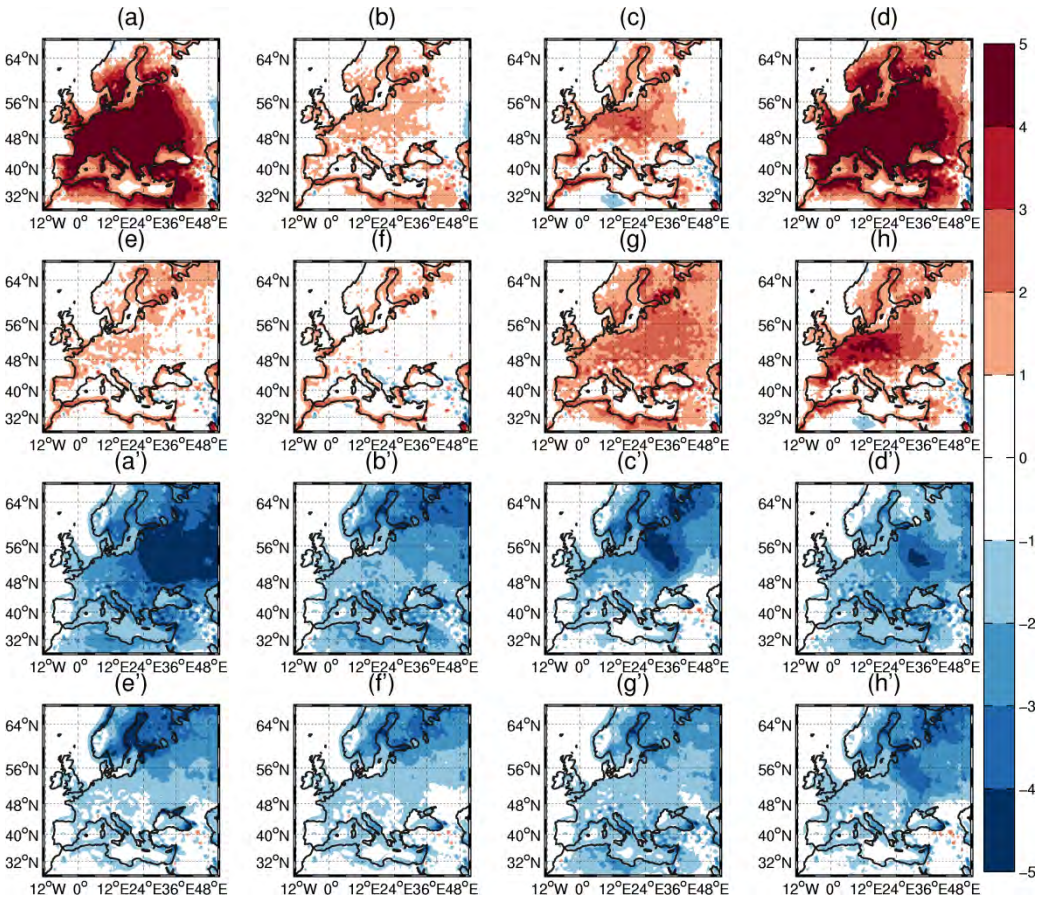

Figure 64: Bais moyen par rapport à la "réalité synthétique" (simulation Big-Brother) des températures pour l'été (encarts a - h) et l'hiver (encarts a' - h'). Les encarts a à h pour l'été (a' à h' pour l'hiver) montrent les résultats de la simulation non guidée, des simulations guidées UV, T, Q, UV-T-Q, UV-T, UV-Q, T-Q avec (UV indiquant le guidage des composantes du vent, T celui de la température et Q celui de l'humidité). Les variables τ_a = 6 h et τ_p = 6 h. Source:(Omrani H. et al., 2013a).

Les meilleurs résultats sont obtenus quand le vent est guidé. Les résultats sont d'autant meilleurs si la température est aussi guidée. Ceci est corrélé à une meilleure simulation du géopotentiel à 500 hPa représentant la circulation de grande échelle. La meilleure simulation du géopotentiel est obtenue quand le vent est guidé car celui-ci est lié à une intégration près au vent géostrophique. L'amélioration avec la température s'explique par le fait que le géopotentiel est aussi lié à 2 intégrations près à la température par l'équation du vent thermique. Les constantes d'intégration n'étant pas contraintes, un biais résiduel demeure sur le géopotentiel, d'autant plus élevé que le nombre d'intégrations est important. Le biais résiduel de géopotentiel pourrait être supprimé en guidant la pression à la surface ce qui pourrait permettre de contraindre les intégrations.

4. Conclusion

La question de l'utilisation du guidage, terme non physique, dans la simulation climatique régionale reste encore objet de débats. L'approche "Big-Brother" permet de mieux comprendre les avantages et limites du guidage. Le principal avantage de la méthode est qu'elle permet de simuler les processus de fine échelle dynamiquement compatibles avec la grande échelle qui les force. Ceci s'est avéré essentiel pour expliquer et supprimer des biais de température simulés dans des études publiées de régionalisation. Sa principale limite est l'absence de rétroaction forte sur la grande échelle qui inhibe en grande partie la variabilité interne du RCM. Néanmoins, la

notion même de variabilité interne d'un RCM à aire limitée qui requiert des conditions aux limités n'est pas aussi claire que pour les GCM. Sa seconde limite est que le champ simulé par le RCM dépend complètement de la qualité du forçage de grande échelle. Si le forçage est mauvais, le champ simulé le sera autant. Ceci dit, la capacité de la cascade inverse à corriger le champ de grande échelle n'est pas démontrée et reste un champ de recherche largement ouvert. Enfin, l'optimisation du temps de guidage par une approche Big-Brother n'assure en aucun cas que la comparaison à des observations sera bonne du fait de biais possible dans les observations et du choix des paramétrisations physiques du modèle qui peuvent s'avérer inadéquates. Cette étude isole uniquement la sensibilité au guidage et nullement aux autres choix possibles pour configurer le modèle WRF.

F. COUPLING GLOBAL AND REGIONAL CTMS: FOCUS ON AEROSOLS

Regional chemistry transport models are usually initialized and driven at the boundaries (top and lateral) by global models outputs or measurements-derived profiles. Usually for PM, global model outputs are used in most of regional models like CHIMERE (Vautard et al., 2005) and EMEP (Simpson et al., 2012).

Very few studies investigated the impact of the long range transport of PM to Europe. The hemispheric transport of PM was assessed by (Brandt et al., 2012) with a chemistry transport model, for particles, the contributions from North America to Europe is around 0.9% (~0.05 µg m^{-3}). (Liu et al., 2009) proposed a receptor modelling study with a global chemistry transport model in order to evaluate domestic versus background origins of PM2.5 concentrations in several regions of the world (Table 45). Their results show that PM2.5 from outside Europe contributed to 30 % of the background PM2.5 concentrations in Europe. The main species contributing to the PM2.5 is dust followed by sulphates. Organic matter and black carbon concentrations have mainly a domestic origin in Europe.

Table 45: Contributions to annual average area-weighted fine aerosol (PM2.5) surface aerosol concentrations (SAC) (units: µg m^{-3}) over each receptor region. 'Total' indicates total fine aerosol (PM2.5) concentrations including ammonium sulphate, black carbon (BC), organic mass (OM), and fine dust; 'Domestic' indicates aerosol concentrations resulting from local emissions; Background is the difference between 'Total' and 'Domestic' concentrations. The percent contribution from each aerosol species to each category (i.e., 'Total', 'Domestic', 'Background') is also quantified. Note: ''DMS'' represents sulphate aerosols derived from DMS, while ''Sulphate'' in the 'Background' category represents sulphate contributed from ROW (ROW= ships, airplanes, volcanoes, etc.). NA : North America, SA : South America, EU : Europe, FSU : Former Soviet Union, AF: Africa, IN: India, EA: East Asia, SE: Southeast Asia, AU: Australia, ME: Middle East. (*Source : Liu et al., 2009)*

	Sources	Unit	Receptors									
			NA	SA	EU	FSU	AF	IN	EA	SE	AU	ME
Total		**µg m^{-3}**	**4.4**	**6.1**	**7.6**	**4.6**	**25.9**	**16.4**	**17.7**	**5.0**	**5.8**	**25.2**
	Sulfate	%	49	18	48	25	5	20	29	40	13	12
	BC	%	5	5	7	2	1	5	6	6	2	1
	OM	%	33	49	27	22	12	30	22	41	21	4
	Dust	%	14	28	18	50	82	45	43	13	64	83
Domestic		**µg m^{-3}**	**3.6**	**5.0**	**5.2**	**3.2**	**24.3**	**9.7**	**15.1**	**2.8**	**5.2**	**15.2**
	Sulfate	%	50	10	53	18	1	28	29	31	7	12
	BC	%	5	6	9	2	1	8	7	8	2	1
	OM	%	39	59	38	28	12	48	23	61	23	4
	Dust	%	5	25	0	51	85	16	41	0	68	83
Background		**µg m^{-3}**	**0.8**	**1.1**	**2.4**	**1.5**	**1.7**	**6.7**	**2.6**	**2.2**	**0.6**	**10.0**
	Sulfate	%	28	37	28	36	42	8	30	48	17	11
	BC	%	1	0	1	2	1	0	2	3	1	1
	OM	%	4	5	5	10	9	4	15	15	9	3
	Dust	%	52	42	58	46	41	87	51	30	27	84
	DMS	%	15	16	8	5	7	2	2	3	46	1

Regarding the temporal frequency of PM boundary conditions to be used in models, some studies provide some guidance. In the frame of the AQMEII project (Schere et al., 2012) show that for both O3 and PM10, using 3-hourly fields at the boundaries contributes to obtaining a slightly larger variability that is more in agreement with the observations for O3 and NO2. The time variability is impaired for PM10 showing that the predictability of dust events (intensity and occurrence) remains difficult as shown (Menut et al., 2009). If dust models can provide a better measure of variability on seasonal or monthly bases, these models could better predict dust concentrations over Europe on a daily basis.

In (Borge et al., 2010) simulations performed with the CMAQ model suggest that model performances were affected by spatial and seasonal factors, the results indicate that model-derived dynamic BC improved CMAQ predictions when compared to those based on static concentrations prescribed in the boundaries.

Concerning the initial conditions, simulation results from (Samaali et al., 2009)suggest the use of a spin-up period of longer than one week for a large (continental) domain and long-term simulation of PM2.5 and O3 rather than the 2–4 days commonly assumed in the literature.

For regional models, dust and sulphate (in a lesser extent) boundary conditions appear to be very important compared to the other aerosol components. However, the time variability of dust outbreaks is difficult to capture by global models and this feature has a direct impact on the quality of the regional simulations.

The way to design a domain can also have a strong impact on regional simulations. For instance, it is well known that the South-West of Russia is affected by frequent agricultural and biomass fires (Witham and Manning, 2007). If the regional domain encompasses this area and if the fire emissions are not accounted for, there will be a lack of PM in this region. Usually global models account for biomass burning emissions; in that case it is suggested to limit the extension to the East in order to benefit from global model boundary conditions. This recommendation also applies to the issue of desert dust emissions in the southern boundaries.

The Salut'AIR project required to revisit changing boundary conditions in order to capture the influence of long range transport in a changing climate. The correspondence between LMDz-OR-INCA and CHIMERE particulate species was thus updated according to Table 46.

Table 46: Matching between LMDz-OR-INCA and CHIMERE particulate Species. The reader is referred to (Bessagnet et al., 2008b) for the exact signification of Chimere lumped SOA.

INCA	CHIMERE
DUST (CIDUSTM)	DUST (pDUST)
Sulphate (ASSO4M)	Sulphate (pSO4)
Black Carbon (AIBCM, ASBCM)	Black Carbon: 0.1-10µm (BCAR)
Primary Organic Matter (AIPOMM, ASPOMM)	Secondary Organic Aerosols (AnA1D, AnBmP, BiA1D, BiBmP) and Organic Carbon (OCAR)

G. COMPLEMENTARY INFORMATION ON THE CBA UNCERTAINTY ASSESSMENT

Table 47 indicates the indicators aggregated for calculating the sensitivity ranges of health benefits in Section 6.2.2.1.

The following two tables are a complement to Section 6.2.2.2. They list the factors that are not accounted for in the modelling and which may bias the balance of costs and co-benefits. Table 48 focuses on the modelling areas emissions modelling, dispersion modelling and health impact assessment; Table 49 on the modelling of air pollution mitigation costs.

Using the scoring system suggested in Holland et al. (2005b and 2005c), any bias that is likely to lead to an underestimation (overestimation) of the variable indicated in the heading of each table is given a negative (positive) rating. A single '-' or '+' denotes a factor considered to have only a small effect, a triple '---' or '+++' denotes a bias likely to be significant, and a double '—' or '++' indicates biases that may or may not be significant.

Table 48 presents sources of potential biases that may affect the overall damage under each scenario and thus the ***benefit*** calculated when passing from CLE1 to CLE2. An underestimation of benefits in an incremental analysis between CLE1 and CLE2 also implies an underestimation of the co-benefit/cost ratio.

Table 49 lists sources of potential biases that may affect the ***air pollution mitigation cost*** under each scenario and thus the overall costs when passing from CLE1 to CLE2. The more important a cost category is that is omitted (or underestimated) in the analysis, the more the cost savings brought about when moving from CLE1 to CLE2 will be underestimated. An underestimation of air pollution cost savings would imply an overestimation of total additional costs (= sum over air pollution mitigation cost savings and additional energy costs), which in turn would imply an underestimation of the co-benefit/cost ratio (and vice versa).

Table 47 : Aggregation of core and sensitivity indicators for the analysis of sensitivity ranges for health damage and benefit calculations

Indicator	Core?	Pollutant	Impact	Core indicator Salutair	Core low VOLY	Core mid VOLY	Core high VOLY	Core low VSL	Core mid VSL	Core high VSL	Sensitivity low VOLY	Sensitivity mid VOLY	Sensitivity high VOLY	Sensitivity low VSL	Sensitivity mid VSL	Sensitivity high VSL
Acute Mortality (All ages) low VOLY	Core	O3	Premature deaths		x			x			x			x		
Acute Mortality (All ages) median VOLY	Core	O3	Premature deaths	x		x			x			x			x	
Acute Mortality (All ages) mean VOLY	Core	O3	Premature deaths				x			x			x			x
Respiratory Hospital Admissions (65yr +)	Core	O3	Cases	x	x	x	x	x	x	x	x	x	x	x	x	x
Minor Restricted Activity Days (MRADs 15-64yr)	Core	O3	Days	x	x	x	x	x	x	x	x	x	x	x	x	x
Respiratory medication use (adults 20yr +)	Core	O3	Days	x	x	x	x	x	x	x	x	x	x	x	x	x
Minor Restricted activity days (65yr+)	Sensitivity	O3	Days								x	x	x	x	x	x
Respiratory symptoms (adults 15yr +)	Sensitivity	O3	Days								x	x	x	x	x	x
Chronic Mortality (All ages) LYL median VOLY	Core	PM	Life years lost		x						x					
Chronic Mortality (All ages) LYL median VOLY	Core	PM	Life years lost	x		x						x				
Chronic Mortality (All ages) LYL mean VOLY	Core	PM	Life years lost				x						x			
Chronic Mortality (30yr +) deaths median VSL	Core	PM	Premature deaths					x						x		
Chronic Mortality (30yr +) deaths mean VSL	Core	PM	Premature deaths						x						x	
Chronic Mortality (30yr +) deaths mean VSL	Core	PM	Premature deaths							x						x
Infant Mortality (0-1yr) median VSL	Core	PM	Premature deaths	x	x			x			x			x		
Infant Mortality (0-1yr) mean VSL	Core	PM	Premature deaths			x			x			x			x	
Infant Mortality (0-1yr) mean VSL	Core	PM	Premature deaths				x			x			x			x
Chronic Bronchitis (27yr +)	Core	PM	Cases	x	x	x	x	x	x	x	x	x	x	x	x	x
Respiratory Hospital Admissions (All ages)	Core	PM	Cases	x	x	x	x	x	x	x	x	x	x	x	x	x
Cardiac Hospital Admissions (All ages)	Core	PM	Cases	x	x	x	x	x	x	x	x	x	x	x	x	x
Restricted Activity Days (RADs 15-64yr)	Core	PM	Days	x	x	x	x	x	x	x	x	x	x	x	x	x
Respiratory medication use (children 5-14yr)	Core	PM	Days	x	x	x	x	x	x	x	x	x	x	x	x	x
Respiratory medication use (adults 20yr +)	Core	PM	Days	x	x	x	x	x	x	x	x	x	x	x	x	x
LRS symptom days (children 5-14yr)	Core	PM	Days	x	x	x	x	x	x	x	x	x	x	x	x	x
LRS among adults (15yr +) with chronic symptoms	Core	PM	Days	x	x	x	x	x	x	x	x	x	x	x	x	x
Restricted Activity Days (RADs >65) - ext. days	Sensitivity	PM	Days								x	x	x	x	x	x
Asthma Consultations (0-14yr)	Sensitivity	PM	Consultations								x	x	x	x	x	x
Asthma Consultations (15-64yr)	Sensitivity	PM	Consultations								x	x	x	x	x	x
Asthma Consultations (65yr +)	Sensitivity	PM	Consultations								x	x	x	x	x	x
Consultations for URDs (0-14yr)	Sensitivity	PM	Consultations								x	x	x	x	x	x
Consultations for URDs (15-64yr)	Sensitivity	PM	Consultations								x	x	x	x	x	x
Consultations for URDs (65yr +)	Sensitivity	PM	Consultations								x	x	x	x	x	x

Table 48: Biases that may affect damages and thus benefits when moving to a more ambitious scenario

Source of bias			likely effect on damage (underestimation = '-', overestimation = '+')	likely effect on co-benefit/cost-ratio (underestimation = '-', overestimation = '+')	Comment
Modelling of emissions to air	Emission starting point bias for air pollutants		+++/---	+++/---	Uncertainty in emission inventories may introduce negative or positive bias.
	Emission factors established via GAINS		0	0	Associated emissions are well researched with no evidence of any signficant bias.
	Emission factors derived via Kuznets curve assumptions		+++/---	+++/---	These assumptions may introduce negative or positive bias on emission factors and thus damages.
Dispersion modelling	Ozone concentrations		0	0	Overall, assumed that average concentrations are reasonable, with no systematic bias. SOA are included in the analysis.
	PM2.5 concentrations		0	0	
	Difference between urban and rural concentrations		0	0	Accounted for in the modelling.
	Hot spot PM		-	-	The modelling chain does not account for an assessment of hot-spot ozone or PM2.5. Not considered very important as the models are calibrated against background concentrations.
	Hot spot		+	+	
	Variability in meteorology		++/--	++/--	Variability in meteorology can be an important source of bias, especially as this study uses a climate model rather than reanalyses. However, in the project this bias is handled in the atmospheric post-processing.
Benefits analysis	Lack of assessment of impacts	On health	-	-	Believed that some health impacts are excluded, moderated by concern over some valuations possibly being too high, e.g. for chronic bronchitis.
		On materials	---	---	Soiling of materials not accounted for in the modelling.
		On materials in cultural heritage	--	--	Effects of acidification not accounted for in the modelling. Might be of limited importance.
		On crops	---	---	Not accounted for in the modelling.
		On other agriculture	--	--	Not accounted for in the modelling. Considered rather unimportant.
		On ecosystems	---	---	Not included. Extent of exceedance of eutrophication (at least at the 2030 horizon, cf. Amann et al, 2013) in particular suggests that this effect may remain significant.
		Outside Europe	---	---	Leads to underestimation of benefits of the reduction of emissions from Europe.
		From different particle species	+++/---	+++/---	Effect on benefits (upward or downward bias) will depend on the level of control for each particle type.
		From reduction in greenhouse gases	---	---	Impacts of reduced greenhouse gases not accounted for in the modelling.
	Quantification of deaths from PM using techniques not based on life tables (use of VSL in sensitivity ranges)		(+++)	(+++)	Potential for double counting of deaths. Only relevant in sensitivity analysis, not in the Salut'air core estimate.
	Use of cut-point for quantification of ozone impacts		-	-	The impact of the cut-point appears limited, given the low share of ozone impacts in overall health impacts (or damage).

Table 49: Biases that may affect air pollution mitigation costs

Source of bias		**likely effect on AP costs (underestimation = '-', overestimation = '+')**	**likely effect on co-benefit/cost-ratio (underestimation = '-', overestimation = '+')**	**Comment**
Modelling of air pollution mitigation cost	Development of costs for abatement measures over time	++	++	Costs considered likely to fall over time as new technologies emerge. Not accounted for in GAINS air pollution mitigation cost data. This might overestimate costs.
	Lack of account of future technical development of existing measures	++	++	Likely bias towards underestimation of future cost-effectiveness of existing measures. Might be counterbalanced by Kuznets curve assumption after 2030 assuming improvement of emission factors with economic growth.
	Costs for abatement measures for VOCs etc. from energy sectors	-	-	Only costs for the reduction of NOx, SO2 and PM2.5 emissions taken into account. Underestimation of mitigation costs is considered limited as CO costs are indirectly related to NOx and as VOC costs in the energy sector are small.
	Costs for abatement measures for non-energy sectors for which MESSAGE is not linked to GAINS	-	-	Likely underestimation of abatement costs, however not assumed to be important.
	Lack of account of behavioural measures and structural change	+	+	Such measures provide additional scope for emission reductions. They are not modelled in GAINS but implicitly taken into account via the activity (energy) scenarios from MESSAGE.

H. REFERENCES

Amann, M., Bertok, I., Borken-Kleefeld, J., Cofala, J., Heyes, C., Höglund-Isaksson, L., Klimont, Z., Nguyen, B., Posch, M., Rafaj, P., Sandler, R., Schöpp, W., Wagner, F., and Winiwarter, W.: Cost-effective control of air quality and greenhouse gases in Europe: Modeling and policy applications, Environmental Modelling and Software, 26, 1489-1501, 2011a.

Amann, M., Borken, J., Böttcher, H., Cofala, J., Hettelingh, J.-P., Heyes, C., Holland, M., Hunt, A., Klimont, Z., Mantzos, L., Ntziachristos, L., Obersteiner, M., Posch, M., Schneider, U., Schöpp, W., Slootweg, J., Witzke, P., Wagner, A., and Winiwarter, W.: Greenhouse gases and air pollutants in the European Union: Baseline projections up to 2030', EC4MACS interim assessment. , 2011b.

Andersson, C., and Engardt, M.: European ozone in a future climate: Importance of changes in dry deposition and isoprene emissions, J. Geophys. Res., 115, D02303, 2010.

Bessagnet, B.: Aerosols et Climat, 2008.

Bessagnet, B., Menut, L., Curci, G., Hodzic, A., Guillaume, B., Liousse, C., Moukhtar, S., Pun, B., Seigneur, C., and Schulz, M.: Regional modeling of carbonaceous aerosols over Europe—focus on secondary organic aerosols, Journal of Atmospheric Chemistry, 61, 175-202, 2008a.

Bessagnet, B., Menut, L., Curci, G., Hodzic, A., Guillaume, B., Liousse, C., Moukhtar, S., Pun, B., Seigneur, C., and Schulz, M.: Regional modeling of carbonaceous aerosols over Europe - focus on secondary organic aerosols, Journal of Atmospheric Chemistry, 61, 175-202, 10.1007/s10874-009-9129-2, 2008b.

Boberg, F., and Christensen, J. H.: Overestimation of Mediterranean summer temperature projections due to model deficiencies, Nature Clim. Change, 2, 433-436, 2012.

Borge, R., López, J., Lumbreras, J., Narros, A., and Rodríguez, E.: Influence of boundary conditions on CMAQ simulations over the Iberian Peninsula, Atmospheric Environment, , 44, 2681-2695, 10.1016/j.atmosenv.2010.04.044, 2010.

Boucher, O., and Pham, M.: History of sulphate aerosol radiative forcing, , Geophys. Res. Lett., 29, 10.1029/2001GL0140148, 2002.

Brandt, J., Silver, J. D., Frohn, L. M., Geels, C., Gross, A., Hansen, A. B., Hansen, K. M., Hedegaard, G. B., Skjoth, C. A., Villadsen, H., Zare, A., and Christensen, J. H.: An integrated model study for Europe and North America using the Danish Eulerian Hemispheric Model with focus on intercontinental transport of air pollution, Atmospheric Environment, 53, 156-176, 2012.

Brandt, J., Silver, J. D., Christensen, J. H., Andersen, M. S., Bønløkke, J. H., Sigsgaard, T., Geels, C., Gross, A., Hansen, A. B., Hansen, K. M., Hedegaard, G. B., Kaas, E., and Frohn, L. M.: Contribution from the ten major emission sectors in Europe and Denmark to the health-cost externalities of air pollution using the EVA model system – an integrated modelling approach, Atmos. Chem. Phys. Discuss., 13, 5871-5922, 2013.

Caldwell, P., Chin, H.-N., Bader, D., and Bala, G.: Evaluation of a WRF dynamical downscaling simulation over California, Climatic Change, 95, 499-521, 2009.

Cattiaux, J., Douville, H., Ribes, A., Chauvin, F., and Plante, C.: Towards a better understanding of changes in wintertime cold extremes over Europe A pilot study with CNRM & IPSL atmospheric models., Climate Dynamics, under review, 2012.

CGDD: Rapport de la Commission des comptes et de l'économie de l'environnement – santé et qualité de l'air extérieur, 2012.

Christensen, J., Carter, T., Rummukainen, M., and Amanatidis, G.: Evaluating the performance and utility of regional climate models: the PRUDENCE project, Climatic Change, 81, 1-6, 2007.

Christensen, J., and Christensen, O.: A summary of the PRUDENCE model projections of changes in European climate by the end of this century, Climatic Change, 81, 7-30, 2007.

Colette, A., Granier, C., Hodnebrog, O., Jakobs, H., Maurizi, A., Nyiri, A., Bessagnet, B., D'Angiola, A., D'Isidoro, M., Gauss, M., Meleux, F., Memmesheimer, M., Mieville, A., Rouïl, L., Russo, F., Solberg, S., Stordal, F., and Tampieri, F.: Air quality trends in Europe over the past decade: a first multi-model assessment, Atmos. Chem. Phys., 11, 11657-11678, 2011.

Colette, A., Granier, C., Hodnebrog, O., Jakobs, H., Maurizi, A., Nyiri, A., Rao, S., Amann, M., Bessagnet, B., D'Angiola, A., Gauss, M., Heyes, C., Klimont, Z., Meleux, F., Memmesheimer, M., Mieville, A., Rouïl, L., Russo, F., Schucht, S., Simpson, D., Stordal, F., Tampieri, F., and Vrac, M.: Future air quality in Europe: a multi-model assessment of projected exposure to ozone, Atmos. Chem. Phys., 12, 10613-10630, 2012a.
Colette, A., Koelemeijer, R., Mellios, G., Schucht, S., Péré, J.-C., Kouridis, C., Bessagnet, B., Eerens, H., Van Velze, K., and Rouïl, L.: Cobenefits of climate and air pollution regulations, The context of the European Commission Roadmap for moving to a low carbon economy in 2050, ETC/ACM - EEA, Copenhagen, 78, 2012b.
Colette, A., Vautard, R., and Vrac, M.: Regional climate downscaling with prior statistical correction of the global climate forcing, Geophys. Res. Lett., 39, L13707, 2012c.
Colette, A., Bessagnet, B., Vautard, R., Szopa, S., Rao, S., Schucht, S., Klimont, Z., Menut, L., Clain, G., Meleux, F., and Rouïl, L.: European atmosphere in 2050, a regional air quality and climate perspective under CMIP5 scenarios, Atmos. Chem. Phys. Discuss., 13, 6455-6499, 2013.
Davies, H. C., and Turner, R. E.: Updating prediction models by dynamical relaxation: an examination of the technique, Quarterly Journal of the Royal Meteorological Society, 103, 225-245, 1977.
Denby, B., Cassiani, M., de Smet, P., de Leeuw, F., and Horalek, J.: Sub-grid variability and its impact on European wide air quality exposure assessment, Atmospheric Environment, 45, 4220-4229, 2011.
Dentener, F., Stevenson, D., Cofala, J., Mechler, R., Amann, M., Bergamaschi, P., Raes, F., and Derwent, R.: The impact of air pollutant and methane emission controls on tropospheric ozone and radiative forcing: CTM calculations for the period 1990-2030, Atmos. Chem. Phys., 5, 1731-1755, 2005.
Déqué, M.: Frequency of precipitation and temperature extremes over France in an anthropogenic scenario: Model results and statistical correction according to observed values, Global and Planetary Change, 57, 16-26, 2007.
Desaigues, B., Ami, D., Bartczak, A., Braun-Kohlova, M., Chilton, S., Czajkowski, M., Farreras, V., Hunt, A., Hutchinson, M., Jeanrenaud, C., Kaderjak, P., Maca, V., Markiewicz, O., Markowska, A., Metcalf, H., Navrud, S., Nielsen, J. S., Ortiz, R., Pellegrini, S., Rabl, A., Riera, R., Scasny, M., Stoeckel, M.-E., Szanto, R., and Urban, J.: Economic valuation of air pollution mortality: A 9-country contingent valuation survey of value of a life year (VOLY), Ecological Indicators, 11, 902-910, 2011.
Dufresne, J.-L., Foujols, M.-A., Denvil, S., Caubel, A., Marti, O., Aumont, O., Balkanski, Y., Bekki, S., Bellenger, H., Benshila, R., Bony, S., Bopp, L., Braconnot, P., Brockmann, P., Cadule, P., Cheruy, F., Codron, F., Cozic, A., Cugnet, D., de Noblet, N., Duvel, J.-P., Ethé, C., Fairhead, L., Fichefet, T., Flavoni, S., Friedlingstein, P., Grandpeix, J.-Y., Guez, L., Guilyardi, E., Hauglustaine, D., Hourdin, F., Idelkadi, A., Ghattas, J., Joussaume, S., Kageyama, M., Krinner, G., Labetoulle, S., Lahellec, A., Lefebvre, M.-P., Lefevre, F., Levy, C., Li, Z. X., Lloyd, J., Lott, F., Madec, G., Mancip, M., Marchand, M., Masson, S., Meurdesoif, Y., Mignot, J., Musat, I., Parouty, S., Polcher, J., Rio, C., Schulz, M., Swingedouw, D., Szopa, S., Talandier, C., Terray, P., and Viovy, N.: Climate change projections using the IPSL-CM5 Earth System Model: from CMIP3 to CMIP5 Climate Dynamics, in press., 10.1007/s00382-012-1636-1, 2013.
EEA: Assessment of ground-level ozone in EEA member countries, with a focus on long-term trends, European Environment Agency, Copenhagen, 56, 2009.
Fiore, A. M., Naik, V., Spracklen, D. V., Steiner, A., Unger, N., Prather, M., Bergmann, D., Cameron-Smith, P. J., Cionni, I., Collins, W. J., Dalsoren, S., Eyring, V., Folberth, G. A., Ginoux, P., Horowitz, L. W., Josse, B., Lamarque, J.-F., MacKenzie, I. A., Nagashima, T., O'Connor, F. M., Righi, M., Rumbold, S. T., Shindell, D. T., Skeie, R. B., Sudo, K., Szopa, S., Takemura, T., and Zeng, G.: Global air quality and climate, Chemical Society Reviews, 41, 6663-6683, 2012.
Flaounas, E., Drobinski, P., Vrac, M., Bastin, S., and Lebeaupin Brossier, C.: Seasonal variability and extremes of precipitation and temperature in the Mediterranean region: Evaluation of dynamical and statistical downscaling methods for the frame of HyMeX and MED-CORDEX, Climate Dynamics, under review, 2011.

Forster, P., Ramaswamy, V., Artaxo, P., Berntsen, T., Betts, R., Fahey, D., Haywood, J., Lean, J., Lowe, D., Myhre, G., Nganga, J., Prinn, R., Raga, G., Schultz, M., and Van Dorland, R.: Changes in atmospheric constituents and in radiative forcing, in: Climate Change 2007: The physical science basis: Contribution of Working Group I to the Fourth Assessment Report of the Intergovernmental Panel on Climate Change edited by: Solomon, S., Qin, D., Manning, M., Chen, Z., Marquis, M., Averyt, K., Tignor, M., and Miller, H., Cambridge University Press, Cambridge, UK 2007.
Giorgi, F., Jones, C., and Asrar, G. R.: Addressing climate information needs at the regional level: the CORDEX framework, WMO Bulletin, 58, 175-183, 2009.
Gobiet, A., and Jacob, D.: A new generation of regional climate simulations for Europe: The EURO-CORDEX Initiative Geophysical Research. Abstracts, 14, 2012.
Grubler, A., Aguayo, F., Gallagher, K., Hekkert, M., Jiang, K., Mytelka, L., Neij, L., Nemet, G., and Wilson, C.: Policies for the Energy Technology Innovation System (ETIS)', in: Global Energy Assessment: Toward a Sustainable Future, 2012.
Guenther, A., Karl, T., Harley, P., Wiedinmyer, C., Palmer, P. I., and Geron, C.: Estimates of global terrestrial isoprene emissions using MEGAN (Model of Emissions of Gases and Aerosols from Nature), Atmos. Chem. Phys., 6, 3181-3210, 2006.
Hamaoui-Laguel, L., Meleux, F., Beekmann, M., Bessagnet, B., Génermont, S., Cellier, P., and Léinois, L.: Improving ammonia emissions in air quality modelling for France, Atmospheric Environment, 2012.
Hauglustaine, D. A., Lathière, J., Szopa, S., and Folberth, G. A.: Future tropospheric ozone simulated with a climate-chemistry-biosphere model, Geophysical Research Letters, 32, L24807, 2005.
Haylock, M. R., Hofstra, N., Tank, A. M. G. K., Klok, E. J., Jones, P. D., and New, M.: A European daily high-resolution gridded data set of surface temperature and precipitation for 1950-2006., Journal of Geophysical Research-Atmospheres, 113, 2008.
Hedegaard, G. B., Brandt, J., Christensen, J. H., Frohn, L. M., Geels, C., Hansen, K. M., and Stendel, M.: Impacts of climate change on air pollution levels in the Northern Hemisphere with special focus on Europe and the Arctic, Atmos. Chem. Phys., 8, 3337-3367, 2008.
Hedegaard, G. B., Christensen, J. H., and Brandt, J.: The relative importance of impacts from climate change vs. emissions change on air pollution levels in the 21st century, Atmos. Chem. Phys. Discuss., 12, 24501-24530, 2012.
Holland, M., Hunt, A., Hurley, F., Navrud, S., and Watkiss, P.: 'Methodology for the Cost-Benefit analysis for CAFE: Volume 1: Overview of Methodology', Service Contract for Carrying out Cost-Benefit Analysis of Air Quality Related Issues, in particular in the Clean Air for Europe (CAFE) Programme, 2005a.
Holland, M., Hurley, F., Hunt, A., and Watkiss, P.: Methodology for the Cost-Benefit analysis for CAFE: Volume 3: Uncertainty in the CAFE CBA: Methods and First Analysis', Service Contract for Carrying out Cost-Benefit Analysis of Air Quality Related Issues, in particular in the Clean Air for Europe (CAFE) Programme, 2005b.
Holland, M., Watkiss, P., and Pye, S.: Cost-Benefit Analysis of Policy Option Scenarios for the Clean Air for Europe programme' Service Contract for Carrying out Cost-Benefit Analysis of Air Quality Related Issues, in particular in the Clean Air for Europe (CAFE) Programme, 2005c.
Holland, M., Wagner, A., Hurley, F., Miller, B., and Hunt, A.: Cost Benefit Analysis for the Revision of the National Emission Ceilings Directive: Policy Options for revisions to the Gothenburg Protocol to the UNECE Convention on Long-Range Transboundary Air Pollution, 2011.
Holland, M.: Cost-benefit Analysis of Policy Scenarios for the Revision of the Thematic Strategy on Air Pollution, 2013.
Hourdin, F., Foujols, M. A., Codron, F., Guemas, V., Dufresne, J., Bony, S., Denvil, S., Guez, L., Lott, F., Gattahs, J., Braconnot, P., Marti, O., and Meurdesoif, Y.: From LMDZ4 to LMDZ5: Impact of the atmospheric model grid configuration on the climate and sensitivity of IPSL climate model, Climate Dynamics, under review, 2012.
Hurley, F., Hunt, A., Cowie, H., Holland, M., Miller, B., Pye, S., and Watkiss, P.: 'Methodology for the Cost-Benefit analysis for CAFE: Volume 2: Health Impact Assessment', Service Contract for Carrying

out Cost-Benefit Analysis of Air Quality Related Issues, in particular in the Clean Air for Europe (CAFE) Programme, 2005.
IPCC: Contribution of Working Group I to the Fourth Assessment Report of the Intergovernmental Panel on Climate Change, Cambridge University Press, Cambridge, United Kingdom and New York, NY, USA., 2007.
Jacob, D., Bärring, L., Christensen, O., Christensen, J., de Castro, M., Déqué, M., Giorgi, F., Hagemann, S., Hirschi, M., Jones, R., Kjellström, E., Lenderink, G., Rockel, B., Sánchez, E., Schär, C., Seneviratne, S., Somot, S., van Ulden, A., and van den Hurk, B.: An inter-comparison of regional climate models for Europe: model performance in present-day climate, Climatic Change, 81, 31-52, 2007.
Jacob, D., and al., e.: EURO-CORDEX: New high-resolution climate change projections for European impact research Regional Environmental Change, submitted, 2013.
Jacob, D. J., Logan, J. A., and Murti, P. P.: Effect of rising Asian emissions on surface ozone in the United States, Geophysical Research Letters, 26, 2175-2178, 1999.
Jacob, D. J., and Winner, D. A.: Effect of climate change on air quality, Atmospheric Environment, 43, 51-63, 2009.
Jacobson, M. Z., Kaufman, Y. J., and Rudich, Y.: Examining feedbacks of aerosols to urban climate with a model that treats 3-D clouds with aerosol inclusions, Journal of Geophysical Research: Atmospheres, 112, D24205, 2007.
Katragkou, E., Zanis, P., Kioutsioukis, I., Tegoulias, I., Melas, D., Krüger, B. C., and Coppola, E.: Future climate change impacts on summer surface ozone from regional climate-air quality simulations over Europe, J. Geophys. Res., 116, D22307, doi:10.1029/2011JD015899 2011.
Kjellström, E., Nikulin, G., Hansson, U. L. F., Strandberg, G., and Ullerstig, A.: 21st century changes in the European climate: uncertainties derived from an ensemble of regional climate model simulations, Tellus A, 63, 24-40, 2011.
Kovats, S., Lloyd, S., Hunt, A. & Watkiss, P.: The impacts and Economic Costs of Climate Change on Health in Europe, N/A.
Krupnick, A., Ostro, B., and Bull, K.: Peer Review of the Methodology of Cost-Benefit Analysis of the Clean Air For Europe Programme, 2005.
Lamarque, J.-F., Bond, T. C., Eyring, V., Granier, C., Heil, A., Klimont, Z., Lee, D., Liousse, C., Mieville, A., Owen, B., Schultz, M. G., Shindell, D., Smith, S. J., Stehfest, E., Van Aardenne, J., Cooper, O. R., Kainuma, M., Mahowald, N., McConnell, J. R., Naik, V., Riahi, K., and van Vuuren, D. P.: Historical (1850–2000) gridded anthropogenic and biomass burning emissions of reactive gases and aerosols: methodology and application, Atmos. Chem. Phys., 10, 7017-7039, 10.5194/acp-10-7017-2010, 2010.
Langner, J., Engardt, M., and Andersson, C.: European summer surface ozone 1990-2100, Atmos. Chem. Phys., 12, 10097-10105, 2012a.
Langner, J., Engardt, M., Baklanov, A., Christensen, J. H., Gauss, M., Geels, C., Hedegaard, G. B., Nuterman, R., Simpson, D., Soares, J., Sofiev, M., Wind, P., and Zakey, A.: A multi-model study of impacts of climate change on surface ozone in Europe, Atmos. Chem. Phys., 12, 10423-10440, 2012b.
Laprise, R.: Regional climate modelling, Journal of Computational Physics, 227, 3641–3666, 2008.
Lathière, J., Hauglustaine, D. A., Friend, A. D., De Noblet-Ducoudré, N., Viovy, N., and Folberth, G. A.: Impact of climate variability and land use changes on global biogenic volatile organic compound emissions, Atmos. Chem. Phys., 6, 2129-2146, 2006.
Liu, J., Mauzerall, D. L., Horowitz, L. W., Ginoux, P., and Fiore, A. M.: Evaluating inter-continental transport of fine aerosols: (1) Methodology, global aerosol distribution and optical depth, Atmospheric Environment, 43, 4327-4338, 10.1016/j.atmosenv.2009.03.054, 2009.
Manders, A. M. M., van Meijgaard, E., Mues, A. C., Kranenburg, R., van Ulft, L. H., and Schaap, M.: The impact of differences in large-scale circulation output from climate models on the regional modeling of ozone and PM, Atmos. Chem. Phys., 12, 9441-9458, 2012.
Maraun, D., Wetterhall, F., Ireson, A. M., Chandler, R. E., Kendon, E. J., Widmann, M., Brienen, S., Rust, H. W., Sauter, T., Themeßl, M., Venema, V. K. C., Chun, K. P., Goodess, C. M., Jones, R. G., Onof, C., Vrac, M., and Thiele-Eich, I.: Precipitation downscaling under climate change. Recent

developments to bridge the gap between dynamical models and the end user, Reviews of Geophysics, 48, 2010.
Marti, O., Braconnot, P., Dufresne, J. L., Bellier, J., Benshila, R., Bony, S., Brockmann, P., Cadule, P., Caubel, A., Codron, F., de Noblet, N., Denvil, S., Fairhead, L., Fichefet, T., Foujols, M. A., Friedlingstein, P., Goosse, H., Grandpeix, J. Y., Guilyardi, E., Hourdin, F., Idelkadi, A., Kageyama, M., Krinner, G., Lévy, C., Madec, G., Mignot, J., Musat, I., Swingedouw, D., and Talandier, C.: Key features of the IPSL ocean atmosphere model and its sensitivity to atmospheric resolution, Climate Dynamics, 34, 1-26, 2010.
Meleux, F., Solmon, F., and Giorgi, F.: Increase in summer European ozone amounts due to climate change, Atmospheric Environment, 41, 7577-7587, 2007.
Menut, L.: Adjoint modeling for atmospheric pollution process sensitivity at regional scale, J. Geophys. Res., 108, 8562, 2003.
Menut, L., Chiapello, I., and Moulin, C.: Previsibility of mineral dust concentrations: The CHIMERE-DUST forecast during the first AMMA experiment dry season, Journal of Geophysical Research: Atmospheres, 114, 10.1029/2008JD010523, 2009.
Menut, L., Tripathi, O. P., Colette, A., Vautard, R., Flaounas, R., and Bessagnet, B.: Evaluation of regional climate model forcing with an air quality perspective, Climate Dynamics, 10.1007/s00382-012-1345-9, 2012a.
Menut, L., Tripathi, O. P., Colette, A., Vautard, R., Flaounas, R., and Bessagnet, B.: Evaluation of regional climate model forcing with an air quality perspective, Climate Dynamics, under review, 2012b.
Menut, L., Bessagnet, B., Khvorostyanov, D., Beekmann, M., Colette, A., Coll, I., Curci, G., Foret, G., Hodzic, A., Mailler, S., Meleux, F., Monge, J. L., Pison, I., Turquety, S., Valari, M., Vautard, R., and Vivanco, M. G.: Regional atmospheric composition modeling with CHIMERE, Geosci. Model Dev. Discuss., 6, 203-329, 2013a.
Menut, L., Tripathi, O., Colette, A., Vautard, R., Flaounas, E., and Bessagnet, B.: Evaluation of regional climate simulations for air quality modelling purposes, Climate Dynamics, 40, 2515-2533, 2013b.
Messner, S., and Strubegger, M.: User's guide for MESSAGE III. , IIASA, Laxenburg, 1995.
Michelangeli, P. A., Vrac, M., and Loukos, H.: Probabilistic downscaling approaches: Application to wind cumulative distribution functions, Geophys. Res. Lett., 36, L11708, doi:10.1029/2009GL038401, 2009.
Miller, B., Hurley, F., and Shafrir, A.: Health Impact Assessment for the National Emissions Ceiling Directive (NECD) – Methodological Issues, 2011.
Nenes, A., Pandis, S., and Pilinis, C.: ISORROPIA: A New Thermodynamic Equilibrium Model for Multiphase Multicomponent Inorganic Aerosols, Aquatic Geochemistry, 4, 123-152, 1998.
OECD: Cost-benefit analysis and the environment - Recent developments, 2006.
OECD: Mortality Risk Valuation in Environment, Health and Transport Policies, 2012.
Omrani H., Drobinski P., and T., D.: Investigation of indiscriminate nudging and predictability in a nested quasi-geostrophic model, Quart. J. Roy. Meteorol. Soc., 138, 158-169, 2012a.
Omrani H., Drobinski P., and T., D.: Spectral nudging in regional climate modelling: how strongly should we nudge?, Quart. J. Roy. Meteorol. Soc., 138, 1808-1813, 2012b.
Omrani H., Drobinski P., and T., D.: Nudging in regional climate modelling: what should we nudge? , Clim. Dyn.,, submitted, 2013a.
Omrani H., Drobinski P., and T., D.: Optimal nudging strategies in regional climate modelling: investigation in a Big-Brother Experiment over the European and Mediterranean regions, Clim. Dyn., doi:10.1007/s00382-012-1615-6, 2013b.
Pankow, J. F.: An absorption model of the gas/aerosol partitioning involved in the formation of secondary organic aerosol, Atmospheric Environment, 28, 189-193, 1994.
Parry, M. L., Canziani, O. F., Palutikof, J. P., van der Linden, P. J., and Hanson, C. E.: Contribution of Working Group II to the Fourth Assessment Report of the Intergovernmental Panel on Climate Change, Cambridge, UK and New York, USA, 2007.

Péré, J. C., Colette, A., Dubuisson, P., Bessagnet, B., Mallet, M., and Pont, V.: Impacts of future air pollution mitigation strategies on the aerosol direct radiative forcing over Europe, Atmospheric Environment, 62, 451-460, 10.1016/j.atmosenv.2012.08.046, 2012.
Pham, M., Boucher, O., and Hauglustaine, D.: Changes in atmospheric sulfur burdens and concentrations and resulting radiative forcings under IPCC SRES emission scenarios for 1990–2100, J. Geophys. Res., , 110, doi:10.1029/2004JD005125., 2005.
Possell, M., Nicholas Hewitt, C., and Beerling, D. J.: The effects of glacial atmospheric CO2 concentrations and climate on isoprene emissions by vascular plants, Global Change Biology, 11, 60-69, 2005.
Prather, M., Gauss, M., Berntsen, T., Isaksen, I., Sundet, J., Bey, I., Brasseur, G., Dentener, F., Derwent, R., Stevenson, D., Grenfell, L., Hauglustaine, D., Horowitz, L., Jacob, D., Mickley, L., Lawrence, M., von Kuhlmann, R., Muller, J.-F., Pitari, G., Rogers, H., Johnson, M., Pyle, J., Law, K., van Weele, M., and Wild, O.: Fresh air in the 21st century?, Geophysical Research Letters, 30, 1100, 2003.
Radu R., Déqué M., and Somot S.: Spectral nudging in a spectral regional climate model. , Tellus A, 60, 2008.
Rafaj, P., Rao, S., Klimont, Z., Kolp, P., and Schöpp, W.: Emissions of air pollutants implied by global long-term energy scenarios, IIASA, Vienna, 2010.
Rao, S., and Riahi, K.: The role of non-CO2 greenhouse gases in climate change mitigation: Long-term scenarios for the 21st century, Multigas mitigation and climate policy, The Energy Journal, 3, 2006.
Rao, S., Chirkov, V., Dentener, F., Dingenen, R., Pachauri, S., Purohit, P., Amann, M., Heyes, C., Kinney, P., Kolp, P., Klimont, Z., Riahi, K., and Schoepp, W.: Environmental Modeling and Methods for Estimation of the Global Health Impacts of Air Pollution, Environmental Modeling & Assessment, 1-10, 2012.
Rao, S.: Better air for better health: Forging synergies in policies for energy access, climate change and air pollution, Global Environ. Change, in press, 2013.
Riahi, K., Gruebler, A., and Nakicenovic, N.: Scenarios of long-term socio-economic and environmental development under climate stabilisation, Technol. Forecast. Soc. Change 74, 10.1016/j.techfore.2006.05.026, 2007.
Riahi, K., Rao, S., Krey, V., Cho, C., Chirkov, V., Fischer, G., Kindermann, G., Nakicenovic, N., and Rafaj, P.: RCP 8.5 A scenario of comparatively high greenhouse gas emissions, Climatic Change, 109, 33-57, 2011.
Riahi, K., Dentener, F., Gielen, D., Grubler, A., Jewell, J., Klimont, Z., Krey, V., McCollum, D., Pachauri, S., Rao, S., van Ruijven, B., van Vuuren, D. P., and Wilson, C.: Energy Pathways for Sustainable Development, in: Global Energy Assessment: Toward a Sustainable Future, edited by: Nakicenovic, N., IIASA, Laxenburg, Austria and Cambridge University Press, Cambridge, United Kingdom and New York, NY, 2012.
Rowell D.P., and Jones R.G.: Causes and uncertainty of future summer drying over Europe. , Clim. Dyn., 27, 2006.
Salameh T., Drobinski P., and Dubos T.: The effect of indiscriminate nudging time on the large and small scales in regional climate modelling: application to the Mediterranean basin., Quart. J. Roy. Meteorol. Soc., 136, 2010.
Samaali, M., Moran, M. D., Bouchet, V. S., Pavlovic, R., Cousineau, S., and Sassi, M.: On the influence of chemical initial and boundary conditions on annual regional air quality model simulations for North America, Atmospheric Environment, 43, 48734885, 10.1016/j.atmosenv.2009.07.019, 2009.
Schere, K., Flemming, J., Vautard, R., Chemel, C., Colette, A., Hogrefe, C., Bessagnet, B., Meleux, F., Mathur, R., Roselle, S., Hu, R.-M., Sokhi, R. S., Rao, S. T., and Galmarini, S.: Trace gas/aerosol boundary concentrations and their impacts on continental-scale AQMEII modeling domains, Atmospheric Environment, 53, 38-50, 2012.
Semenov, M. A., Brooks, R. J., Barrow, E. M., and Richardson, C. W.: Comparison of the WGEN and LARS-WG stochastic weather generators for diverse climates, Climate Research, 10, 95-107, 10.3354/cr010095, 1998.

Shindell, D. T., Lamarque, J. F., Schulz, M., Flanner, M., Jiao, C., Chin, M., Young, P., Lee, Y. H., Rotstayn, L., Milly, G., Faluvegi, G., Balkanski, Y., Collins, W. J., Conley, A. J., Dalsoren, S., Easter, R., Ghan, S., Horowitz, L., Liu, X., Myhre, G., Nagashima, T., Naik, V., Rumbold, S., Skeie, R., Sudo, K., Szopa, S., Takemura, T., Voulgarakis, A., and Yoon, J. H.: Radiative forcing in the ACCMIP historical and future climate simulations, Atmos. Chem. Phys. Discuss., 12, 21105-21210, 2012.
Simpson, D., Benedictow, A., Berge, H., Bergstrom, R., Emberson, L. D., Fagerli, H., Flechard, C. R., Hayman, G. D., Gauss, M., Jonson, J. E., Jenkin, M. E., Nyiri, A., Richter, C., Semeena, V. S., Tsyro, S., Tuovinen, J. P., Valdebenito, A., and Wind, P.: The EMEP MSC-W chemical transport model - technical description, Atmos. Chem. Phys., 12, 7825-7865, 2012.
Skamarock, W. C., Klemp, J. B., Dudhia, J., Gill, D. O., Barker, D. M., Duda, M. G., Huang, X. Y., Wang, W., and Powers, J. G.: A Description of the Advanced Research WRF Version 3, NCAR, 2008.
Solazzo, E., Bianconi, R., Pirovano, G., Matthias, V., Vautard, R., Moran, M. D., Wyat Appel, K., Bessagnet, B., Brandt, J., Christensen, J. H., Chemel, C., Coll, I., Ferreira, J., Forkel, R., Francis, X. V., Grell, G., Grossi, P., Hansen, A. B., Miranda, A. I., Nopmongcol, U., Prank, M., Sartelet, K. N., Schaap, M., Silver, J. D., Sokhi, R. S., Vira, J., Werhahn, J., Wolke, R., Yarwood, G., Zhang, J., Rao, S. T., and Galmarini, S.: Operational model evaluation for particulate matter in Europe and North America in the context of AQMEII, Atmospheric Environment, 53, 75-92, 2012a.
Solazzo, E., Bianconi, R., Vautard, R., Appel, K. W., Moran, M. D., Hogrefe, C., Bessagnet, B., Brandt, J. r., Christensen, J. H., Chemel, C., Coll, I., Denier van der Gon, H., Ferreira, J., Forkel, R., Francis, X. V., Grell, G., Grossi, P., Hansen, A. B., Jericevic, A., Kraljevic, L., Miranda, A. I., Nopmongcol, U., Pirovano, G., Prank, M., Riccio, A., Sartelet, K. N., Schaap, M., Silver, J. D., Sokhi, R. S., Vira, J., Werhahn, J., Wolke, R., Yarwood, G., Zhang, J., Rao, S. T., and Galmarini, S.: Model evaluation and ensemble modelling of surface-level ozone in Europe and North America in the context of AQMEII, Atmospheric Environment, 53, 60-74, 2012b.
Stevenson, D. S., Dentener, F. J., Schultz, M. G., Ellingsen, K., van Noije, T. P. C., Wild, O., Zeng, G., Amann, M., Atherton, C. S., Bell, N., Bergmann, D. J., Bey, I., Butler, T., Cofala, J., Collins, W. J., Derwent, R. G., Doherty, R. M., Drevet, J., Eskes, H. J., Fiore, A. M., Gauss, M., Hauglustaine, D. A., Horowitz, L. W., Isaksen, I. S. A., Krol, M. C., Lamarque, J. F., Lawrence, M. G., Montanaro, V., Müller, J. F., Pitari, G., Prather, M. J., Pyle, J. A., Rast, S., Rodriguez, J. M., Sanderson, M. G., Savage, N. H., Shindell, D. T., Strahan, S. E., Sudo, K., and Szopa, S.: Multimodel ensemble simulations of present-day and near-future tropospheric ozone, J. Geophys. Res., 111, D08301, 10.1029/2005JD006338 2006.
Szopa, S., Hauglustaine, D. A., Vautard, R., and Menut, L.: Future global tropospheric ozone changes and impact on European air quality, Geophys. Res. Lett., 33, L14805, 10.1029/2006GL025860 2006.
Szopa, S., Balkanski, Y., Schulz, M., Bekki, S., Cugnet, D., Fortems-Cheiney, A., Turquety, S., Cozic, A., Déandreis, C., Hauglustaine, D., Idelkadi, A., Lathière, J., Lefevre, F., Marchand, M., Vuolo, R., Yan, N., and Dufresne, J. L.: Aerosol and ozone changes as forcing for climate evolution between 1850 and 2100, Climate Dynamics, 1-28, 2012a.
Szopa, S., Cozic, A., Schulz, M., Balkanski, Y., and Hauglustaine, D.: Aerosol and Ozone changes as forcing for Climate Evolution between 1850 and 2100, Climatic Change, under review, 2012b.
Szopa S., Hauglustaine, D., Vautard, R., and Menut, L.: Evolution of the tropospheric composition in 2030: impact on European air quality, Geophys. Res. Lett., 33, doi:10.1029/2006GL025860, 2006.
Thunis, P., Cuvelier, C., Roberts, P., White, L., Post, L., Tarrason, L., Tsyro, S., Stern, R., Kerschbaumer, A., Rouil, L., Bessagnet, B., Builtjes, J., Schaap, M., Boersen, G., and Bergstroem, R.: Evaluation of a Sectoral Approach to Integrated Assessment Modelling including the Mediterranean Sea, JRC, Ispra, Italy, 2008.
van Loon, M., Vautard, R., Schaap, M., Bergström, R., Bessagnet, B., Brandt, J., Builtjes, P. J. H., Christensen, J. H., Cuvelier, C., Graff, A., Jonson, J. E., Krol, M., Langner, J., Roberts, P., Rouil, L., Stern, R., Tarrasón, L., Thunis, P., Vignati, E., White, L., and Wind, P.: Evaluation of long-term ozone simulations from seven regional air quality models and their ensemble, Atmospheric Environment, 41, 2083-2097, 2007.

Vautard, R., Honoré, C., Beekmann, M., and Rouil, L.: Simulation of ozone during the August 2003 heat wave and emission control scenarios, Atmospheric Environment, 39, 2957-2967, 2005.
Vautard, R., Brankovic, C., Colette, A., Deque, M., Fernandez, J., Gobiet, A., Goergen, K., Nikulin, G., Guettler, I., Keuler, K., Warrach-Sagi, K., Teichmann, C., and Halenka, T.: The simulation of European heat waves from an ensemble of regional climate models within the EURO-CORDEX project, Climate Dynamics, in revision., 2012.
Vautard, R., Gobiet, A., Jacob, D., Belda, M., Colette, A., Déqué, M., Fernandez, J., Garcia-Diez, M., Goergen, K., Güttler, I., Halenka, T., Karacostas, T., Katragkou, E., Keuler, K., Kotlarski, S., Mayer, S., Meijgaard, E., Nikulin, G., Patarcic, M., Scinocca, J., Sobolowski, S., Suklitsch, M., Teichmann, C., Warrach-Sagi, K., Wulfmeyer, V., and Yiou, P.: The simulation of European heat waves from an ensemble of regional climate models within the EURO-CORDEX project, Climate Dynamics, 1-21, 2013.
Vidale, P., Lüthi, D., Wegmann, R., and Schär, C.: European summer climate variability in a heterogeneous multi-model ensemble, Climatic Change, 81, 209-232, 2007.
Von Storch H., Langenberg H., and Feser F.: A spectral nudging technique for dynamical downscaling purposes. , Mon. Wea. Rev., 128, 3664–3673, 2000.
Vrac, M., Stein, M., and Hayhoe, K.: Statistical downscaling of precipitation through nonhomogeneous stochastic weather typing, Climate Research, 34, 169-184, 10.3354/cr00696, 2007.
Vrac, M., Drobinski, P., Merlo, A., Herrmann, M., Lavaysse, C., Li. L., and Somot, S.: Dynamical and statistical downscaling of the French Mediterranean climate: uncertainty assessment, Natural Hazards and Earth System Sciences., under review, 2012.
WHO: Health relevance of particulate matter from various sources, 2007.
WHO: Review of evidence on health aspects of air pollution –REVIHAAP – First results, 2013a.
WHO: Health risks of air pollution in Europe – HRAPIE – Summary of recommendations for question D5 on “Identification of concentration-response functions” for cost-effectiveness analysis, 2013b.
Wilkinson, M. J., Monson, R. K., Trahan, N., Lee, S., Brown, E., Jackson, R. B., Polley, H. W., Fay, P. A., and Fall, R. A. Y.: Leaf isoprene emission rate as a function of atmospheric CO2 concentration, Global Change Biology, 15, 1189-1200, 2009.
Wilks, D. S., and Wilby, R. L.: The weather generation game: a review of stochastic weather models, Progress in Physical Geography, 23, 329-357, 10.1177/030913339902300302, 1999.
Witham, C., and Manning, A.: Impacts of Russian biomass burning on UK air quality, Atmospheric Environment, 41, 8075-8090, 10.1016/j.atmosenv.2007.06.058., 2007.
Young, P. J., Archibald, A. T., Bowman, K. W., Lamarque, J. F., Naik, V., Stevenson, D. S., Tilmes, S., Voulgarakis, A., Wild, O., Bergmann, D., Cameron-Smith, P., Cionni, I., Collins, W. J., Dalsoren, S. B., Doherty, R. M., Eyring, V., Faluvegi, G., Horowitz, L. W., Josse, B., Lee, Y. H., MacKenzie, I. A., Nagashima, T., Plummer, D. A., Righi, M., Rumbold, S. T., Skeie, R. B., Shindell, D. T., Strode, S. A., Sudo, K., Szopa, S., and Zeng, G.: Pre-industrial to end 21st century projections of tropospheric ozone from the Atmospheric Chemistry and Climate Model Intercomparison Project (ACCMIP), Atmos. Chem. Phys. Discuss., 12, 21615-21677, 2012.
Zhang, Y., Wen, X. Y., and Jang, C. J.: Simulating chemistry-aerosol-cloud-radiation-climate feedbacks over the continental U.S. using the online-coupled Weather Research Forecasting Model with chemistry (WRF/Chem), Atmospheric Environment, 44, 3568-3582, 2010.